Titre: Title:	Regionalized Life Cycle Impact Assessment (LCIA) Fate and Characterization Factors for Microplastic Emissions in the Marine Environment
Auteur: Author:	Carla AlChahir AlHajjar
Date:	2025
Type:	Mémoire ou thèse / Dissertation or Thesis
Référence: Citation:	AlChahir AlHajjar, C. (2025). Regionalized Life Cycle Impact Assessment (LCIA) Fate and Characterization Factors for Microplastic Emissions in the Marine Environment [Thèse de doctorat, Polytechnique Montréal]. PolyPublie. https://publications.polymtl.ca/63401/

POLYTECHNIQUE MONTRÉAL
affiliée à l'Université de Montréal

Regionalized life cycle impact assessment (LCIA) fate and characterization factors for microplastic emissions in the marine environment

CARLA ALCHAHIR ALHAJJAR
Département de génie chimique

Thèse présentée en vue de l'obtention du diplôme de *Philosophiæ Doctor*
Génie chimique

Janvier 2025

POLYTECHNIQUE MONTRÉAL
affiliée à l'Université de Montréal

Cette thèse intitulée :

Regionalized life cycle impact assessment (LCIA) fate and characterization factors for microplastic emissions in the marine environment

présentée par **Carla ALCHAHIR ALHAJJAR**
en vue de l'obtention du diplôme de *Philosophiæ Doctor*
a été dûment acceptée par le jury d'examen constitué de :

Marie-Claude HEUZEY, présidente
Anne-Marie BOULAY, membre et directrice de recherche
Cécile BULLE, membre et codirectrice de recherche
Philippe ARCHAMBAULT, membre
Rosalie VAN ZELM, membre externe

DEDICATION

To Carla on her first day as a PhD student, this is for you...

To my family, Arianna, Tony, Lara, Michel, Elia, this is also for you...

To my resilient country Lebanon, I will forever love you...

To the tiny project underway "Marc", I can't wait to see you...

To the future, I am ready for you...

A Carla en son premier jour en tant que doctorante, ceci est pour toi ...

A ma famille, Arianna, Tony, Lara, Michel, Elia, ceci est aussi pour vous ...

A mon pays résilient, le Liban, je t'aimerai toujours ...

Au petit projet en cours "Marc", j'ai hâte de te voir ...

Au futur, je suis prête pour toi ...

ACKNOWLEDGEMENTS

Growing up singing "*Life in plastic, it's fantastic*", I never imagined that years later, I would dedicate my work to understanding the real impact of plastics - and realizing that it's not always so fantastic. This journey would not have been possible without the many incredible individuals who have supported, guided and inspired me over the past six years. First and foremost, I thank my supervisors, Anne-Marie Boulay and Cécile Bulle, for their insightful discussions, constant encouragement, support, and guidance. Anne-Marie, thank you for your guidance and support throughout this project. I appreciate integrating me into the MarILCA working group and the plastic team at CIRAIG. Being part of the discussions of these teams enriched my knowledge regarding plastic impacts and life cycle assessment. Cécile, I truly appreciate your immense patience and availability, especially during last-minute revisions and urgent meetings. Your guidance has been invaluable. A special thanks to Manuele Margni for always taking the time to answer my ecotoxicity-related questions whenever he visited Montreal. I am also grateful to Isabel Jalòn-Rojas for hosting me in Bordeaux and supporting me while working with the TrackMPD model.

To my family - Arianna, Tony, Lara, Michel, and Elia - thank you for your unwavering support, no matter the distances. Michel, I cannot thank you enough for your patience in answering all my coding questions, engaging in endless brainstorming sessions, and helping me solve engineering challenges, no matter the time zone. To my childhood friends back home - Anthony, Christine, Gaby, Georgy, Michelle, Jhonny, Paul, and Eliane - thank you for still being there after all these years, despite the miles between us.

A heartfelt thank you to my roommate and dear friend Laura Prieto Saavedra - your support made all the difference. Thank you for introducing me to the Super Computer (which I could not have completed this project without), for being my family in a foreign country, and for all the late night discussions and shared moments of joy. Layal, Davide, and Elise, I am equally grateful for the time we shared throughout these years and for all the crazy laughs and art nights.

To the incredible CIRAIG team, thank you for making the work environment so dynamic, fun, and supportive. You made the pandemic years much more bearable, and I am grateful for that. A special thanks goes to Ivan Viveros Santos, my first friend in CIRAIG, whose support has been constant throughout this journey. From answering my technical questions to helping me visualize my results and mentoring me in teaching, you have been an amazing colleague and friend. Your calm approach and attention to detail made every collaboration

enjoyable. Another special thanks goes to Maxime Agez, my second friend in CIRAIG, who was always there to support me, no matter what. Thank you for patientl helping me with coding over the pasti six years, answering my endless questions, and listening to me whenever I needed. To Elliot, thank you for our virtual and in-person hugs that always lifted my spirit. Han, thank you for being an amazing friend. Laura, thank you for the countless nights spent together and the unforgettable travels. Marit, thank you for being an amazing office partner. To Ivan, Han, Marie, Iris, Marit, and Maxime, thank you for your kindness and support during the difficult times my beloved country, Lebanon, was going through.

In the end, I acknowledge the usage of "Writefull" for proofreading my thesis.

RÉSUMÉ

La pollution des plastiques dans l'environnement, notamment l'environnement marin, est devenue un enjeu au niveau international au cours des années, à cause de leurs propriétés persistentes et leurs impacts dans l'environnement. Les déchets microplastiques (1 μm - 5 mm) dans l'environnement marin sont préoccupants à cause de leur petite taille et leur facilité à exposer les organismes marins. Les microplastiques (MPs) émis dans les océans sont transportés par différents mécanismes tel que, les courants d'eau, les vagues, les turbulences, etc., ainsi que leurs propriétés physiques (densité, taille, forme). Plusieurs mécanismes sont aussi responsables du changement des propriétés des particules tel que, la salissure, l'aggrégation, le transport par le biote, etc. Dépendemment de toutes ces propriétés environnementales, océanographiques, ainsi que des propriétés des particules, les microplastiques émis dans l'environnement marin sont dispersés et transportés vers différents endroits. Par conséquent, leurs impacts dépendent de leur compartiment de sort ultime et les organismes qui y sont exposés. Les impacts des microplastiques sur l'écosystème marin ont toujours été associés à leur (éco)toxicité, liée à leurs additifs. Cependant, différents impacts ont été récemment liés à la physiologie des particules et leur présence dans le corps des organismes. Ceux-ci incluent la détérioration de la croissance, fausse satiété, limitation de la reproduction, obstruction du tube digestif, ou même la mort. Pour cette raison, l'analyse et la quantification de ces impacts est importante.

L'analyse du cycle de vie (ACV) est une méthodologie qui vise à analyser les impacts environnementaux potentiels d'un produit ou service, sur l'ensemble de son cycle de vie. Une ACV est réalisée en quatres phases, d'après les règles ISO14040 et 14044. Ces phases incluent: la définition des **objectifs et champs de l'étude**, **l'inventaire du cycle de vie (ICV)**, **l'évaluation des impacts du cycle de vie (ÉICV)**, et **l'interprétation des résultats**. Différentes initiatives ont visé à inclure les impacts des MPs en ACV, tout en développant des facteurs de caractérisation (FCs) pour la phase ÉICV. MarILCA est un groupe de recherche international, qui propose un cadre méthodologique pour le développement des facteurs de caractérisation pour les déchets plastiques dans l'environnement, notamment l'environnement marin. Ce cadre méthodologique s'harmonise avec les méthodes ÉICV déjà existantes GLAM et IMPACT World+. Au sein de leur cadre méthodologique, une catégorie d'impacts a été proposée spécifiquement pour les "effets physiques sur le biote" des plastiques émis. Différentes études ont déjà tenté de développer des FCs pour les microplastiques dans l'environnement marin, pour la catégorie d'impacts "effets physiques sur le biote". Ces FCs ont cependant une grande incertitude liée aux compartiments marins non considérés ainsi

qu'à la grande variabilité des mécanismes de sort non quantifiés. Ceci a soulevé la nécessité d'affiner le cadre méthodologique du sort et par conséquent, des FCs. Ce cadre devrait prendre en considération tous les mécanismes de sort qui n'ont pas été considérés et influencent le transport des particules. Puisque plusieurs mécanismes varient spatialement, par exemple les courants d'eau, il est aussi nécessaire de tenir compte de la variabilité spatiale lors de la quantification des FCs. Ceci amène à l'objectif principal de cette thèse "régionaliser les facteurs de sort et les facteurs de caractérisation pour les microplastiques émis dans l'environnement marin, dans le but d'estimer l'importance de la variabilité spatiale comparée à la variabilité due aux propriétés physiques des particules".

Pour répondre à l'objectif principal, trois sous-objectifs ont été identifiés et addressés dans cette thèse. Le premier sous-objectif était de développer un cadre méthodologique affiné pour modéliser les facteurs de sort (FFs) et les facteurs de caractérisation (FCs) des MPs émis dans l'environnement marin. Comprendre ces mécanismes a aidé à prioriser les paramètres pour la quantification des FFs et FCs dans les étapes futures. Suivant une revue de littérature, l'environnement marin est élargi pour inclure plusieurs sous-compartiments marins à plusieurs niveaux (plage, eau de surface, colonne d'eau, sédiments au niveau continental, et niveau global). Ces sous-compartiments sont connectés par les mécanismes de sort responsables de la redistribution des MPs dans l'environnement marin. Par conséquent, des FFs et des FCs mécanistiques sont proposés. Pour s'harmoniser avec les FCs déjà existants, les FCs proposés suivent la structure des FCs existants pour l'(éco)toxicité. Le deuxième sous-objectif vise à identifier les paramètres influants sur les taux de chute et de sédimentation, ainsi que sur les FFs et les FCs. Ainsi, en utilisant un modèle numérique nommé "TrackMPD", les trajectoires des microplastiques, émis virtuellement dans trois points d'émissions d'une même région, sont analysées. Dans une première étape, une analyse de sensibilité est adoptée en faisant varier sept paramètres environnementaux et physiques des MPs entre leur minimum et leur maximum. Dans une deuxième étape, les taux de chute et de sédimentation sont quantifiés d'après les trajectoires des particules. En utilisant ces taux, ainsi que d'autres taux quantifiés d'après des données de la littérature, les matrices de transfert $\mathbf{K}$ sont construites, lesquelles sont ensuite utilisées pour établir les matrices de sort. Une autre analyse de sensibilité est réalisée pour tester l'influence des taux quantifiés sur les FFs. Dans une troisième étape, les FFs sont utilisés avec des facteurs d'exposition-effets (EEFs) pour développer des FCs. Une analyse de sensibilité est également réalisée pour tester l'influence des taux quantifiés et du EEF sur les FCs. Les résultats mettent en évidence une influence notable des propriétés physiques des particules sur les taux de chute et de sédimentation, ainsi que sur les FFs et les FCs. De plus, les propriétés environnementales (par exemple la turbulence) présentent également une influence sur les taux, les FFs et les FCs. Ceci indique que la régionalisation

doit être analysée davantage. Le troisième sous-objectif vise alors à régionaliser les FFs et FCs pour tenir compte de la variabilité spatiale des FCs. Ceci aide à comparer son influence à celle des propriétés physiques des MPs. En utilisant le même modèle numérique "TrackMPD", neuf polymères, de deux formes et cinq tailles, sont émis dans sept régions différentes. Ces régions ont été choisies car elles représentent les lieux d'émission de 92 % des MPs émis à l'océan depuis les rivières. En se basant sur la trajectoire des particules, les taux de transferts sont quantifiés, par exemple, le taux de transfert de la surface d'eau vers la plage ou de la surface d'eau vers le niveau global, etc. Ces taux sont ensuite utilisés avec d'autres taux provenant de la littérature (quantifiant d'autres mécanismes), pour construire les matrices de **K**. Par conséquent les matrices de FFs et FCs sont construites pour chaque particule testée dans chaque région d'émission. Les FCs sont quantifiés pour deux des méthodes ÉICV les plus à jour: IMPACT World+ et GLAM. En analysant la variabilité des FCs, il a été remarqué que l'influence de la régionalisation est significative sur les FCs de certaines particules. Celles-ci incluent les particules denses, pour toutes les tailles et formes, et les grandes particules légères, pour toutes les formes. Ceci est du à la longue dispersion de ces particules dans l'environnement marin, ce qui les rend sensibles à la direction des courants de chaque zone d'émission. On peut conclure qu'en quantifiant et analysant les impacts des MPs dans l'environnement marin, il n'est pas seulement important de comprendre quels types de particules sont émis, mais aussi à quel endroit est ce qu'elles sont émises dans l'environnement marin.

Les FCs développés pour les deux approches, sont aggrégés en des FCs pour deux continents (l'Afrique et l'Asie) et en FCs globaux, en utilisant les émissions totales de MPs des rivières vers les océans comme facteurs de pondération. Ces FCs agrégés tiennent donc compte de la variabilité spatiale des MPs aux points d'émissions les plus importants dans l'environnement marin. Ils prennent par ailleurs en considération cinq compartiments environnementaux dans la modélisation du sort des particules, ce qui permet une analyse fine en comparaison des FCs déjà existants.

ABSTRACT

Plastics pollution in the environment, notably the marine environment, has become an international issue over the years due to their persistent properties and impacts on the environment. Microplastic (1 μm - 5mm) littering in the marine environment was of particular concern, due to their small size and ease of exposure to the marine ecosystem. Microplastics (MPs) emitted into the oceans are driven by various mechanisms such as water currents, waves, turbulence, etc., as well as their physical properties (size, density and shape). Several marine mechanisms are also responsible for changing the properties of MPs leading to their redistribution, such as biofouling, aggregation, biota transfer, etc. Depending on all these environmental, oceanographic, and physical properties of MPs released into the marine environment, the particles are dispersed and transported to different locations. Consequently, their impacts depend on their ultimate fate compartment and the organisms exposed to them. The impacts of MPs have always been associated with their (eco)toxicity, linked to their additives and chemicals attached to them. However, different impacts have recently been linked to the physiology of the particles within the body of marine species. These include growth deterioration, false satiation, reproduction limitation, obstruction of the digestive tract, or even mortality. Therefore, it is important to assess the impacts of these particles on marine ecosystems.

Life cycle assessment (LCA) is an international tool used to assess environmental impacts of products and services over their entire life cycle. It is done over four phases according to ISO14040 and 14044. They include the **goal and scope definition**, **life cycle inventory LCI**, **life cycle impact assessment LCIA**, and **results interpretation**. Several initiatives have tried to include impacts of MPs in LCA through developing characterization factors (CFs) for the LCIA phase. MarILCA is an international working group that proposed a framework to develop CFs for plastic emissions, mainly in the marine environment, in a harmonized way with already existing LCIA methods IMPACT World+ and GLAM. In their framework, a new impact category was added to address "physical effects on biota" of emitted plastics. Several studies attempted to develop CFs for MP emissions for this impact category. However, their CFs presented high uncertainty due to unaccounted fate mechanisms and marine sub-compartments. This raised the need to refine the fate framework and consequently, the CF framework. This framework should account for all environmental and oceanographic properties that influence the fate of MPs in the marine environment, along with their physical properties. Since many fate mechanisms (e.g., water currents) vary among regions, it is important to assess the influence of this variability on developed CFs. This leads to the

main objective of the present thesis "regionalize the fate and characterization factors (CFs) of microplastic emissions in the marine environment, to assess the impact of spatial variability on CFs compared to the variability driven by the physical properties of microplastics".

In order to achieve the objective of this thesis, three sub-objectives are defined and achieved. The first sub-objective necessitates the development of a comprehensive more refined framework for the development of FFs and CFs for MP emissions in the marine environment. Understanding these mechanisms will help prioritize the parameters for quantification of FFs and CFs in future steps. Based on a comprehensive literature review, fate mechanisms responsible for the redistribution of MPs are identified. The marine environment is expanded to include several sub-compartments at two different scales (beach, water surface, water column, sediments at the continental scale, and the global scale). Based on this framework, mechanistic FFs and CFs are proposed. They are harmonized with the structure of emission-based CFs for (eco)toxicity. The second sub-objective includes the identification of influencing parameters on the settling of MPs, as well as influencing parameters on the FFs and CFs. Thus, using a numerical model "TrackMPD", the trajectories of virtually emitted MPs in the marine environment are tracked. In a first step, a sensitivity analysis is done where seven parameters, including environmental and MP physical properties, were changed between their minimum and maximum. In a second step, sinking and sedimentation rates are quantified using TrackMPD in three emission points in a specific region. These rates along with other rates, quantified based on literature data, are used to construct rate matrices for MPs tested. Other sensitivity analyses are done to address the influence of quantified rates on the FFs. In a third step, using FFs developed and already-existing exposure-effect factors (EEFs), CFs for MPs tested are quantified. A sensitivity analysis is then followed to test the sensitivity of CFs on quantified rates and EEFs. Results showed that MP physical properties have high influence on the sinking and sedimentation rates, and thus, on developed FFs and CFs. In addition, environmental properties (e.g., turbulence), that spatially vary in the marine environment, also showed high influence on sinking and sedimentation rates, FFs and CFs. Therefore, the need to address regionalization in future steps is identified. The third sub-objective accounts for the regionalization of FFs and CFs to analyze its variability compared to that of MP physical properties. Using the same numerical model "TrackMPD", nine polymers of five size classes and two shapes, are virtually emitted in seven different locations in the marine environment. These locations represent 92% of MP emissions from rivers into seas. Based on the trajectories of emitted particles, transfer rates between marine sub-compartments, e.g., transfer rate between water surface and beach, water surface and the global scale, etc., are quantified. These transfer rates are then used with other rates, quantified based on literature data, to construct rate matrices $\mathbf{K}$. Consequently, $\mathbf{FF}$ and $\mathbf{CF}$

matrices are quantified for every particle tested in each of the seven emission regions. CFs are constructed for the two most updated LCIA approaches: IMPACT World+ and GLAM. Analyzing the variability of CFs, it can be observed that regionalization has a significant influence on the CFs of certain particles. They include small particles of all sizes and shapes, and low density large particles of all shapes. This is because these particles are greatly dispersed in the marine environment. Thus, their fate is greatly influenced by the direction of water currents in each emission region. Therefore, when assessing the impacts of MPs in the marine environment, it is equally important to understand what particles are emitted and where in the marine environment.

Developed CFs for the two approaches are later aggregated into continent CFs (Africa and Asia) and global CFs using MP exports from rivers to oceans. These CFs address the spatial variability of MPs in highest emission points around the world marine environment. They address five emission marine sub-compartments and provide a more accurate fate modeling, compared to already existing CFs.

TABLE OF CONTENTS

LIST OF TABLES

LIST OF FIGURES

LIST OF SYMBOLS AND ACRONYMS

AoP	Area of Protection
AoC	Area of Concern
CDOM	Dissolved color organic matter
CH_4	Methane
CF	Characterization factor
CMS	Connectivity Modeling System
CO_2	Carbon dioxide
CTU	Comparative Toxicity Unit
deg	degradation
EEF	Exposure-effect factor
EF	Effect factor
EPS	Expanded polystyrene
FF	Fate factor
frag	fragmentation
FU	Function Unit
FSLCI	Forum for sustainability through life cycle innovation
ILCD	International Reference Life Cycle Data System
ISO	International Organization for Standardization
JRC-IES	European Commission's Joint Research Center - Institute for Environment and Sustainability
LC	Life cycle
LCA	Life cycle assessment
LCI	Life cycle inventory
LCIA	Life cycle impact assessment
MariLCA	Marine impacts in life cycle assessment
MMP	Marine Microplastic Potential
MPs	Microplastics
MT	Million tons
PAF	Potentially affected fraction
PAH	Polycyclic aromatic hydrocarbons
PCB	Polychlorinated biphenyls
PDF	Potentially disappeared fraction
PE	Polyethylene

PET	Polyethylene terephtalate
PFN	Plastic Footprint Network
PLP	Plastic Leak Project
POPs	Persistent organic pollutants
PP	Polypropylene
PVC	Polyviny chloride
SF	Severity Factor
SETAC	Society of Environmental Toxicology and Chemistry
TRWP	Tyre and road wear particles
UNEP	United Nations Environment Program
UV-A	Ultraviolet A rays
UV-B	Ultraviolet B rays
XF	Exposure factor

LIST OF APPENDICES

CHAPTER 1 INTRODUCTION

The increase in plastic pollution in the world's oceans is becoming a major concern because of their detrimental effects to the ecosystem [5]. Annual plastics emissions into the aquatic environment are estimated to reach 53 million tonnes per year by 2030 [6]. Microplastics (MPs), between 1 µm and 5 mm [4], have been detected on world beaches [7, 8], water surfaces [9], water columns, and even deep sediments [10]. MPs have been very widespread in the marine environment. They have traveled from Antarctica to Arctic regions [11], where they expose marine ecosystems. The distribution of MPs greatly depends on their persistence and physical properties (size, density, shape) [12]. In addition, environmental and oceanographic conditions play a key role in their redistribution, such as ocean currents, turbidity currents, turbulence, water density, wave and wind mixing, and formation of microbial films [13, 14]. The widespread accumulation of growing MP pollution raises concerns about their impacts on marine ecosystems and requires its evaluation.

Life cycle assessment (LCA) is an international decision-making tool for the evaluation of environmental impacts of products/services throughout their life cycle stages. Impacts are evaluated in numerous impact categories, such as ecotoxicity, human toxicity, climate change, etc. [3, 15, 16]. The evaluation of impacts in LCA is carried out in a phase called Life Cycle Impact Assessment (LCIA), where pollutants are characterized using characterization factors (CF) [3, 16]. A CF is a mathematical quantification of a cause-effect chain of the pollutant considered for a certain impact category. For (eco)toxicity emission-based CFs, the cause-effect chain is constructed through two factors: a fate factor FF and an exposure-effect factor EEF. FFs quantify the distribution of pollutants emitted within the environment, and EEFs assess the impacts of these bioavailable pollutants distributed on the receiving ecosystem. Thus, a CF is needed to be able to assess the impacts of considered MPs on the marine ecosystem. For this purpose, an international working group MarILCA (Marine Impacts in LCA) was founded in 2018, with the support of the UN Environment Program and the Forum of Sustainability through Life Cycle Innovation (FSLCI) [17], to establish a harmonized framework for the evaluation of plastic pollution in LCIA, with a focus on the marine environment. In order to separate impacts linked to the (eco)toxicity of polymers (e.g., additives), an additional impact category was proposed to only consider the "physical effect on biota" of emitted plastics. Within MarILCA's framework, simplified characterization factors were developed for MPs based on a simplified fate framework [18, 19] and exposure-effect factors for water and sediment ecosystems [18–21]. The simplified fate factor was based on the degradation of MPs in one marine compartment (water) in which the settling of MPs was estimated

in a simplified way [18, 19]. Simplified FFs developed resulted in a high uncertainty on the CFs due to unconsidered mechanisms (such as water currents and turbulence) and marine sub-compartments (such as beaches, sediments, etc.). This raised the need to refine the fate model by expanding it to include more marine sub-compartments and account for unconsidered mechanisms that play an important role in the distribution of emitted MPs. Since most of these mechanisms are spatially dependent, especially water currents, it is equally important to regionalize FFs and subsequently CFs. This will allow a better understanding of the importance of regionalization, compared to the physical properties of MPs, on the CFs. Therefore, the main objective of this doctoral thesis is to regionalize fate and characterization factors of MP emissions to the marine environment, for the LCIA impact category "Physical effect on biota".

The second chapter of this thesis presents a comprehensive literature review that led to the development of the research hypothesis. The third chapter describes the research hypothesis, general objective, and sub-objectives along with an overview of the thesis structure. An overview of the general methodology in provided in chapter 4 while chapter 5 presents the detailed methodology of the third sub-objective. Chapters 6, 7 and 8 then present the work that led to achieve each of the defined sub-objectives. In particular, chapter six answers the first sub-objective where a comprehensive, more refined framework is proposed for the development of FFs and CFs for MP emissions in the marine environment. This led to the first scientific article, entitled *Life cycle impact assessment framework for assessing physical effects on biota of marine microplastic emissions*, which was published in the *International Journal of Life Cycle Assessment*. Chapter seven presents the results of answering the second sub-objective, where the influence of MP physical properties as well as environmental parameters on the settling of MPs is assessed. In addition, the influence of quantified fate mechanisms on the CFs is evaluated. This resulted in the second scientific article, entitled *Identifying influencing physical and environmental parameters through the development of site-specific fate and characterization factors for microplastic emissions in the marine environment* that was accepted, on the 28^{th} of November 2024, in the *International Journal of Life Cycle Assessment*. Chapter eight then answers the third sub-objective where the regionalization of fate and characterization factors is accomplished. The importance of the physical properties of MPs is also assessed compared to the regionalization. Finally, this thesis concludes with a general discussion of contributions, thesis project limits, and suggests some recommendations for research in Life Cycle Inventory (LCI) and Life Cycle Impact Assessment (LCIA) for regionalization.

CHAPTER 2 LITERATURE REVIEW

This chapter aims at presenting and criticizing different definitions, elements, and concepts necessary for the comprehension of the following thesis. This literature starts by presenting the problems of plastic waste in the marine environment with a focus on microplastics (section 2.1). Then, MP transport mechanisms (section 2.2) and weathering processes (section 2.3) are discussed. This is followed by a description of the numerical modeling used to represent the fate of MPs in the marine environment (Section 2.4). The impacts of MPs on marine species are then presented in section 2.5. Life cycle assessment, with a specific focus on the life cycle impact assessment phase, is later introduced in section 2.1. Finally, the state-of-the-art of microplastics in life cycle assessment is presented in section 2.7.

2.1 Plastics in the marine environment

Marine litter has become a global environmental threat and concern due to its exponential increase over the years. The presence of plastics strongly prevails over that of other items, such as glass and ceramics, metals, papers, textiles, rubber, and woods in all marine subcompartments [22]. Despite global efforts to reduce plastic emissions, it is estimated that between 20 and 53 million tons per year [Mt/year] of plastics will reach aquatic environments by 2030 [23]. Microplastics are small plastic particles that range in size from 1 µm to 5 millimeters [24]. They reach the oceans as primary or secondary microplastics. Primary MPs are produced on the microscale, such as pellets, while secondary microplastics result from the physical fragmentation of larger macroplastics [24]. Land-based MPs are the main source of marine primary microplastics through river transport [1] that feed marine water surfaces. Marine activities (e.g., fishing) [25] are responsible for secondary microplastics through fragmentation of larger macroplastics in the marine environment. Although the presence of MPs is predominant in coastal surface waters and coasts, mainly around densely populated areas [26], it has also been detected in large proportions in deep-sea water and sediment samples [27]. As they linger in the marine environment, various mechanisms affect their transport and residence time, leading to potential impacts.

2.2 Transport of microplastics in the marine environment

Understanding and modeling the transport of MPs in the marine environment have been very challenging because various physical, chemical, and biological processes, influenced by the

physical properties of the particles (size, density, shape), play an important role [28]. The densities of MP have a significant influence on their distribution in the marine environment. Low density particles (positively buoyant) float at the water surface [29, 30] while particles denser than seawater (negatively buoyant) sink in the water column until they reach the sediments, where they accumulate [31]. In addition to their density, the size and shape of MPs also have a significant influence on their settling velocities [32]. Depending on their presence, plastics can be affected by different oceanographic mechanisms and processes. Lighter particles are mainly driven by windage that transports them at the surface of the water; slightly buoyant particles are controlled by the celerity of their fouling; and heavy microplastics are mainly affected by their sinking velocity [29, 33]. The following sections (section 2.2.1, section 2.2.2, section 2.2.3 and section 2.3) summarize all fate mechanisms. More details on these mechanisms can be found in section 6.3 of chapter 6.

2.2.1 Horizontal transport at the beach and the water surface

Positively buoyant MPs, which are less dense than their surrounding water, are driven primarily by advection and diffusion, influenced by mixing processes of turbulence [34]. Their horizontal dispersion is affected by buoyancy, Stokes drift (wave-induced motion), and Langmuir circulation (wind-induced motion) [35]. The influence of turbulence on MPs is greatly related to their size. The larger MPs are much less affected by turbulent mixing than the smaller ones [36]. Stokes drift causes MPs to drift in the direction of wave propagation [37] however, it remains challenging to model the movement of floating MPs with Stokes drift [38]. Wind-induced turbulence on the surface traps MPs in strong vertical flows, called Langmuir circulation [29] and push them deeper in the water [39, 40]. Positively buoyant particles eventually resurface at different velocities depending on their shape and size [41, 42]. Because larger macroplastics have higher velocities, they float in shallower layers compared to MPs that settle in deeper layers [42]. Floating macroplastics, influenced by stronger Stokes drift in shallower layers, become trapped in coastal waters [43–45]. The action of waves and tides [30], the high exposure to UV lights and mechanical abrasion of the sand [46] then result in their fragmentation near the shore. Resultant MPs drift offshore [44] and become more abundant than macroplastics as we move horizontally away from the shore [30, 47]. Beaching time of macro- and microplastics therefore depends on their terminal velocities, linked to their size, shape, and buoyancy, as well as the steepness of the waves [45]. Ekman drift, caused by the wind and Earth's rotation, leads to the formation of the ocean's convergence zones, where MPs accumulate [14, 48–50]. However, these MPs are gradually removed from these zones through processes such as biofouling (section 2.2.2), aggregation (section 2.2.2) and ingestion by marine organisms [51] (section 2.2.2).

2.2.2 Vertical transport in the water column

Negatively buoyant microplastics, having densities larger than that of the surrounding seawater, start to sink as soon as they reach the marine environment. They settle at different settling velocities depending on their size and shape. The settling velocity of MPs is directly proportional to their size [32]. Thus, the larger the particle for the same shape and density, the faster it reaches the sediments. Positively buoyant MPs mainly float at the shallow layers of the ocean, as explained in section 2.2.1. However, many marine mechanisms and environmental conditions alter their density, resulting in their vertical transport to deep benthic layers of the ocean [52]. Although these mechanisms still require a lot of research, the vertical transport of buoyant MPs has been greatly associated with biofouling (section 2.2.2). Aggregation (section 2.2.2), biota interactions (section 2.2.2) and sea ice transfer (section 2.2.2) have also been documented as a key factor in the settling of positively buoyant MPs.

Biofouling

In the seawater, algae and microorganisms accumulate as biofilms on the surface of marine litter, herein microplastics. This process known as biofouling has been widely reported to be the main reason for the settling of positively buoyant MPs [53, 54]. The celerity of biofouling depends on the polymer type, surface area and roughness [46]. Negatively buoyant MPs, having a rapid settling velocity, might sink close to their emission points before biofouling can take place [53]. However, positively buoyant floating MPs must undergo biofouling in order to sink and eventually reach the sediments [55, 56]. Biofouling rates depend on the size of the particles and the surface area to volume ratio, with smaller particles fouling faster and sinking sooner than larger particles [29, 57]. The shape of MPs plays a role in the celerity of MP biofouling as well. Films were shown to foul faster than fibers, followed by spherical MPs [29]. Furthermore, biofilms grow unevenly on the surface of MPs, leading to instabilities in their sinking, which reduces their settling velocity [58]. This illustrates the complex role of biofouling in the vertical transport of MPs.

In addition to the physical properties of MPs [59], biofilm growth is influenced by various other factors, including the chemical composition of MPs (additives), and environmental conditions such as salinity [60], seasonality [57], and geographical locations [61]. Biofouling communities vary across oceans, with slower biofilm growth in areas of low biological activity, such as subtropical gyres. This results in a longer residence time on the surface of the ocean. In contrast, high biological activity in the equatorial regions results in a faster sinking of microplastics due to high algae concentrations [57, 62]. In addition, biofouling rates are higher in spring and summer due to algal blooms [57, 63]. While biofouling generally

reduces microplastics buoyancy, studies have shown varied effects in different aquatic environments (rivers and estuaries). If the density of the biofilm is smaller than that of MPs, the overall density of the fouled particles could decrease, reducing their settling velocity [64, 65]. These studies highlight the need for further research on the dual role of biofouling in vertical transport of microplastics, particularly in marine environments.

The growth of biofilms also depends on water conditions, light limitations, and predation [46, 66]. For instance, in deeper water layers, the light needed for algae respiration and growth is attenuated. When biofouling conditions needed for biofilm growth are not present, defouling might occur. This creates a fouling-defouling cycle depending on water conditions. This leads to an increase-decrease cycle of MP densities that results in an oscillatory movement within the water column [53]. However,it has been shown that biofilms grow faster in deeper layers compared to water surfaces. This is related to hydrodynamic forces that slow the growth of biofilms and reduce the accumulation of biofilm mass at the water surface. Moreover, ultraviolet radiation, which is highly present at the water surface, decreases biofouling rates and leads to potential defouling [63]. Extreme weather conditions and strong waves might also cause the detachment of biofilms from the surface of MPs [67]. All these environmental conditions are challenging not only to capture but also to model and quantify. This reflects the complexity of modeling all fate mechanisms that influence MP transport in the marine environment.

Aggregation

Marine snow consists of aggregates of particulate organic matter (POM), microorganisms and clay minerals, which are formed from detritus, plankton, and biological aggregation of smaller particles, including fecal pellets from plankton, fish, and marine mammals [68]. Larvaceans, which are marine organisms, create mucus-based structures known as "houses" that they use for locomotion and feeding [69]. Recent studies suggested that biological transport, due to aggregation to larvacean houses and marine snow, may also play a significant role in the redistributing of microplastics (MPs) from surface waters to deep sea sediments [70, 71]. Marine snow can carry MPs of varying densities, shapes, and sizes from the surface to the seafloor, increasing their availability to benthic organisms [72–74]. This process enhances the sinking rates of dense particles and decreases the buoyancy of floating MPs [74–79].

Biota Transfer

Marine animals, including fish, turtles, and invertebrates, are exposed to MPs through different exposure routes (section 2.5). Once ingested, MPs can either be retained in the body

of the prey or egested in their fecal pellets. Microplastics embedded in fecal pellets have a higher settling velocity than free MPs [71]. Similarly, MPs retained in the body of organisms with a slow ingestion-excretion rate are ingested at the surface and ejected at the bottom [80]. This indicates that marine organisms can contribute significantly to the accumulation of positively buoyant MPs in sediments, especially MPs smaller than 1 mm [81]. However, retention-excretion rates, which vary by species, are still not very well explored and quantified [82].

Sea ice transfer

During ice formation in the Arctic and Antarctic, MPs become entrapped in the early stages of sea ice formation [83, 84]. During ice melting, trapped MPs are released and vertically distributed in the euphotic zone [85]. Floating ice horizontally migrates in the water, resulting in the horizontal distribution of MPs upon melting [86]. Thus, seasonal formation and melting of sea ice can serve as a temporary delay for sedimentation of trapped MPs [87]. This increases their duration of exposure to marine organisms [84]. However, more research is still needed in this new field to better understand the interaction of MPs with sea ice and the influence on their fate [88].

2.2.3 Transport in sediments

Settling microplastics eventually reach the sediments. In coastal areas, enhanced turbulence near the bottom can resuspend MPs from the sediments [89, 90]. Depending on the physical properties of the particles and the turbidity currents, some of the particles might suspend, in the stream of turbulence, without having contact with the sediment bed [91]. Thus, they can move along the sediment bed through water velocity and turbulence [92] similarly to natural sediments [93, 94]. When they finally settle on the sediment bed, they can undergo bedload transport, similarly to sediment particles, through sliding, rolling, or successively jumping, a process also known as saltation [91, 95]. The bedload transport of MPs depends on several factors. The physical properties of MPs play a key role in their interaction with sediment particles. Although size has a small influence, the density of MPs significantly affects their transport. Higher density MPs require higher shear stress to move along the sediment bed compared to lighter particles of the same size and shape. In addition, spherical particles always move earlier than other shapes because they have the smallest surface contact with sediment particles. Thus, they require less resistance and drag force to move. In addition, spherical particles have a tendency to roll over the surface of sediments rather than saltation. This is because they require a stronger lifting force. Alternatively, cylindrical and

irregular shape MPs require more drag force to move because they can get trapped within the interspaces of sediment particles [92, 96]. For this reason, they tend to travel shorter distances compared to regular-shaped particles [96].

The slope of the sediment surface [96] and the type of sediment particles also influence the behavior of settled MPs. Fine gravel sediments have a higher drag force followed by coarse sand and medium sand [92]. Although MP saltation, the dominant bedload transport, has been found analogous to that of natural sediments [95], the variety of MP characteristics in terms of size, shape, and density results in a more complex transport compared to natural sediments. Although MPs and sediment particles might share similar size ranges, natural sediments generally exhibit higher densities and less variety within their characteristics. Thus, the transport of natural sediments is more uniform than that of MPs [97]. Therefore, more research is still required to understand and capture the bedload transport dynamics of MPs and their interactions with sediment particles.

While bedload transport of MPs horizontally moves the particles along the sediment surface, the settled MPs can also exhibit vertical transport due to turbidity currents [98]. Once settled, MPs are gradually buried by sedimentation, a process that occurs at slow rates. In addition, benthic organisms, known as bioturbators, play a dual role in distributing MPs in sediments: they can both resuspend MPs [99] and enhance their burial in deeper sediment layers. This process is known as bioturbation [100, 101]. The extent of this process depends on species's behaviors, traits, and feeding modes [102]. Once buried in deep sediment layers, MPs are less likely to move to the surface of sediments [103].

2.3 Weathering of plastics

Fragmentation irreversibly changes the shape of plastics and breaks them into smaller polymer fragments [46]. Macroplastics fragment into microplastics which in turn fragment into nanoplastics [104]. Fragmentation occurs through mechanical forces such as wind, waves, and water movement [105–107]. Further degradation of plastics converts polymers into monomers, leading to eventual mineralization through the formation of carbon dioxide [108]. Depending on stabilizing additives, environmental conditions and polymer properties, fragmentation and degradation can take several years to occur [109].

Photodegradation, through exposure to UV-A and UV-B radiation, is the most significant weathering mechanism in the marine environment [108]. In the presence of oxygen, this process is referred to as photooxidation [110] and is crucial to initiating weathering mechanisms [46, 111]. Photooxidation begins at the outer surface of the particles, exposed to

UV radiation [112] and gradually penetrates deeper at slower rates due to light attenuation and limited oxygen diffusion [113]. The resulting embrittlement and cracks depend on their length, the stresses that act on them, and the fracture toughness of the polymer [113]. Photooxidation occurs primarily on the beach and the sea surface where the required conditions are satisfied [114]. In addition, coastal areas provide significant mechanical forces, due to hot and dry sands, and the action of waves and sand abrasion. These conditions enhance the formation of secondary microplastics obtained as a result of the fragmentation of macroplastics [33, 104].

Biofragmentation is the process through which marine organisms break down plastics physically (through ingestion) or biologically (through enzymes) [108]. This process justifies the presence of nanoplastics in the fecal pellets of marine organisms [77, 115]. Further biodegradation is mainly responsible for the mineralization of plastic polymers into carbon dioxide, water, and methane [116]. While photodegradation and photooxidation dominate on beaches and the sea surface, biodegradation is primarily responsible for plastic degradation in the water column and sediments [117]. Nonetheless, biodegradation occurs at significantly slower rates than light-induced photooxidation [46].

Seasonal variations also have an influence on the degradation rates of polymers. The increase in UV intensity in summer accelerates the degradation, whereas in winter it decelerates because of the reduced intensity. Similarly, plastics in the equatorial regions experience higher weathering rates due to longer exposure to stable, intense UV light compared to those in polar areas [118].

Various environmental and water conditions can affect the fragmentation and degradation of plastics in the marine environment [119]. Reduced water temperature, compared to beach, can slow degradation rates [113]. Furthermore, biofouling (section 2.2.2) can shield the plastic surface from UV light and cause it to sink further away from weathering conditions [120]. Uneven biofilm growth can influence the degradation rates at the surface of the particles [121]. Negatively buoyant MPs tend to remain intact due to fast settling and limited weathering conditions in the water column and sediments [117]. The type of polymers also plays a key role in their weathering processes. For instance, polypropylene is less resistant to degradation than polyethylene. In addition, foamed expanded polystyrene is particularly vulnerable to fragmentation because it is composed of multiple thin layers [122].

2.4 Simple and numerical modeling

All the aforementioned environmental and marine mechanisms emphasize the complexity of capturing and modeling the behavior of MPs in the marine environment. However, several modeling attempts managed to replicate one or more of these behaviors. SimpleBox4Plastics [2] is a non-dynamic multimedia fate model developed to estimate the transport of MPs in several environmental media, including the marine environment. Several fate mechanisms, such as resuspension and burial in sediments, as well as the transfer between the water and sediment sub-compartments (sedimentation) are modeled in a simplified way. Sedimentation is quantified for a variety of MP densities and sizes. However, SimpleBox4Plastics only accounts for spherical MPs. Biofouling is not taken into account in the model. Alternatively, aggregation is assumed in one step only. This means that if the overall density of the aggregated MP does not exceed the surrounding seawater density, the particle will never settle. This assumption leads to inaccurate results that counteract the observations in the literature, where positively buoyant particles have been detected in deep marine sediments [123]. In addition, the influence of advection is quantified using a simplified value of water flow (expressed in m^3/s). This influences the settling velocity that is based on a simple gravitational settling velocity, without taking into account the influence of water currents in 3D, as well as other oceanographic processes such as Stokes drift, wind effect, etc. SimpleBox4Plastics can be used to quantify some fate mechanisms that have not been widely studied in the literature (such as resuspension and burial). However, in order to predict the three-dimensional distribution of MPs, it is important to understand the uncertainty this model presents due to the simplifications of many oceanographic and environmental mechanisms.

Tracking the transport and distribution of marine plastics requires the consideration of combined influence of hydrodynamic water currents, microplastic physical properties, and all the physical, chemical, and biological mechanisms in marine sub-compartments. Thus, it is very challenging to model the trajectories of emitted particles because of the complexity of combining all the needed mechanisms and conditions. Numerical modeling has been used to trace the particles of marine litter, such as plastic debris, while considering a variety of marine processes. It is becoming a useful tool commonly used to predict the transport and accumulation of MPs. There are mainly two complementary approaches currently used in numerical modeling. The first approach is the Eulerian framework that uses ocean velocity fields to track tracers in the ocean. This approach does not track the distribution of individual particles but rather their distribution in terms of their mass or volume. It is commonly used to simulate plastic transport in sediments (e.g. Michallet et al. (2004) [124]

and Chauchat et al. (2018) [125]). The Eulerian framework is also used to simulate plastic transport in one- (1D) or two-(2D) dimension models. For example, it is used to simulate the one-dimensional vertical transport of MPs in the ocean surface layer due to turbulence, based on surface measurements [36,41,126]. The second approach is the Lagrangian framework that is advantageous for simulating marine debris, such as plastics, in complex flow fields while accounting for a variety of mechanisms (such as dispersion, aggregation, etc.). This approach focuses on the transport of individual particles. Thus, it is commonly used to simulate the three-dimensional transport of MPs. Lagrangian approach uses precomputed Eulerian velocity fields derived from observations or from ocean general circulation models (OGCMs). Several models have been developed to trace macroplastic and microplastic emissions in the marine environment by integrating the spatially and temporarily varying velocity fields in time. Among these Lagrangian models, there are those adapted to simulate the transport and fate of MPs in open oceans, that is, "Plasticparcels" [127] based on the "Probably A Really Computationally Efficient Lagrangian Simulator" (Parcels) [128] and "OceanParcels" models [128,129], OpenDrift [130], and the Pol3DD model [50,131]. Other Lagrangian models are used for smaller spatial scales such as coastal and regional seas. Among these models are the "Poseidon pollutants transport model" (PPTM) [132], the Delft3D-PART model [133], and the "Track Marine Plastic Debris" (TrackMPD) model [12]. Other models can be used for both coastal and open oceans, such as the Ichthyop model [134, 135].

The aforementioned models have been widely used for a variety of MP applications. However, despite efforts to integrate as much as possible of fate mechanisms along with the influence of MP physical properties, these models still lack, to a certain extent, a variety of important mechanisms and parameters needed to accurately model the transport of MPs in the marine environment. For instance, the Ichthyop model does not account for the physical properties of MPs, beaching, vertical transport, and biofouling [134, 135]. While the PPTM model is considered a more advanced model by integrating additional Stokes drift, wind effects, and vertical transport, compared to the Ichtyhyop mode, it does not integrate MP physical properties and biofouling [132]. Nevertheless, some applications managed to incorporate them while employing the model [136]. The Pol3DD model was used mainly for the transport of MPs at the water surface [50, 131]. The Delft3D-PART can be used for 3D tracking [133] however, it has been applied for 2D tracking where the vertical movement of MPs was ignored. While the results showed agreement with the measurements, the model presented inaccurate results by overestimating and underestimating the distribution of MPs in some of the regions tested [137]. The OceanDrift model framework was developed and used primarily for oil spill studies [138], but it has been applied to drifter and microplastic studies in coastal zones. However, differences in terminal settling velocities linked to the physical properties of MPs

were not taken into account [139].

Nevertheless, some of these models are quite promising to capture the behavior of MPs in the marine environment, as they include most relevant mechanisms for their transport. The TrackMPD model is a Lagrangian model that can track MPs in 2D and 3D motion. It can calculate the forward and backward trajectories of virtually emitted MPs. It is compatible with a wide variety of OGCMs (such as FVCOM, MARC, MARS, POM, NEMO, etc.) depending on the target region and the needed level of accuracy of hydrodynamic data. The model includes many physical mechanisms such as advection-diffusion. It can also account for additional horizontal and vertical dispersion that might not be accounted for in the OGCM data. In addition, sinking, washing-off, beaching, and resuspension are accounted for. The model can also be used for a variety of physical properties of polymers (density, size, and shape). Biofouling and degradation that influence MP transport are also taken into account with a wide variety of formulations that can be applied, such as the sinking/rising velocity based on the size of the particles, the increase of the settling velocity with biofouling, and the increase of the particles density with biofouling [12]. Although it is challenging to use this model for large-scale simulations, due to the high computational time and data needed, this model presents great flexibility in testing the physical properties of MPs and fate mechanisms, as well as various parameters that influence these mechanisms, such as biofouling and degradation. Most recently, the "Plasticparcels" model [127], based on the OceanParcels model, emerged with the main goal of tracking virtual plastics released in the oceans. "Parcels" team has been integrating the transport of plastics in their model "PlasticParcels" by systematically including a wide variety of mechanisms in a variety of studies, such as modeling the transport of buoyant particles [27], modeling the influence of MP size and their fragmentation on their transport [140], modeling the vertical transport of biofouled particles [13, 57], etc. It was not until recently that these quantified mechanisms were merged together into the PlasticParcels model (`https://github.com/OceanParcels/plasticparcels/blob/main/docs/paper/paper.md`. However, the ability of this model to track the transport of plastics until their final fate on the sediments remains unclear.

The widespread of MPs in the marine environment, due to the interaction between the particle properties and the environmental and oceanographic conditions, has played a role in exposing marine organisms to MPs on beaches, water surface and even deep benthic sediment layers. Hence, understanding the interaction of MPs with marine biota is crucial to assess their impacts.

2.5 Impact of microplastics on marine species

Microplastics are more bioavailable than macrolitter items due to their small size. The presence of microplastics has been reported in various small organisms such as deposit- and detritus feeders (such as lugworms [141] and amphipods [142]), filter- and suspension feeders (such as barnacles [143], copepods [144] and mussels [145]), echinoderms (such as sea cucumbers [146] and starfish [147]), phytoplankton [148], and other types of crustaceans (such as shrimps [149], lobsters [150], and crabs [147]). Larger creatures, such as whales [151, 152], fishes [6], and turtles [153] have also been shown to have traces of microplastics. Marine organisms are vulnerable to MPs through primary (direct) ingestion from the marine environment [154] or indirect feeding (secondary ingestion) of contaminated prey in the trophic chain [155]. Ingestion can be deliberate, due to misdirected feeding behaviors, or accidental, due to confusion with prey items [154]. The size of MPs plays an important role since it is related to the size of the organism [156]. Thus, the size of MPs through secondary ingestion is smaller than through primary ingestion because it is scaled to the size of the prey [156]. Different feeding behaviors can expose organisms to various types of MPs. For instance, crabs and starfish tend to ingest particles with hollows and cracks on their surfaces, while sea anemones ingest microplastics with smooth surfaces [147]. In addition, biofilm presence (section 2.2.2) might reduce the consumption of MPs as well as their retention times (e.g., in anemones) [157]. In addition, feeding behaviors can expose marine organisms through water, passively through sediments [155], or both [158].

Once inside the body, microplastics can either accumulate, be translocated between body tissues [145], or can be eliminated through excretion or egestion. They might even be stored in the body without following excretion [155]. Before being eliminated, microplastics can present various sublethal impacts on marine biota depending on the ingesting organism. These include internal and/or external injuries, blockage of the digestive tract resulting in false satiation sensation and physiological stress [157], reduction in feeding [144,159], growth retardation, alteration of morphology (e.g. weight reduction) [157], immunological responses and gene expression profiles [145], reduction in reproduction [159] and fertility [160], fecundity and survival rate of progeny [161], influence on lipid accumulation [144], abnormal growth development [144], bladder blocking and/or rupture [156]. Lethal effects have also been observed with elevated mortality rates [156, 159]. Despite all these recorded impacts of MPs on marine organisms, there is still a large knowledge gap about their possible negative impacts on some species; for example, whale species [151], and still require further research.

In addition to their physical impacts, microplastics can introduce toxic compounds into marine organisms [162] through chemical additives mixed during the manufacturing process

to enhance the properties of polymers [163]. Leaching from microplastic particles, chemical additives can introduce various lethal and sublethal effects to marine ecosystems such as reduced mobility, growth or reproduction rate, mutations, behavioral changes, and variations in biomass or photosynthesis rate and even mortality [164]. In addition to additives, it has been confirmed that MPs can adsorb other pollutants on their surface from the marine environment, such as persistent organic pollutants POPs and heavy metals. However, this exposure, which has become a growing concern [145], is still unexplored and requires further research.

Since plastic litter in the marine environment will continue to increase in the future [23], it is important to assess the impacts of their interactions with marine organisms.

2.6 Life cycle Assessment

The life cycle assessment (LCA) is an environmental method that aims to evaluate the potential environmental impacts of products, processes, or services throughout their entire life cycle, which consists of the following steps: 1) extraction and treatment of raw materials, 2) manufacturing processes, 3) transport and distribution, 4) use and reuse of final products, and 5) recycling or waste management at the end of life [3]. Due to its holistic approach, LCA assists in: 1) evaluating the different stages of the product life cycle and thus improving their environmental performances at these stages, 2) identifying environmental indicators for evaluation and analysis, 3) informing industries and/or organizations in decision making, and 4) marketing of the products and services that are being studied [3].

2.6.1 General description of LCA

LCA is an iterative method that is carried out in four phases according to the International Organization for Standardization (ISO) standards [3, 16] (figure 2.1):

1. Goal and scope definition
2. Life cycle inventory (LCI)
3. Life cycle impact assessment (LCIA)
4. Results interpretation

LCA is generally used on a comparative basis (e.g., two products). In the **goal and scope definition** phase, the function and functional unit (FU) are identified. The FU serves as the

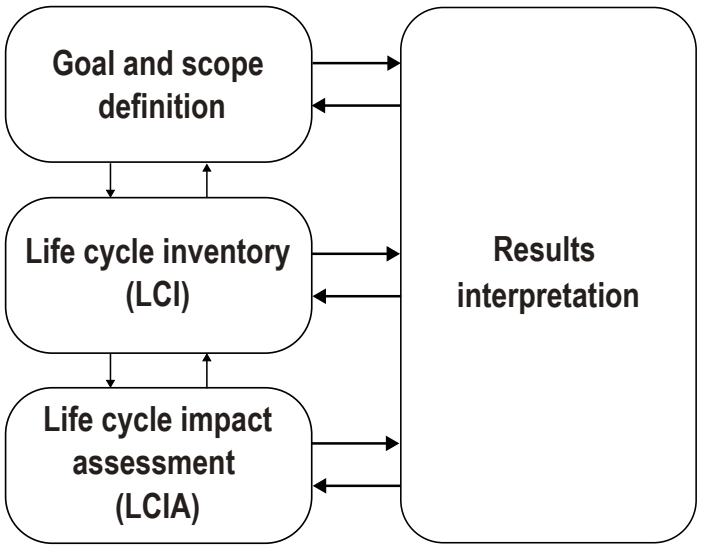

Figure 2.1 Life cycle assessment phases, adapted from [3]

basis of comparison based on which the product, process, or service studied is analyzed or compared. In addition, the product/process/service system and its boundaries are defined in this phase. The **life cycle inventory (LCI)** consists of collecting all the data needed to perform the LCA. Two types of flows are defined: elementary flows where all exchanges with the biosphere are collected; i.e., the extraction of primary resources and emissions of pollutants to the environment. Intermediary or economic flows are defined as the exchanges within the technosphere as input and output flows. The **life cycle impact assessment (LCIA)** phase addresses the potential impacts of elementary flows associated with the life cycle of the system studied. The elementary flows of LCI collected are converted into their potential impact scores in identified impact categories (such as climate change) using characterization factors (CFs). Each flow is associated with a CF, obtained by quantifying a defined cause-effect chain for each of the impact categories studied. This thesis mainly addresses the LCIA phase, specifically the development of characterization factors for microplastic emissions in the marine environment. Therefore, this phase will be elaborated mostly throughout this thesis. The **interpretation** phase consists of analyzing the results of the LCA with a complete and coherent reasoning. Consequently, the scope of the study, the quality of LCI flows, and the adopted LCIA methodology could be changed or improved in an iterative revision. In this phase, sensitivity and uncertainty analyses might also be applied to reinforce the analysis.

2.6.2 Life cycle impact assessment and characterization factors

In order to assess the impacts of elementary LCI flows, LCIA consists of different steps. According to ISO 14044, these steps are classified as mandatory or optional [16]. Mandatory steps consist of the following:

1. *Selection of impact categories, category indicators, and characterization models* where impacts that need to be addressed are selected relative to the goal and scope defined in the first phase [165].

2. *Assignment of LCI results (classification)*: LCI elementary flows are assigned to one or more of the selected impact categories at a midpoint and/or endpoint level, such as freshwater ecotoxicity, human toxicity, etc. [165].

3. *Calculation of category indicator results (characterization)*: This step consists of characterizing the emission and extraction flows to represent their environmental contribution to selected impact categories using characterization factors [165].

Characterization factors are the result of a mathematical representation of a cause-effect impact pathway for an impact category. This chain is a succession of different environmental processes that start with environmental emissions and/or extractions and end with their relative impacts [166]. Following a cause-effect chain for the ecotoxicity impact category, a widely known consensus "USEtox" [167] develops characterization factors by multiplying three matrix-based factors: fate factor (FF), exposure factor (XF) and effect factor (EF), as presented in equation 2.1. A severity factor can also be added to transform impacts at midpoint levels into impacts at damage levels (endpoints) [15].

$$CF^{sk} = SF^{sk}.EF^{sk}.XF^{sk}.FF^{sk} \tag{2.1}$$

where CF_i^{sk} is the element of the CF^{sk} matrix representing the characterization factor for the impact category k and the elementary flow s emitted to a considered environmental compartment.

A fate factor represents the environmental processes and mechanisms that lead to the distribution and transformation of emitted pollutants into environmental compartments and sub-compartments [168]. It links the emissions in a compartment to the increase in mass or concentration of the emitted substance in a receiving compartment [15]. It is based on multimedia exchanges and is quantified in a square fate matrix **FF**, where columns represent

emission compartments and rows represent receiving compartments. In this **FF** matrix, diagonal elements indicate the residence time of the pollutant in the considered compartment, while off-diagonal elements represent the increase in mass after a pollutant emission. FFs are expressed in [$kg_{compartment}$ per $kg_{emitted}/day$] [167]. **FF** matrix is obtained from a square non-singular transfer rate matrix **K** [day^{-1}] that accounts for intermedia transfer and removal rates (e.g., degradation).

An exposure factor differs in definition between the impact category being assessed. For the characterization of ecological impacts, XF denotes the bioavailability of pollutants emitted to the exposed ecosystem [169]. Since the current thesis focuses on the impacts of MPs on marine ecosystems, only ecotoxicity will be addressed in the CF construction approach.

An effect factor EF quantifies the adverse effects resulting from exposure to pollutants emitted through different exposure pathways. An **EF** matrix presents the receiving compartments in its columns and the resulting effects in its rows, such as freshwater ecotoxicity for ecotoxicological impacts [169]. EFs are expressed in $PAF.m^3/kg$ for ecotoxicology (PAF stands here for the "Potentially Affected Fraction of species" in each m^3).

As a result of multiplying the factors mentioned above, the characterization factor would have units of $PAF.m^3.day/kg_{emitted}$ for ecotoxicology [169], which is equivalent to the Comparative Toxic Unit [$CTU_e/kg_{emitted}$] of USEtox in the midpoint impact category "freshwater ecotoxicity" [167]. This $PAF.m^3.day$ unit allows to consider that the impact increases when the fraction of species affected in each m^3 increases, when the volume increases, or when the duration of the impact increases. Using a severity factor [170], midpoint CFs can be transformed into endpoint (damage) CFs expressed in $PDF.m^3.day/kg_{emitted}$ for "Ecosystem Quality" [171]. PDF stands here for the potentially disappeared fraction of species (in each m^3 each day).

In LCIA, endpoints (damage) are aggregated into an Area of Protection (AoP) of recognizable value to society [165], for example, "Ecosystem Quality". Impact categories, such as "Ecotoxicity" and "Physical effect on biota", are part of the "Ecosystem Quality" area of protection. Depending on the LCIA method, the units of CFs for "Ecosystem Quality" differ. IMPACT World+ [15] and GLAM [172] are currently two of the most updated LCIA impacts methods. Each method adopts different units that have different significance and thus are to be interpreted differently.

IMPACT World+ method

The IMPACT World+ (IW+) method adopts the units $PDF.m^2.yr$, which represent the potentially disappeared fraction of species (a local impact in each m^2) integrated over a certain surface area (m^2) and given duration (year). This means that if we increase the affected surface area or the duration of exposure, the impact increases. These units allow for the comparison of two ecosystems over a surface area for a year. They can also be seen as having as a reference unit: disappearance 100% of species over 1 m^2 during a year (1 $PDF.m^2.yr$). Thus, if we make disappearance 50% of species over 2 m^2 during a year, it is equivalent to disappearance 50% of species over 1 m^2 during 2 years. The philosophy behind these units is based on the hypothesis of protecting the ecosystem as a whole, rather than a single species. In other words, adopting these units means that having disappeared 5% of species over 1 m^2 of a tropical (rich) ecosystem is considered as important as having disappeared 5% of species over 1 m^2 of a desert (scarce) ecosystem, during a year. Therefore, $PDF.m^2.yr$ units give more intrinsic values to species that live in a scarce species ecosystem compared to a rich ecosystem. Less value is given to a species that lives in a rich ecosystem because there are relatively more species to replace it. However, in a species scarce ecosystem, there is less resilience, and each species is key to maintaining the whole ecosystem [173, 174]. For the IMPACT World+ method, the endpoint units (damage) of USEtox are converted to $PDF.m^2.year$, by dividing the endpoint units ($PDF.m^3.d$), with the depth of the water compartment [meters] and a conversion of the time unit (1 year = 365.5 days), in order to harmonize and compare the impacts with other endpoint units for the AoP ecosystem quality.

GLAM approach

GLAM is the recently developed Global Guidance on Environmental Life Cycle Impact Assessment Indicators [172]. It considers the fraction of species that has disappeared over a year in the whole ecosystem of study. Thus, it adopts the units $PDF.yr$. Following the example presented before, the disappearance 50% of the species is no longer considered relative to the surface area of the compartment, but rather the 50% of the species is considered to have disappeared from the whole ecosystem considered. For example, 1 PDF.yr is similar to having disappeared 100% of species in the whole marine ecosystem during a year. To determine the fraction of species that disappeared in the whole marine ecosystem, the total number of species in the marine ecosystem must be determined and the number of species affected identified. Hence, contrary to IW+, this approach gives the same intrinsic value to every species. This means that species that disappear in a rich environment (e.g. estuaries) have the same value as species that disappear in another less rich environment (e.g.

deep-ocean zones). This also implies that the compartment that hosts more species is given more importance than those with fewer species. In other words, adopting these units means that if 5% have disappeared from an ecosystem that hosts 100 species, it is equivalent to 0.5% of the disappeared species from an ecosystem that hosts 1000 species. For the GLAM approach, the endpoint units (damage) of USEtox are converted into $PDF.yr$, by dividing the endpoint units ($PDF.m^3.d$), with the volume of the aquatic environment [m^3] and a time unit conversion (1 year = 365.25 days). In this approach, a global extinction probability factor (GEP) is used later to account for the vulnerability to extinction of species. However, this is outside the scope of the present thesis.

Assessing microplastic emissions in the marine environment requires the development of specific characterization factors that are coherent and harmonized with existing LCIA approaches, to ensure comparable metrics.

2.7 State of art of plastics in LCA

Different initiatives have been launched to integrate plastic pollution in LCA in the LCI and LCIA phases. The Plastic Leak Project (PLP), launched in 2020 by Quantis and the environmental consulting firm EA, addressed the shortcomings of plastics in LCI by quantifying plastic leakage into the environment. They developed various inventory flows for macroplastic and microplastic emissions into ocean, freshwater, and terrestrial environments. They presented inventory flows for 1) macroplastic leakage from plastic waste, 2) microplastic leakage from textiles, 3) microplastic leakage from tire abrasion during transport, and 4) microplastic leakage from plastic production [175]. Additional flows followed later, for five types of micro- and macroplastic losses into the ocean from lost fishing gears (macroplastics), marine coatings (MPs), plastic pellets during plastic production (MPs), tire abrasion (MPs) and plastic mismanaged at the end of life (macroplastics). PLP is now expanded into the Plastic Footprint Network (PFN) (`https://www.plasticfootprint.earth/`) which takes a broader approach, evaluating the overall impact on the life cycle of plastic usage. Following the PLP guidelines and flows, PFN added flows for macroplastic leakage from packaging and macroplastic leakage from textiles [176].

To address the LCIA gaps, different independent approaches emerged. Saling et al. (2020) [177] developed fate and characterization models for microplastic emissions in the marine environment. Their characterization factors are expressed in Marine Microplastic Potential (MMP) at the midpoint level. The MMP is obtained as a function of a fragmentation rate, time factor, and effect factor. In their fate model, the marine environment was considered as a single compartment and only fragmentation and degradation were estimated. The dis-

tribution of MPs based on various fate mechanisms that are faster than slow weathering mechanisms was not taken into consideration. Fragmentation and degradation rates are surface specific and therefore depend on the surface area of particles that varies with their shape and size (section 2.3) [18,19]. However, in their model, all MPs are considered spherical with a fixed diameter of 100 µm. Thus, differences linked to the physical properties of the particles were not addressed, which does not accurately represent all MPs found in the marine environment. The effect factors were quantified using effect concentrations (EC50) and lethal concentrations (LC50). Their EFs are dimensionless ratios as they represent the relative toxicity of MPs compared to a reference type (microbeads) [177]. Their model can be used to have an estimate of MP toxicity in the marine environment at the midpoint level. However, since their units are not harmonized with existing LCIA methods for ecotoxicity [165], they are not comparable to other impact categories at the endpoint (damage) and AoP levels. In a more recent approach, the impacts of MP emissions in various environmental compartments, i.e., river sediments, soil, marine water, and marine sediments, were quantified [178]. Similarly to Saling et al. (2020) [177], they ignored the differences related to the shape and size of the particles. They also accounted for degradation to estimate the persistence of MPs in the compartments. The distribution of MPs between marine water and sediments was mainly linked to the density of the particles. This means that if a particle is less dense than seawater, it will linger in the water and never reach the sediments, while high density particles immediately reach the sediments. This assumption contradicts observations in the literature where positively buoyant MPs are detected in deep ocean sediments due to biofouling, aggregation, etc. (sections 2.2.2 and 2.2.2). Therefore, their FFs do not adequately address the fate mechanisms and influencing parameters responsible for the redistribution of MPs within the marine environment. In their study, FFs are expressed in kilograms of plastic pollution equivalent per kilograms of plastic emitted [$kg_{PPe}/kg_{emitted}$] [178]. Their units are not harmonized with adopted FF units for ecotoxicity. Therefore, they do not allow for the comparison of MP impacts with other impact indicators.

In parallel to these individual attempts, an international working group "Marine Impacts in LCIA" (MarILCA) was founded in 2019 under the support of FSLCI and the Life Cycle Initiative [17]. The main objective of MarILCA is to develop CFs for marine litter for LCIA, with a specific focus on plastics. Within the framework of MarILCA, a new impact category was added to address the "Physical effect on biota" of plastic litter [24]. A first effect factor was proposed for the entanglement of plastic waste on marine ecosystems [4]. This EF was further extended to address the spatial distribution of plastic debris and species habitats where entanglement incidents have been observed [179]. Developed EFs, coupled with the geographical ranges of marine species, were then combined with a fate model that

predicts the spatial distribution of plastic debris after release from fishing activities. As a result, spatially explicit CFs are obtained to quantify the impacts of entanglement on marine species (mammals, birds, and reptiles) [180]. In addition to the physical impacts of plastics through entanglement, an EF was developed to account for the ecotoxicity of plastic additives [164] to include 17 more chemicals than already existing EFs [181]. In order to address the physical impacts of MPs on marine ecosystems, an effect factor was initially developed based on HC50EC50: hazardous concentration derived from the geometric mean of EC50 (effect concentration affecting 50 % of species) [20]. A simplified fate model was then developed and used with these EFs, to develop CFs for MP physical impacts on biota. The simplified fate model considered the marine environment as a single compartment and developed degradation rates based on the physical properties of MPs (size, density, and shape). In addition, three different degradation rates (slow, medium, fast) were developed for each MP, which is an improvement to previously developed fate models [177, 178]. Moreover, the fate model addressed the removal of positively buoyant MPs from water to sediments based on estimates of sedimentation rates of various tested MPs [18]. Additional CFs were then quantified for more polymers with updated effect factors developed based on HC20EC10: hazardous concentration derived as the geometric mean of EC10 (effect concentration affecting 10 % of species) for MP emissions in the marine and freshwater environment [19]. A more recent study addressed impacts of MPs in sediments and introduced the Species Distribution Fraction (SDF) matrix. SDFs represent the percentage of species that live or feed in an environment. They are used to aggregate impacts (CFs) across marine sub-compartments in order to scale them to the level of impacts on the overall marine ecosystem [21]. Despite the enhancements made in the fate model, none of the aforementioned studies considered the distribution of MPs in marine sub-compartments: water surface, water column, sediments and the global scale. Sedimentation rates were only developed as a removal rate from the water [18, 19, 177]. Sediments, where most of MPs eventually accumulate [182] were not considered as a separate sub-compartment [18, 19, 177]. In addition, existing LCIA fate models are still lacking fate mechanisms, environmental parameters, and oceanographic conditions that influence the transport of MPs in the marine environment. Moreover, while the physical properties of MPs were addressed in the degradation rates of Corella-Puertas et al. (2022) and (2023) [18, 19], they haven't been addressed with the fate mechanisms that depend on the size, shape, and density of MPs (such as biofouling). This explains the high uncertainty observed in the FFs and CFs developed in the simplified models [18, 19]. Furthermore, the beach, where a large quantity of MPs eventually accumulate [27, 183] was never addressed in the existing models. Thus, the distribution of MPs quantified in these models might overestimate or underestimate the presence of MPs, which leads to an imprecise estimation

of MP impacts. Therefore, in order to reduce the uncertainty linked to unconsidered fate mechanisms, a more refined fate model is needed where different marine sub-compartments and associated fate mechanisms are considered. As previously explained in this chapter, fate mechanisms, oceanographic parameters and the physical properties of MPs interact with each other within the marine environment. For instance, the interaction between the biofouling celerity and MP size, the turbulence and MP size, the settling/rising velocity with MP size, density and shape, etc. The importance of these interactions when modeling the fate and characterization factors of MPs has never been assessed. Similarly, water currents and fate mechanisms responsible for the redistribution of MPs in the marine environment vary spatially. However, no study so far has evaluated the importance of regionalization compared to the physical properties of microplastics, especially in the context of LCIA. Therefore, it is essential to address the spatial variability of MP impacts, along with their physical properties, by regionalizing the fate and CF model, which was never tackled in the existing models.

CHAPTER 3 REASEARCH HYPOTHESIS AND OBJECTIVES

3.1 Research hypothesis

Based on current understanding and need identified in the literature review, the following research hypothesis is developed: The variability of fate and characterization factors due to regionalization is important relative to the variability due to the physical properties of emitted microplastics.

To validate this hypothesis, two criteria have to be analyzed. First, the order of magnitude of spatial variability has to be of the same order of magnitude or higher than that of the variability related to the physical properties of MPs. Second, the rank of MP impacts between regions of emissions should have a low rank correlation (less than 0.9 - 0.9 correlation factor being interpreted to represent a very strong correlation [184]). If at least one of these two identified criteria is observed in the results, this thesis hypothesis is considered validated.

3.2 Thesis objectives

The main objective of this thesis is to "regionalize the fate and characterization factors (CFs) of microplastic emissions in the marine environment, to assess the impact of spatial variability on CFs compared to the variability driven by the physical properties of microplastics".

In order to achieve this objective, the following sub-objectives are defined:

1. *Develop a comprehensive refined framework for the development of fate and characterization factors for microplastic emissions in the marine environment.* This is important to understand what fate mechanisms and parameters are important to consider for the regionalization of FFs and CFs.

2. *Identify influencing parameters on microplastic transfer rates in the marine environment and the influence of transfer rates on fate and characterization factors.* This is important to assess whether the identified influencing parameters are related to regionalization or only MP physical properties. This step highlights where efforts should be made to operationalize the fate and characterization framework proposed in the first sub-objective.

3. *Regionalize the FFs and CFs to assess the importance of spatial variability compared to the variability linked to the physical properties of emitted MPs.* This step is important

to validate or invalidate the thesis hypothesis.

This project takes part of MarILCA's framework [4]. The achievement of the objectives of this thesis contributes significantly to key areas within this framework, as highlighted in figure 3.1.

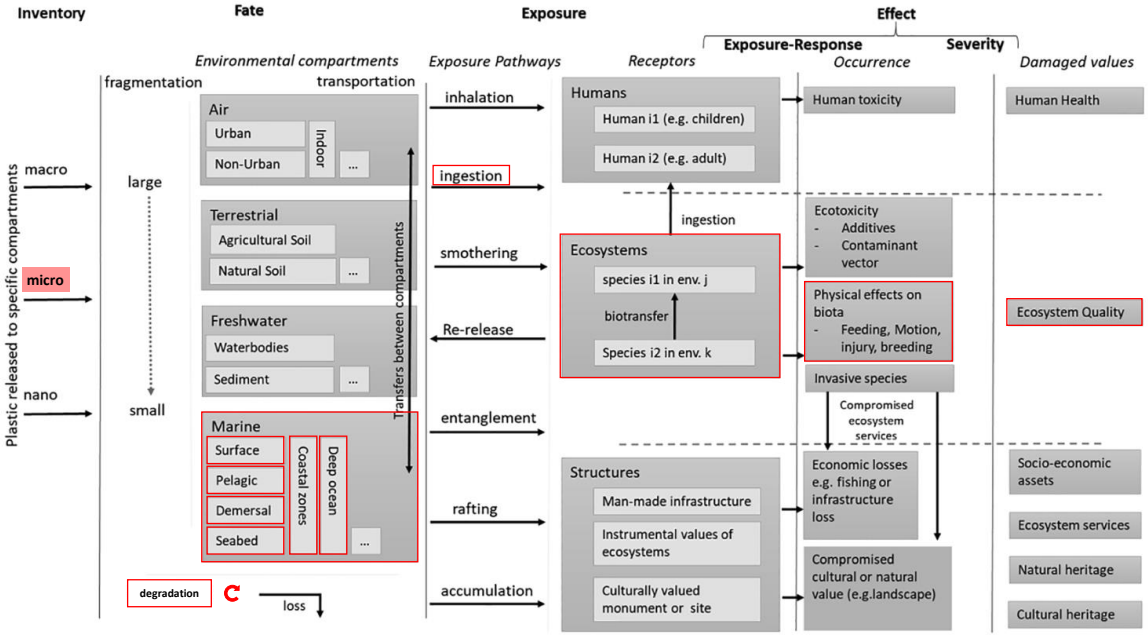

Figure 3.1 MarILCA's LCIA framework summarizing the impact pathways of plastics in the environment. Boxes outlined in red represent the relevant areas addressed in this thesis. Adapted from source: [4]

3.3 Overview of thesis structure

The following sections of this thesis are structured around answering each of the identified sub-objectives mentioned before, as summarized in figure 3.2. A general methodology, which briefly introduces and links the methodologies of the three sub-objectives, is presented in chapter 4. Chapter 5 will later detail the methodology for answering the third sub-objective. Answering the first two sub-objectives led to two scientific articles. Thus, in order to avoid redundancy, the methodologies of the first and second scientific articles will be presented, along with their results and discussions, as published in the articles (chapters 6 and 7). The results of the third sub-objective will be presented later in chapter 8.

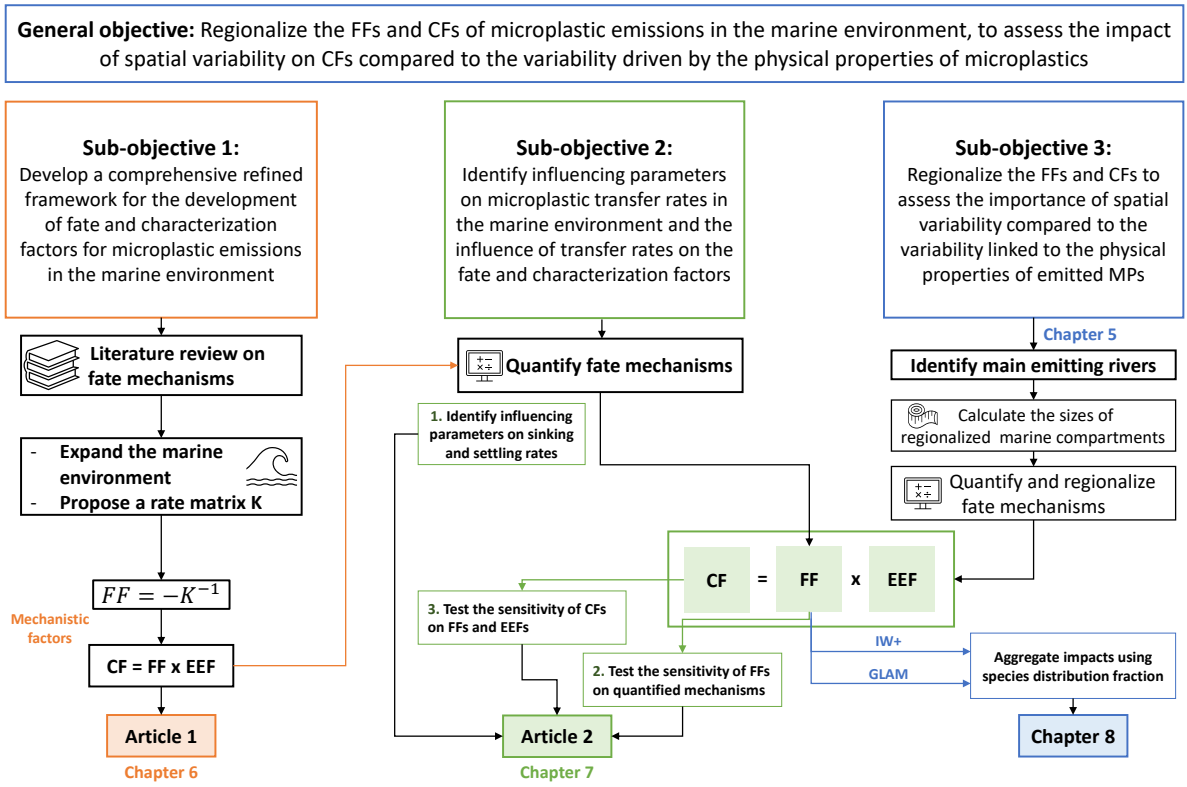

Figure 3.2 Overview of the general methodology that led to the achievement of each sub-objective defined in this thesis

CHAPTER 4 OVERVIEW OF THE GENERAL METHODOLOGY

This section presents the general methodology developed to achieve the sub-objectives of this thesis, as summarized in figure 3.2.

4.1 Develop a comprehensive refined framework for the development of FFs and CFs for MP emissions in the marine environment

This first sub-objective corresponds to the first part of the general methodology (figure 3.2). A framework is needed to propose mechanistic fate and characterization factors for MarILCA's impact category "Physical effects on biota" (figure 3.1). In order to have units comparable and coherent to the already existing LCIA emission-based CFs for (eco)toxicity, a matrix approach similar to that of the USEtox consensus model [167] is adopted. Several steps are followed to propose the framework for fate and characterization matrices.

A comprehensive knowledge of the fate of MPs in the marine environment is essential. Thus, in a first step, a literature review is conducted to identify all the fate mechanisms and envi-ronmental parameters that are responsible for the transport of MPs emitted in the marine environment. Based on this literature review, a fate framework is proposed that expands the marine environment into multiple well-defined sub-compartments connected via identi-fied fate mechanisms. The fate framework is represented in a square fate matrix **FF** [day] that has emission sub-compartments on its columns and receiving sub-compartments on its rows. Fate factors FFs presented on the diagonal represent the residence time of MPs in the corresponding sub-compartment. Off-diagonal FFs relate MP emissions to their mass in-crease in a receiving sub-compartment. **FF** is obtained from the inversion of a non-singular square matrix **K** $[day^{-1}]$ that has the same structure as **FF**. Elements on the diagonal of **K** represent the total removal rate from the corresponding sub-compartment, while off-diagonal elements connect identified sub-compartments through fate mechanisms of transport.

In a second step, mechanistic characterization factors are obtained through matrix calculation of **FF** with exposure-effect factors (EEFs) [185]. CFs are presented in a matrix that has emission compartments in its columns and impacts on exposed ecosystems on its rows, herein physical effects on biota.

4.1.1 Identify influencing parameters on microplastic transfer rates in the marine environment and the influence of transfer rates on the FFs and CFs

This second sub-objective corresponds to the second part of the general methodology (figure 3.2). In order to operationalize the framework proposed in the first sub-objective, it is important to assess the significance of various parameters on FFs and CFs. This step is essential to understand whether most influencing parameters are mainly linked to the physical properties of MPs and/or to the spatial variability of certain fate mechanisms. The second sub-objective is a key step that highlights where efforts should be directed for the development of FFs and CFs for MP emissions in the marine environment. To accomplish this, several steps are followed to quantify all identified fate mechanisms in the first sub-objective. Some of these mechanisms are quantified based on literature data while others are modeled using numerical modeling. The tracking model 'TrackMPD' [12] is used because it allows for the evaluation of various spatially variable mechanisms (such as advection, turbulence, biofouling, etc.) along with the physical properties of MP (size, density, shape). TrackMPD model is chosen instead of Plasticparcels, described in section 2.4, because it was the most complete and suitable model to achieve this objective of the thesis at the time. The steps followed are summarized below:

In a first step, water current data are extracted for the North-East of the US. These data only serve as a case study to allow testing of the parameters by running simulations using TrackMPD. A sensitivity analysis is performed where six parameters (size, density, shape, biofouling rate, vertical dispersion, and horizontal dispersion) are varied between their minimum and maximum values. Based on the "least-square model", the magnitude of influence of each parameter on the sedimentation time is presented in a "Pareto plot".

In a second step, the transfer from the water surface to the water column (sinking rate) and the transfer from the water column to the sediments (sedimentation rate) are quantified using TrackMPD. Resuspension, burial, degradation, and resurfacing rates are quantified based on literature data. Consequently, the rate and fate matrices are quantified. In order to understand the influence of quantified rates on the FFs, a sensitivity analysis is conducted in which a 10% increase is systematically added to each quantified rate.

In a third step, the characterization factors are calculated using developed FFs and already existing exposure-effect factors EEFs [18–20]. A sensitivity analysis is also performed where a 10% increase is systematically added to the quantified rates and the EEF used. These sensitivity analyzes help to provide recommendations for improving the modeling of fate and characterization factors. Understanding the variability and sensitivity of parameters tested serves as a guide to propose ways to categorize microplastic FFs and CFs based on their

physical properties (size, density, and shape). It also gives an indication for the need to regionalize fate and, subsequently, characterization factors.

4.1.2 Regionalize FFs and CFs to quantify their spatial variability, and assess its importance with regards to the variability linked to the physical properties of emitted MPs

This third sub-objective corresponds to the third part of the general methodology (figure 3.2). In order to accomplish this sub-objective, several steps are followed:

In a first step, the main emission points are identified based on the export of MPs from rivers to the ocean. Water currents for each region are later extracted for each emission region. Seven regions are considered that represent 92% of MP emission from rivers to oceans [1].

In a second step, TrackMPD is used to model the transport of MPs in each emission region. Consequently, transfer rates between marine sub-compartments (for instance, beaching rate, sinking rate, etc.) are quantified. Using these rates along with other rates quantified from literature data (for instance, resuspension rate, degradation rate, etc.), **K** and **FF** matrices are quantified.

In a third step, developed **FF**s are used with exposure-effect factors and species distribution fractions (SDFs) to calculate **CF** matrices for nine polymers (EPS, PP, LDPE, HDPE, PS, PET, PLA, PVC, TRWP), of two shapes (sphere, fiber) and five size classes (1, 10, 100, 1000, 5000 μm), for two LCIA approaches (IMPACT World+ and GLAM). Consequently, the variability of CFs linked to regionalization is compared to that linked to the physical properties of MPs for the two approaches. This analysis allows to answer the main objective of this article and provide regionalized CFs for MP emissions in the marine environment, for MarILCA's impact category "Physical effects on biota", and the area of protection (AoP) "Ecosystem Quality" of two LCIA methods. The detailed methodology of this sub-objective is further explained and detailed in the following chapter.

CHAPTER 5 METHODOLOGY FOR THE THIRD SUB-OBJECTIVE: REGIONALIZE FF AND CF TO ASSESS THE IMPORTANCE OF SPATIAL VARIABILITY COMPARED TO THE VARIABILITY LINKED TO THE PHYSICAL PROPERTIES OF EMITTED MP

Regionalized characterization factors are developed using two approaches for two LCIA methods: IMPACT World+ (IW+) approach and GLAM approach (section 5.1). In order to understand the influence of regionalization on CFs, the first step is to regionalize the fate model. Initially, the main microplastic emissions sites are identified (section 5.2). Site-specific continental and global marine sub-compartments are then built (section 5.3). Spatially variable mechanisms are quantified in different regions (section 5.4), for which regionalized rate **K** and fate **FF** matrices are developed (section 5.5). Seasonality is also assessed to understand its influence on regionalized FFs and CFs (section 5.5). The quantification of fate mechanisms extends over the methodology followed to accomplish the second sub-objective, detailed in chapter 7, to account for the regionalization. For this reason, some similarities might be found between both methodologies. Using exposure-effect factors (section 5.6) and species distribution fractions (section 5.7), site-specific CFs are developed, then aggregated into continent and global CFs (section 5.8). More details on this chapter can be found in Appendix C or in the **Supplementary Information**.

5.1 Characterization Factors CFs

Characterization factors CFs, for MP emissions in every marine sub-compartment, are obtained by multiplying **FFs** [$kg_{compartment}$ per $kg_{emitted}/d$] with **EEFs** [$PAF.m^3/kg_{compartment}$], according to the matrix-structure equation [185]:

$$CF = FF \times EEF \tag{5.1}$$

The CF matrix is a square matrix in which emission compartments are represented on the columns and receiving ones on the rows (equation C.1). These CFs are referred to as "partial" CFs as they represent impacts on a specific ecosystem in a receiving sub-compartment (e.g., water surface) and not on the overall marine ecosystem. They are expressed in $PAF.m_i^3.d$ that describe the potentially affected fraction of species (PAF) in the volume of the considered marine sub-compartment i. A severity factor SF is used to convert the potentially affected fraction of species (PAF) into the potentially disappeared fraction of species (PDF). The

severity factor is equal to 1 according to the latest recommendations for ecotoxicity [186]. In addition, using a time conversion factor (1 year = 365.25 days), $PAF.m_i^3.d$ is converted to $PDF.m_i^3.yr$. In order to generate CFs at the level of the whole marine ecosystem, two approaches can be used as explained below:

5.1.1 The IMPACT World+ approach

As described in section 2.6.2, the IMPACT World+ (IW+) approach [15] considers the potentially disappeared fraction of species (PDF) over a surface area m^2 over a duration ($PDF.m^2.yr$). Thus, the damage to the ecosystem increases when a) the fraction of affected species increases; b) the affected surface increases; c) the duration of the impacts increases. As previously presented, the underlying assumption behind the choice of this $PDF.m^2.yr$ approach is that all ecosystems have the same value, no matter the density of species. Hence, CFs [$PDF.m^2.yr$] for this approach are obtained by dividing each row of sub-compartment specific CFs [$PDF.m_i^3.yr$] (partial CFs) by the volume (V_i [m^3]) of its corresponding sub-compartment i to obtain the fraction of potentially disappeared species in the overall sub-compartment (in $PDF.yr$, but the PDF here is no longer applied to a m_i^3, but to the overall sub-compartment "box"). Overlapping sub-compartments within a considered scale (for instance, water surface, water column, and sediments of the continental scale) (figure 5.1) are aggregated using their relative species distribution fraction (SDF) between different sub-compartments, relative to the continental scale box, as a weighting factor. This allows to obtain the fraction of potentially disappeared species in the whole continental scale "box" (in $PDF.yr$, with the PDF being applied here to the continental box). Since all ecosystems have the same value, SDF has an influence in overlapping sub-compartments within a considered scale (in this case, the sub-compartments of the continental scale). More details about the species distribution fraction are provided in section 5.7. The resulting CFs are then multiplied by the surface area of each scale (beach, continental, and global) to convert $PDF.yr$ to $PDF.m^2.yr$. Therefore, in this approach, the depth of the compartments plays a role in increasing or reducing the impacts (mathematically dividing by the volume, then multiplying by the surface area is equivalent to dividing by the depth). A bigger depth can "dilute" the impacts in a certain sub-compartment.

5.1.2 The GLAM approach

As described in section 2.6.2, the GLAM approach, used in the recently developed Global Guidance on Environmental Life Cycle Impact Assessment Indicators GLAM [172], considers the disappeared fraction of species over a year in the entire ecosystem of study, herein

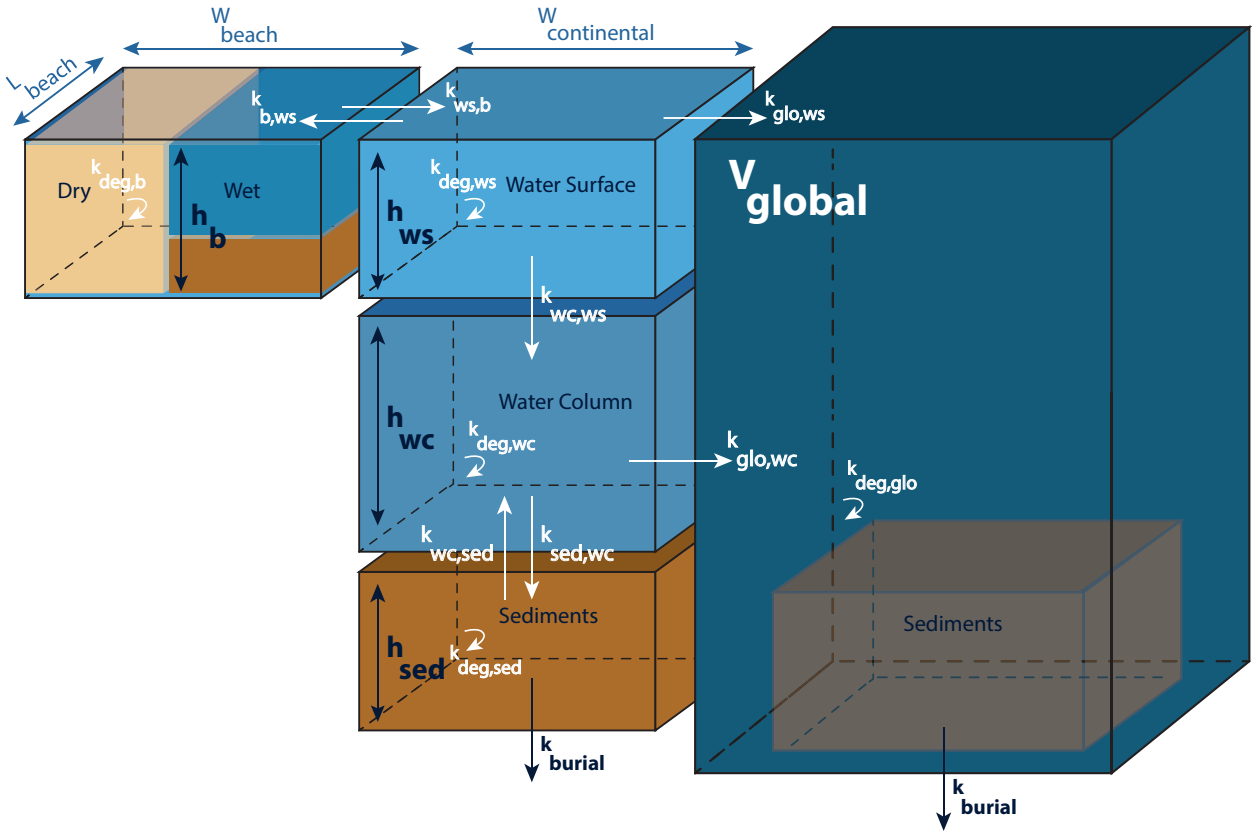

Figure 5.1 Marine sub-compartments as considered in the third sub-objective, connected through different transfer rates. Sediments in the global scale are not considered as a separate compartment. L: length, W: width, h: height, b:beach, ws: water surface, wc: water column, sed: sediments, deg: degradation. $k_{j,i}$ represents the transfer rate from compartment i to j.

the marine ecosystem [$PDF.yr$]. As explained previously, in this approach, species that disappear in a rich environment have the same intrinsic value as species that disappear in another environment with lower species richness. CFs for the GLAM approach are therefore obtained by dividing the sub-compartment specific CF matrix (partial CFs) ($PDF.m^3.yr$) by the volume of each sub-compartment (similarly to what is done in the IW+ approach), to transform impacts into $PDF.yr$ in each sub-compartment ($PDF.yr$ where PDF represents the potentially disappeared fraction of species in the sub-compartment box). Hence, dividing by a larger compartment leads to a smaller $PDF.yr$. The resulting CFs [$PDF.yr$] are then aggregated using the species distribution fraction, for each sub-compartment (overlapped or not), relative to the overall marine ecosystem. Hence, a compartment with a lower species density has a smaller contribution to the overall impact. Therefore, in this approach, the size of the sub-compartment and the species distribution fraction are very influencing. More details about the species distribution fraction are provided in section 5.7.

In order to regionalize the CFs for the two approaches, the regionalization of fate factors is initially accomplished according to the following steps.

5.2 Main emission sites of MPs in the marine environment

Since rivers are the main source of MPs in the marine environment, the model of Schmidt et al. (2017) [1], which allows assessing the emissions of all rivers around the globe, is used to determine the regions with the highest MP transfers from rivers to the ocean. In this study, they collect plastic debris data in rivers and estimate the amount of mismanaged plastic waste generation to estimate the export load of plastics from rivers to coastal seas. The results of their Model 1 are used since they are based on microplastic data without taking into account macroplastic emissions. Table 5.1 presents the results of 12 rivers that release MPs to seas in various regions. Other rivers that released less than 1% MPs are not considered. Due to data and time availability, the following sites of emissions are prioritized: East China Sea, Arabian Sea (Indus), Yellow Sea, Mediterranean Sea, Bay of Bengal, Okhotsk Sea, Gulf of Guinea and Banana Point (Congo), where 92% of the total MP emissions from rivers to sea take place.

5.3 Marine compartments at continental and global scales

The marine environment is divided into several compartments and sub-compartments, as presented in figure 5.1. The size of each marine compartment and sub-compartment is defined depending on the specification of each emission region. The length of the beach is taken as the distance of the extracted domain (see section 5.4.1). The depth of the beach is taken as the depth of the intertidal region [187], which is exposed at low tides and submerged at high tides [188]. Coasts are classified as microtidal when the mean spring tide range is less than 2 meters, mesotidal between 2 and 4 meters, macrotidal between 4 and 6 meters, and megatidal when it is greater than 6 meters [188]. The beach depth of every emission region is taken according to the classification and specification of [188]. The width of the beach is taken as 100 meters, which is the width most observed for open coast beaches [189]. Continental and global scales are defined based on the topography of marine sediments and the abundance of marine ecosystems. The continental scale is taken as the continental shelf where a higher species richness is observed [190–192] due to the availability of primary conditions needed for metabolisms and reproduction [193]. It is defined at an average depth of 200 meters [193, 194], where most types of habitat are present due to light availability and high temperature [194]. The width of the continental shelf (horizontal dis-

Table 5.1 Main rivers emitting MPs in various receiving seas. Taken from Schmidt et al. (2017) [1]

River	Receiving Sea	Continent	MP load [tons/year]	Percentage of emission
Yangtze river	East China Sea	Asia	1.47E+06	64%
Indus	Arabian Sea	Asia	1.64E+05	7%
Huang He (Yellow river)	Yellow Sea	Asia	1.24E+05	5%
Hai He	Yellow Sea	Asia	9.19E+04	4%
Nile	Mediterranean	Africa	8.48E+04	4%
Meghna, Bramaputra, Ganges	Bay of Bengal	Asia	7.28E+04	3%
Zhujiang (Pearl River)	South China Sea	Asia	5.3E+04	2%
Amur	Sea of Okhotsk	Asia	3.83E+04	2%
Niger	Gulf of Guinea	Africa	3.52E+04	2%
Mekong	South China Sea	Asia	3.34E+04	1%
Shatt el Arab/Karun	Persian Gulf	Asia	2.33E+04	1%
Congo	Atlantic (Banana Point)	Africa	1.34E+04	1%

tance from the coast) exhibits a high variability depending on geographical locations [193]. In order to determine the width of regionalized continental sub-compartments, the topography of each chosen site is analyzed to determine where the water depth becomes more than 200 meters. The bathymetry file used is downloaded from the Copernicus Marine Environment Monitoring Service (CMEMS, `http://marine.copernicus.eu/`). The product name is "GLOMFC_024_mask_bathy". A median distance is calculated using Vincenty's algorithm [195] to represent the width of each regionalized continental scale sub-compartment. The median depth of defined continental regions is then taken to represent the depths of continental water for each region. Depths of regionalized water surface sub-compartments are determined based on the dissolved color organic matter (CDOM) responsible for the absorption of UV lights in the oceans [196]. Regionalized water surface depths are defined at the depths below which photooxidation is reduced because of UV light attenuation. They are determined from the measurements of [196]. Accordingly, depths of regionalized water column sub-compartments are obtained as the difference between the depth of continental water and that of the corresponding water surface. The volume of the global scale is calculated using the global surface area estimated in the scientific consensus model for (eco)toxicity USEtox [167] and the global water depth ($Depth_{global}$ = 3.68 km [197]).

5.4 Quantification of fate mechanisms

The transfer between various marine sub-compartments includes the quantification of several fate mechanisms (summarized in figure 5.1), which are the intermedia transfer rates (section 5.4.1) and the removal rates (sections 5.4.1 and 5.4.2). All these rates are quantified based on various models and data from the literature, as presented in the following sections and

summarized in figure 5.2.

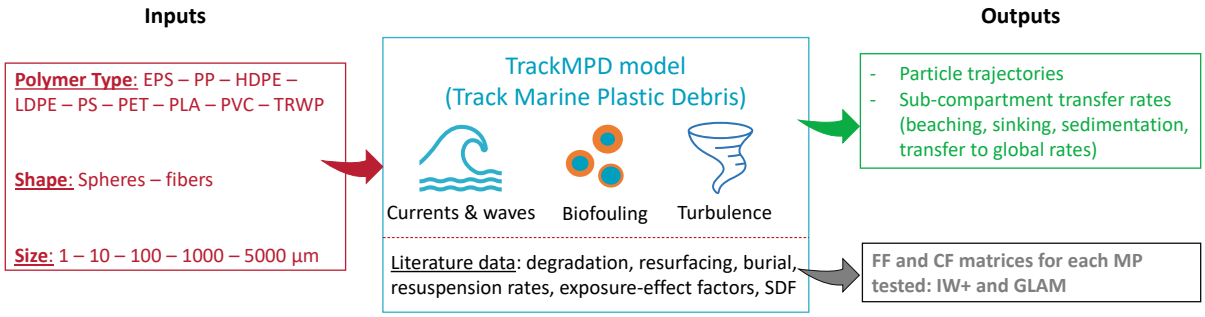

Figure 5.2 The methodology followed for the production of regionalized FFs and CFs for IW+ and GLAM approaches for all MPs tested

5.4.1 Intermedia transfer rates

Beaching, sinking, sedimentation, and transfer to the global scale

Beaching, sinking, sedimentation rates, as well as transfer rates from the continental to the global scale depend on several oceanographic properties, i.e., water currents, which vary spatially. In order to account for the variability of these parameters, the TrackMPD v.2.3 model [12] is used. TrackMPD model tracks the three-dimensional movement of emitted microplastics, using three-dimensional water currents. Microplastics are emitted in defined sites n (section 5.2). The parametrization of TrackMPD model can be found in section 5.4.1. The time of transfer calculated during the simulations is recorded and then used to calculate the transfer rates. Beaching (from the water surface to the beach), sinking (from the water surface to the water column) rates, as well as transfer rates to the global scale, are calculated according to the following equation:

$$k_{j,i}^{n} = \frac{1}{t_{j,i}^{n}} \tag{5.2}$$

where $k_{j,i}$ and $t_{j,i}$ are the transfer rate $[day^{-1}]$ and time [day] (from TrackMPD) from the emission sub-compartment i to the receiving sub-compartment j for the emission site n.

The transfer from the water surface sub-compartment to the beach ($k_{b,ws}$) is defined when the particles reach the coast, and thus their final fate is "beached". The transfer from the water surface to the water column sub-compartment ($k_{wc,ws}$) is determined when the particles emitted at the water surface cross the depth of the water surface sub-compartment, as defined

in section 5.3. Transfers from the water surface ($k_{glo,ws}$) and the water column ($k_{glo,wc}$) to the global scale are determined when the particles horizontally cross the width of the continental scale, as defined in section 5.3. Since TrackMPD uses real marine topography, emitted particles reach the sediments at different depths. Therefore, the rate of transfer from the water column to the sediments ($k_{sed,wc}$) is determined using a scaling ratio, as seen in equation 5.3:

$$k^n_{sed,wc} = \frac{D_{real}}{D^n_{wc}} . \frac{1}{t^n_{sed,wc}} \tag{5.3}$$

where $k^n_{sed,wc}$ and $t^n_{sed,wc}$ are the transfer rate [day^{-1}] and the transfer time [day] (from TrackMPD) from the water column to the sediment sub-compartments. D_{real} [m] is the real depth at which the particles reach the sediments and $D_{wc.C^n}$ is the depth of the water column sub-compartment, as defined in section 5.3, for the emission site n.

Parametrization of TrackMPD

TrackMPD v.2.3 [198] is used to simulate three-dimensional transport of microplastics in the marine environment. This particle-tracking Lagrangian model advects particles using hydrodynamic data and the 4th-order Runge-Kutta method, incorporating processes such as horizontal diffusion and vertical mixing (via a random walk approach), settling, buoyancy, and resuspension, all as functions of particle physical properties including density, size, shape, and biofilm coverage. Additionally, the model accounts for beaching and refloating phenomena. Readers can refer to Jalón-Rojas et al. (2019) [12] for a full description of the model.

Daily hydrodynamic data are extracted from Copernicus Database Global Ocean Physics Reanalysis [199]. These data have a horizontal resolution of $1/12^o$ and 50 depth levels, and a temporal resolution of 24 hours. The data include three-dimensional water velocity fields. In each emission site (section 5.2), 250 particles are emitted in five different locations (50 particles/location) (figure 5.3, tables C.1 and C.2). A sensitivity analysis showed consistent transport trends with higher particle numbers (refer to section C.1.2 for details). Particles are randomly emitted the 1st of January 2016 in order to ensure sufficient simulation time and data availability. In order to address the influence of seasonality, particles are emitted the 1st of July 2016, after the variation in ocean currents due to seasonal monsoons. Simulations of seasonality are only done for spherical 5000 μm EPS and fibrous 1000 μm HDPE particles in every emission site, because these particles provided a high spatial variability based on preliminary results.

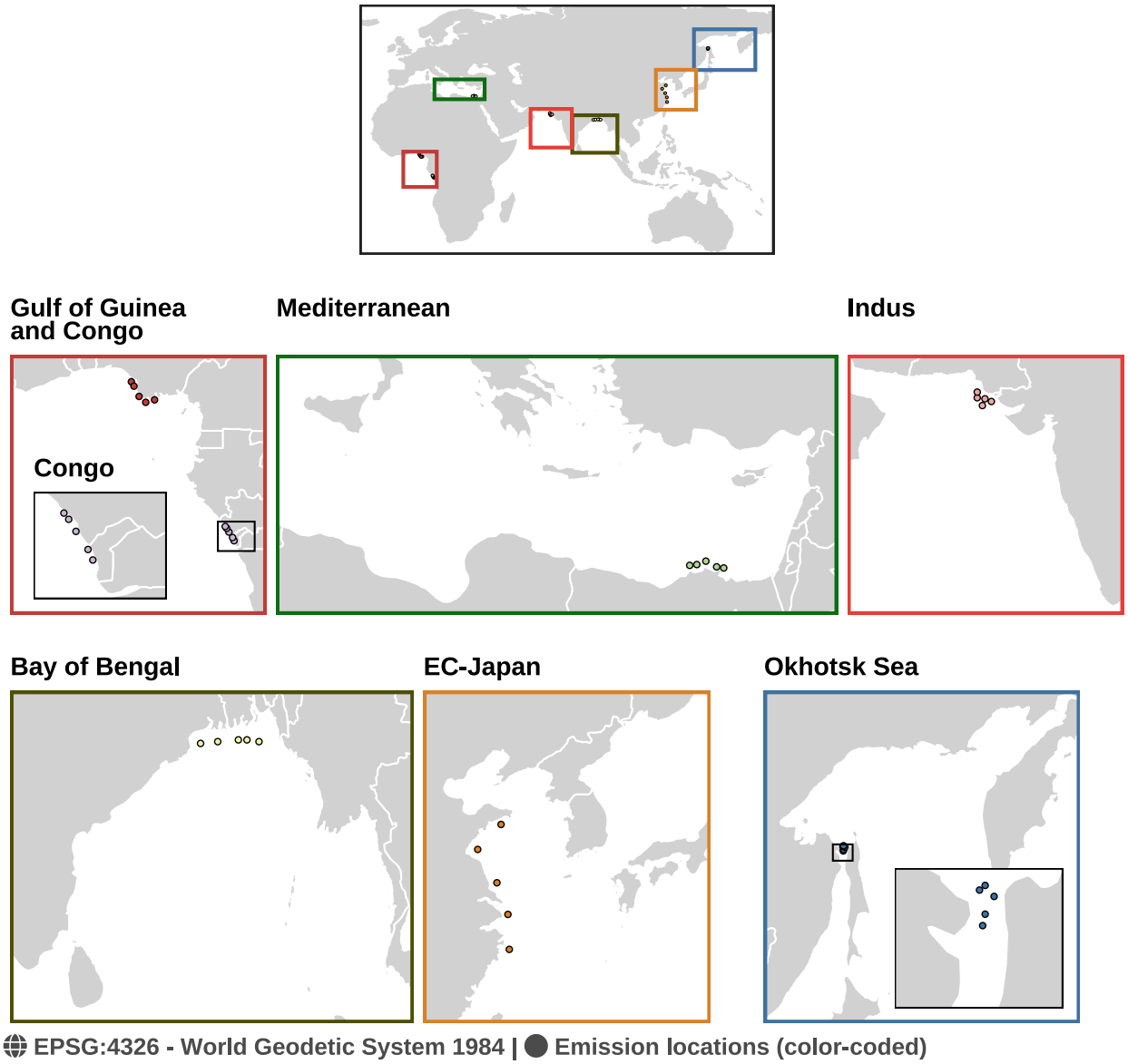

Figure 5.3 Microplastic emission locations in every emission site, presented in table 5.1. EC-Japan refers here to emissions in East China Sea

Simulations are run on the Narval distributed memory cluster of the "Digital Research Alliance of Canada". During simulations, the internal time step is taken as 1 hour. For high density particles (i.e. polystyrene) that settle within minutes, the internal time step is taken as 1 minute to be able to capture the sedimentation time. The duration of the simulations is defined as 910 days to allow the particles to reach their final fate, i.e., when particles are either beached, settled, and/or transported to the global scale. Horizontal and vertical dispersion coefficients are added in TrackMPD to account for turbulence effects that were not accounted for in the water current data from the hydrodynamic model (i.e., Langmuir circulation [12, 200]). The horizontal dispersion is thus calculated based on the following equation [201, 202]:

$$k_h = k_0.(\frac{l}{l_0})^{(4/3)} \tag{5.4}$$

where k_h is the horizontal dispersion $[m^2/s]$, k_0 the reference diffusivity $k_0 = 1\ m^2/s$ [201,202], l the local grid resolution ($1/12^o$, or approximately 8 km for the data used) and l_0 the reference length scale $l_0 = 1$ km. This equation gives a horizontal dispersion of 16 m^2/s adopted for all simulations in all geographical sites. The globally averaged value of the vertical dispersion $k_v = 1 \times 10^{-4}\ m^2/s$ [203] is adopted for simulations in all geographical sites as well.

The settling velocity of microplastic particles tested depends on their physical properties, summarized in table C.5. Since high density large particles settle rapidly after being released to the water, one polymer (polystyrene, $\rho = 1.06 g/cm^3$) is tested using TrackMPD. The settling and sinking velocities obtained represent all high density polymers (1.06-1.2 g/cm^3). In TrackMPD, the settling velocity is calculated using the formulation of Waldschlager et al. (2019) [92], for spherical and cylindrical particles larger than 100 micrometers, as this formulation demonstrated its good performance for large microplastics [58, 92, 204]. Since adequate formulations are still lacking to calculate the settling velocities of small particles, it is assumed that their settling velocities are similar to those of sediments [12]. Therefore, the formulation of Zhiyao et al. (2008) [205] is used for spherical particles and Khatmullina et al. 2017 [206] for cylindrical particles, as recommended in TrackMPD v.1 [12]. Details about the three formulations, as well as their parameters, are provided in section C.1.2.

Biofouling density is taken as 1.24 g/cm^3, which is the average of values found in the literature (table C.8). The biofouling rate applied in the simulations is 3.07E-06 m/d, calculated based on the weight increase of biofouled MPs [67]. Biofouling rates can be implemented in TrackMPD as a function of increase in the settling velocity or density. However, little to no experiments have quantified the change in these parameters due to biofouling. The study of

Karkanorachaki et al. (2021) [67] tested the influence of biofouling on specific types of MPs (only films: PP, LDPE, HDPE, PS, PET, and pellets: PP, LDPE, HDPE) of fixed diameter. In order to run simulations for MPs of various sizes, shapes, and densities (table C.5), an idealized approach is adopted for scenario testing due to its flexibility to be applied for various combinations of polymer properties. The biofouling rate in this approach represents the increase in the thickness of the biofilm thickness [m/d] at the surface of the particles, calculated based on the empirical data of Karkanorachaki et al. (2021) [67]. More details on the development of this rate can be found in section C.1.2.

Resuspension, burial, and resurfacing rates

Resuspension and burial rates depend on the physical properties of MPs [207] as well as turbidity currents [98] and the bioturbation activity [99], which vary spatially. Since there is little data to account for these distinctions, a simplified approach is followed where a single value is used for all MPs and all geographical locations ($k_{resuspension}$ = 2.3E-04 day^{-1} and k_{burial} = 2.4E-05 day^{-1}). Resuspension and burial rates are calculated based on the resuspension and burial velocities found in the Simplebox4plastic model [2]. More details about their quantification are found in chapter 7. The burial rate is applied in the continental beach and sediment sub-compartments, as well as in the global compartment. Similarly, the resurfacing rate, which is the transfer from the beach to the water surface ($k_{ws,b}$), depends on the properties of the particles, as well as the oceanographic conditions, i.e., waves, water currents, types of beaches, etc. However, there are few data to quantify it. In addition, modeling this rate using numerical modeling is challenging due to the high resolution of oceanographic hydrodynamic data required near the shore. For this reason, a single value ($k_{resurfacing}$ = 4.5E-01 day^{-1}) is calculated based on the rates of transfer of beach sediments to the water, as designed in the artificial beach of Kamphuis et al. (1991) [208]. More details on the calculation of the resurfacing rate can be found in chapter 7.

5.4.2 Removal rates

According to Corella-Puertas et al. (2023) [19], degradation rates depend on a surface degradation rate that varies with the density, size, and shape of the polymers. Currently, there are no compartment-specific degradation rates available to account for differences related to UV exposure and mechanical abrasion [114]. Therefore, medium and slow degradation rates are taken from Corella-Puertas et al. (2023) [19]. In order to differentiate between the degradation rates within marine sub-compartments, fast rates are applied for beach sub-compartments ($k_{b,deg}$) where mechanisms enhancing the weathering of MPs are pro-

nounced [114]. Medium rates are used for the water surface ($k_{ws,deg}$), and slow rates for the water column ($k_{wc,deg}$) and sediments ($k_{sed,deg}$) at the continental scale, and for the global scale ($k_{glo,deg}$).

5.5 Rate and fate matrices

The rate matrix needed for the construction of the fate matrix is presented in equation 5.5. Transfer rates ($k_{j,i}$) [day^{-1}] from an emission sub-compartment i, on the columns, to a receiving sub-compartment j, on the rows, are presented in off-diagonal elements. Diagonal elements present the total removal rate of the corresponding sub-compartment. While the continental scale is detailed into beach (b), water surface (ws), water column (wc), and sediment (sed) sub-compartment, the global scale is assumed as a single compartment that includes both global water and sediment. Mechanisms of removal from the global scale are considered as deep burial in the sediments and degradation in the water compartment. Merging the global sub-compartments into one sub-compartment is a simplification because of the complexity of this scale. Emitting particles in the global scale closer to the continental scale might be different than emitting in the open ocean. Since simulation times are very high, especially when using large data, it is challenging to include the entire global scale in the simulations. In addition, it is predicted to have lower impacts in the global scale, due to its large size, compared to the continental scale.

$$\mathbf{K} = \begin{bmatrix} k_{b.C,b.C} & k_{b.C,ws.C} & 0 & 0 & 0 \\ k_{ws.C,b.C} & k_{ws.C,ws.C} & 0 & 0 & 0 \\ 0 & k_{wc.C,ws.C} & k_{wc.C,wc.C} & k_{wc.C,sed.C} & 0 \\ 0 & 0 & k_{sed.C,wc.C} & k_{sed.C,sed.C} & 0 \\ 0 & k_{glo,ws.C} & k_{glo,wc.C} & 0 & k_{glo,glo} \end{bmatrix} \tag{5.5}$$

Moreover, as hypothesized in the multimedia model used to develop CFs for freshwater ecotoxicity; USEtox [167], the transfer from the global scale to the continental scale is negligible compared to transfers from the continental to the global scale. Thus, transfer rates from the global scale ($k_{j,glo}$) are assumed to be zero. Continental sub-compartments that are not directly connected together also present a zero transfer rate from one to another. Intermedia transfer rates (off-diagonal elements) are quantified as explained in sections 5.4.1 and 5.4.1

while total removal rates $k_{i,tot}$ (diagonal elements) are quantified according to:

$$\begin{aligned} k_{b,tot} &= k_{b,deg} + k_{ws,b} + k_{b,burial} \\ k_{ws,tot} &= k_{ws,deg} + k_{b,ws} + k_{wc,ws} + k_{glo,ws} \\ k_{wc,tot} &= k_{wc,deg} + k_{sed,wc} + k_{glo,wc} \\ k_{sed,tot} &= k_{sed,deg} + k_{wc,sed} + k_{sed,burial} \\ k_{glo,tot} &= k_{glo,burial} + k_{glo,deg} \end{aligned} \tag{5.6}$$

A rate matrix $\mathbf{K}$ $[day^{-1}]$ is constructed for each microplastic defined for each scenario (table C.5) and for each geographic emission site (section 5.2). A site-specific fate matrix **FF** [day] is then obtained by inverting the rate matrix according to equation 5.7 [185]:

$$\mathbf{FF_p^n} = -\mathbf{K_p^n} \tag{5.7}$$

where p is the corresponding microplastic polymer and n the corresponding emission site. The structure of the **FF** matrix is presented in equation C.10.

5.6 Exposure-effect matrix EEF

The exposure-effect matrix **EEF** is presented in equation C.11. EEFs in the matrix are expressed in $[PAF.m^3/kg]$. They are developed from the hazardous concentration (HC20) obtained as the geometric mean of concentrations affecting 10% of species (EC10) [209]. Various EEFs have been developed to account for MP impacts on marine species depending on their exposure route. An EEF_w is an exposure-effect factor developed for species exposed to MPs via water. It is developed based on data for virgin MPs (EEF_w = 1067.5 $PAF.m^3/kg$) [19, 20]. It is applied for water surface and water column sub-compartments, as well as the global compartment. EEF_{sed} (EEF_{sed} = 16.2 $PAF.m^3/kg$) is an exposure effect factor recently developed for marine species exposed to MPs through sediments. It is also developed solely on data derived for virgin MPs [21] and is applied to the sediment sub-compartment. As presented in figure 5.1, the beach sub-compartment is modeled as a dry beach (sands) and a wet beach hosting the submerged part of the beach (water and sediments). Thus, the effect-exposure factor for the beach EEF_b quantifies the impacts for both terrestrial (dry part of the beach) and aquatic species (wet part of the beach). The percentages of weighting between the two ecosystems are derived from the International Union for Conservation of Nature (IUCN) database [210]. Species for marine coastal/supratidal

habitats are taken to represent the dry beach and marine intertidal habitat to represent the wet beach, as defined in section 5.3. These percentages are regionalized according to the emissions sites of this study (section 5.2). More details about the regionalization of species distributions across emission sites are further explained in section 5.7. The terrestrial EEF ($EEF_{terrestrial} = 1.38\ PAF.m^3/kg$) is developed by Tunali et al. (in preparation) [211] from data derived for virgin MPs, except for one species (*Zea mays L*) where MPs used contained additives. For the wet part of the beach, EEF_w is used for the water part with a percentage of 44.6% and EEF_{sed} for the sediment part with a percentage of 54.6%. These percentages, developed by Saadi et al. (2024) [21] using WoRMS database [212], represent the distribution of species that feed from water and from sediments, respectively. All the aforementioned EEFs are applied for all MPs modeled in this study since it was proven that there is no significant influence between the physiology of MPs and their impacts on the aquatic ecosystem [20].

5.7 Species distribution Fractions SDF

The species distribution fraction, as presented in section 2.7, is used to aggregate impacts within marine sub-compartments to represent the impact on the overall marine ecosystem [21]. The aggregation differs depending on the IW+ or GLAM approach (section 5.1). For the IW+ approach, the aggregation is performed on the basis of the affected surface [m^2]. Thus, ecosystems over a certain surface area [m^2] are equivalent. Therefore, ecosystems in beach, continental, and global scales are equivalent over their surface area. Their SDFs are then equal to 100%. Overlapping ecosystems that share the same surface (water surface, water column, sediments), are aggregated using their species distribution fractions, to represent their species contribution of the overall continental-scale ecosystem. The distribution of marine species between water and sediment sub-compartments is distinguished based on the feeding behavior of species. According to Saadi et al. (2024) [21], WoRMS database gives a total of 774438 species ($SDF_w = 44.6\%$) that feed from water while 92549 feed from sediments ($SDF_{sed} = 55.4\%$). In order to distinguish the SDF between the water surface and water column, the vertical species gradient from Costello et al. (2017) [190] is used. In this study, the density gradient of species as a function of depth is provided. However, data at depths lower than 100 meters are lacking. Therefore, we used the value of 0-100m (66. 2%) for the water surface sub-compartment as the species richness in this sub-compartment is considered where most marine species thrive due to light availability and temperature. The species distribution in the continental water column is therefore taken between 100-200 meters (26.8%), which is the depth of the water at the continental scale (section 5.3). Since little data exist regarding the feeding behavior and habitats of these sub-compartments, these

SDFs are not regionalized.

For the GLAM approach, the species distribution fraction of each sub-compartment is determined relative to the overall marine ecosystem. The distribution of species between water and sediments and within the water compartments is determined based on the feeding behavior of species and their habitats, as for the IW+ approach. The distribution between the beach, continental sub-compartment and global scale is determined based on the habitats of species. IUCN database provides the species richness of all marine habitats for fishing areas as defined by the European Commission [210]. Thus, SDFs are regionalized according to the fishing area in which emission sites are located. Based on IUCN habitats, the species of each sub-compartment are taken as follows. As presented in section 5.6, species of the dry beach are taken from the supratidal habitat in the IUCN database and the wet beach from the marine intertidal habitat [210]. The continental scale is classified as the marine neritic habitat. The global scale is taken as marine deep benthic and marine oceanic habitats. The global scale represents species in the world's deep oceanic environment.

5.8 Continent and global CFs

According to equation 5.1, multiplying obtained fate factors (section 5.5), exposure-effect factors (section 5.6) and the species distribution fraction (section 5.7), emission-site characterization factors are obtained for IW+ and GLAM methods. Emission-site CFs are then aggregated into continent CFs, and subsequently a global CF, using the percentage of MP emissions of each site (table 5.2), according to equation 5.8. Two continental CFs are obtained for Africa and for Asia. The CF for the Mediterranean Sea is considered in the continent of Africa since the emissions to the Mediterranean were considered from the Nile river.

$$CF^k = CF^n . \frac{E^n}{E^k_{tot}} \tag{5.8}$$

where CF^k and CF^n are CFs for the continent k and the emission site n, respectively. E^n and E^k_{tot} are MP emissions in site n and total MP emissions in the continent k, respectively.

CHAPTER 6 ARTICLE 1 : LIFE CYCLE IMPACT ASSESSMENT FRAMEWORK FOR ASSESSING PHYSICAL EFFECTS ON BIOTA OF MARINE MICROPLASTICS EMISSIONS

This first article addresses the first objective. It presents the proposed fate model based on a comprehensive literature review. The model serves as the basis for the development of mechanistic fate and characterization factors for microplastic emissions in the marine environment, for the LCIA impact category "Physical effect on biota". This article was published the 9^{th} of September 2023 in *International Journal of Life Cycle Assessment* (`https://link.springer.com/10.1007/s11367-023-02212-7`). The co-authors of this article are Cécile Bulle and Anne-Marie Boulay. Supplementary information of this article can be found in Annex A. The literature review on the fate mechanims was presented in the workshop *Linking the Life Cycle Inventory and Impact Assessment of Marine Litter and Plastic Emissions* that was held online in March 2020. The methodological framework was presented in the *Life Cycle Innovation Conference* that was held online in August 2020. It was also presented in the *Society of Environmental Toxicology and Chemistry SETAC Europe - 30^{th} Annual Meeting* that was held online as well in May 2020. This article will be cited throughout this thesis as (Hajjar et al., 2023).

6.1 Abstract

Purpose The international working group MariLCA has proposed a framework aiming towards integrating the impacts of plastic pollution in life cycle impact assessment (LCIA). Filling one of the identified mechanisms, this paper proposes a harmonized LCIA framework for the development of mechanistic fate factors (FFs) and consequently characterization factors (CFs) for microplastics (MPs) emissions in the marine environment, for the proposed impact category "Physical effects on biota".

Methods Based on a literature review, fate mechanisms and environmental factors influencing MPs in the marine environment are identified. Dominant fate mechanisms are determined; based on which the marine environment is divided into homogeneous sub-compartments. Following on this framework and multimedia fate models adopted in LCIA, rate matrices for different types, shapes, and sizes of MPs are constructed. Fate matrices are obtained by negatively inverting rate matrices. Similar to emission-related impact categories, CFs matrices are constructed by multiplying FF matrices with exposure-effect matrices.

Results and discussion The marine environment is divided into marine sub-compartments at two different scales: continental and global. Marine sub-compartments include beach, water surface, water column, and sediments at the continental scale; and water surface, water column, and sediments at the global scale. Due to the dependency of MPs fate on their physiology (shape, size, and density), different rate and fate matrices can be obtained. Mechanistic characterization factors for water surface and water column sub-compartments are obtained by multiplying the fate matrix with already existing exposure-effect factors for aquatic ecosystem. However, in order to develop CFs for beach and sediments sub-compartments, this framework suggests the development of new exposure and effect factors specific to these sub-compartments.

Conclusion Since LCA is known as a holistic approach, marine litter should be integrated in its impact assessment. This proposed framework fills one of the gaps of MariLCA's framework that aims towards integrating plastic litter in LCIA by proposing fate and CFs matrices for different types of microplastics emitted to the marine environment.

6.2 Introduction

Plastic pollution has become a global environmental issue especially in the marine environment because of its impacts on the marine ecosystem. Land-based sources of plastics eventually enter the ocean through different pathways. A recent study stated that around 20 million tons (MT) of global plastic wastes are emitted in aquatic environments and this value is expected to triple as of 2030 [23]. Plastic debris are globally widespread traveling from Antarctic to Arctic regions [11]. They are mainly concentrated around densely populated areas before being transported long distances [26]. They are found in all marine environments, from coasts to open water [213], at the water surface and on the seafloor, and even in deep sea sediments [10, 56].

Plastic additives leaching into the marine environment are available to exposed ecosystem [163]. Plastics also play a role as a vector for hazardous contaminants to marine organisms [214] such as organic pollutants, i.e. polycyclic aromatic hydrocarbons (PAHs) and polychlorinated biphenyls (PCBs) [215], and heavy metals [162]. Apart from their ecotoxicity, impacts have also been linked to their physiology. Marine organisms are exposed to microplastics (MPs), ranging from 1µm to 5 mm [24] by ingestion, egestion, uptake, accumulation and tissue transfer, causing internal and external wounds, blockage of the digestive tract, or hindering growth. Impaired feeding can cause reduced capacity and/or false satiation leading to starvation or even mortality [31,216]. Although identified as an environmental threat, plastic pollution is likely to continue increasing in the future. Therefore, it is important to assess

their potential impacts in the environment, including within Life Cycle Assessment (LCA).

Numerous LCAs have assessed the potential benefits of different plastic alternatives [217,218]. However, LCA still lacks impact assessment approaches for potential impacts of plastic litter in the environment, specifically marine litter. This is limiting the comparison of the magnitude of potential marine litter impacts with other environmental problems in LCA [24]. Plastic Leak Project (PLP) has already started providing inventory data for macro- and microplastics emissions for life cycle inventory (LCI) [219]. Few recent studies have proposed different LCIA approaches for the generation of CFs for plastics emissions in the marine environment. In their paper, Saling et al. (2020) [177] suggested a characterization model based on a Marine Microplastic Potential (MMP) that is a function of a fragmentation rate, a degradation rate, and an effect factor. The fate of MPs was mainly linked to their residence time that influence their exposure duration to the marine ecosystem. The marine environment was considered a single compartment which doesn't allow the differentiation between transport mechanisms in marine sub-compartments and related specific exposure. In a more recent study, Maga et al. (2022) [178] developed CFs for plastics emissions in different environmental compartments, including marine compartment. In their approach, the fate of plastics was also linked to the degradation rates of polymers. Since fragmentation and degradation are considered slow mechanisms and change in rates between marine sub-compartments [113], some particles might settle or beach prior to their removal through weathering mechanisms. This is mainly linked to different transport mechanisms and MPs physical properties (density, size, and shape) that weren't accounted for in the aforementioned approaches. While these individual initiatives proposed CFs for marine plastic litter in LCA, an international working group, MariLCA (Marine impacts in LCA), was launched in parallel in 2018 with the support of the UN Environment Program and the Forum of Sustainability through Life Cycle Innovation (FSLCI). Its main target is to improve LCIA models by developing harmonized CFs for environmental impact pathways of marine litter [17]. In their framework, they identified different gaps along the impact pathway to develop CFs for plastics pollution for different areas of protection (AoPs). They have proposed to model macroplastics, microplastics, and nanoplastics potential impacts in separate models that are linked, because their fate mechanisms differ within the marine environment as well as their potential impacts (i.e., entanglment for macroplastics) [24]. All these aspects were not accounted for in Saling et al. (2020) [177] and Maga et al. (2022) [178]. Within MariLCA's framework, an effect factor (EF) was developed for the micro/nanoplastics physical impacts on biota in the aquatic environment (freshwater and marine water) [20]. Using these EFs, preliminary fate factors were provided to develop simplified CFs for MPs emissions in the marine environment [18]. Since fragmentation and degradation are not considered sufficient to adequately quantify the

fate of MPs in the marine environment, as proposed by Saling et al. (2020) [177] and Maga et al. (2022) [178], Corella-Puertas et al. (2022) [18] accounted for sedimentation rates in their fate model based on literature values and expert estimates. They have also considered fragmentation and degradation rates based on Chamas et al. (2020) [220] and Maga et al. (2022) [178] but updated them to be polymer and particle specific. Corella-Puertas et al. (2022) [18] considered the marine environment as a single water compartment. However, results reflected the importance of developing a more refined fate model, and subsequently CFs model, due to the high uncertainty linked to fate mechanisms that differ with MPs physiology and within marine sub-compartments [18].

To the date of this article, the literature still lacks studies that tackle a rigorous and detailed analysis for the importance and influence of MPs fate mechanisms in the marine environment. Therefore, the main objective of this paper is to present a consistent and harmonized framework for developing characterization factors (CFs) for microplastics emitted to the marine environment. In order to address this, the following steps are followed:

1. A literature review is done to identify different processes, parameters, and mechanisms responsible for the distribution and removal of microplastics in oceanic sub-compartments.

2. Based on the literature review, a fate framework is proposed to set the methodological basis and key principles for the development of rate matrices, and subsequently fate matrices. The framework expands the marine environment modelled in Corella-Puertas et al. (2022) [18] to include various marine sub-compartments that need to be considered with additional fate mechanisms and refine the ones previously developed.

3. A framework is proposed for the integration of proposed FFs with EFs in order to provide CFs for the area of protection "Physical effects on marine biota" proposed by MariLCA [24]. This paper aims to support quantitative modelling for fate factors and characterization factors for MPs in the marine environment. Operational FFs and CFs are not in the scope of this paper but remain ongoing work within the MariLCA working group.

6.3 Review on Fate Mechanisms

Different mechanisms are responsible for the transport of microplastics in the marine environment. They are influenced by physical properties of the particles and environmental conditions [29]. Although coastal areas account for high concentrations of plastic litter [221,222],

coastal hydrodynamics transporting them are significantly different than the ones in the open ocean. They are mainly driven by winds, waves, tides, and influenced by the topography of the seafloor considering the shallow coastal water depth [223]. These differences make the understanding of marine plastics' behaviour highly challenging and the 3D modeling of their transport very complex, especially due to the limited knowledge on the behaviour of particles with respect to their physical properties [33]. Based on their mass balance model, Koelmans et al. (2017) [224] found that almost 99.8% of initially buoyant plastics, emitted to the oceans in 1950, had settled below the ocean surface layer [224] while Lebreton et al. (2019) [183], using a different simple box model, found that the majority of plastic litter also entering the oceans in 1950, are rather trapped near the shoreline and only a small fraction had escaped off to the open ocean. In a recent study based on modeling methodologies and in situ field measurements, Kaandorp et al. (2020) [202] estimated that almost 50% of plastics that have entered the Mediterranean Sea have sunk down (37-51%) and nearly 50% have accumulated in the coastlines (49-63%). This could be linked to the variation in hydrodynamics and marine parameters in different geographic locations or to the behaviour of plastics based on their physical properties and the factors that influence them. Despite the reason behind these differences, those results emphasize the complexity of fully understanding and modeling the fate of plastics in the oceans which requires a deep comprehension of chemical, physical, and biological processes. The following sections; horizontal transport (section 6.3.1), vertical transport (section 6.3.2), sedimentation (section 6.3.3), fragmentation and degradation (section 6.3.4), summarize all mechanisms, environmental factors, and physical properties that intervene in the horizontal and vertical distribution of microplastics between marine sub-compartments.

6.3.1 Horizontal transport

Positively buoyant MPs, less dense than the surrounding water, are mainly driven by advection and diffusion which accounts for the turbulence mixing processes [34]. The horizontal dispersion of microplastics is influenced by their buoyancy, Stokes drift (wave-induced motion), and Langmuir circulation (wind-induced motion) [35] (figure 6.1). Stokes drift represents the particle's drifting motion in the direction of waves propagation [37]. It is highly dependent on the shape of waves, and it is more pronounced in the shallower layers of the water. Despite the fact that the complex relation between floating particles transport and Stokes drift requires more research and understanding, it is considered an important criteria for modeling drifting of floating plastic particles as seen in the model developed by Onink et al. (2021) [38]. Actions of winds and heat fluxes generate turbulence at the ocean surface in the wind mixing layer [225] where plastics are intensely mixed [33]. Within the shal-

low mixed layer, the wind-induced flow results in the formation of counter-rotating vortices (windrows) at the water surface with their horizontal axes parallel to wind direction [226] (figure 6.1). This process, known as Langmuir circulation, traps an important part of the positively buoyant MPs in the upper mixed ocean layers [33]. Strong vertical flows, generated in Langmuir circulation, deeply submerge smaller MPs having low buoyancy away from the surface [39, 40]. Positively buoyant particles, intensely mixed in the mixed layer, resurface due to their vertical buoyancy force [41] at different velocities depending on their size (surface area and volume) and shape [42]. Having larger surface area, bigger particles rise faster while smaller MPs remain below the shallow water surface. Therefore, the wind-induced mixing results in a size selective transport where MPs size decreases in deeper layers [42]. This vertical distribution, along with size sampling limits, can explain the underestimation of plastic abundance during surface tow measurements even under mild wind conditions [41,47]. Larger macroplastics floating in shallower layers, are more influenced by Stokes drift that is faster at the surface than in deeper layers. They are trapped in coastal waters where they are constantly being washed ashore then carried back to the oceans by the actions of waves and tides [30]. This near-shore trapping increases the residence time of macroplastics onshore making them more susceptible to fragmentation [43] due to UV solar light on beaches and mechanical fragmentation by means of sand abrasion and actions of waves and tides [46] (section 6.3.4). Resultant microplastics, intensely mixed in deeper layers escape the near-shore trapping and drift offshore against the propagation of waves [33] leading to another size selective transport where the size decreases as we move away to the open ocean [30, 47]. Another ocean surface circulation mechanism, Ekman drift, is induced by surface winds and earth's rotation. The earth's rotation deflects the wind's direction resulting in a clockwise motion of the surface current in the Northern Hemisphere and counter-clockwise motion in the Southern Hemisphere [14]. Ekman transport creates convergence and divergence zones at the surface of the oceans. Convergence zones, found in the five sub-tropical gyres, accumulate transported macro- and microplastics [48–50]. However, it has been demonstrated that MPs do not remain indefinitely in the gyres but different processes play a role in there removal such as biofouling (section 6.3.2), aggregation (section S1.1), and ingestion by mesopelagic fishes [51] (section S1.2).

Very light particles, such as foamed polystyrene ($\rho = 0.0365 g/cm^3$), float at the surface with a protruding area above the water. They are subjected to winds, waves, and currents [29]. 'Windage' is referred to as the direct wind drag exerted on the exposed area causing the particle to move at the water surface [34]. It is important to understand the difference between windage and the wind-induced flow that is considered and accounted for in the surface current [227]. The overall force of windage, water current, and the opposite drag of the

water exerted on the particle result in a rolling motion over the surface almost four times faster than the current speed. Because the size of microplastics is much smaller than the length of surface waves, rolling motion is not affected by small or moderate waves [29]. This rapid rolling prevents any other altering mechanism to happen, such as biofouling (section 6.3.2) [228]. The residence time of floating microplastics, their drifting and beaching depend on the ratio of the surface exposed to air to the submerged surface of the particle [229]. Windage is quantitatively dependent on this buoyancy ratio which in turn depends on the physical properties of the particles [34, 230]. In addition, thermohaline global ocean circulation can transfer floating plastics long distances from the North Atlantic up to the Arctic seas. This could be the final destination for plastics where they might accumulate on Arctic benthic sediments if required time is given for vertical transport mechanisms to occur [231] (sections 6.3.2, S1.1, S1.2). A detailed review for the transport of floating marine plastic litter is presented by [14].

Little is known about the exchange of microplastics at the ocean-atmosphere interface [232]. However, some studies have proven that small-sized suspended atmospheric microplastics (SAMPs) could be possibly transported to the oceans [233, 234]. It has been estimated that 1.21 tonnes of SAMPs could be annually transported for long distances from land-based sources to the marine environment [235]. While some researchers suggest the possibility of MPs transport from the atmosphere to the oceans, other suggest a possible transfer from the ocean surface to the atmosphere from bubble action/jet expulsion. However, more research is still needed on this topic [236].

6.3.2 Vertical transport

Arriving in the marine environment, MPs having densities larger than that of the surrounding water (negatively buoyant) are expected to imminently start sinking until they reach benthic sediments. Their fate is dependent on their settling velocities; the larger their velocity, the closer they settle to their release point, while slower MPs travel with the water current as they settle [224]. Positively buoyant MPs have been detected in the water column and sediments hence suggesting that other factors might modify their properties [52, 237]. While positively buoyant microplastics represent around half (by mass) of all plastics, van Sebille et al. (2015) [238] estimated that only 1% of global plastics waste that has entered the ocean in 2010 has accumulated on the water surface. In order to understand the vertical transport of floating microplastics in the marine environment, it is important to understand various challenging processes. Wind induces what is referred to as upwelling and downwelling fronts [239]. Upwelling, referring to the vertical upward movement of deep and cold water towards

the surface, transport microplastics into the shallower layers of the ocean. Downwelling, which is the opposite of upwelling, drives the particles downwards as the warm surface water moves towards deeper layers [240]. The intensity of these movements depends on various processes such as, coastal topography and Ekman transport (section 6.3.1) [239]. Wind turbulence-induced vortices formed due to Langmuir circulation (section 6.3.1) induces also the vertical movement of microplastics due to upwelling and downwelling movements [39]. In addition to ocean currents and MPs densities, multiple transformation processes might alter their properties leading to their redistribution in the ocean. Despite the fact that these processes are still poorly understood [74], the vertical transport of buoyant microplastics has been linked to different mechanisms, such as biofouling (section 6.3.2), aggregation (section S1.1), biota interactions (section S1.2), and sea ice transfer (section S1.3), as discussed below.

Biofouling

Biofilms are aggregates of microorganisms that adhere onto a surface in water, such as plastics [241]. It starts by the formation of a conditioning film of ions and organics on the surface of the particles [53] followed by a thin layer of biofilms within a couple of weeks which progressively grows within hours with bacteria, algae, etc. [242]. In general, biofilm growth increases the overall density, hence increases the settling velocity of microplastics (figure 6.1). In shallow waters, negatively buoyant MPs might reach benthic sediments before biofouling takes place [53]. As for floating microplastics, biofouling reduces their buoyancy by increasing their overall density until it surpasses that of the surrounding water [55, 56, 242]. Biofouling rate is a trade-off between the size and the surface-to-volume ratio of a particle. Larger particles have higher collision rates leading to a faster biofouling while smaller microplastics require less algae to reach the density of the seawater [66]. Investigations show that smaller MPs, having a larger surface area to volume ratio, are fouled faster than larger macroplastics hence, start sinking sooner [29, 57, 242]. This supports the size selective transport suggested by Cózar et al. (2014) [243] and then supported by Kooi et al. (2017) [66] and Egger et al. (2020) [244] where the size reduces in deeper layers. Therefore, the vertical movement of floating plastic particles is not only influenced by the wind-induced mixing but also the rate of biofouling below the mixed layer [62]. Similarly to their size, the shape of microplastics also influences their settling rates, with films becoming biofouled faster than fibers, followed by spheres [29]. In addition, the nonuniform distribution of biofilms on the surface of MPs sheets causes a motion instability in the water reducing their vertical velocity no matter the increase in density. This reflects the double role biofouling plays for the vertical transport of microplastics [58].

Defouling might occur at a certain depth in the water column [242] due to physical mechanisms, light limitations, feeding fishes, or seasonal changes [66, 242]. Microplastics, no longer denser than the surrounding seawater, resurface until biofouling takes place again. This fouling-defouling relationship results in an oscillatory movement of MPs in the water until persistent biofilms are formed [53]. This up-and-down movement is size-dependent. Larger MPs, having larger sinking and rising velocities, have higher oscillation frequency than smaller ones [53, 62]. Biofilm's thickness depends on the number of colonizing agents such as algae which is related to collision, growth, mortality, and respiration. This results in oscillatory movements following a seasonal cycle or a circadian cycle (24 hours) if algae's growth is light-dependent [66]. Algal respiration is also temperature and oxygen dependent. Respiration increases with temperature thus, reduces with depth [66]. It also increases with oxygen concentration thus, enhancing biofouling [245]. Since marine water salinity, thus density, increases with depth, sinking biofouled MPs slow down and suspend at deep water levels until biofilms grow enough for sinking to proceed [28, 110].

In addition to MPs physical properties (size, shape, density), different parameters influence biofilm growth such as MPs chemical composition (i.e. presence of additives), salinity that enhances biofouling [60], seasonality [57], and MPs geographical locations [61]. Fouling communities vary within oceans [104]. In regions where biological activity is low (i.e. subtropical gyres), biofilm thickness grows slowly, and larger particles take longer to start sinking which enhances their presence at the surface. In equatorial regions, where biological activity is high due to high algae concentrations, microplastics sink faster than other regions in the oceans [57, 62]. Moreover, buoyant MPs sink faster during spring season due to algal blooming [57].

In general, biofouling has been associated to the reduction of microplastics buoyancy. However, other studies, in different aquatic environments, have shown a different behavior for the transport role of biofouling. In Hawkesbury River, Australia, biofouled negatively-buoyant polyurethane showed a 50% reduction in their settling velocity [64]. Another study in the Seine watershed showed that biofouling reduced the settling velocity of small heavy tyre and road wear particles (TRWPs) (diameter: 18 µm) while it had insignificant effect on the settling velocity of larger TRWP particles (diameter: 152 µm) [246]. In addition, Miao et al. (2021) [65] showed that biofouling in three different rivers in China has increased the settling velocity of negatively buoyant PET and PVC particles while reduced the density of floating PP. Aforementioned studies were tested in aquatic systems but none of them were reported in the oceans as to the date of this literature review was carried. Thus, it is important to emphasize on the need for additional research on the double role of biofouling on the vertical transport of MPs in the marine environment.

In addition to biofouling, other mechanisms also play a role in the vertical transport of microplastics in the marine environment. These mechanisms are aggregation (section S1.1), transport by biota (section S1.2), and sea ice transfer (section S1.3) that are more elaborated in the supplementary information.

6.3.3 Sedimentation

Microplastics have been detected in the deepest layers of oceans (i.e. Mariana Trench) [247]. They have been detected in sea sediments at water depths ranging up to 5000 meters [10,56]. Turbidity currents at the bottom sediments, known to transport sediment and organic carbon from shallow waters, can similarly transport and bury MPs in deeper layers. Suspension and deposition behavior of MPs within the turbulence layer is linked to the frequency of turbidity currents and the interactive and cohesive forces between particles and suspended materials (e.g. clay) [98]. Settling velocities of MPs have a great influence on their behaviour because they vary with their size and shape with the shape effect only pronounced for larger particles. For instance, settling rates of cylindrical polycaprolactone plastics start deviating from those of spherical shapes at a diameter close to 2mm [206]. Having smaller surface area to volume ratio, fragments settle faster, uninfluenced by their shape, than elongated fibers easily mixed in the turbulent eddies [98]. Upon their final deposition on sediments, MPs become buried by subsequent sedimentation. At estimated sedimentation rates between 0.00014 and 2.5 cm/yr, this physical process is considered slow [248]. Benthic organisms (bioturbators) play a double role in the distribution of MPs. While they might facilitate their resuspension [99], they might also strongly enhance their mixing [249] leading to their burial in deeper sediment layers, a process also known as "bioturbation" [100,101]. Burial rate and intensity of bioturbation depend on species behaviors including their traits, activities, feeding modes, etc. [100–102]. Once in deep layers, it is less probable for these particles to be transported back to the surface of sediments [103]. A worldwide mean depth of nearly 10 cm is estimated for bioturbation [250, 251] while subsurface benthic feeders generally feed at the surface [101]. It can be hypothesized that MPs detected deep in the sediments might have a reduced exposure to benthic organisms. In order to better understand and assess the ultimate fate and potential impacts of MPs in the marine environment, specifically sediments, their vertical distribution by turbidity currents and bioturbation still need more investigation.

In coastal waters where the topography of the seafloor is influenced by turbidity currents, tides, and breaking waves, turbulence is enhanced near the bottom [89] causing the resuspension of MPs from the sediments [90]. Therefore, the shallowness of water near the coast, along with wind, waves, tides, and coastline morphology, is important for the understanding

of MPs complex 3D circulation in the oceans.

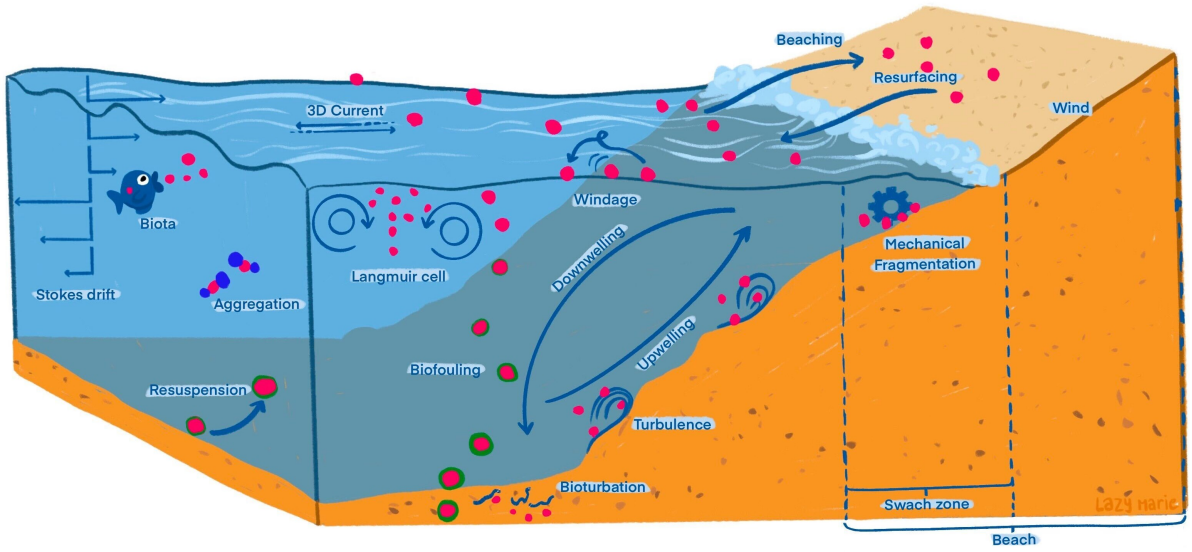

Figure 6.1 Schematic of mechanisms transporting microplastics in the marine environment

6.3.4 Fragmentation and degradation

Weathering refers to the biotic or abiotic degradation of plastics that modifies their mechanical, physical, and chemical properties by reducing their molecular weights [104]. As a result, embrittled plastics form new smaller fragments of microplastics and/or nanoplastics under mechanical forces such as sand abrasion and friction actions due to wind, waves, tides movements [105] and milder mechanical stresses of water [106, 107]. This process, referred to as fragmentation [46], irreversibly changes the shape of plastics and breaks them down into smaller polymers [252]. Further degradation results in the conversion of polymers into their monomers and ultimately the mineralization of monomers [108] when carbons present in plastics chains are converted into carbon dioxide [46]. Total mineralization is reached when all carbons are converted [121].

Fragmentation and degradation might take up to thousands of years to be reached due to the longevity of polymers, their properties, and surrounding environmental conditions [109]. Weathering in the marine environment proceeds through different mechanisms: 1) photodegradation under sunlight exposure, 2) thermooxidative degradation due to slow oxidation at moderate temperatures [46], and 3) biodegradation by marine living organisms (i.e., fungi, yeast, bacteria, algae and their enzymes) [112]. Exposure to ultraviolet (UV) radiation, primarily UV-A (315-400nm) and UV-B (290-315nm), initiates photodegradation [108] which

is the most important degrading mechanism in the environment [46]. In the presence of oxygen, this light-initiated degradation (photodegradation) is referred to as photooxidation or oxidative photodegradation [252]. Once it is initiated, the degradation can proceed by oxidation without further exposure to UV light [110]. Embrittlement initially starts at the outer surface exposed to sunlight where yellowing occurs and microcracks form [112]. It then propagates into the bulk of the particles where the rate decelerates because of light attenuation and low oxygen diffusion. Crack growth depends on its length, stresses applied on it, and the fracture toughness of the polymer [113]. Light-induced embrittlement is essential to initiate degradation as a precondition to the actions of mechanical forces for fragmentation to occur [111]. For this reason, photooxidation of plastics is mainly initiated in sea surface (in the euphotic or epipelagic zone) and on hot dry sands, where direct exposure to sunlight occurs [114]. Intense forcing is mainly provided in coastal zones where macroplastics entrapped near the shore are fragmented and generated secondary MPs are carried to the ocean by winds and waves [33, 104].

Biodegradation is the mechanism by which plastics are deteriorated by marine organisms either physically (through ingestion) or biologically (through enzymes) [108]. Biofragmentation generates smaller fragments; for example, nanoplastics have been detected in faecal pellets of marine organisms following their ingestion of MPs [77, 115]. In freshwater amphipods, biofragmentation can occur rapidly within a maximum of 96 hours [253]. Further biodegradation can result in complete transformation of polymers into CO_2, H_2O, and CH_4 as final products [116]. For non biodegradable plastics, biological decomposition is considered negligible in the marine environment, compared to photooxidation on beaches and on sea surface, due to slow kinetics and low oxygen availability [113]. While photodegradation and photooxidation are dominant at the surface of the ocean, biodegradation is the main reason for plastics degradation below the euphotic zone (epipelagic) [117]. However, biodegradation rates are several orders of magnitude slower than light-induced photooxidative reactions [46].

Environmental factors and water properties, alter the degradation rates of plastics in the marine environment [119]. Temperature doesn't affect the rate of weathering initiation but influences the rate of degradation that decelerates in water because of the absence of heat buildup [113, 121, 254] and low oxygen diffusion [114]. In addition, biofouling in water shields the surface of plastics from being exposed to UV light and leads to their sinking away from the surface which delays their weathering [120]. This is implied by the presence of less cracks on the surface of plastics sampled from the water surface compared to the ones sampled from the beach [228]. Very light small plastics (< 2 mm) rolling fast at the surface of the seawater prevent biofouling from occurring and hence, result in an even degradation on all faces of the particles. Conversely, nonuniform fouling in the water results in an uneven degradation

at the surface of the particles [121]. Therefore, UV sunlight attenuation [254], reduced temperature and oxygen availability, and slow biodegradation increase the persistence of plastics in the oceans below a certain depth in the photic zone, mainly on benthic sediments [117]. Negatively buoyant microplastics sinking at fast rates remain intact due to limited fragmentation and degradation in the water column.

In addition to environmental and water properties, observed degradation and fragmentation rates vary with the physiology of the particles [220]. Microplastics are more susceptible to weathering processes compared to macroplastics because they have larger surface area to volume ratio hence, they produce higher numbers of fragments [111] and present higher mineralization rates [104]. Thinner particles produce more MPs than thicker ones as they present lower mechanical robustness to fragmentation. Because photodegradation is initiated at the surface, thicker particles facilitate the formation of fibers as predominant MPs generated compared to the formation of fragments [106]. The rate of degradation also depends on the type of polymers [108]. To elaborate, polypropylene (PP) is less resistant than polyethylene (PE) but both require UV exposure for initiation to take place and mechanical abrasion for fragmentation to proceed. However, foamed EPS, formed through multiple thin layers, is more susceptible to fragmentation than PP and PE plastics hence, can produce a large number of micro-and nanoplastics, in a short period of time, through mechanical friction on sands [111, 122]. As for the shape of the particles, specifically cubic shaped light particles are found to have higher degradation rates than other shapes [228]. The color of MPs also plays a role in their degradation rates where darker plastics tend to absorb more UV-light than lighter ones resulting in an increase in temperature and accelerated weathering [113].

During the synthesis of plastics, chemicals and additives are added to enhance their properties and performance [255]. Additives such as UV stabilizers enhance the persistence of plastics by shifting their activation energy towards longer wavelengths [255]. As a result, prolonged exposure to higher UV light intensity is required to enhance the weathering of plastics [220]. Consequently, seasonal variations might accelerate or decelerate degradation rates by increasing UV intensity during summer and decreasing it during winter. Similarly, longer exposure to high stable intensity UV light in the equator increases weathering rates of plastics compared to their exposure in the Poles [118]. Upon the degradation of plastics, chemicals and additives are released. Some additives might easily biodegrade while others might persist contributing to the chemical pollution of the marine environment [256].

The influence of different environmental and water properties along with plastics physiology emphasize on the complexity of measuring slow fragmentation and degradation rates, especially with limited experimental data [118].

6.4 Methodology

Assessing potential impacts of microplastics in the marine environment follows on the recommendation of ISO14040 and is based on modeling an identified cause-effect pathway. With the intention of harmonization with LCIA models for emission-related impact categories, for instance the UNEP/SETAC toxicity consensus model USEtox [167] adopted in Impact World + [15] and LC-Impact [257], a similar multimedia model structure has been adopted for the development of characterization factors for MPs emitted to the marine environment for the impact category "Physical effect on biota". This model was recommended by different assessment models including the European Commission's Joint Research Centre – Institute for Environment and Sustainability (JRC-IES) in the International Reference Life Cycle Data System (ILCD) Handbook [258]. Developing a model coherent with a robust consensus grants a good harmonization within LCIA. Similarly to all the emission related impact, the model is presented according to the following equation:

$$\text{Characterization factor} = \text{Fate Factor} \times \text{Exposure Factor} \times \text{Effect Factor} \tag{6.1}$$

Characterization factors are expressed in $[PAF.m^3.day/kg_{emitted}]$ which corresponds to the Comparative Toxicity Unit $[CTU_e/kg_{emitted}]$ from USEtox at the midpoint level for the impact category "freshwater ecotoxicity". In order to obtain endpoint CFs for the impact category "ecosystem quality", the units are transformed into $[PDF.m^3.day/kg_{emitted}]$, equivalent to Comparative Damage Units $[CDU_e/kg_{emitted}]$ from USEtox, by multiplying midpoint CFs with a severity factor [170]. As proposed by Bulle et al. (2019) [15] for the IMPACT WORLD+ LCIA method, final units used are expressed in $[PDF.m^2.year/kg_{emitted}]$ obtained by dividing endpoint CFs with the water depth [m], to allow for comparison with other endpoint units for Ecosystem Quality.

The three components of the characterization factor are independently modeled. While Lavoie et al. (2021) [20] developed an exposure-effect factors, expressed in $[PAF.m^3/kg_{compartment}]$ for MPs in the aquatic environment, fate factors can be developed following the framework below.

6.4.1 Fate model

LCA fate factors link emissions to the mass or concentration of pollutants in each compartment after an emission flow [171]. An LCIA fate model for plastic litter takes into consideration the environmental multimedia distribution and residence time of plastics within spatially-defined marine compartment and sub-compartments [24]. It identifies accumula-

tion zones with high littering concentrations where exposure to the ecosystem is pronounced and potential impacts must be considered. The fate model represents fragmentation, degradation, and transport mechanisms of plastics within the environment which are key determinants of their residence time and redistribution within the ocean. After identifying fate mechanisms and environmental factors that influence the transport of MPs (section 6.3), an overall multimedia fate framework is developed by dividing the marine environment into sub-compartments, such that relevant fate processes and ocean hydrodynamics are appropriately considered as well as oceanic topography and exposed ecosystem. According to these mechanisms, sub-compartments are identified to distinguish different residence times of MPs in the ocean. This framework holds as a comprehensive basis for the quantification of fate mechanisms that helps identifying most dominant ones and most influencing factors. The size of each box is defined in such a way that homogeneous well-understood fate mechanisms are present. Since marine species diversity and density is much higher in the coastal area compared to the global ocean [259], this framework follows on USEtox proposition [167] and distinguishes between the two scales.

Each sub-compartment is represented by a simple homogeneous well-mixed box described by its total volume, water and solid phases, and contaminants (herein microplastics). Water phases consist of a suspended matter phase and a biota phase. Suspended matter refers to any abiotic substance non dissolved in the water phase, such as fecal pellets, sands, and clay, that can bind to microplastics leading to their redistribution between identified boxes. Transfers between sub-compartments are based on all identified predominant and well understood mechanisms (section 6.3) responsible for the dispersal of MPs out of a considered sub-compartment and into another. Transformation processes, i.e., fragmentation and degradation, are considered to determine whether microplastics will remain in a considered sub-compartment or will be removed. Fate factors quantify the residence time and the mass increase of MPs in the marine sub-compartments. In accordance with multimedia environmental fate models, based on Mackay et al. (2002) [260] previously adopted in LCIA, mechanistic fate factors (FFs) are developed based on a series of mass balance equations applied to each sub-compartment according to the following general equation:

$$\frac{dm_i(t)}{dt} = S_i - m_j \times k_{i \leftarrow j} + m_i \times (k_{j \leftarrow i} - k_{deg,i} - k_{frag,i}) \tag{6.2}$$

Where m_i is the mass [kg] of MPs in compartment "i", S_i [kg/day] is the emission flow rate, $k_{i \leftarrow j}$ and $k_{j \leftarrow i}$ $[day^{-1}]$ are the intermedia transfer rate from compartment "j" into compartment "i" and from compartment "i" to compartment "j" respectively. $k_{deg,i}$ and $k_{frag,i}$ $[day^{-1}]$ are degradation and fragmentation rates of MPs in compartment "i".

The series of differential equations obtained are solved using matrix algebra solving techniques as the most straightforward and transparent technique for the interpretation of physical processes within the matrices [261, 262]. The fate factor is obtained as the time-integrated solution of pollutant mass released into environmental compartments [169]. Following the linear relationship between the steady-state solution of a continuous flux and the fate factor [260,263], the steady-state solution resulting in the mass [kg] of MPs in each sub-compartment is obtained according to the general matrix formula:

$$\mathbf{m} = -\mathbf{K}^{-1}.\mathbf{S} = \mathbf{FF}.\mathbf{S} \tag{6.3}$$

The fate is represented by the fate matrix **FF**, where columns represent the source emitting sub-compartments and rows the receiving sub-compartments. The size of the matrix is determined by the number of identified sub-compartments. Each source compartment can be a receiving one, therefore **FF** is a square non-singular matrix. As shown in equation 6.3, **FF** is obtained by the negative inversion of the rate matrix **K** [185]. As a result, the rate matrix has the same size as **FF** and represents MPs exchanges between adjacent sub-compartments and losses to characterize their spatial distribution. In order to obtain the **K** matrix, fate processes that influence plastic particles emitted to the oceans need to be quantified. As seen in section 6.3, these processes are influenced by MPs physical characteristics (size, shape, and density), physical environmental forces (mainly gravity force and Archimedean buoyance force), environmental and marine conditions (seawater density, seabed topography, flow velocity, turbulence, etc.) [90]. For these reasons, these differences should be accounted for while quantifying transfer, degradation, and fragmentation rates for the development of rate and fate matrices. This quantification will help identifying most dominant mechanisms as well as fate mechanisms that have the least significance on the transport of the particles. Since fate mechanisms vary with the physiology of the particles, several polymer-specific rate, hence fate matrices should also be developed.

6.4.2 Characterization factors

The calculation framework for the generation of characterization factors according to equation 6.1 provides the sub-components (fate and exposure-effect models) needed to provide CFs for each type of MPs. Multiple fate factors are combined with the exposure-effect factors to provide the full set of CFs for each type of polymer and particle (size and shape). Following the same matrix-algebra-based calculation framework adopted in LCIA and presented in

the fate model (section 6.4.1), equation 6.1 is written as the following matrix equation:

$$\mathbf{CF} = \mathbf{FF} \times \mathbf{EEF} \tag{6.4}$$

Mechanistic characterization factors for MPs emitted in the marine environment are then obtained in the **CF** matrix by multiplying the **FF** with the exposure-effect matrix **EEF** [185].

6.5 Results

The following sections present the proposed multimedia fate framework (section 6.5.1) for the development of fate factors for MPs emissions in the marine environment. Mass balance equations and rate matrices development are presented in section 6.5.2 followed by the development of characterization factors in section 6.5.3.

6.5.1 Multimedia fate framework

The proposed framework represents marine environment at two scales: continental and global scale. The continental scale includes beach, water surface, water column, and sediments subcompartments and the global scale includes only water surface, water column, and sediments (figure 6.2). According to Shaked et al. (2011) [264], and then adopted by USEtox, the continental scale is defined at 60 km coastal zone, which is the average distance that includes most of the continental shelf and the water depth of the section adjacent to land is less than 150m [167, 264]. Since degradation and fragmentation of microplastics are mainly initiated by exposure to UV sunlight and then enhanced by mechanical fragmentation near the coast (section 6.3.4), beach sub-compartment is defined where highest exposure to UV light and greater weathering of plastics are dominant. It is defined as the zone that extends from the uppermost limit of waves to the low tide limit [189]. It includes the backshore, which is the zone above the high tide line that only gets wet with high waves (i.e. storm waves), and the swash zone that represents the region between the low and high tide lines. The swash zone is therefore submerged during high tides and exposed during low tides [265]. Mechanical forces, due wave breaking and sediments motion, are high in the swash zone enhancing the fragmentation of plastics that are light-initiated on the backshore (section 6.3.4) [33]. In general, the width of the beach can range from few meters up to several kilometers [189]. In this framework, the width of the beach sub-compartment is chosen to be 100 meters which is mostly observed for open coastal beaches [189]. The water surface layer is determined as the shallow layer of the epipelagic zone that transports light microplastics through windage and advection and influenced by different types of wind and waves drifts. Since weathering of microplastics

is also pronounced at the surface of the water compared to deeper layers, the depth of the water surface sub-compartment is determined as the depth below which photooxidation is limited due to UV light attenuation. This is measured by dissolved color organic matter (CDOM) that absorbs UV-lights in seawater by Tedetti et al. (2006) [196]. Coastal waters, containing a higher concentration of CDOM, attenuate UV light more effectively than the open ocean [196]. Therefore, it penetrates deeper at the global scale than in the continental scale. For this reason, the depth of water surface sub-compartments are defined as 6 meters and 10 meters for the continental and global scale respectively, corresponding to the level at which 10% of surface UV radiation remains (Z10% in meters) and 90% is absorbed [196]. Within this depth, hydrodynamic physical processes (i.e. windage, advection, wave and wind currents) transporting MPs at the surface are also considered. The depth of the water column sub-compartment can vary from few meters to several thousand meters depending on geographical locations. Following on the proposition of USEtox, the water column depths are taken as 94 and 140 meters for continental and global scales respectively, in order to obtain a total water depth of 100 and 150 meters, respectively. However, it is important to mention that these depths are not representative of the actual water column depths of oceans around the world and should be replaced when the model is regionalized. According to the recommendation of Fantke et al. (2018) [259] for persistent contaminants, sediments are considered as a separate sub-compartment rather than a layer within the water column. It is defined where MPs are deposited by sedimentation and bioturbation. The depth below which bioturbation is no longer pronounced is considered as the maximum boundary of the sediment sub-compartment as MPs are no longer resuspended and their exposure to marine ecosystem is considered negligible. Sediments sub-compartment is thus defined at a depth of 10 cm in the seafloor which is the worldwide mean depth of bioturbation [250, 251].

As previously seen, marine biota can transport MPs from the water surface to the sediments through biofouling (section 6.3.2), ingestion and excretion with fecal pellets (section S1.1 and S1.2). Marine organisms can also play a role in the fragmentation of microplastics into smaller nanoplastics and the complete mineralization through biodegradation (section 6.3.3). Therefore, marine biota act as an embedded multimedia compartment within the marine environment responsible for the redistribution of MPs within identified sub-compartments. The interaction of marine biota with marine MPs is summarized in figure S1.

Following on AQUATOX model [266], marine biota includes different species of marine organisms, algae, and microphytes that interact with MPs. Based on the assumption of Arnot et al. (2004) [267], microplastics are considered homogeneous within the body of marine organisms. In order to properly account for the exchanges of MPs between marine biota and marine sub-compartments, information regarding the ingestion and excretion within different

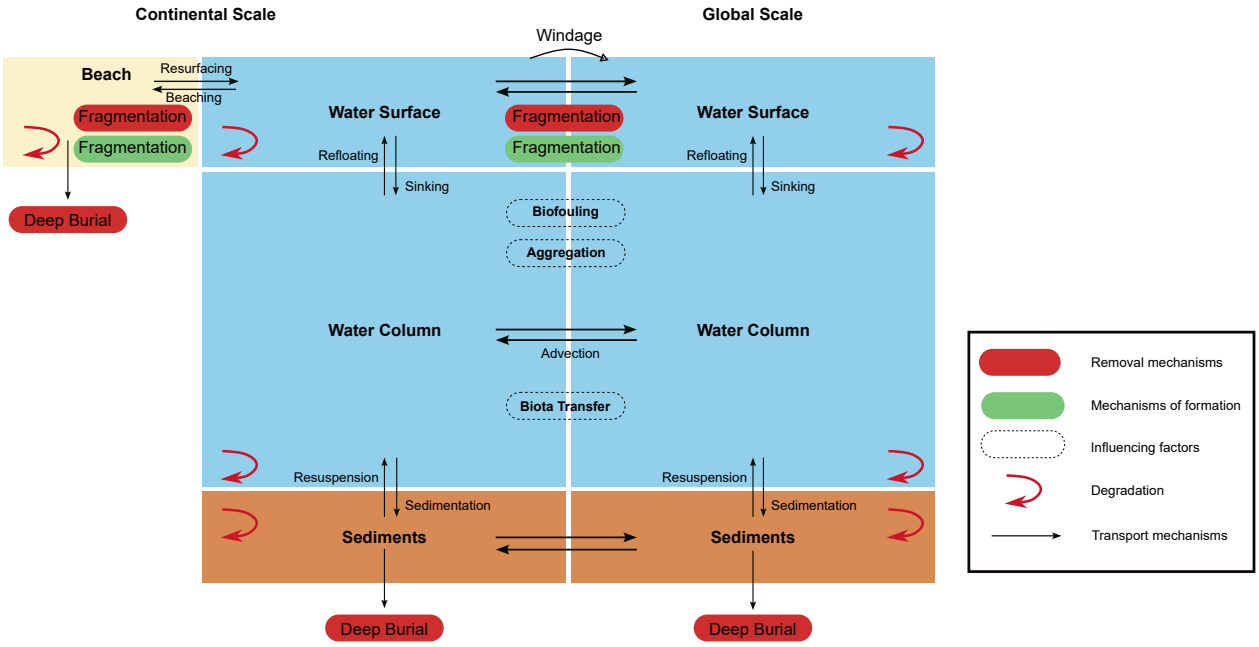

Figure 6.2 Fate framework for microplastics in the marine environment.

marine organisms and in different sub-compartment should be taken into consideration. For instance, excretion and uptake through the gills of fishes and crabs in the water and the sediments, as well as marine mammals and small phytoplankton (section S1.2) should be accounted for differently. In addition to that, mortality of marine organisms as well as predation relations between different species should be taken into consideration to properly define the biota sub-compartment and the mass transfer of MPs within this compartment. However, information regarding the residence time of MPs within marine organisms are still lacking and require significant research. Moreover, the model should account for how significantly could industrial fishing influence the removal of MPs from the marine sub-compartment through the removal of MPs enriched biota. Since degradation of microplastics is a slow process, it is assumed that MPs ingestion/excretion rates are faster than the fragmentation and degradation within the organisms. For this reason, marine biota is not considered as a separate marine sub-compartment in this framework but rather interactions are considered within transport rates mechanisms as identified in section 6.5.1.

After identifying each sub-compartment, dominant hydrodynamic processes and transformation mechanisms that determine the residence time of MPs and their intermedia exchanges between adjacent sub-compartments are categorized as follows (figure 6.2): 1) mechanisms of formation and removal; 2) transport mechanisms.

Mechanisms of formation and removal

As previously explained in section 6.3.4, MPs are formed due to fragmentation of larger macroplastics (in green) exposed to UV solar light and mechanical forces on beaches and at the water surface [46]. Although the formation of nanoplastics due to fragmentation of MPs is still not very well understood, recent studies have explored it [122, 268] and therefore, it is considered as a mechanism of removal for MPs. As proposed within MariLCA's framework, nanoplastics potential impacts will be modeled in a separate specific model where the formation of nanoplastics from the fragmentation of MPs, considered as a removal mechanism in this framework, will be considered as a mechanism of formation. Fragmentation and degradation processes are mainly considered on the beach and in the water surface where they are initiated by high exposure to UV light and mechanical forces due to wind friction, sand abrasion, and actions of tides and waves. Slow biodegradation also occurs in the water column and sediments. Degradation is thus considered as a removal mechanism in each sub-compartment (red arrows in the figure). Surface benthic feeders generally feed at the surface of the sediments [101]. Therefore, potential impacts of MPs present deeper than 10cm in the sediments are considered negligible and MPs are considered removed by deep burial. Burial in the beach sediments is also considered as a removal mechanism where plastics no longer reach the water.

Transport mechanisms

MPs circulate horizontally and vertically between marine sub-compartments through identified intermedia transfer mechanisms and influenced by different environmental factors. Positively buoyant MPs generated on the beach alternate between onshore sands and water through tides and waves. Particles transported to the beach are considered 'beached'. They remain exposed to sunlight on sands until fragmented or carried back to the ocean water where they are free from nearshore trapping and therefore drift out of the continental water surface into global water surface by advection. Particles are considered out of the beach sub-compartment when they are in the water and no longer return to the beach. Drifting MPs are influenced by waves, Stokes drift, Ekman drift, Langmuir circulation and wind-induced current (section 6.3.1) within 20 meters depth. These mechanisms should be taken into consideration when determining the rate of advection between the two surface sub-compartments of the continental and global scale. In addition, very light MPs, floating with an exposed part to air, are transported at the surface by windage from the continental to the global scale. Microplastics in the shallow layer can be transported to air due to wind movement and wave breaking. Although this mechanism needs further investigations, its consideration

in this framework is important for future development.

Water surface and water columns sub-compartments exchange MPs through vertical transport. The rate of sinking of negatively buoyant particles is influenced by their sinking velocity upon their arrival to the water and is enhanced by further biofouling [224]. However, sinking of low-density MPs is a function of different processes that reduce their buoyancy and increase their density until it surpasses that of the surrounding water. They include biofouling (section 6.3.2), aggregation (section S1.1), and biota transfer (section S1.2) that increase the residence time of positively buoyant MPs in the water compared to negatively buoyant ones. Defouling is not considered as a permanent process since fouling/defouling processes can follow a circadian or seasonal cycles and it is overcome by the formation of persistent biofilms. For this reason, an intermedia transfer from the water column to the water surface through refloating is not accounted for in this framework. However, defouling should be taken into consideration when calculating the sinking rates as it increases the residence time of MPs in the water column prior to their arrival to the sediments. Moreover, as the density of the water increases in depth, sinking MPs might become neutrally buoyant at a certain depth until their density exceeds again that of the seawater due to further biofouling, aggregation, or biota transfer [28,110]. Therefore, suspension in water column also increases the residence time of MPs before being transferred out of the water sub-compartment.

Sinking microplastics are transported out of the water column into sediments, at both scales, through sedimentation. Due to turbulence caused by turbidity currents, waves, tides and seabed topography, microplastics resuspend into the water column. This process is mainly pronounced at the continental scale where the depth of the seawater in coastal zones is shallower and benthic sediments are influenced by wind current and waves at the surface. In addition to resuspension, sedimented microplastics undergo horizontal transport along with bedload alternating between continental and global sediments [98].

6.5.2 Mass balance equations and rate matrices

Mass balance applied to each sub-compartment generates a system of equations structured in a matrix format [185]. Intermedia exchanges are quantified by transfer rates (expressed in day^{-1}) presented in the rate $\mathbf{K}$ matrix [day^{-1}]:

$$\mathbf{K} = \begin{bmatrix} -k_{b.C,tot} & k_{b.C,ws.C} & 0 & 0 & 0 & 0 & 0 \\ k_{ws.C,b.C} & -k_{ws.C,tot} & 0 & 0 & k_{ws.C,ws.G} & 0 & 0 \\ 0 & k_{wc.C,ws.C} & -k_{wc.C,tot} & k_{wc.C,sed.C} & 0 & k_{wc.C,wc.G} & 0 \\ 0 & 0 & k_{sed.C,wc.C} & -k_{sed.C,tot} & 0 & 0 & k_{sed.C,sed.G} \\ 0 & k_{ws.G,ws.C} & 0 & 0 & -k_{ws.G,tot} & 0 & 0 \\ 0 & 0 & k_{wc.G,wc.C} & 0 & k_{wc.G,ws.G} & -k_{wc.G,tot} & k_{wc.G,sed.G} \\ 0 & 0 & 0 & k_{sed.G,sed.C} & 0 & k_{sed.G,wc.G} & -k_{sed.G,tot} \end{bmatrix} \quad (6.5)$$

Off-diagonal elements represent intermedia transfer rates $k_{j\leftarrow i}$ ($k_{j,i}$) from an emission sub-compartment i to a receiving sub-compartment j while diagonal elements represent total removal rates ($k_{i,tot}$) from each sub-compartment. Indices b, ws, wc, and sed represent the illustrated sub-compartments proposed in the framework (section 6.5.1): beach, water surface, water column, and sediments. Indices C and G represent continental and global scales, respectively. Rates between sub-compartments that are not directly connected, i.e continental beach and global water surface, are assumed to be zero.

Based on identified mechanisms (section 6.3) and the framework presented in section 6.5.1 above, transfer rates in the **K** (equation 6.5) are defined. Rate expressions for vertical transport (sinking and sedimentation) depend on aggregation, biofouling, biota transfer, and advection. They are developed as follows for the continental scale. Global scale expressions are similarly developed (Equation S1).

$$\begin{aligned} k_{wc.C,ws.C} &= k_{sinking} = k_{aggregation} + k_{biofouling} + k_{biotatransfer} + k_{advection} \\ k_{sed.C,wc.C} &= k_{sedimentation} = k_{aggregation} + k_{biofouling} + k_{biotatransfer} + k_{advection} \\ k_{sed.C,wc.C} &= k_{resuspension} \end{aligned} \quad (6.6)$$

For the horizontal transport, the rate of transfer between beach and water surface sub-compartments ($k_{ws.C,b.C}$ and $k_{b.C,ws.C}$) is mainly driven by advection. However, this rate should also account for all turbulence factors that play an important role in the off-shore transport. These factors include, Stokes drift, wind, Langmuir circulation, and Ekman transport. Intermedia transfer between continental and global water surface sub-compartment ($k_{ws.G,ws.C}$ and $k_{ws.C,ws.G}$) also account for advection influenced by the same factors as well as windage. Transfer rate between continental and global water column and sediments sub-compartments ($k_{wc.G,wc.C}$ and $k_{sed.C,sed.G}$) are mainly driven by advection. A summary of all transfer mechanisms can be found in table S1.

Constant rates of sedimentation, sinking, beaching, and transfers between identified subcompartments are still unavailable in literature. They depend on identified aformentioned mechanisms, environmental conditions, ocean topography, and water currents which are specific to every geographical region. For this reason, it is important while determining these rates to take into consideration all environmental and oceanic factors as well as the spatial variability that might influence them. Three-dimensional tracking models could be used to calculate horizontal and vertical transfer rates, i.e. TrackMPD model [12] and TOPIOS model [269]. In the absence of full 3D models, some constant rates can be estimated using equations previously adopted for nanoparticles, assuming MPs and nanoparticles have similar behaviors. This framework proposes the following equations, previously adopted for the fate of nanoparticles in the Rhine River [270], for the resuspension and sediment deep burial constant rates:

$$k_{resuspension} = \frac{\nu_{resuspension}}{h_{sediments}} \quad \text{and} \quad k_{burial} = \frac{\nu_{burial}}{h_{sediments}} \tag{6.7}$$

Where $\nu_{resuspension}$ and ν_{burial} are MPs average resuspension velocity and deep burial velocity, respectively, expressed in [m/s].

Total transfer rates (diagonal elements) representing removal mechanisms from each subcompartment depend on transfer rates in addition to other removal processes. They are presented in equation 6.8 below for the continental scale. Similarly, total removal rates for global scale are developed in equation S2.

$$\begin{aligned}
k_{b.C,tot} &= k_{b.C,deg} + k_{b.C,frag} + k_{ws.C,b.C} \\
k_{ws.C,tot} &= k_{ws.C,deg} + k_{ws.C,frag} + k_{b.C,ws.C} + k_{ws.G,ws.C} + k_{wc.C,ws.C} \\
k_{wc.C,tot} &= k_{wc.C,deg} + k_{sed.C,wc.C} + k_{wc.G,wc.C} \\
k_{sed.C,tot} &= k_{sed.C,deg} + k_{sed.G,sed.C} + k_{wc.C,sed.C} + k_{burial}
\end{aligned} \tag{6.8}$$

Where deg and $frag$ refer to degradation and fragmentation of MPs.

In order to properly account for all mechanisms, fragmentation and degradation rates must consider biofragmentation and biodegradation even if the rates are slower than the ones at the beach and the water surface. In addition, fragmentation and degradation removal rates should be separately accounted for in the total transfer rates equations because mineralized MPs are no longer polymers. However, fragmented nanoplastics are considered as a removal mechanism since they are no longer in the microscopic scale considered in the framework but should be accounted for when modeling the impacts of nanoplastics in the marine environ-

ment. Degradation rates of nanoplastics will then need to be quantified. However, current studies cannot determine them separately due to experimental challenges and limitations. In general, these rates are determined through the mass loss of plastics that can be the result of both degradation and fragmentation. For this reason, this framework follows on the proposition of Corella-Puertas et al. (2023) [19] where both rates are represented by a single rate that varies with the size, shape, and type of polymers. Similarly, transfer rates between marine sub-compartments depend on the physical properties of MPs. A single fate matrix therefore doesn't adequately represent the fate of all MPs polymers within the marine environment and they should be classified according to differences influencing the fate linked to their physiology where each MP category is represented by a fate matrix.

As proposed in MariLCA, modeling the formation of MPs from the fragmentation of macroplastics is to be modelled in a separate model to account for all transport mechanisms that influence macroplastic particles [24]. The two models can be linked in different ways. As proposed in this framework, the marine environment is divided into seven sub-compartments at two different scales. A transfer between size classes (i.e, macroplastics into microplastics) could be accounted in additional identified sub-compartment that represent the size class considered. Therefore, the rate **K** matrix could be expanded from seven sub-compartments into 14 sub-compartments and 21 if the fragmentation of microplastics into nanoplastics is to be considered. Fragmentation from a bigger size class (i.e, macroplastics) into a smaller size class (i.e., microplastics) in a considered sub-compartment could be represented by a transfer rate from the considered sub-compartment of the bigger size class (example: continental water surface for macroplastics) into the same sub-compartment for the smaller size class (example: continental water surface for microplastics). Exchanges and transfers for the same size class could be considered among their representative sub-compartments with their specific rates identified.

6.5.3 Characterization factors

According to the matrix equation 6.1, the fate matrix obtained from the inversion of rate constant matrix **K** is multiplied by the exposure-effect factor developed by Lavoie et al. (2021) [20] and updated by Corella-Puertas et al. (2023) [19]. The EEF is based on three aquatic and marine trophic levels (as recommended by USEtox [167]) for a variety of endpoints (growth, mortality, reproduction, energy balance, metabolic activity, immobilization, and behaviour).). It is calculated using the hazardous concentration (HC50) obtained as the geometric mean of EC50s (effect concentration affecting 50% of species). However, following the new recommendations of GLAM (Owsianiak et al., 2023), a new EEF has been developed

based on $HC20_{EC10}$ Corella-Puertas et al. (2023) [19]. For all the data used, MPs tested were virgin particles to only account for their physical impacts. Although FFs might be influenced by the physical properties of MPs however, according to (Lavoie et al., 2021), the physiology of the particles doesn't significantly influence the exposure-effect factor. Therefore, a single EEF was provided for all shapes, types, and sizes. Since EEFs take into consideration aquatic species, their consideration is taken in all water compartments and CFs are obtained for water surface and water column sub-compartments. In order to generate CFs for beach and sediments sub-compartments, specific exposure and effect factors should be developed because the exposure of the ecosystem to MPs differ between water and soil compartments, i.e. beach and sediments, even if they are considered "wet" compartments. The resultant **CF** matrix $[PAF.m^3.d/kg_{emitted}]$ has the following format:

$$\mathbf{CF} = \begin{bmatrix} CF_{b.C} & CF_{ws.C} & CF_{wc.C} & CF_{sed.C} & CF_{ws.G} & CF_{wc.G} & CF_{sed.G} \end{bmatrix} \tag{6.9}$$

Fisheries activities [271], emissions from waste mismanagement [23], and rivers [272] are considered to be connected to the water surface near the coast. Therefore, the water surface at the continental scale is considered as an emission compartment and $CF_{ws.C}$ can be used to connect life cycle inventory (LCI) to MPs potential impacts on the impact category "Physical effects on biota". However, since MPs can be formed in the marine environment through fast fragmentation at the beach and water surface at the continental scale, and slow (bio)fragmentation in the water column and sediments at both scales, all identified sub-compartments are considered as emission compartments. As previously mentioned, the formation of microplastics through fragmentation of larger macroplastics is an ongoing project within MariLCA's framework and outside the scope of this paper. However, using effect factors for macroplastics potential impacts in the marine environment, a CF matrix using the expanded **K** matrix can be obtained for different size classes of plastic particles.

As proposed in section 6.5.2, different FF matrices are required to represent the differences linked to the influence of MPs physical properties on their fate. Consequently, different CFs are obtained for each MP category. CFs can then be aggregated into a single CF for MPs emitted in the marine environment depending on the availability of LCI data and the need of the LCA practitioner.

6.6 Discussion

The proposed framework serves as basis for the development of fate factors and characterization factors for microplastics emissions in the marine environment for the life cycle impact

assessment LCIA phase. It represents the marine environment in simple boxes and accounts for the fate of MPs using simplified equations. The steady-state approach adopted in LCIA and used for the development of mechanistic **FF** and **CF** matrices in this framework does not represent the actual dynamic fate of microplastics emissions into oceans. For this reason, it only serves as an approach to quantify a potential rather than an actual impact on marine ecosystem, which is the case of all LCIA models. However, despite its simplicity, the fate framework proposed integrates all fate mechanisms that might influence the fate of MPs in the marine environment which hasn't been previously considered in the models of Saling et al. (2020) [177], Maga et al. (2022) [178], and Corella-Puertas et al. (2022) [18]. Being highly persistent, it is crucial to consider transport mechanisms that might redistribute the particles before any degradation or fragmentation takes place. For this reason, marine sub-compartments were identified at two different scales to represent the difference in MPs behaviors based on dominant fate mechanisms. That matrix framework chosen for the development of rate and fate matrices presents the flexibility to add or remove sub-compartments by simply extending or reducing the matrices by a row and a column [185]. In addition, identified sub-compartments can be modified in size and volume while determining transfer rates. It can be adjusted to different continents where hydrodynamic fate mechanisms might change due to seasonal variations and environmental changes. Depending on modeling techniques adopted to quantify rates of MPs transport and removal, the depth of water column in both continental and global scale can be adjusted to represent a specific region. The proposed values can serve as a reference when simplified fate mechanisms are used for the generation of FFs. However, the depth of the water column can represent the actual water depth based on the geographical location of MPs emissions. In addition, water currents can also be determined using ocean general circulation models (OGCM) to represent the potential spatial variability of advective transfer rates and consequently the fate; a subject that should be tackled while developing operational FFs and CFs in future steps. Moreover, although the framework summarizes all fate mechanisms that might play a role in the redistribution of MPs, it is important to mention that research on fate of plastic litter in oceans is still growing and different data needed for the generation of rate constants are still missing, i.e., separated degradation and fragmentation rates for different polymer types and in different oceanic sub-compartments.

Marine biota vertically transports MPs from the surface of the water either through diurnal migration (section S1.2), or through aggregation with denser fecal pellets (section S1.1). Marine organisms might also fragment MPs into smaller nanoplastics (section 6.3.4). Since fragmentation and degradation rates, as well as the interaction of marine biota with MPs still require significant research, biota-associated mechanisms are quantified as separate

rates within identified transport and removal rates. The alternative of considering marine biota as a separate compartment within the marine environment may be explored in future steps. Interactions could then be quantified similarly to AQUATOX that models the environmental fate of pollutants in aquatic ecosystems [266]. Different ingestion and excretion mechanisms would be taken into consideration for different organisms and in different marine sub-compartments. The sensitivity to MPs will be separately considered for different species based on the availability of data. In addition, all factors and environmental conditions i.e., respiration, mortality, biomass, etc. will be taken into consideration.

As it is presented in literature, rivers are considered as a source pathway for MPs littering in the marine environment [273]. River plumes represent the region where riverine and marine water are joined [274]. Floating plastics and microplastics litters can be trapped in these plumes due to different water properties and hydrodynamic processes [275]. This part being a boundary layer between rivers and oceans is not considered in this framework. However, the understanding of riverine transport into oceans is very important and should be considered in future steps when combining MPs transport from inputs into oceans.

The EEFs used for the development of CFs are developed using data testing virgin polymers with no additives or chemicals attached, to consider the impacts linked to the physiology of the particles [20]. The ecotoxicity of MPs on freshwater and marine ecosystems can be accounted for using the impact pathway adopted in USEtox for freshwater ecotoxicity [167] and is an ongoing work within MariLCA [24]. In their work, [20] presented that there are no statistical differences in data between micro- and nanoplastics influence and a single EEF is representative for their potential impacts on aquatic species inseparably. For this reason, the removal of MPs through fragmentation into nanoplastics and the separate fate model for nanoplastics (as suggested by Woods et al. (2021) [24]) might not be needed. This is particularly pertinent if other fate mechanisms are proven not to differ between micro- and nanoplastics. EEFs are calculated using the hazardous concentration (HC50) obtained as the geometric mean of EC50s (effect concentration affecting 50% of species). However, following the new recommendations of GLAM [209], a new EEF has been developed based on $HC20_{EC10}$ [19] and should be used when developing operational CFs.

While inventory modeling is not within the scope of this framework, it is important to emphasize on the need for maintaining harmonization between characterization factors developed in impact assessment modelling and inventory data [24]. The Plastic Leak Project (PLP), generating LCI data for plastics emissions, accounts for two types of fate: an initial fate that represents the first emissions of plastic littering in the environments, i.e., MPs transported from rivers into oceans [219]. This framework only represents the marine compartment (no

freshwater compartment or other non aquatic compartments) and should be consistent between LCI and LCIA modelling. Generated fate factors and hence characterization factors, based on this framework, must be combined with LCI data considering the final fate of MPs. Therefore, PLP inventory flows should account for MPs emissions into marine environment whether from a direct emission into the ocean, fragmentation of macroplastics, or transfers from rivers, soils, or atmosphere. Moreover, in order to account for compatible units, LCI data must have the units of kilograms of plastics leaked into marine environment [kg] and should have specific information regarding geographic locations of emissions as well as polymers characteristics (size, shape, and density) in case this framework would be operationalized in a regionalized way. The reason behind this is the variation of MPs fate based on geographical locations and different hydrodynamical and environmental mechanisms influencing different types of polymers. Following on the size classification proposed in [24], MPs have an upper size limit of 5mm and a lower limit of 1 micrometer. The compatibility of MPs size between LCI data and CFs is important to facilitate LCI data collection and maintain the harmonization between LCI and LCIA modelling.

The proposed framework is consistent with USEtox [167] used in IMPACT WORLD + [15] where the fate boxes are considered homogeneous boxes and MPs are well-mixed in marine sub-compartments. Therefore, accumulation zones in ocean gyres are not represented in the water sub-compartment at the global scale. The reason behind this is that IMPACT WORLD + approach doesn't differentiate between species density between environmental compartments [15]. However, the global scale can be refined in future steps if data regarding species variability in the marine environment are available and different LCIA modeling approach is to be used.

Terrestrial species, such as sea birds, ingest MPs from beaches and water surfaces [276]. Ingestion is associated with trophic transfer through contaminated preys [277] or direct consumption of MPs by planktonic organisms due to their shapes and colors [278]. However, it has been observed that microplastics impacts on sea birds are less severe than that of macroplastics [5]. These potential impacts should be quantified using a cause-effect chain for the development of CFs for potential impacts of marine MPs on terrestrial ecosystem, which is out of the scope of this paper.

6.7 Conclusion

With the ongoing growth of plastics production and use, it is important to assess their potential environmental impacts, especially in the marine environment where they are accumulating. Lacking LCIA CFs for microplastics emissions in the marine environment, LCA

practitioners are unable to account for their potential impacts in the environment. This article proposes a methodological framework for the development of mechanistic characterization factors CFs for MPs emitted to the marine environment for the new impact category "Physical effects on biota". The multimedia fate framework presented above serves to support the development of mechanistic fate factors as the first step for the development of CFs. It provides a detailed representation of MPs circulation in the ocean. The framework harmonizes with previously validated and adopted models in LCIA which facilitates its integration in existing LCIA methods.

Acknowledgment

The authors would like to acknowledge the valuable support from their respective institutions and the funding which supported this work. The Life Cycle Initiative (UN Environment) contributes financially to MarILCA supporting research. The CIRAIG would like to thank its industrial partners for their financial support: ArcelorMittal, Hydro- Québec, LVMH, Michelin, Nestlé, OPTEL, Solvay, Total and Umicore. They would like to also thank Marie Lourioux for her support in the development of figure 2 of the manuscript.

CHAPTER 7 ARTICLE 2 : IDENTIFYING INFLUENCING PHYSICAL AND ENVIRONMENTAL PARAMETER THROUGH THE DEVELOPMENT OF SITE-SPECIFIC FATE AND CHARACTERIZATION FACTORS FOR MICROPLASTIC EMISSIONS IN THE MARINE ENVIRONMENT

This second article addresses the second objective. It provides identified influencing environmental parameters and physical properties of MPs on their sinking and settling. It equally identifies the rates and factors that influence the fate factors FFs and characterization factors CFs for microplastic emissions in the marine environment. This article was accepted the 28th of November 2024 (available online the $23^r d$ of January 2025), in *International Journal of Life Cycle Assessment*. The co-authors of this article are Cécile Bulle, Maxime Agez, Elena Corella-Puertas, and Anne-Marie Boulay. Supplementary information of this article can be found in Appendix B. This article will be cited throughout this thesis as (Hajjar et al., 2024).

7.1 Abstract

Purpose Within the international working group Marine Impacts in Life Cycle Assessment MarILCA, a mechanistic fate framework was proposed to refine the fate factors (FFs) and subsequently characterization factors (CFs) of microplastics (MPs) emitted to the marine environment, for the impact category "Physical effects on marine biota". To operationalize this framework with parsimony, this paper quantifies different identified fate mechanisms and determines the most influencing parameters on the fate. This will help determine a minimum set of variables based on which FFs could be categorized and clarify the need for regionalization in the operationalization of the framework.

Methods Based on different studies and models, fate mechanisms are quantified. A simulation plan is adopted to test the influence of microplastic and environmental properties on the settling of the particles using TrackMPD. Fate and CF matrices are developed for defined microplastic categories based on the simulation plan. A local sensitivity analysis is then applied in order to test the influence of various fate mechanisms on the fate and CF matrices.

Results and discussion The physiology of the particles (size, density, shape) and oceanic properties significantly affect the fate of the particles. The interaction between various influencing parameters highlights the complexity of quantifying the fate of MPs in the marine environment. Large particles of low density presented the highest residence time in water sub-compartments compared to smaller particles and negatively buoyant ones due to their slow settling. The final fate for all microplastics analyzed is benthic sediments. This highlights the need to develop effects factors (EFs) for sediment species to better understand the sensitivity of species exposed through sediments compared to species exposed through water. The sensitivity of fate mechanisms on the FFs and the variability of influencing parameters indicate the need for categorizing the fate, and subsequent CFs, based on the physiology of the particles. It also implies that regionalization is needed in future steps to account for the variability of water currents, biofouling celerity, and turbulence.

Conclusion This article supports one of MariLCA's objectives of integrating marine litter in Life Cycle Impact Assessment (LCIA). Testing the variability of fate parameters and identifying the importance of their influence assists in the operationalization of the framework previously proposed. This will help refine the fate factors and CFs already existing in the literature, increasing the accuracy linked to the variability and influence of combined physical and environmental parameters (biofouling, size, density, shape, etc.).

7.2 Introduction

While plastic pollution is clearly becoming an environmental problem, different mitigation strategies have been implemented to regulate plastic waste. However, despite these efforts, plastics emissions and littering in the environment are predicted to increase [279]. Plastics in the marine environment present ecological consequences [280]. Microplastics (MPs), ranging between 1µm and 5mm [24], are of particular concern because they expose a wide variety of marine organisms in water and sediments [26]. MP lethal and sublethal impacts, such as growth alteration, feeding activity and growth reduction [281], influence the structure and functions of marine ecosystems [280] and need to be assessed.

Life cycle assessment (LCA) is an internationally recognized and standardized methodology supporting environmental decision-making. In recent attempts to assess potential impacts of plastic littering [18, 177, 178], the international working group MariLCA (Marine Impacts in LCA) was founded in late 2018, with the support of the UN Environment Life Cycle Initiative and the Forum for Sustainability through Life Cycle Innovation (FSLCI) [17]. MariLCA's main objective is to develop characterization factors (CFs) for plastic littering to link plastic emissions with their potential impacts on different impact categories already existing in LCA

(i.e. human toxicity, ecotoxicity). In addition to MP ecotoxicity, a new impact category was added within MariLCA's framework, "Physical effects on biota" [24], to account for potential impacts on ecosystems linked to MP physical characteristics (size, density, shape); such as blockage of digestive tract, false satiation, mortality, etc. [5]. Within the framework of MariLCA, several attempts were made to quantify the components needed to develop characterization factors (CFs) for MP physical impacts on marine ecosystem [18–20]. These CFs followed the structure of emission-based CFs for (eco)toxicity. They account for the fate, exposure and effect of MPs. The fate factor FF links the mass of pollutants emitted to a compartment with their mass in different environmental compartments [169]. It is obtained from the inversion of a rate matrix **K** that accounts for removal rates (i.e., degradation) and environmental transfer rates (e.g, from air to ocean). For MP physical impacts on biota, it is challenging to quantify the exposure of MPs to marine ecosystem. Therefore, exposure and effect factors are combined in an exposure-effect factor (EEF) that relates the quantity of pollutants in an environmental compartment to their impacts quantified as a potentially affected fraction (PAF) of exposed organisms [185].

Initially, an exposure-effect factor was developed for micro/nanoplastics physical effects on biota in the aquatic environment (marine and freshwater) [20]. Corella-Puertas et al. (2022) [18] developed CFs for potential physical impacts of expanded polystyrene and tire road wear microplastics in the marine environment based on existing effect factors and a simplified marine fate model. CFs for nine different polymers were then added in their latest update with more refined FF and EF [19]. In their approach, they considered the marine environment as a single water compartment. Water surface and water column were not distinguished, and beach and sediments were not considered. Thus, they did not account for specific fate mechanisms and environmental conditions that connect marine sub-compartments. They accounted only for the fragmentation and degradation of polymers, which was previously considered in existing individual models [177, 178]. These individual models attempted to develop fate and CFs for MPs in the marine environment; however, they only linked the fate to the weathering of microplastics. In order to account for these unconsidered fate mechanisms, Corella-Puertas et al. (2023) [19] quantified sedimentation rates for different types, sizes, and shapes of polymers based on expert estimates. Biofouling, responsible for increasing the density of MPs by the accumulation of fouling organisms on the surface of MPs [57] were assumed in the sedimentation rates in a very simplified way. Water currents in 3D, responsible for the distribution of MPs, were not considered but rather, advection was represented by a simple single flow rate value. In addition, turbulence caused by winds and waves was not accounted for. Other fate mechanisms, such as resuspension and deep burial, beaching, etc. were also not quantified. Moreover, the marine environment was not distinguished

into two scales (close to the coast and global scales). This does not adequately reflect the impacts of MPs on the exposed ecosystem where the highest abundance is close to the coast [191]. The high uncertainty of their simplified fate model was linked to the variability of the fate mechanisms considered: degradation and sedimentation. This raised the need for the development of a more refined fate model, and subsequently CF model, to quantify MP potential impacts in the marine environment with less uncertainty and additional fate mechanisms and marine sub-compartments. To address this issue, a detailed fate and CF framework was proposed in Hajjar et al. (2023) [187] where the marine environment was divided into different sub-compartments at two different scales. Fate mechanisms influencing the distribution of microplastics within each sub-compartment were identified. Mechanistic rate and fate matrices were then constructed based on determined sub-compartments and fate mechanisms. Accordingly, mechanistic CFs for MPs emitted in the marine environment were then proposed by the multiplication of FFs and existing EEFs for each type of polymer (density, size, and shape). Operational FFs and CFs following this proposal are still missing.

In order to operationalize the proposed fate model, identified fate mechanisms should be quantified within a **K** matrix. Hajjar et al. (2023) [187] proposed different approaches and models that can be used. The Simplebox4plastics [2] is one of the multimedia models developed outside of Life cycle impact assessment (LCIA) scope, that quantifies the fate of plastics in various environmental compartments, including the marine environment. It accounts for the resuspension rates (from sediments to water) and burial rates (from sediments to deep layers) that can be adopted in the **K** matrix. They also quantify the transfer between marine water and sediments sub-compartments using a proposed water current velocity and particles sinking velocities [2]. However, these transfer rates depend on three-dimensional water currents and physical forces among which are the gravity force, buoyancy force, and the drag force [29], that were not accounted for in the Simplebox4plastics approach and need to be addressed. Consequently, numerical modeling, where water velocity fields in 3D are used, is an important tool used to predict the distribution of marine litter, such as microplastics [282]. Numerical modeling can be used to understand the variability of various parameters and fate mechanisms (e.g., dispersion, advection, biofouling, etc.), that vary spatially and temporarily, for different physical properties of MPs (size, density, shape). Thus, most influencing factors and parameters for MP three-dimensional transport in the marine environment can be identified. This step is essential to propose recommendations on how to simplify the fate model needed for LCIA. In addition, this will help determine the need to regionalize the proposed fate model and to categorize it based on the physiology of MPs, when operationalizing. Therefore, the main objectives of this article are:

1. Identify influencing parameters on the transfer rates of MPs between marine sub-compartments (e.g. water surface and water column) and understand their variability using numerical modeling

2. Test the sensitivity and the variability of quantified rates on the fate and characterization factors

In order to answer the second objective, two sub-objectives are defined: 1) complete and improve the modeling of fate mechanisms in marine sub-compartments, and 2) give recommendations for the categorization of FFs and CFs based on MPs physical properties and environmental factors.

7.3 Methodology

To achieve the objectives of this article, several steps are followed as summarized in figure 7.1

7.3.1 Quantification of intermedia transfer and degradation rates

In order to operationalize the mechanistic model proposed by Hajjar et al. (2023) [187], fate mechanisms identified in the mechanistic rate **K** matrix proposed are quantified. Depending on data availability, each intermedia transfer and degradation rate is quantified as presented in figure 7.1.

Sinking and sedimentation rates

Sinking and sedimentation rates depend on different marine mechanisms that vary with geographical locations and transport the particles at different speeds. Some of these mechanisms also depend on the physical properties of MPs. For this reason, as proposed by Hajjar et al. (2023) [187], numerical modeling is used to quantify these rates while testing the variability of all parameters on influencing the transport of MPs. There are essentially two complementary approaches in numerical modeling to estimate the pathway of marine litter in the ocean. The first one is based on Eulerian modeling which directly uses ocean velocity fields to track tracers in the oceans. However, it is mainly used for one- and two-dimensional setups to account for transport influenced by turbulent diffusion (i.e. vertical mixing), such as Enders et al. (2015); Kukulka et al. (2012) [36, 41] and Poulain et al. (2019) [126]. The second approach uses Lagrangian models which are commonly used in oceanography for computing the three-dimensional transport of virtual particles in the ocean (e.g. microplastics). These models use

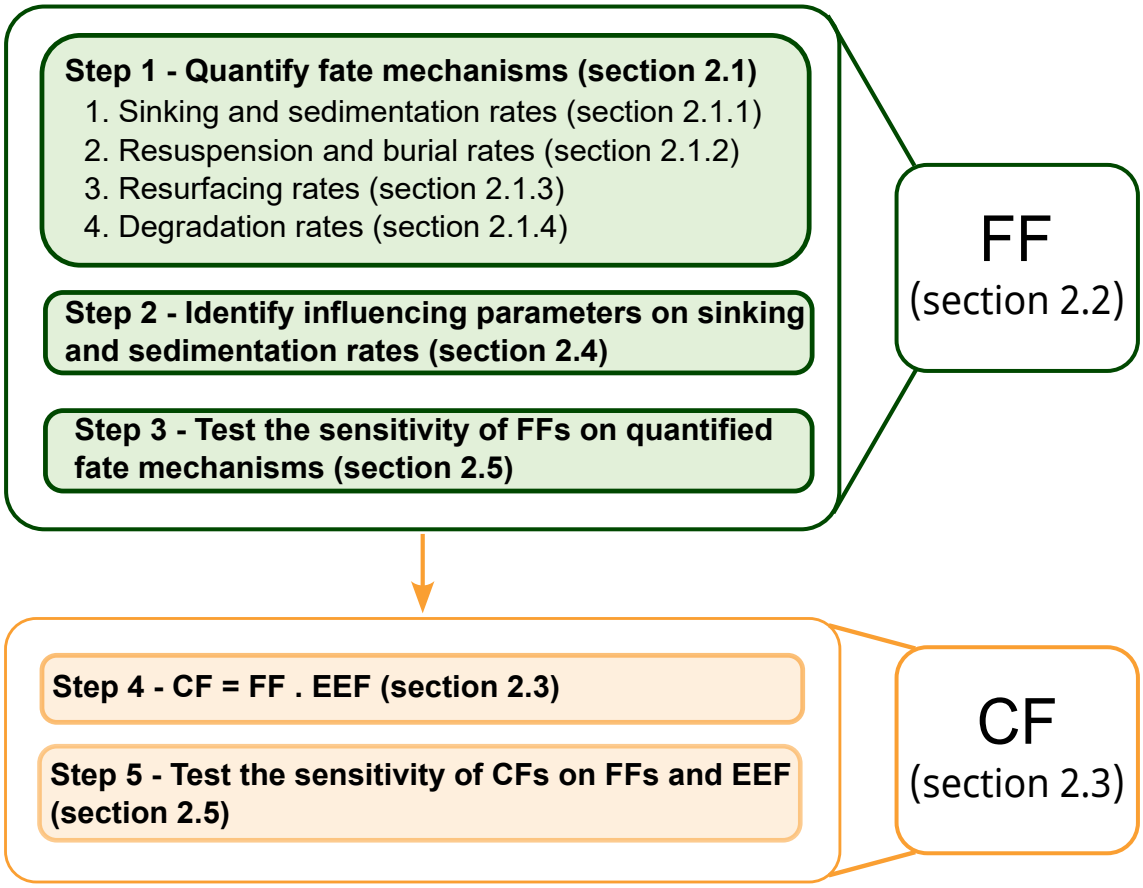

Figure 7.1 Overview of the methodology followed to quantify the fate mechanisms and test the sensitivity of different parameters

pre-computed spatial and time integrated Eulerian velocity fields from ocean general circulation models (OGCMs) [283]. Different Lagrangian numerical models have been developed to compute the distribution of floating marine litter including the effect of current, waves, and wind such as Jalón-Rojas et al. (2019) [12] and Lebreton et al. (2021) [284]. In these models, pre-computed Eulerian velocity is used to model the transport of virtual particles by integrating in time the spatially- and temporarily varying velocity fields [283]. Track Marine Plastic Debris (TrackMPD) is a 3D numerical Lagrangian model that tracks virtual MPs in the marine environment. It takes into consideration differences in environmental properties (i.e., dispersion, biofouling, etc.) and physical properties of MPs (size, shape, density) [12]. Therefore, TrackMPD is used since it is a comprehensive fate model that allows to identify most influencing parameters through testing the variability of several fate mechanisms while

accounting for the variability of MP physical properties. Details about the parametrization of TrackMP can be found in section (7.3.1).

Since TrackMPD model tracks the movement of particles in the marine environment, the time of transport is recorded. The rate of transfer from the water surface to the water column "sinking rate" ($k_{wc,ws}$) [day^{-1}] is thus calculated using the time it takes the particles to cross the depth of the water surface sub-compartment as defined in Hajjar et al. (2023) [187] at 6 meters, which is the average depth below which UV-A and UV-B, responsible for photooxidation, are absorbed, as follows:

$$k_{wc,ws} = \frac{1}{t_{wc,ws}} \tag{7.1}$$

Where $t_{wc,ws}$ [day] represents the transfer time from the water surface to water column sub-compartments. Because the particle might be transported up and down the 6 meters proposed during sinking, the time is recorded when particles cross the threshold for the last time.

Similarly, the rate of transfer from the water column to the sediments "sedimentation rate" ($k_{wc,ws}$) [day^{-1}] is calculated using the time of transfer from a depth of 6 meters until benthic sediments. Since TrackMPD uses velocity fields from Ocean General Circulation Models (OGCMs) that model water currents for real marine topography, particles would settle at different depths depending on their trajectory. In order to harmonize sediments depth at which particles settle with the depth of the water column proposed in [187] - which is 94 meters-, it is assumed that the particles settle in the water column at an average constant velocity and thus, the rate of transfer from the water column to sediments sub-compartments is calculated using a scaling ratio, as shown in equation 7.2:

$$k_{sed,wc} = \frac{D_{real}}{D_{wc}} \cdot \frac{1}{t_{sed,wc}} \tag{7.2}$$

where D_{real}/D_{wc} [-] represents the ratio of real settling depths to the depth as identified in the framework for the water column sub-compartment (94 meters) [187]. $t_{sed,wc}$ [day] is the sedimentation time from a depth of 6 meters to the real simulated benthic depths.

Resuspension and burial rates

Resuspension and burial rates are considered as advective processes occurring over the upper and bottom layers of sediments (as seen in figure S1). Little data exist about the quantification of MPs in marine benthic sediments. Following the hypothesis proposed by Quik et al. (2023) [2] that advective processes are independent of the substance properties or type, it is

assumed that MPs behavior is similar to those of sediment particles. Different studies have estimated the resuspension and burial velocities of sediment particles in different aquatic environments (freshwater [2, 285], lagoons [286] and lakes [287, 288]). The Simplebox4Plastics model [2] provides a specific plastics resuspension rate from marine benthic sediments which is adopted in this article. The Simplebox4Plastics model equally provides a burial rate for plastics in the marine sediments according to equation 7.3 below. This equation comes in accordance with the proposition of Hajjar et al. (2023) [187], which in turns harmonizes with the methodology of Praetorius et al. (2012) [270].

$$k_{burial} = \frac{\nu_{burial}}{h_{sediments}} \tag{7.3}$$

where v_{burial} [m/day] is the burial velocity from the sediments to deeper layers. $h_{sediments}$ [m] is the depth of the sediment sub-compartment taken as 10 cm as defined in Hajjar et al. (2023) [187].

The Simplebox4Plastics model defines a marine sediment compartment at a depth of 3 cm. Therefore, the burial rate is calculated from plastics burial velocity proposed by Simplebox4Plastics model and a sediment depth of 10 cm. The burial rate in the beach sub-compartment is assumed to be the same as the one in sediments sub-compartment.

Resurfacing rate

The rate of MPs transport from the beach back to the water - "resurfacing rate" - depends on various processes such as waves, beach slope, particle characteristics, etc. [33]. Quantifying this rate using numerical modeling, such as the TrackMPD model, is challenging as it requires a high resolution for the shoreline characteristics and the water currents close to it. For this reason, this rate is estimated based on literature studies where MPs are assumed to behave similarly to beach particles. Nevertheless, the resurfacing rate varies significantly with sand characteristics and is highly site-specific [289]. However, considering the lack of data, this rate is estimated based on Kamphuis et al. (1991) [208] where they created an artificial beach with wave propagation to estimate the rate of sediments transported from the beach to the water and the distribution of sediments at steady-state for a given sediment load, which led us to obtain a $k_{resurfacing}$ $[day^{-1}]$ by applying a mass balance. More details regarding the development of this rate are provided in section S1.1.2.

Degradation rates

Degradation rates (k_{deg} $[day^{-1}]$) are taken from Corella-Puertas et al. (2023) [19]. Since these rates are highly dependent on the physiology of the particles, Corella-Puertas et al. (2023) [19] developed degradation rates for different types of polymers of different shapes and sizes that are used in this article. In order to consider differences in degradation rates in different marine sub-compartments, fast rates are used for beach sub-compartment where the highest mechanical abrasion and exposure to UV lights occur [114]. Medium rates are used for the water surface and slow degradation rates are used for water column and sediment sub-compartments.

TrackMPD setup to calculate sinking and sedimentation rates

TrackMPD v.1 [12] is used to simulate the three-dimensional transport of virtual MPs. This model considers different transport mechanisms: advection, turbulence, biofouling, degradation, sinking, and deposition, for both macro-and microplastics. The mode of settings chosen to run TrackMPD is 5 where the simulations are run for different densities, shapes, and sizes. Biofouling parameters (biofouling density and biofouling rates) are not constant over time. Furthermore, due to the challenges in considering biofouling and degradation mechanisms at the same time, degradation is not quantified in this mode [12]. However, it is accounted for separately, as discussed in section 7.3.1. Due to the high computational time of the TrackMPD v.1 model, large global hydrodynamic data cannot be used. Therefore, it cannot be implemented to develop global transfer rates adequate for the global **K** matrix needed in LCIA. However, since the main objectives of this work are to address the variability of fate mechanisms and identify most influencing factors and properties on the fate of MPs (objectives 1 and 2), available regional data are used. These site-specific 3D velocity fields can provide a concrete scenario to test the variability and sensitivity of the parameters. Three-dimensional weekly-averaged velocity fields are obtained from the hindcasts of the US Northeast Coastal Ocean Forecasting System (NECOFS) nested in the Finite-Volume Community Ocean Model (FVCOM) that can be found in their databases (`http://134.88.228.119:8080/fvcomwms/`). The coastal domain is defined using data for the "Canadian Atlantic Coast" from the *Marine Region* database (`https://doi.org/10.25504/FAIRsharing.5164e7`). The dataset has a 50m resolution. Fifty virtual microplastic particles are released at three different locations (figure 7.2 and table S1) to account for the variability of ocean currents and topography. Emissions are done at a depth of 50 cm below the surface of the water. Releasing date is chosen to be the first of March 2010 to ensure sufficient simulation time and data availability.

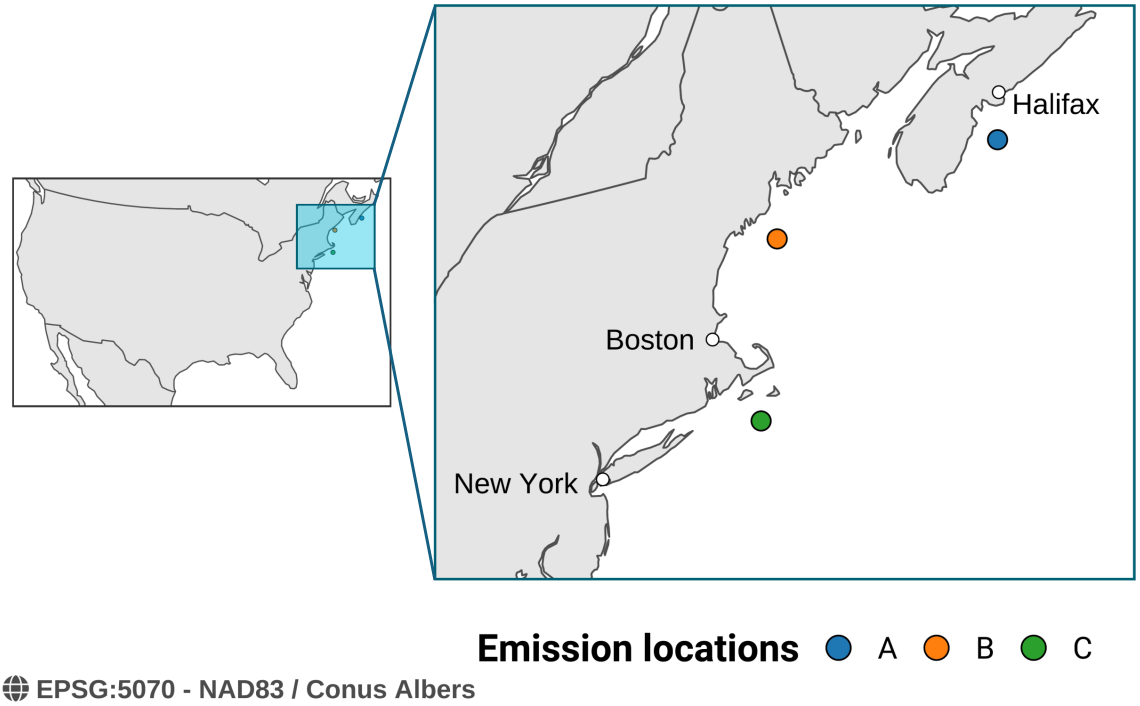

Figure 7.2 Emission locations of microplastics in the NorthEast of the US, used to run the simulations of TrackMPD

Hypotheses and assumptions for the development of the rate K matrix

Different hypotheses and simplifications were adopted for the development of the **K** matrix.

1. Hajjar et al. (2023) [187] identified two scales: continental and global. Thus, in order to operationalize this model, intermedia transfers between the two scales need to be quantified. However, since the objectives of this article are mainly to determine the influencing parameters on the transport of the particles as well as to test the variability and sensitivity of quantified rates on the **K** and **FF** matrices, only one scale is considered for simplicity. For this reason, the rate matrix, proposed in Hajjar et al. (2023) [187], is simplified to only represent single beach, water surface, water column and sediment sub-compartments. Accordingly, rate equations are simplified (as seen in matrix 7.4) and indices ".C" and ".G" used in [187] to indicate continental and global scales, respectively, are removed. Nevertheless, this distinction has to be addressed in future steps when developing regionalized and global **FF** and **CF** matrices.

2. The fragmentation of microplastics into nanoplastics involves different mechanisms and factors which are outside the scope of this article. It has also been shown that the fragmentation of microplastics into nanoplastics is much smaller than the degradation of

microplastics [290]. In addition, according to Lavoie et al. (2021) [20], effect factors developed account for the impacts of both micro- and nanoplastics inseparably. Therefore, the fragmentation of micro- into nanoplastics is not quantified in the **K** matrix.

3. While marine organisms can play a role in the transport of microplastics from the water surface to the bottom sediments [187], this transport rate is not quantified in this article due to the complexity of interacting mechanisms and the lack of available data needed to document them. However, it remains an aspect to be developed.

4. Aggregation was identified as the transport of MPs through attachment to marine snows [187]. Little data is known regarding this mechanism and therefore, it is assumed that biofouling is the main mechanism altering the density of MPs in the marine environment. Therefore, the aggregation rate is not quantified in this article.

5. TrackMPD accounts for biofouling while tracking the transport of microplastics in the marine environment. Therefore, the rate of biofouling is not quantified separately but rather considered within sinking and sedimentation rates.

6. Low density MPs might resurface from the water column to the water surface following defouling in the marine water [42]. However, it is difficult to quantify this behavior and little data exist to represent it. Therefore, as proposed in Hajjar et al. (2023) [187], it is assumed that once biofouling begins and the particles' densities start to increase, no defouling occurs and the particles keep on sinking from the water surface to the water column arriving to the sediments. Therefore, the rate of transfer from the water column back to the water surface is set to zero.

7.3.2 Rate and fate matrices

Following on these assumptions, the simplified **K** matrix is presented below:

$$\mathbf{K} = \begin{bmatrix} -k_{b,tot} & k_{b,ws} & 0 & 0 \\ k_{ws,b} & -k_{ws,tot} & 0 & 0 \\ 0 & k_{wc,ws} & -k_{wc,tot} & k_{wc,sed} \\ 0 & 0 & k_{sed,wc} & -k_{sed,tot} \end{bmatrix} \tag{7.4}$$

Zero values represent sub-compartments that are not in contact with each other and thus do not interact. For instance, there is no transfer to the sediments from an emission in the beach without passing through the water surface and column. Therefore, the rate $k_{sed,b}$ holds a zero value. Intermedia transfer and degradation rates are quantified as explained in sections 7.3.1, 7.3.1, 7.3.1, 7.3.1 and summarized in table 7.1. Based on the assumptions presented before, the transfer rate from the water surface to the water column ($k_{wc,ws}$) and from the water column to the sediments ($k_{sed,wc}$) represent sinking and sedimentation rates implicitly influenced by water currents and biofouling.

Table 7.1 Summary of the different fate mechanisms quantified in the rate **K** matrix

Mechanism	Rate	Equation or Reference	Spatial definition
Transfer rate from water surface to water column	$k_{wc,ws}$	Equation 7.1	Spatially modelled in TrackMPD
Transfer rate from water column to sediments	$k_{sed,wc}$	Equation 7.2	Spatially modelled in TrackMPD
Resuspension rate	$k_{resuspension}$	[2]	Global average assumption
Burial rate	k_{burial}	Equation 7.3	Global average assumption
Resurfacing rate	$k_{ws,b}$	Section S1.1.1	Global average assumption
Degradation of microplastics	$k_{i,deg}$	[19]	Global average assumption

Total removal rates ($k_{i,tot}$), which are diagonal elements, are simplified as follows:

$$\begin{aligned} k_{b,tot} &= k_{b,deg} + k_{ws,b} + k_{b,burial} \\ k_{ws,tot} &= k_{ws,deg} + k_{b,ws} + k_{wc,ws} \\ k_{wc,tot} &= k_{wc,deg} + k_{sed,wc} \\ k_{sed,tot} &= k_{sed,deg} + k_{wc,sed} + k_{sed,burial} \end{aligned} \tag{7.5}$$

Where "b" represents beach sub-compartment., "tot" and "deg" indicate total removal rates and degradation rates, respectively.

The fate matrix [$kg_{compartment}$ per $kg_{emitted}/day$] is then obtained by inverting the **K** matrix [day^{-1}] [185]. The fate matrix has the same size as the rate matrix (matrix 7.4). Off-diagonal elements represent the mass increase of MPs in each receiving sub-compartment (row) after an emission in the emission sub-compartment (column). Diagonal elements represent the residence time of MPs in the considered sub-compartment.

7.3.3 Characterization factors

CF matrices [$PAF.m^3.d/kg_{emitted}$] are obtained by the multiplication of **FF** matrices with updated exposure-effect factors (equation 7.6). Based on the latest recommendations of the

USEtox group for ecotoxicity [209], EEFs are based on the hazardous concentration (HC20) obtained as the geometric mean of EC10s (hazardous concentration affecting 20% of species based on their EC10s. $HC20_{EC10}$ is derived from a species sensitivity distribution (SSD) curve of EC10s [209] - EC10s represent the concentrations affecting 10% of species) [19, 209]. A single EEF (EEF = 38.4 $PAF.m^3/kg$) for all MP categories is used to account for the physical impacts of MPs because the physiology of the particles does not have a significant influence on the EEF [20]. EEFs are only applied for water sub-compartments (water surface and water column) since only studies on aquatic species were used for their development [19, 20]. Therefore, only CFs for water sub-compartments are obtained in order to test their sensitivity on quantified fate mechanisms and EEF used.

$$CF = FF.EEF \tag{7.6}$$

7.3.4 Identification of parameters influencing sinking and sedimentation rates

As presented in section 7.3.1, transfer rates in the marine environment are influenced by several factors that depend on geographical locations and the physical properties of MPs. In order to understand the most influencing parameters on the transport of MPs between marine sub-compartments, all variables that can be modified in TrackMPD (see section 7.3.1 for model setup) are tested. The variability of the water surface density and the biofouling density was neglected because the density of the seawater surface doesn't vary greatly and limited data exist for the biofouling density. Variables tested include the physiological properties of the particles (size, density and shape), biofouling rate, horizontal and vertical dispersion. Physical properties have a wide variability ranging from 1µm to 5mm [24] in size and from positively buoyant to negatively buoyant in density. Other environmental properties include the horizontal (kh) and vertical dispersion (kv) to account for ocean turbulence. Limited data exist on these coefficients, and they are highly site-specific [291]. Biofouling rate is important to be tested, as it is a key mechanism in the settling of positively buoyant particles [29]. The celerity of biofouling does not only vary with the size of MPs, where smaller particles are biofouled faster than larger ones, but also depends on geographical locations [13, 287]. In order to address the individual influence and the interactions of these parameters that have wide variability, a simulation plan is developed. Because of the high computation time required for each simulation using TrackMPD, a half fraction design is developed based on Dunn et al. (2022) [292]. Each variable is tested between a minimum and a maximum value, as presented in table 7.2, to cover the entire range of most common values found for each variable. Density values were chosen for foamed expanded polystyrene (EPS)

and polyethylene terephtalate (PET) to represent low- and high-density particles. Cylindrical and spherical shapes are tested. The size of spherical particles was chosen to represent the upper and lower limits of microplastics size class as adopted in Woods et al. (2021) [24]. Cylindrical particles were chosen to represent the largest and smallest fibers for microplastic particles [18]. The values of environmental properties, i.e., biofouling rate and horizontal and vertical dispersion, were chosen according to the lowest and highest values found for different ocean locations. For dispersion coefficients, vertical dispersion is much lower than horizontal dispersion but can vary with one order of magnitude between the globally averaged value ($1 \times 10^{-4} m^2/s$) and the directly observed value in the oceans ($1 \times 10^{-5} m^2/s$) [203]. These two values, which are common values observed in marine systems [12, 203], are taken as the maximum and minimum values for kv. Horizontal dispersion varies with space and time [293]. It can reach a value of $10^4 m^2/s$ with high spatial variability [203]. The true value of this coefficient is unknown [291]. However, in the shallow coastal marine environment, kh could range between 5 and $20 m^2/s$ [291]. In order to represent a certain variability in ocean turbulence, these values are taken as minimum and maximum values.

Table 7.2 Minimum and maximum values for variables tested in the simulation plan

Parameter	**Minimum Value**	**Maximum Value**	**Units**	**Reference**
Density	0.379	1.37	g/cm^3	[12]
Shape	Sphere	Cylinder	$(-)$	
Size				
-Sphere	$D = 1.0E{-}03$	$D = 5$	mm	[24]
-Cylinder	$D = 1.0E{-}03$	$D = 1.0E-01$	mm	[19]
	$L = 1.0E-01$	$L = 5$	mm	
BR	$1.0E{-}07$	$1.0E{-}05$	m/d	[12]
kh	5	20	m^2/s	[293]
kv	$1.0E{-}05$	$1.0E{-}04$	m^2/s	[203]

A total of 32 simulations were run with different sets of minimum and maximum values for each variable as detailed in section S1.3. MPs are tracked until they reach the sediments (preliminary results showed that none of the emitted particles reached the beach). The time taken by the particles to pass from the surface to the sediments (settling time) is then recorded for each particle in each run. Based on this output, the median value of the particles emitted per run in the full region tested is initially taken. Based on linear modeling "least-square model", the coefficient of each parameter describing the magnitude of influence of each variable on the output is obtained. A Pareto plot is then constructed to represent the magnitude of effect, in absolute, of each parameter on the settling time of MPs. Similarly, a

median value for every particle emitted at each emission location (see section 7.3.1) is used to construct a regional Pareto plot to understand the influence of water dynamics. More details on the construction of the simulation plan and the Pareto Plot is found in Section S1.3. The model setup and descriptions of simulations are explained in section 7.3.1.

7.3.5 Sensitivity analysis

In addition to understanding the influence of MPs physical properties and environmental properties on the settling of the particles, it is important to understand the influence of the other rates quantified in section 7.3.1 on the fate factors (e.g. the influence of the degradation, resuspension, burial, etc. rates on the the fate factors). For this reason, a sensitivity analysis is done on different rate matrices developed per simulation (section 7.3.4). In order to better understand the influence of fate mechanisms for different MPs tested and based on the results of section 7.3.4), the 32 TrackMPD simulations run to quantify the sinking and sedimentation rates are classified based on MPs physical properties (size, shape, and density) defined in table 7.2. As a result, eight MP categories are obtained with four simulations in each category (as presented in table S3). Accordingly, eight rate **K** matrices are obtained. For each category, sinking and sedimentation rates are obtained according to equations 7.1 and 7.2 with transfer times recorded for the four simulations of each category. Table S3 summarizes the number of simulations per category and respective degradation rates as taken from Corella-Puertas et al. (2022) [18]. Since little data exist on the resurfacing rate, a single value is used for all eight categories (section 7.3.1). Resuspension and burial rates are the same for all categories as well since these rates are independent of the particle's physiology [2].

For each microplastic category, a 10% increase on each quantified rate mechanism is tested consecutively. A new rate **K** matrix, and subsequently FF matrix, are then obtained. A matrix showing the relative differences between the original and the new FF matrix is then calculated as follows:

$$FF_{i,percentage} = \frac{|FF_{i,original} - FF_{i,10\%}|}{FF_{i,original}} \times 100 \tag{7.7}$$

Where $FF_{i,percentage}$ is the percentage of influence on the FF matrix of each microplastic category i, $FF_{i,original}$ the original fate matrix, and $FF_{i,10\%}$ the new fate matrix obtained after the 10% increase on each rate mechanism. Similarly, the percentage CF matrix for each microplastic category is obtained to account for the influence of fate mechanisms on the characterization factors. In addition, the sensitivity of effect factors (EF_{ws} and EF_{wc}) are analyzed, by consecutively adding 10%, to compare it with the influence of fate mechanisms

on the CFs.

7.4 Results

After quantifying all required rates, as described in section 7.3.1 and presented in table S3, including the sedimentation and sinking rates needed to build the fate matrix and do the sensitivity analysis, the results are presented in the following order: section 7.4.1 - Identification of parameters influencing sedimentation and sinking rates; section 7.4.2 - Sinking and sedimentation time; section 7.4.3 - the variability of fate factors with tested parameters; section 7.4.4 - the variability of characterization factors with MP physical properties and environmental parameters; and section 7.4.5 - Sensitivity analysis. All quantified rates used for the construction of rate and fate matrices are presented in table S3.

7.4.1 Identification of parameters influencing sedimentation and sinking rates

The Pareto plot obtained for the entire region (emission points A, B, and C combined) is presented in figure 7.3 (a) below. As it is shown, the physiology of the particles has a significant influence on their settling time. This emphasizes the need of categorizing FFs and CFs based on MPs physical properties to account for the variability linked to them. The interactions between the variables tested also have an influence on the settling time and their importance can be greater than that of individual parameters. While density is the third most influencing parameter, the size of the particles is of least significance. However, the influence of their interaction (density:size) is of the most significance on the settling time. This can be explained by the fast biofouling and thus, the settlement of smaller buoyant MPs compared to larger ones due to their higher surface area-to-volume ratio [29, 57]. In addition, the effect of MPs physical properties has a negative coefficient, which means that increasing those parameters from their minimum values to their maximum values reduces the settling time. This is supported by a higher settling velocity of larger, dense MPs compared to smaller ones [42]. Biofouling rate (BR) and vertical dispersion (kv) also show an important influence on the fate by reducing their settling time (negative coefficient). While horizontal dispersion (kh) has a low influence as an independent parameter, its interaction with other environmental and physical properties is an important effect (i.e., density:kh:kv). Comparing the interactions of different parameters, it can be seen that the interactions among environmental properties are of lower significance compared to their interactions with the physical properties of the particles. Horizontal and vertical dispersion are influenced by the water currents, hence vary geographically. This is also the case for biofouling rate which may be influenced by the water temperature, and algal concentrations and bloom [57]. The variability related to

those parameters suggests the relevance of regionalizing the proposed framework and the characterization factors in future steps.

Although the order of importance slightly changes among the three emission locations (figure 7.3 (b), (c) and (d)), the same conclusions still hold. The density, BR, and the interaction between the density and the size, remain the most influencing parameters; however, their order of influence might vary. It can also be noticed that the magnitude of effect of parameters in location A is larger than that of point B and C. This can be linked to the topography of the region where particles settle deeper when emitted in point A compared to points B and C. Therefore, they would require more time to reach the sediments.

7.4.2 Sinking and sedimentation time

Figure 7.4 presents the sinking ($t_{wc,ws}$) and sedimentation ($t_{sed,wc}$) times for each of the eight categories of MPs (see section 7.3.5). Settling and sedimentation times for high density (HD) big (B) spherical (Sp) and cylindrical (Cy) particles ($1.11E-02$ day for Sp-HD-B and $2.53E-01$ day for Cy-HD-B) are negligible compared to other categories because they have higher settling velocities than other particles. Thus, they settle within minutes in coastal shallow regions. Low density (LD) small (S) particles have almost similar settling times as high density small ones of the same shape. This is due to the rapid biofouling of small particles having high surface area-to-volume ratio. As a result, they become negatively buoyant in a short time and start settling in a manner similar to that of high density particles. This also supports longer sedimentation (from water column to sediments) compared to sinking (from water surface to water column) for all impact categories, except for low density big spherical and cylindrical particles (Sp-LD-B and Cy-LD-B). The latter two categories spend more time at the water surface (15.7 days and 3.24 days) than in the water column (8.11 days and 1.47 days) due to slower biofouling for large particles compared to smaller ones. It is also noticed that Cy-LD-B particles spend significantly less time in water compared to spherical ones (Sp-LD-S) because spherical particles have the minimum surface area of all particle's shapes. Therefore, their fouling time, which is linearly dependent on the characteristic length scale of the particle, is two orders of magnitudes slower than that of cylindrical shapes [29]. Therefore, they start sinking sooner. The settling behavior of cylindrical particles vary with the density of the particles but shows no differences in reference to their size. This can be due to the settling velocity equation, used in TrackMPD, which is based on Khatmullina et al. (2017) [206] where cylindrical particles depend on the size unlike spherical particles that depend on both size and shape.

In addition to settling and sinking times, it can be noticed that the depth at which the

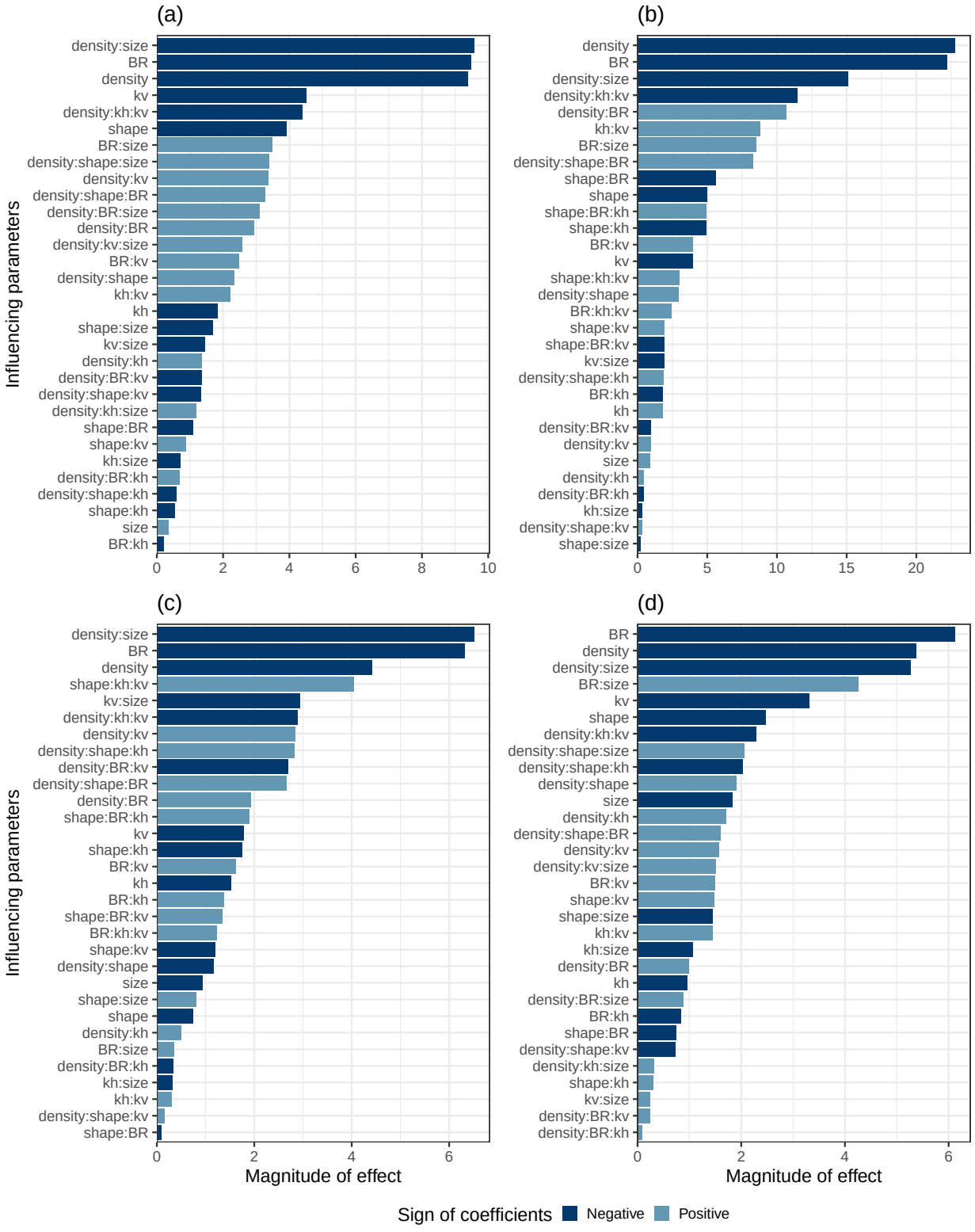

Figure 7.3 Pareto plot showing the influence of parameters and their interactions on the settling time of MPs in the full region tested (a), emission location A (b), emission location B (c), and emission location C (d) (i:j represents the interactions between parameters i and j). kh: horizontal dispersion, kv: vertical dispersion, BR: biofouling rate

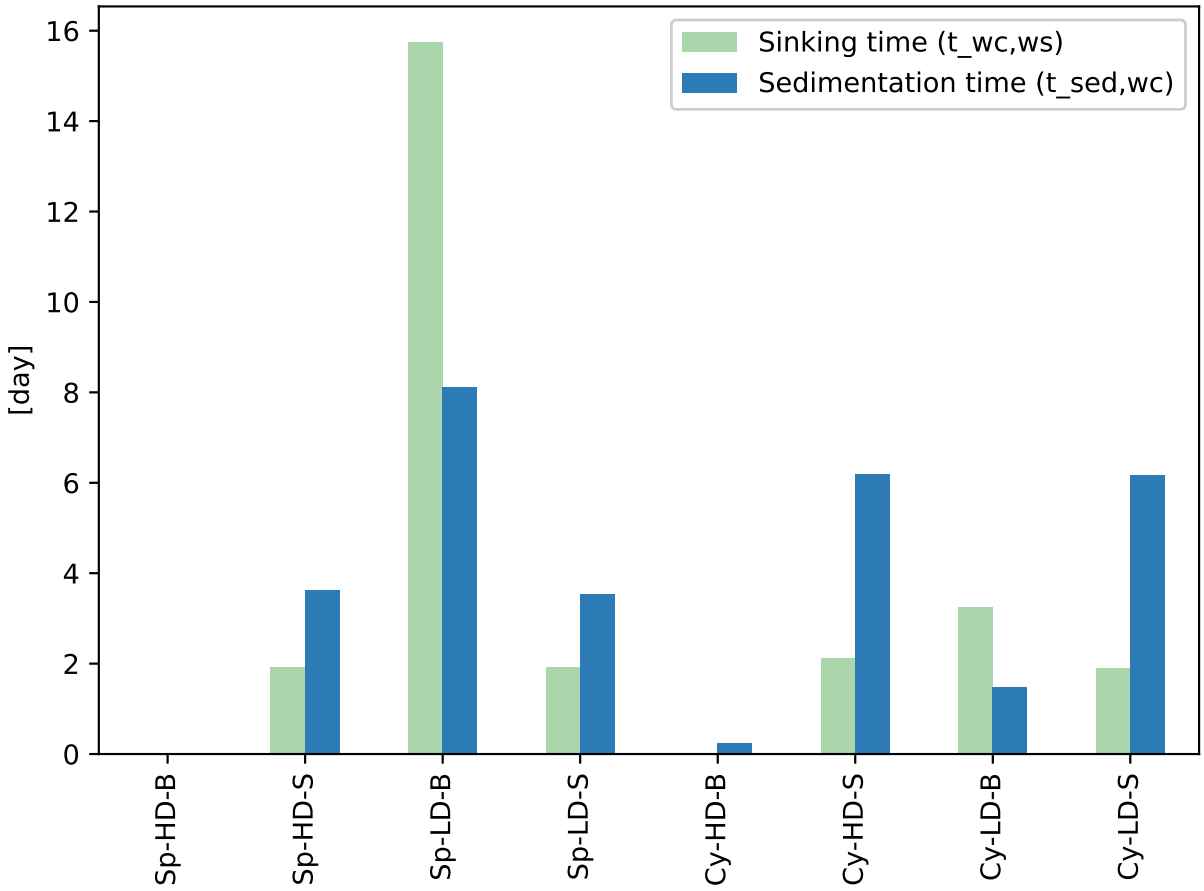

Figure 7.4 Transfer time between water sub-compartments for each MPs category (Sp and Cy represent spherical and cylindrical shapes, HD and LD indicate high and low densities, and B and S indicate big and small particles)

particles reach the sediments, in all 32 simulations, is less than 100 meters. According to Hajjar et al. (2023) [187], the depth of the continental scale is defined at a depth of 100 meters maximum. This indicates that these particles have settled in the continental scale. However, upon calculating the horizontal distance at which the particles have reached the sediments, it can be noticed that some particles have settled at a distance larger than 60km from the coast. According to Hajjar et al. (2023) [187], the global scale is defined at a distance larger than 60km from the coast, which indicates that these particles might have reached the global scale. If the distance from the coast is taken as a criteria, the particles would be considered moved to the global scale however, if the depth of the continental scale is taken as a criteria, the particles would be considered settled in the continental scale. Therefore, a redefinition of the continental and global scales is required according to the depth of the water compartments and the distance from the coast. These two parameters spatially vary, which supports the

need to regionalize the **FF** matrix and the size of marine sub-compartmental boxes according to the topography of the region (depth of the water sub-compartments) and the distance from the coast. The results of all 32 simulations, including the calculated horizontal distance, can be found in the supporting information (excel workbook).

7.4.3 The variability of fate factors with tested parameters

All fate matrices can be found in section S2.2. Table 7.3 presents minimum and maximum FF values among microplastic categories. The residence time of MPs in the beach ($FF_{b,b}$) varies between $3.64E-01$ day for Sp-HD-S and $2.22E+00$ days for spherical low density big (Sp-LD-B) particles. $FF_{b,b}$ is mainly controlled by the degradation of the particles on the beach as there is no transfer from the water surface to the beach in the region where the simulations are held, and the same values for burial and resurfacing rates are applied for all types of MPs. Spherical small PET particles have the highest degradation rate (2.3 day^{-1}) compared to other categories while spherical big EPS particles degrade the slowest ($2.63E-04$ day^{-1}) [19] and therefore, remain the longest on the beach. $FF_{ws,b}$ is the fate factor that represents the mass increase of microplastics in the water surface for an emission to the beach. It is also viewed as the product of a transfer fraction from the beach to the water surface ($f_{b\rightarrow ws}$) and the residence time in the water surface $FF_{ws,ws}$. This factor ranges between a minimum of $4.9E-04$ day for spherical high density particles (Sp-HD-B) and a maximum of $15.75E+00$ days for spherical low density big particles (Sp-LD-B). This is explained by the residence time in the water surface mainly driven by the sinking rate ($k_{wc,ws}$) since the degradation in the water is significantly slower. The sinking rate is the highest for high density big particles that settle the fastest among MP categories while low density big particles spend more time at the surface before starting to settle (figure 7.4). Similarly, $FF_{wc,ws}$ ranges between a minimum value of $8.7E-02$ day corresponding to Sp-HD-B and a maximum value of $150.8E+00$ days corresponding to Sp-LD-B. This is linked to the residence time in the water column mainly driven by the sedimentation time that is the highest for high density big particles while it is the slowest for low density big ones (figure 7.4). $FF_{sed,b}$, $FF_{sed,ws}$, and $FF_{sed,sed}$ indicate the tendency of MPs to reach the sediments after an emission to the beach, water surface, and water column through direct (if applicable) and indirect intercompartmental exchanges. Indirect transfer occurs via the water surface and the water column. These factors are significantly larger than other FFs due to high residence time in sediments $FF_{sed,sed}$ which is in turn significantly larger than the residence time in other sub-compartments. This is explained by fate mechanisms responsible for the removal of MPs from the sediments. As explained in section 7.4, microplastics reaching the sediments are either buried in deep layers at a burial rate of $2.4E-05$ day^{-1}, resuspended

into the water column at a resuspension rate of $2.3E-04\ day^{-1}$, or degraded through slow biodegradation (e.g. $4.4E-09\ day^{-1}$ for Sp-HD-B). All these mechanisms take a long time to occur compared to settling and therefore, lead to the accumulation of MPs in benthic surfaces.

Figure 7.5 presents the residence time of microplastics in the sediments for the various categories tested. It can be noticed that these factors vary mainly with the size of the particles regardless of their shape and density. Naturally, bigger MPs demonstrate longer residence time compared to smaller ones which degrade faster. Spherical big high (Sp-HD-B) and low density particles (Sp-LD-B) remain in the sediments for 41659 and 41644 days, respectively, while smaller ones (Sp-HD-S and Sp-LD-S) stay for 21775 and 11140 days. Similarly for cylindrical big high (Cy-HD-B) and low density particles (Cy-LD-B), the residence time in marine sediments ($FF_{sed,sed}$) is 41883 and 40828 days, while smaller ones (Cy-HD-S and Cy-LD-S) remain in the benthic zone for 24723 and 13634 days, respectively. This is related to the degradation rate being inversely proportional to the size of the particles [19]. The bigger the particle, the longer it takes to degrade and therefore, reside longer in sediments. The fate of microplastics is driven by various mechanisms that are greatly influenced by the physiology of the particles. While settling depends on the size, shape, and density of the particles, degradation depends on their size and polymer type. All of them lead to different fate factors and residence times. Therefore, it is important to distinguish differences linked to the physical properties of emitted MPs when developing the fate **FF** matrix. Rate and fate matrices for all 32 simulations as well as the eight categories are presented in supplementary information.

Figure 7.6 presents the distribution of MPs for an emission to beach sub-compartment at steady-state (based on the FF which gives the quantity accumulated in each compartment at steady-state for a given rate of emission in the emission compartment). It is obtained as the mass fraction in the receiving sub-compartment for an emission to the beach sub-compartment. This is equivalent to dividing the fate factor (e.g., $FF_{ws,b}$) by the sum of factors in the beach sub-compartment column ($\sum FF_{b,j}$, where j is the receiving sub-compartment). Almost 100% of MPs remaining in the system at steady-state is accumulating in benthic

Table 7.3 Minimum and maximum FF values [days] among all microplastic categories

	Beach	**Water Surface**	**Water Column**	**Sediments**
Beach	(3.6E-01 - 2.22E+00)	(0 - 0)	(0 - 0)	(0 - 0)
Water Surface	(4.9E-04 - 15.74)	(4.94E-04 - 15.75)	(0 - 0)	(0 - 0)
Water Column	(8.7E-02 - 150.7)	(8.7E-02 - 150.8)	(8.7E-02 - 150.8)	(7.9E-02 - 136.4)
Sediments	(2.8E+03 - 4.2E+04)	(1.1E+04 - 4.2E+04)	(1.1E+04 - 4.2E+04)	(1.1E+04 - 4.2E+04)

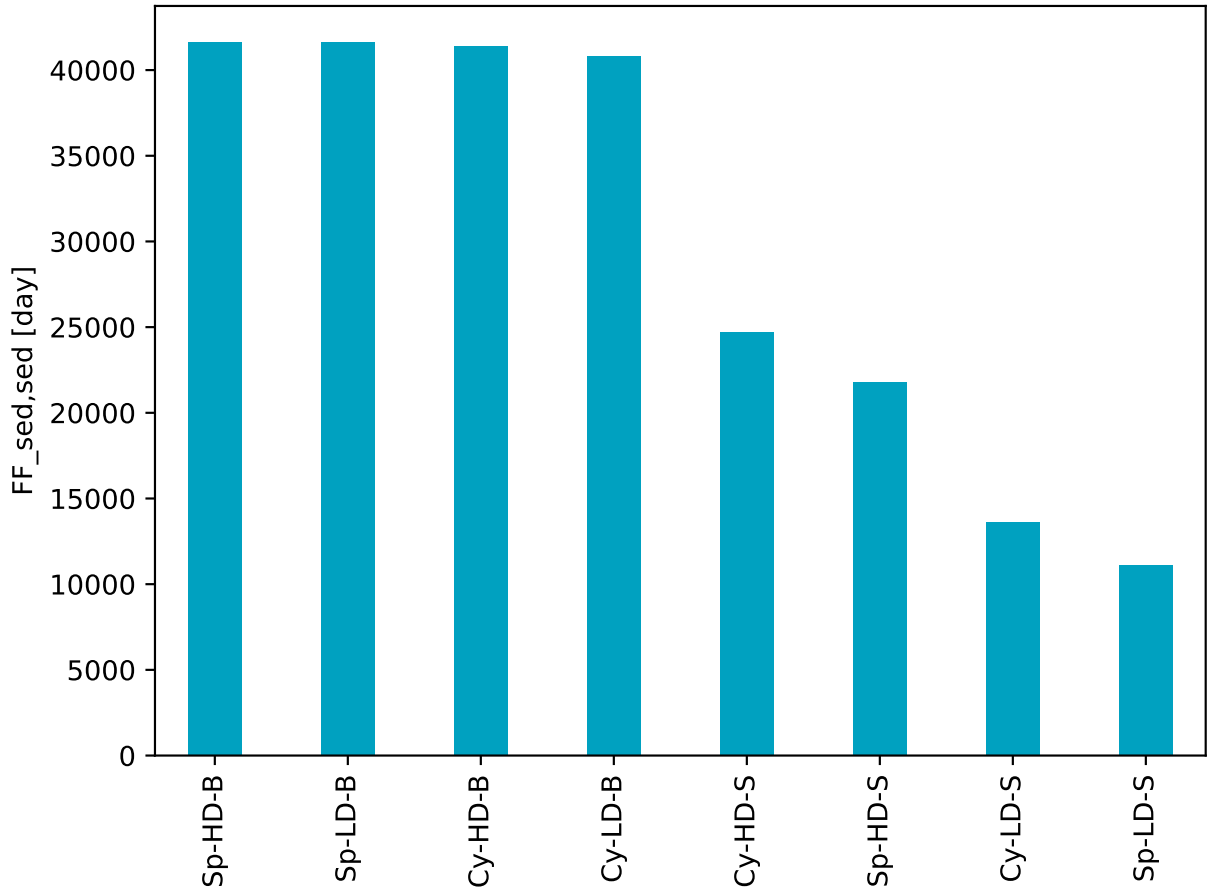

Figure 7.5 Residence time in sediments for all microplastic categories [day]

sediments for all categories. The percentage that accumulates in water sub-compartments is several orders of magnitude smaller. For instance, because of their high settling velocity, $1.2E-06\%$ and $2.1E-04\%$ of spherical high density big microplastics (Sp-HD-B) have a longer residence time in water surface and water column sub-compartments, respectively. Spherical low density big MPs (Sp-LD-B), that take the longest time to exceed water density and start settling compared to other categories (figure 7.4), also accumulate at steady-state in majority in sediments with a percentage of 99.6%. Percentages in beach (0.005%), water surface (0.04%), and water column (0.4%) are also considered negligible. Comparing spherical to cylindrical shapes, the same conclusions can be seen with smaller values for cylindrical particles due to faster biofouling and shorter residence time in water sub-compartments (figure 7.4). All microplastic categories accumulate at steady-state in sediments no matter the emission sub-compartment (all distribution matrices are presented in table S6) where they reside for a long period of time (as shows their residence time in the sediment, which

corresponds to the fate factor from sediment to sediment in the matrices presented in table S5). This emphasizes the importance of refining the fate and effect modeling in this sub-compartment in future steps to better examine the consequences on benthic species due to long exposure.

7.4.4 The variability of characterization factors with MP physical properties and environmental parameters

Table 7.4 demonstrates minimum and maximum CF values among MP categories for water surface and water column sub-compartments. All CF values for all MP categories and all sub-compartments are presented in table S7. The maximum value (6397.1 $PAF.m^3.d/kg$) is for spherical low density big particles that are the slowest to leave the water surface. The lowest impacts (3.35 $PAF.m^3.d/kg$) are for the particles that spend the shortest period of time in the water due to fast settling. Since the same value for the effect factor (38 $PAF.m^3/kg$ [19]) is used in the water surface and water column, differences in CFs are mainly linked to the fate factors. Therefore, the variability of the CFs is mainly linked to the variability of microplastic physical properties and environmental properties.

In order to analyze the influence of environmental parameters, eight sets of categories, based on the environmental properties tested, are defined (table S8). Details on how these categories are developed can be found in section S2.3.1. Since degradation rates, needed for the construction of the rate matrices, are polymer-specific, various rates are considered within the same environmental category set. In order to avoid the confusion with the influence of microplastic physical properties on the fate, the analysis of the influence of environmental properties is based on the characterization factors. Average, minimum and maximum CFs for each category are presented in figure 7.7. Since the same effect factor is applied to the water surface and the water column, the variability of the characterization factors is linked to the fate factors, that vary with differences in environmental properties among the categories (kh, kv, BR). It can also be noticed that within each category, characterization factors vary with several orders of magnitude for every emission compartment (vertical black lines in figure 7.7 starting from the minimum to the maximum CFs within each category and for every emission sub-compartment). CFs for the beach and sediment sub-compartments can

Table 7.4 Minimum and maximum characterization factors for MPs emitted in the water surface and water column sub-compartments

	Water surface	**Water column**
CF $[PAF.m^3.d/kg]$	3.37E+0 - 6.4E+03	3.35E+0 - 5.79E+03

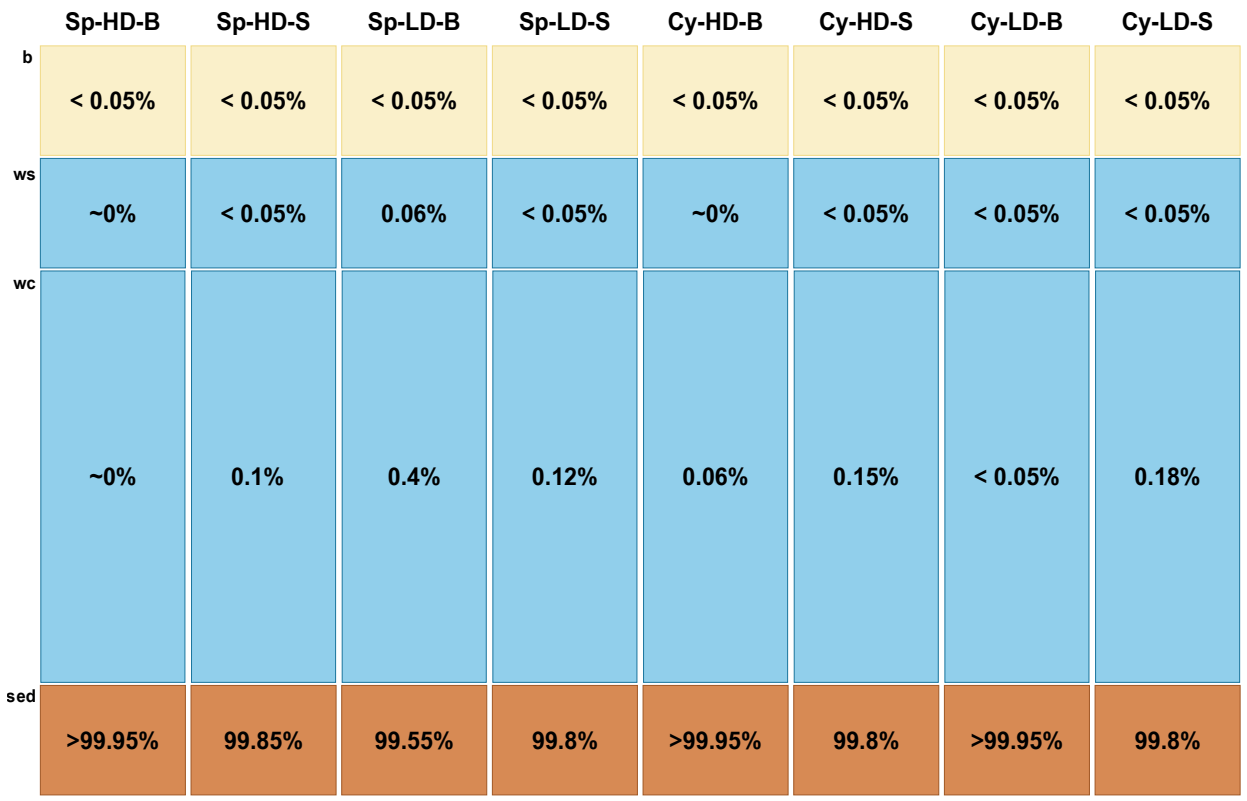

Figure 7.6 Percentage of distribution of microplastics, at steady-state, for an emission in beach sub-compartment (b: beach, ws: water surface, wc: water column, sed: sediments / Sp and Cy represent spherical and cylindrical shapes, HD and LD indicate high and low densities, and B and S indicate big and small particles)

be found in figure S4. These differences are mainly linked to the physiology of the particles. However, comparing differences between categories, it can be observed that the variability of these environmental parameters influences the CFs which emphasizes, once again, the relevance for regionalization to account for the spatial variability of these parameters. The influence of all the environmental properties on the characterization factors can be found in the supplementary information (section S2.3.1).

7.4.5 Sensitivity analysis

Figure 7.8 presents the result of the sensitivity analysis for the spherical low density small particle category "Sp-LD-S". A 10% increase in the burial rate results in a larger influence on the residence time in the sediments ($FF_{sed,sed}$) with a 2.6% decrease. Consequently, $FF_{sed,b}$, $FF_{sed,ws}$, and $FF_{sed,wc}$ obtained as the product between the residence time in the sediment (receiving sub-compartment) and the transfer fraction from an emission sub-compartment

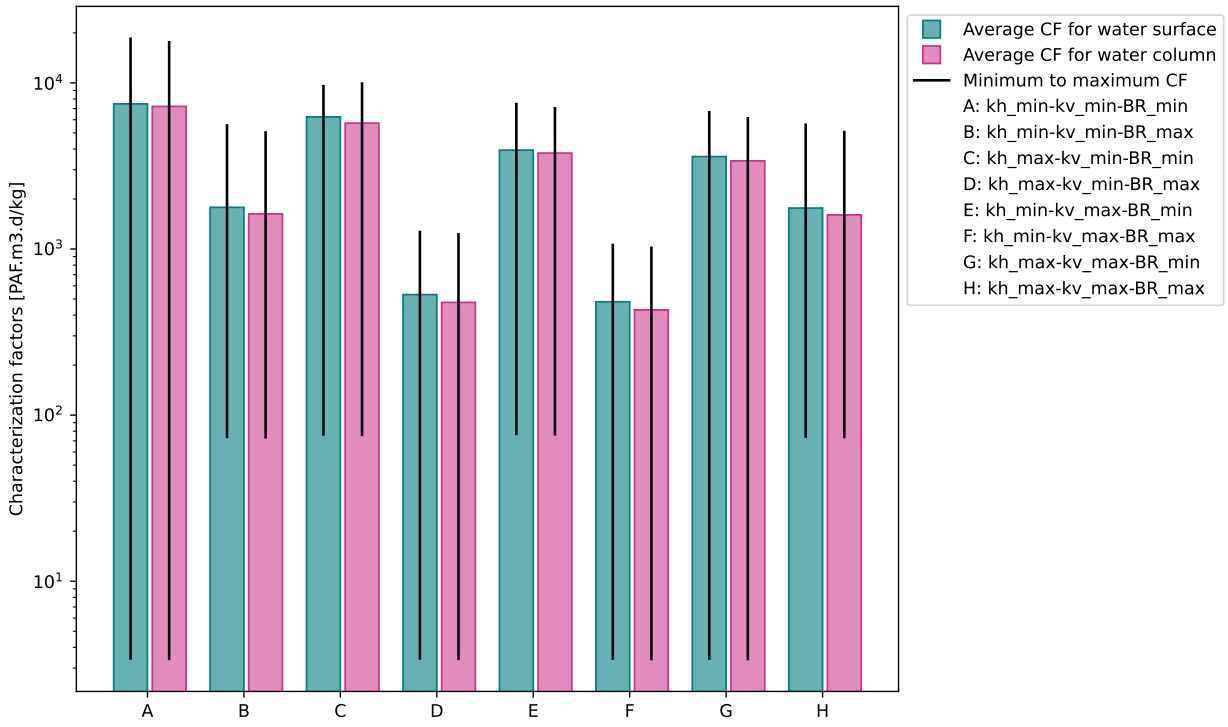

Figure 7.7 Average, minimum and maximum characterization factors $[PAF.m^3.d/kg]$, in log scale, classified based on a fixed set of environmental parameters. Vertical lines represent the minimum and maximum CFs for each category and for the water surface and water column sub-compartments. Kh: horizontal dispersion, kv: vertical dispersion, BR: biofouling rate, min: minimum, max: maximum

(beach b, water surface ws, and water column wc) to a receiving one ($FF_{j,i} = FF_{j,j} \times f_{j,i}$), are influenced by the change in the burial rate. In addition, an increase in the burial rate indicates that less MPs are resuspended into the water column due to burial in sediments. As a result, the residence time in the water column ($FF_{wc,wc}$) is affected by 1.9%, as well as $FF_{wc,ws}$.

Three degradation rates (fast, medium, slow) are used in the construction of the rate matrices (section 7.4). An increase in the fast degradation significantly reduces the residence time in the beach by 6.9%. A faster degradation in the beach implies a smaller fraction of microplastics transferred to the water surface, water column, and sediments. Thus, $FF_{ws,b}$, $FF_{wc,b}$, and $FF_{sed,b}$ are also influenced by 6.9%. An increase in the medium degradation at the water surface slightly affects the residence time in the water surface and therefore, doesn't affect related factors. This is because the particles will leave the water surface, due to faster sinking rate, before they have time to degrade. An increase in the slow degradation reduces the residence time in the water column and sediments. This is explained by a 4.9% reduction

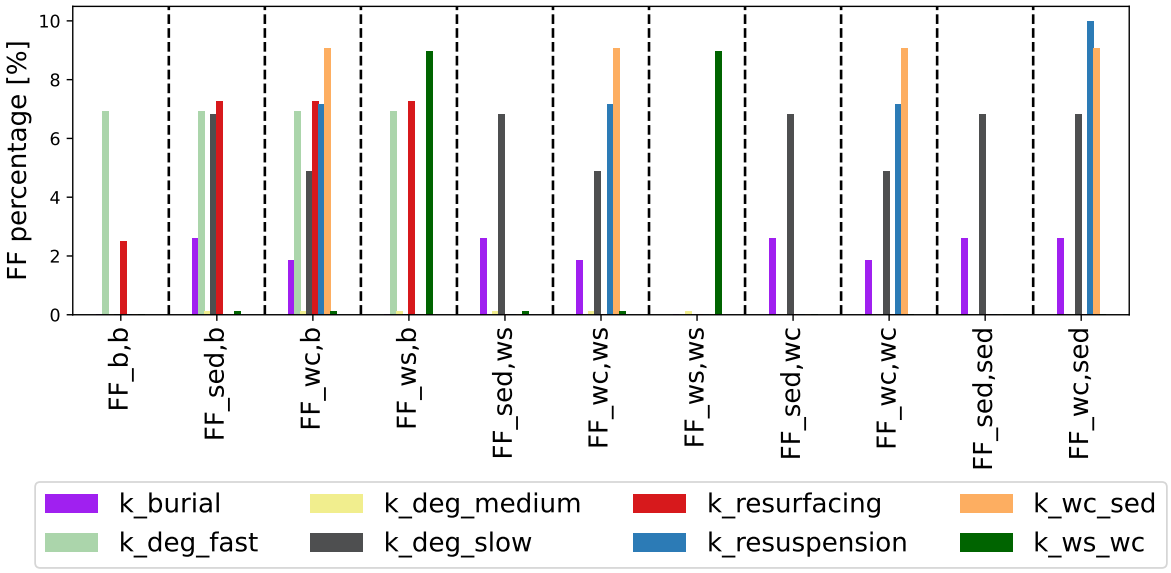

Figure 7.8 Sensitivity analysis of different quantified rates on the fate matrix of "Sp-LD-S" category (b: beach, ws: water surface, wc: water column, sed: sediments - k_deg_i: degradation rates for different intensities i, k_ws_wc: transfer rate from the water surface to the water column, k_wc_sed: transfer rate from the water column to the sediments)

in $FF_{wc,b}$, $FF_{wc,ws}$, and $FF_{wc,wc}$, and a 6.8% in $FF_{sed,b}$, $FF_{sed,ws}$, $FF_{sed,wc}$, $FF_{wc,sed}$, and $FF_{sed,sed}$.

A 10% increase in the resurfacing rate implies a higher fraction of microplastics leaving the beach towards the water surface. This has a significant direct influence on the mass increase in the water surface (7.3%) and indirect influence in the water column and sediments with the same percentage. Although the sensitivity to the resurfacing and fast degradation rates is not the highest among the rates tested, it is significant in the beach sub-compartment. This gives an indication that refining the mechanisms of this sub-compartment is necessary in the future.

Increasing the resuspension rate leads to a bigger transfer fraction of microplastics back to the water. Although it doesn't have an influence on the majority of FFs (figure 7.8), it presents the highest sensitivity, among all rates tested, with a 10% influence on $FF_{wc,sed}$. In addition, as a consequence to this increase, the residence time in the water compartment is reduced by 7.2%. As a result, fate factors where water sub-compartment is a receiving one ($FF_{wc,b}$ and $FF_{wc,ws}$) are equally affected. Therefore, it is crucial to refine the resuspension rate as it depends on the particle density, size, and shape as well as its fouling and degradation states [294].

Increasing the rate of transfer from the water surface to the water column $k_{wc,ws}$ significantly reduces the residence time in the water surface, and eventually $FF_{ws,b}$ with a 8.98% as microplastics sink faster to the water column. As a result, $FF_{wc,b}$, $FF_{sed,b}$, $FF_{wc,ws}$, and $FF_{sed,wc}$ are not affected (0.1% which is not significant). Similarly, increasing the rate of transfer from the water column to the sediments $k_{sed,wc}$ greatly influences the residence time in the water column with a 9.1% reduction. Transfer rates between water sub-compartments are the second and third most sensitive on the fate after the resuspension rate (10% influence). $FF_{wc,b}$ is sensitive to six out of eight rates tested with varying importance. This can be explained by the role of the fate matrix in accounting for both direct and indirect transfers among sub-compartments, unlike the rate matrix that only considers direct exchanges. $FF_{b,ws}$, $FF_{b,wc}$, $FF_{b,sed}$, $FF_{ws,wc}$, and $FF_{ws,sed}$ are not displayed in the graph since these factors are equal to zero due to the absence of inter-compartmental interactions, as explained in section 7.4. The results of the sensitivity analysis of quantified rates for all microplastic categories are presented in figure S5.

The sensitivity of different quantified rates, as well as the effect factors, on the characterization factors of the same tested category (Sp-LD-S) is presented in figure 7.9. Since fate factors, having the beach as an emission sub-compartment, are the most sensitive to most quantified rates, CF_b is the most sensitive among all characterization factors tested. Coming from the fate, resuspension, resurfacing, and the sedimentation transfer rates are the most sensitive on the CFs. EF_{ws} slightly influences CFs in the water surface and the beach only because they are affected by the residence time in these sub-compartments. EF_{wc} has an influence on all CFs. Its sensitivity is as significant as the resuspension rate on CF_{sed} and slightly more important than the influence of the sedimentation rate on CFs in other sub-compartments. This is because the EF_{wc} is only applied to the water column sub-compartment which is not connected by transfers to the water surface and beach sub-compartments. This indicates that CFs for microplastic emissions in the marine environment are driven by both the fate factors and effect factors. Consequently, influencing fate mechanisms need to be refined and specific considerations to the sensitivity of marine species should be taken into account. The sensitivity analysis on CFs for all microplastic categories are provided in figure S6.

7.5 Discussion

Comparing the rates calculated with those found in the literature, we find that $k_{resurfacing}$ ($4.5E-01\ day^{-1}$) obtained from Kamphuis et al. (1991) [208] aligns with the values proposed by Critchell et al. (2016) [291] (between $1E-01$ and $4E-01\ day^{-1}$). Sedimentation rates ($k_{sed,wc}$) calculated using TrackMPD are compared to the ones calculated in the Sim-

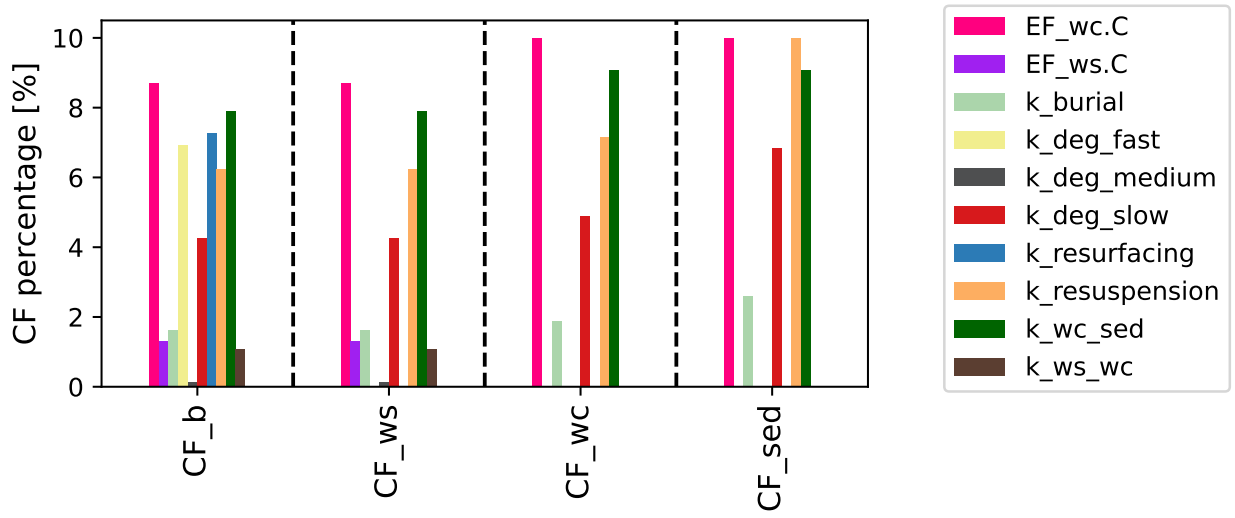

Figure 7.9 Sensitivity analysis of effect factors and different quantified rates on the CF matrix of "Sp-LD-S" category (b: beach, ws: water surface, wc: water column, sed: sediments - k_deg_i: degradation rates for different intensities i, k_ws_wc: transfer rate from the water surface to the water column, k_wc_sed: transfer rate from the water column to the sediments)

plebox4plastics model [2]. The depth of their seawater compartment is modified to match the one proposed by [187] and adopted in this article. Since Simplebox4plastics does not provide sedimentation rates for different particle shapes, only rates for spherical particles are compared (table 7.5). Sedimentation rates for high density particles are several orders of magnitude larger for big particles compared to smaller ones, which corroborates with our results. For big particles, the rates are close, with one order of magnitude difference, while for small ones, a three order of magnitude difference can be observed. This can be linked to the simple gravitational settling velocity used in the Simplebox4plastics that does not account for the influence of the water current. For low density particles, the Simplebox4plastics provides zero sedimentation rates for both free and aggregated particles. They assume aggregation in one step only. Therefore, if the overall density does not exceed that of the surrounding water, the particle floats infinitely in the system [2]. This contradicts our results and observations in the literature, where positively buoyant microplastics reach the sediments due to biofouling, which depends on the size and shape of the particles.

The water surface reports higher concentrations than the water column. This is related to positively buoyant microplastics that need time to be biofouled and start sinking [57]. These results come in accordance with the observations in literature for microplastic samplings in the marine environment [10, 295].

Table 7.5 Comparison of sedimentation rates [day^{-1}] obtained with Simplebox4plastics [2]

	Sphere			
	High density		Low density	
	Big	Small	Big	Small
k_sed,wc (this work)	1.19E+02	2.45E-01	6.9E-02	2.74E-01
Sedimentation of free MPs [2]	4.65E+03	1.86E-04	0	0
Sedimentation of aggregated MPs [2]	4.65E+03	1.98E-04	0	0

Cylindrical particles showed lower settling time than spherical ones due to faster biofouling and higher settling velocities. This explains the dominance of fibrous particles in sediment sampling [56,182]. Although the same conclusion would still hold, it is important to mention that the first version of TrackMPD used in this article uses Khatmullina et al. (2017) [206] for the settling velocity equation of cylindrical particles. However, it has been demonstrated that the irregular distribution of biofilms modifies the orientation of fibers leading to a higher settling velocity. Based on that, the theoretical formulation of Waldschläger et al. (2019) [92] presents a better fit for the settling velocity of fibers [58], which should be considered in future versions.

Since the compartment in which microplastics accumulate at steady-state is in the sediments, it is important to refine mechanisms occurring within this sub-compartment. The resuspension rate is considered a single value for all microplastic categories. However, it depends on the physiology of the particles, as well as their biofouling and degradation states [294]. Following on its significant sensitivity on FFs and CFs (figures 7.8 and 7.9), it is important to improve this resuspension rate in future steps by considering the critical shear stress thresholds for resuspension [296] that differ between particle properties. In addition, it would be important to account for the hiding effects of particles by sediments linked to the difference in size between microplastic and sediment particles. For instance, larger microplastics, lying on the bed surface formed of smaller sediment particles, are more exposed to be transported than smaller microplastic particles shielded within larger sediment particles [92]. Aside from the resuspension rate, it is important to refine the resurfacing rate as well since fate and CFs are highly sensitive to it. FFs and CFs are also found to be sensitive to fast and slow degradation rates which are applied for the beach and sediments total removal rates (diagonal elements in the rate matrix **K** (equation 7.5). These degradation rates are based on experimental data in marine water [18,19]. Therefore, it is recommended to refine those rates based on experiments in beach and/or sands.

As explained in section 7.3.3, available effect factors are used for the development of CFs.

Current effect factors include aquatic/marine ecosystems only [19, 20]. For this reason, they are applied for water sub-compartments. New EFs are currently under development in MariLCA specifically for the sediment sub-compartment [21] and should be taken into consideration when developing global and regionalized CFs for MP emissions in future steps. It is also important to mention that primary microplastic emissions are mainly occurring at the water surface and beach. CFs for the beach, water column, and sediments can however be used for the emissions of secondary microplastics resulting from the fragmentation of larger macroplastics in these sub-compartments.

Marine/terrestrial species, such as seabirds, also feed on marine sub-compartments. They are therefore, exposed to microplastics that can circulate throughout their entire body causing serious damages [297]. The effect of marine MPs on these species is still not accounted for and it is outside the scope of this article. However, it is important, in future steps, to account for these impacts by developing effect factors for species feeding on both terrestrial and marine sub-compartments. These EFs would then be combined with marine FFs to develop CFs for MPs emitted to the marine environment for the impact category "Terrestrial ecosystem".

Previous studies have proposed fate models to develop fate factors and eventually characterization factors for microplastics in the marine environment. Saling et al. (2020) [177] have developed fate factors based on the fragmentation and degradation rates of plastics in the marine environment. Different sub-compartments (e.g., sediments) were not taken into consideration nor were various mechanisms altering the fate and redistributing microplastics, such as biofouling or burial. Hence the finding that microplastics accumulate in the sediments was not presented in the aforementioned study. In addition, as it is presented in table S2, the degradation of microplastics is much slower than other fate mechanisms. Therefore, developing the rate based on degradation rates only, misinterprets the fate of the particles. Moreover, the weathering of plastics in the marine environment takes place at different rates in marine sub-compartments depending on various oceanographic conditions [114]. This differentiation was not taken into consideration either in Saling et al. (2020) [177]. However, as explained in section 7.4.3, the distinction in degradation rate within each sub-compartment has an influence on the fate factors developed (figure 7.5 and table S4). In a more recent study, Maga et al. (2022) [178] considered marine water and marine sediments separately. However, transfer rates between them were not accounted for but rather, a final transfer rate percentage was used. This means that all negatively buoyant microplastics are fully present in the sediments and none of positively buoyant particles reach the sediments. They float in the water with no alteration to their densities by environmental conditions. Their approach does not adequately describe the trajectory of the particles since, depending on their size and shape, high density particles could take some days in the water before they reach the

sediments (figure 7.4), exposing water species along the way. In addition, positively buoyant particles do not float infinitely in the water but rather, eventually reach the sediments (figure 7.4) where they accumulate (table 7.5 and figure 7.6) and expose benthic species. While our results contradict those of the aforementioned studies, they confirm with literature observations where light particles are detected in benthic sediment samplings [52]. Latest MariLCA's project used the weathering approach of [178] to build on more refined degradation rates. In their project, Corella-Puertas et al. (2023) [19] considered different sedimentation rates, based on expert estimates, to account for the biofouling process responsible for the sinking of light microplastics. Similar to Maga et al. (2022) [178], Corella-Puertas et al. (2023) [19] considered the marine environment as a single water compartment. Water surface was not defined as a separate sub-compartment. In addition, beach and sediments were not considered and subsequently, resuspension, burial, and resurfacing rates, quantified in this work, were not examined. Following the sensitivity analysis performed, the fate is mostly sensitive to the resuspension rate (figure 7.8) and therefore, its consideration is important. Moreover, their simplified fate model did not account for water hydrodynamic currents, waves, and water turbulence that are modeled in the ocean general circulation model used in this article. These environmental parameters greatly influence sinking and sedimentation rates (figure 7.3) to which the fate is sensitive (figure 7.8). Therefore, it is important to account for their variability when modeling the fate.

Characterization factors developed in this article serve as an example on how to operationalize the framework proposed in Hajjar et al. (2023) [187] and as a basis to identify key influential parameters on the fate of microplastics. Although different parameters are tested within their variability ranges, water current data are extracted for the specific region in the Northeast of the US. For this reason, these CFs cannot be used for the global approach adopted in the holistic life cycle assessment (LCA). Therefore, we do not recommend to use these CFs as they were only developed to analyze their sensitivity to the EFs and the variability of the transfer rates with the physical properties of MPs and environmental parameters.

Climate change is responsible for ocean warming and increase of the seawater temperature. As a consequence, the degradation of MPs might be enhanced as well as biofilm growth due to bacterial and algal blooming [298]. This might lead to an increase in the settling velocity of MPs and a shorter residence time in water sub-compartments. The increase in seawater temperature results in a decrease of the seawater density [299] as well, which in turn affects vertical and horizontal mixing processes in the ocean. This would alter the density of positively buoyant microplastics, which would also accelerate their settling and reduce their residence time in water. In addition, increased temperatures can lead to polar melts and increased river flux which reduces the salinity and the density of seawater [300].

Moreover, the sea level rise caused by the ocean warming increases coastal wave heights and current speeds [301], and influences the sediment dynamics and sediment transport [302]. This might also influence the resuspension, burial, and microplastics trapping near the shores. Furthermore, climate change might alter the water current circulation [303] leading to the distribution and transport of MPs in new areas. The influence of climate change on the fate of MPs in the marine environment is outside the scope of this article however, it is important to account for it when developing FFs and CFs for MP emissions in the marine environment in future steps.

7.6 Conclusion

This study identifies the most important parameters that influence the fate of microplastics emitted to the marine environment in the direction of proposing recommendations for regionalizing the fate factors and categorizing them based on microplastic physiology. Consequently, it aims at operationalizing the framework proposed in MarILCA through quantifying identified fate mechanisms and developing site-specific fate and characterization factors. According to that, this article provides site-specific FFs and CFs for different marine sub-compartments which was not previously considered in the literature. The influence of MPs physiology and environmental properties reveal the challenges and complexity of modeling the fate of MPs in the marine environment due to the variability linked to these parameters. This supports the need for categorizing the fate factors and subsequently CFs based on MPs physical properties and eventually regionalizing them.

This article analyzes the influence of different physical properties and environmental parameters on the settling rates of microplastics in the marine environment. The sensitivity analysis on the fate factors shows that they are mostly sensitive to the resuspension rate, followed by the transfer rates between aquatic sub-compartments and the fast degradation rate on the beach. Characterization factors were seen to be mostly sensitive to the effect factor in the water column. This indicates that CFs are driven by both the fate and effect on the ecosystem. Therefore, CFs need to be carefully quantified by accounting for all mechanisms and parameters that have influence on the fate, as well as developing effect factors specific for every sub-compartment where species and their exposures could differ.

CHAPTER 8 REGIONALIZED FATE AND CHARACTERIZATION FACTORS FOR MICROPLASTIC EMISSIONS IN THE MARINE ENVIRONMENT

This chapter addresses the third objective of this thesis. It provides regionalized CFs for MP emissions in the marine environment, with a special focus on the main locations of MP emissions. It also assesses the influence of regionalization and seasonality on CFs, compared to the physical properties of microplastics. Additional information and results for this chapter can be found in Appendix C and in Supplementary Information (Zenodo: `http://doi.org/10.5281/zenodo.14427312`. Github: `https://github.com/carlahajjar1/Regionalized-CFs-for-MP-emissions-in-the-marine-environment-for-IW-and-GLAM`).

Before presenting the results of this chapter, it is important to differentiate between the three defined scales: beach, continental, and global. While beach takes part of the continental scale (as presented in chapters 6 and 7), it is taken as a separate scale in this chapter. The continental scale here is used to refer to overlapping sub-compartments (water surface, water column, sediments). This distinction was not made in the first and second sub-objectives, where beach takes part of the continental scale. Nevertheless, this distinction is adopted in this chapter in order to avoid confusion when calculating the size of the compartments (section 5.3), and addressing the species distribution fraction (section 5.7).

The results of this chapter are presented in several sections. The first section (section 8.1) starts by presenting the general results obtained following the methodology presented in chapter 5. Two examples are also presented. The second section addresses the first criterion to answer the research hypothesis (section 8.2). It presents a comparison between the variability of CFs due to regionalization and MP 1) densities, 2) sizes, and 3) shapes. The third section addresses the second criterion of the research hypothesis (section 8.3). It presents the variation of MP ranking orders of impacts between emission regions. The fourth section presents the variability of CFs with the physical properties of MPs, between each emission region (section 8.4) for the two approaches. The fifth section then presents the variability of CFs for each MP tested in every emission region, for the two approaches (section 8.5). This section presents an in-depth analysis that aims at understanding the underlying reasons for the variability of CFs.

8.1 General presentation of the results

For each particle tested (Table C.5) in every emission region (table 5.1), a rate **K** matrix is obtained according to the trajectories generated using TrackMPD. For example, the trajectories of 5000 μm EPS spherical particles and 1000 μm PP fibrous particles in East China Sea (EC) are plotted in figure 8.1. Based on these trajectories, it can be seen that the EPS particles are more dispersed than the PP particles because they are larger. Thus, they take more time to biofoul up to the water density compared to the PP particles. In addition, once biofouled, fibrous particles settle at a higher velocity than spherical particles. Therefore, the PP particles settle sooner than the EPS. Based on these trajectories, the rate of transfer between marine sub-compartments is calculated for every particle. Consequently, a rate matrix for each particle in every region is constructed. All rate matrices for every MP tested in every location can be found in **Supplementary Information**. Based on these rate matrices, FF matrices are also obtained for every particle emitted in every region. All FF matrices are also presented in the **Supplementary Information**.

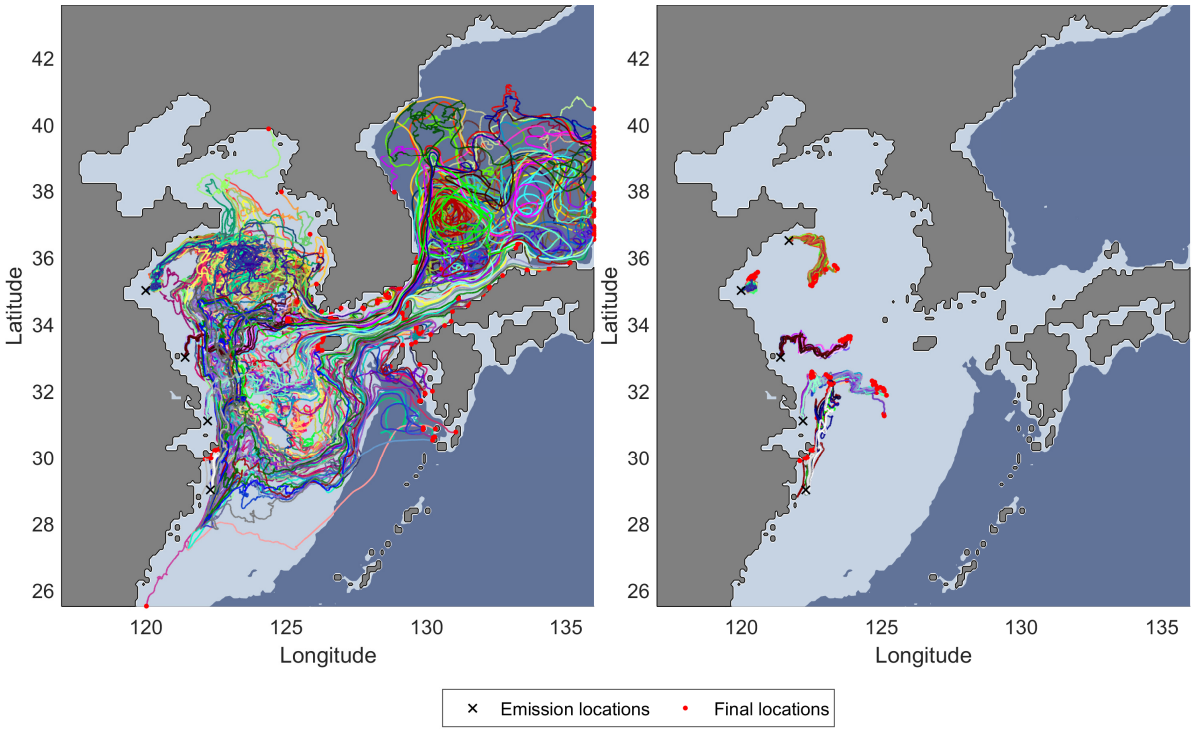

Figure 8.1 The trajectory of EPS 5000 μm spherical (left) and PP 1000 μm fiber (right) emitted in East China Sea. Light blue: continental scale, dark blue: global scale

Due to the lack of region-specific data, the exposure-effect matrix is the same as that used for every emission region for the two approaches considered. Because EEF does not depend

on the physical properties of MPs [20], the same **EEF** is also used for all the particles tested. Regionalized EEF matrices can also be found in **Supplementary Information**.

Little regionalized data exist on the species distribution between the water surface, water column, and sediments. Thus, the **SDF** developed for the IW+ approach is used the same for each emission region. It is based on the feeding behavior of species between water and sediments [21] and the habitats of species between the water surface and the water column [190]. The same generic SDF between these three sub-compartments is used for GLAM, combined with regionalized data of the IUCN database [210], which allow to know the number of species in beach, continental, and global scales. Both matrices, used for the generation of CFs for both approaches, are presented in the **Supplementary Information**.

CFs for both approaches are obtained using the FFs, EEFs, and SDFs. All are presented in the **Supplementary Information**. Two examples are presented below for the particles plotted in figure 8.1:

For IW+ approach $[PDF.m^2.yr/kg]$:

$$\mathbf{CF^{EC}_{EPS}} = \begin{matrix} \text{Beach} & \text{Water surface} & \text{Water column} & \text{Sediments} & \text{Global} \\ \big[1.21\text{E+}03 & 1.21\text{E+}03 & 1.03\text{E+}04 & 1.03\text{E+}04 & 3.35\text{E+}01\big] \end{matrix} \tag{8.1}$$

$$\mathbf{CF^{EC}_{PP}} = \begin{matrix} \text{Beach} & \text{Water surface} & \text{Water column} & \text{Sediments} & \text{Global} \\ \big[9.12\text{E+}03 & 9.12\text{E+}03 & 9.11\text{E+}03 & 9.11\text{E+}03 & 2.94\text{E+}01\big] \end{matrix} \tag{8.2}$$

For GLAM approach $[PDF.yr/kg]$:

$$\mathbf{CF^{EC}_{EPS}} = \begin{matrix} \text{Beach} & \text{Water surface} & \text{Water column} & \text{Sediments} & \text{Global} \\ \big[2.41\text{E-}10 & 1.93\text{E-}10 & 1.29\text{E-}09 & 1.29\text{E-}09 & 5.68\text{E-}14\big] \end{matrix} \tag{8.3}$$

$$\mathbf{CF^{EC}_{PP}} = \begin{matrix} \text{Beach} & \text{Water surface} & \text{Water column} & \text{Sediments} & \text{Global} \\ \big[1.36\text{E-}09 & 1.31\text{E-}09 & 1.14\text{E-}09 & 1.14\text{E-}09 & 5.00\text{E-}14\big] \end{matrix} \tag{8.4}$$

It can be observed that both polymers have impacts of the same orders of magnitude for the two approaches despite differences linked to their fate. This is particular to this emission

region because of the large size of its continental scale. As can be observed, EPS particles are transported to the beach, sediments, and global scale. Their dominant fate mechanism is the sedimentation rate. Their highest partial impacts ($PDF.yr/kg$) are observed on the beach and in the sediments. Since the surface of the continental scale ($3.05E+06\ km^2$) is four orders of magnitude larger than that of the beach ($8.39E+02\ km^2$), impacts in sediments predominate those on the beach. PP particles are transported to the beach and the sediments. Similarly to EPS particles, their impacts are more pronounced on the beach and in sediments. However, their impacts over a surface area predominate in the sediments. Therefore, both particles present similar impacts. Impacts at the global scale are negligible compared to those at the beach and sediments. This explains the smaller CFs for EPS compared to those of PP.

This example indicates the challenges in understanding the influence of each parameter when assessing the impacts of MPs. The interaction of several factors plays an important role in determining the impacts of each MP particle in every emission region. Therefore, it is important to analyze the influence of each individual parameter, as well as its interaction with other parameters. Before going into a detailed analysis, an overview of general observations in the results is first presented.

8.2 Comparison of CF variability due to regionalization, MP size, density and shape

In order to evaluate the importance of each parameter tested: spatial variability, MP size, density and shape, the difference in CFs of each parameter is calculated. For instance, to evaluate the variability of CFs due to the shape of the particles, the difference of CFs for spherical and fibrous particles is calculated for all possible combinations of other parameters (for example, the difference between the CFs of EPS $1\mu m$ spherical particle and EPS $1\mu m$ fibrous particle, the difference between the CFs of EPS $1\mu m$ spherical particle and PP $1\mu m$ fibrous particle, etc.). The largest difference is then taken to represent the largest variability in CFs due to the parameter considered. In order to obtain the relative difference, the ratio of the highest value relative to the smallest one is calculated. For IW+ approach, the largest difference in CFs presented a relative increase of a factor of **13 000** due to the shape, **100 000** due to the size, **1 300** due to the polymer density and **83 000** due to the spatial variability. For the GLAM approach, the largest difference in CFs presented a relative increase of a factors of **1 200** due to the shape, **1 400 000** due to the size, **17 000** due to the density of the polymer, and **14 000 000** due to spatial variability. This is equivalent to saying that the shape, size, polymer density, and spatial variability influence the CFs by an order of

magnitude of 2, 3, 1, 2, respectively for the IW+ approach. For GLAM, shape, size, polymer density and spatial variability influence CFs by an order of magnitude of 1, 4, 2, and 5, respectively.

Table 8.1 presents these same differences in CFs but in absolute values. It can be seen that each parameter presents a CF variability of similar orders of magnitude. These similarities demonstrate the challenges in quantifying the impacts of MPs in the marine environment because of the significant importance of underlying parameters that play a role in the fate and hence the impacts of MPs. The absolute variability in CFs due to regionalization is of the same order of magnitude as the variability related to the physical properties of MPs. This confirms that spatial variability is equally important for the development of CFs for MP emissions. This satisfies the first criterion that validates the research hypothesis. These similarities also present the importance of MP physical properties, density, shape, and size on the modeling of their impacts.

Table 8.1 Absolute differences of CF values for each parameter tested: regionalization, MP size, density and shape for IMPACT World+ $[PDF.m^2.yr/kg]$ and GLAM $[PDF.yr/kg]$ approaches.

	Shape variability	**Size variability**	**Density variability**	**Spatial variability**
IMPACT World+	1.00E+04	2.95E+04	2.19E+04	2.95E+04
GLAM	1.06E-07	2.40E-07	2.38E-07	2.40E-07

8.3 The variation of MP ranking orders of impacts between emission regions

The ranking of CFs is determined for each MP tested in each emission region. Then, the Spearman rank correlation coefficient (SCC) is calculated for the rankings between emission regions to analyze the influence of regionalization on altering the impact ranking of MPs. The results are presented in figure 8.2 for the IW + approach and figure 8.3 for the GLAM approach. It can be observed that the ranking of MPs in the majority of regions presents a rank correlation coefficient less than 0.9. This indicates that emission regions do not present a "very strong" correlation due to regionalization. This satisfies the second criterion that validates the research hypothesis. Few exceptions are observed between the Mediterranean and the Bay of Bengal (SCC = 0.94), Okhotsk Sea and East China Sea (EC-Japan) (SCC = 0.97) for the IW+ approach. For the GLAM approach, exceptions are also observed between the Mediterranean and Indus (SCC = 0.91) , and Sea of Okhotsk and East China Sea (EC-Japan) (SCC = 0.94). These exceptions might be related to a similar MP fate between these regions.

If we reduce the rank correlation coefficient to 0.7, above which data are considered to have a "strong" correlation [184], it can be observed that for the IW+ approach, the majority of countries would have a strong correlation, except Indus and Congo (SCC = 0.49), and Sea of Okhotsk and Indus (SCC = 0.68). This is mainly related to the fate of large high density particles that settle fast and reach the sediments regardless of the emission point. However, for the GLAM approach, the majority of countries would still present a low ranking correlation of impacts (below 0.7), regardless of similarities in the fate of large high density particles. This is because the GLAM approach is more influenced by spatial variability, due to the regionalized sizes of marine sub-compartments and species distribution fraction **SDF**, compared to the IW+ approach (section 5). Nevertheless, in order to better understand the differences and similarities in MP impacts to assess the influence of regionalization and physical properties of MP, a detailed analysis of fate and characterization factors is required.

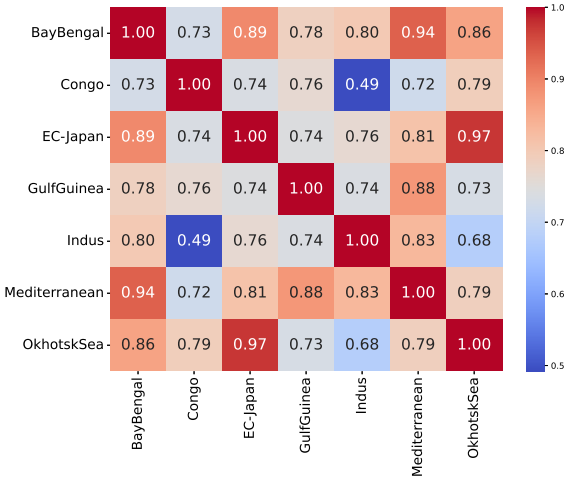

Figure 8.2 Rank correlation coefficients of CFs among emission regions, for IW+ approach (EC-Japan: East China Sea)

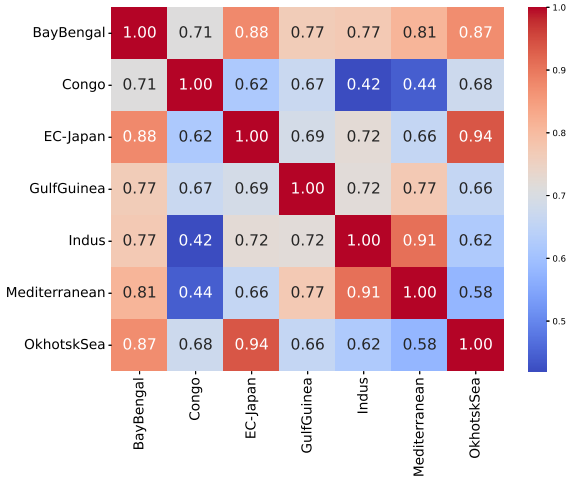

Figure 8.3 Rank correlation coefficients of CFs among emission regions, for GLAM approach (EC-Japan: East China Sea)

Following the satisfaction of both criteria, it can be concluded that the research hypothesis of the present thesis is validated. That means that regionalization is equally important to the development of CFs as is the physical properties of MPs. However, the importance of spatial variability and the variability associated with physical properties need to be further addressed. In the following sections, a more detailed analysis is presented to understand how the physical properties of MPs and regionalization interact and influence the development of CFs for MP emissions in the marine environment.

8.4 The variability of CFs due to MP physical properties within each region

In this section, the variability of CFs due to the physical properties of MPs is assessed and compared between emission regions. This analysis helps to identify whether the variability of CFs due to the physical properties of the MP is similar in every emission region. This section also presents an explanation to some of the differences observed.

8.4.1 The IMPACT WORLD+ approach

The variability of CFs $[PDF.m^2.yr/kg]$ due to the physical properties of MPs in each region, for the IW+ approach at the endpoint level, is presented in figure 8.4. The variability of CFs with the physical properties of MPs ranges up to two orders of magnitude for emissions at the sediments and the global scale, and up to three orders of magnitude for emissions at the beach, water surface, and water column, for every emission region. This variability also differs between emission regions. This indicates that the influence of MP physical properties on the CFs is significant in some regions, where the variability is high (Bay of Bengal, Congo, Indus, Mediterranean, Gulf of Guinea) but less important in others (Okhotsk Sea and East China Sea). This is related to the fate of the particles controlled by the currents of water and removal mechanisms. In the Okhotsk Sea and East China Sea, the majority of emitted particles, regardless of their properties, end up in continental sediments (table C.9). Thus, the physical properties of MPs are not important when emissions are in the Okhotsk Sea and East China Sea (less than one order of magnitude difference between the 25th and 75th percentile in figure 8.4). The highest variability of CFs observed in the Bay of Bengal, Congo, Gulf of Guinea, Indus, and the Mediterranean also depends on the fate of the particles in these regions. For example, large low density particles (such as 5000 μm EPS spherical particles), emitted in Congo, are completely transported to the global scale (figure 8.5) where their impacts are reduced in the large volume of the global scale. Alternatively, 10 μm EPS fibrous particles, also emitted in Congo, contribute to the highest impacts of EPS particles in this region, because they remain in the continental scale, where the impacts are higher (figure 8.5). Thus, the fate of particles differs between emission regions as a result of the interaction between the physical properties of MPs and the water currents. This shows that regionalization is also important as the physical properties of MPs for the development of CFs. However, this raises the need to investigate further the influence of regionalization on CFs compared to each combination of physical properties tested (section 8.5.1).

Water currents can differ greatly between emission regions. The Gulf of Guinea and Congo river are present in the same domain (figure 7.2) and are relatively close to each other. How-

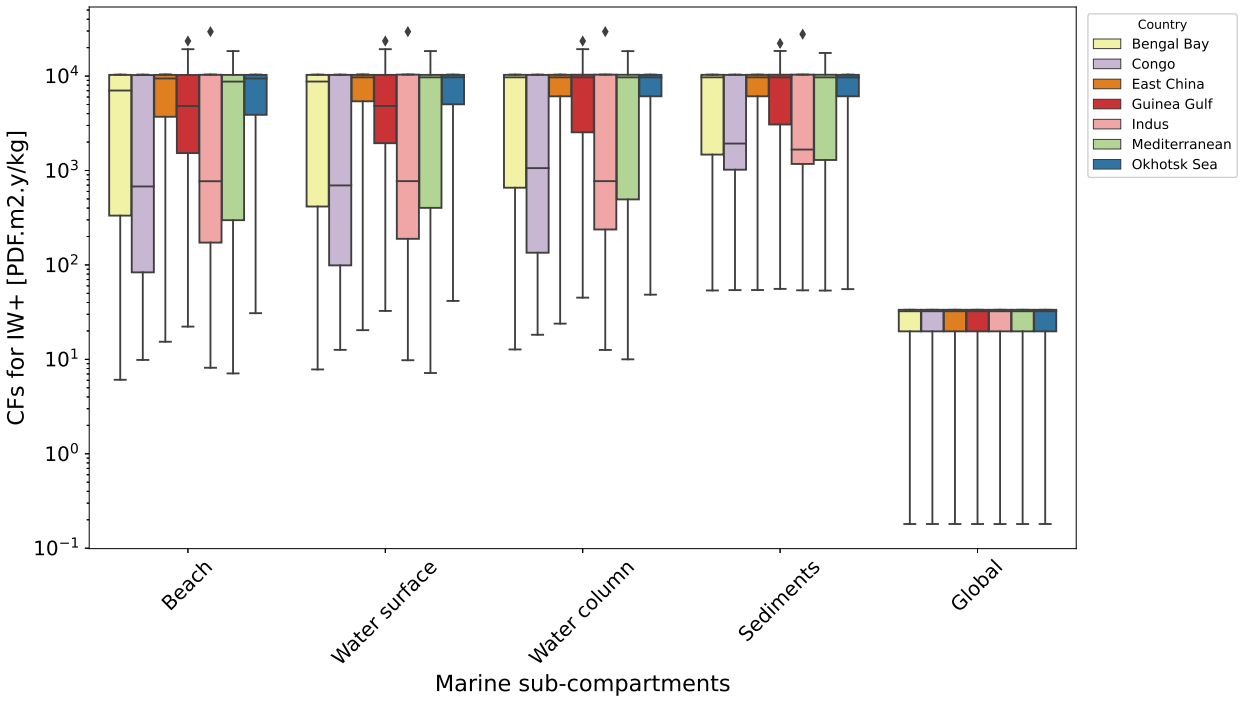

Figure 8.4 The variability of regionalized CFs with the physical properties of MPs, for every emission region, at the endpoint level of IW+ approach

ever, water currents can drift the particles differently in both emission regions. For instance, 1000 μm fibrous EPS particles emitted in Congo are all transported to the global scale. Whereas, the same particles emitted in Gulf of Guinea all beach on the small island next to the coast (figure 8.6). This results in a two-order-of-magnitude difference between CFs of both regions. For an emission at the water surface, CF_{Congo} = 3.54E+01 $PDF.m^2.yr/kg$ while $CF_{GulfGuinea}$ = 4.77E+03 $PDF.m^2.yr/kg$. Therefore, this emphasizes the high influence of regionalization on the impacts of MPs. Thus, it is very important to understand where MPs are emitted when assessing their impacts in the marine environment.

When comparing the orders of magnitude between emission compartments, it can be observed that at the continental scale, the variability of CFs for emissions at the water surface, water column, and sediments has similar orders of magnitude for all emission locations. The final fate of MPs emitted at the water surface and water column is on the beach, in sediments, or in the global scale. The residence time of MPs in the sediments is high (the maximum value is for spherical 5000 μm PVC in Bay of Bengal: 42186.3 days = 115.5 years) due to slow resuspension ($k_{resuspension} = 4.51E-01\ day^{-1}$), burial ($k_{burial} = 2.37E-05\ day^{-1}$) and degradation rates. Thus, MPs reside for a long period of time in the sediments, where they expose 55.4% of continental marine species. Therefore, the high impacts of emissions at the

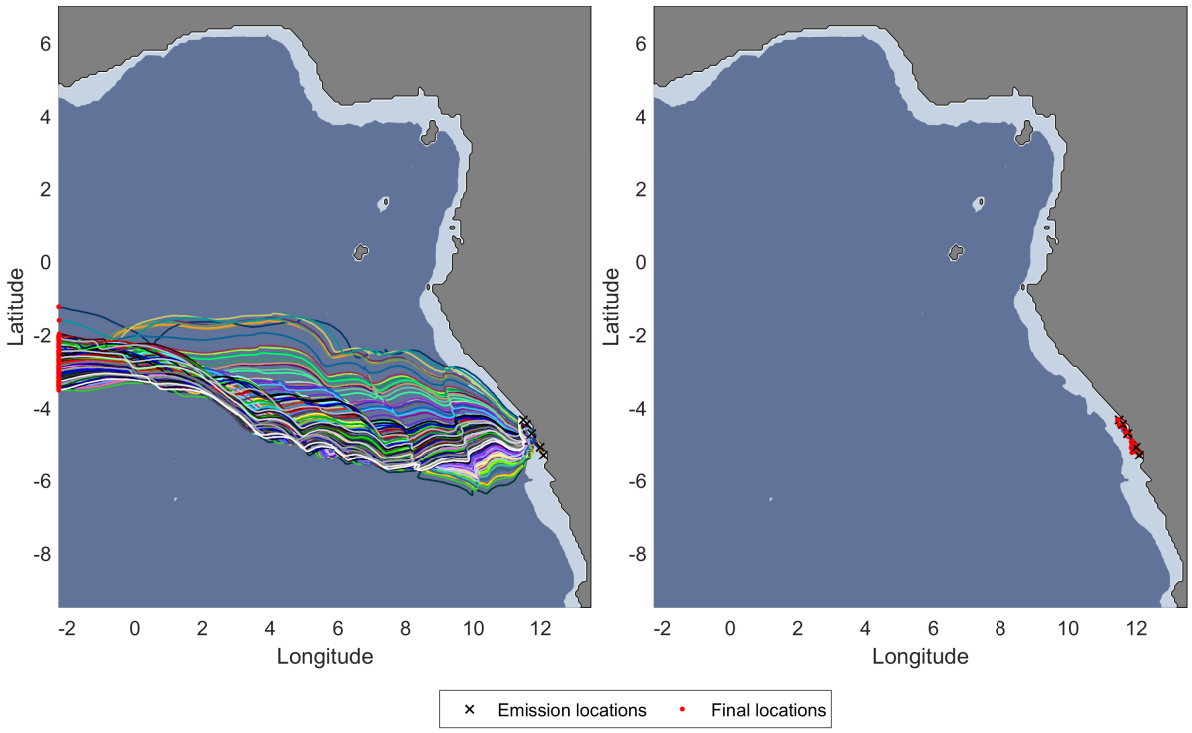

Figure 8.5 Trajectories of 5000 μm spherical EPS (left) and 10 μm fibrous EPS (right) in Congo. Light blue: continental scale, dark blue: global scale

water surface, water column, and sediments are due to the accumulation of MPs where a large fraction of species is exposed.

Although the beach sub-compartment is several orders of magnitude smaller than other marine compartments (table 8.2), and its corresponding EEF ($EEF_{beach} = 441.1\ PAF.m^3/kg$) is always smaller than that of water compartments ($EEF_{water} = 1067.5\ PAF.m^3/kg$), beach emissions have CFs of similar orders of magnitude as those for the water surface, water column, and sediments. This is because the residence time in the beach is at least one order of magnitude smaller than the residence time in other sub-compartments (diagonal elements in the **FF** matrix) due to fast degradation and transfer to the water surface ($k_{resurfacing}$ = 4.5E-01 day^{-1}). Therefore, impacts for an emission at the beach are mainly linked to impacts of MPs reaching continental sub-compartments (water surface, water column, and sediments).

The variability of CFs for emissions at the global scale is almost three orders of magnitude smaller than that of emissions at the beach and continental sub-compartments. Since the EEF at the global scale is considered equal to the one for the continental water surface and water column, which is the highest EEFs among marine compartments (EEF = 1067.5

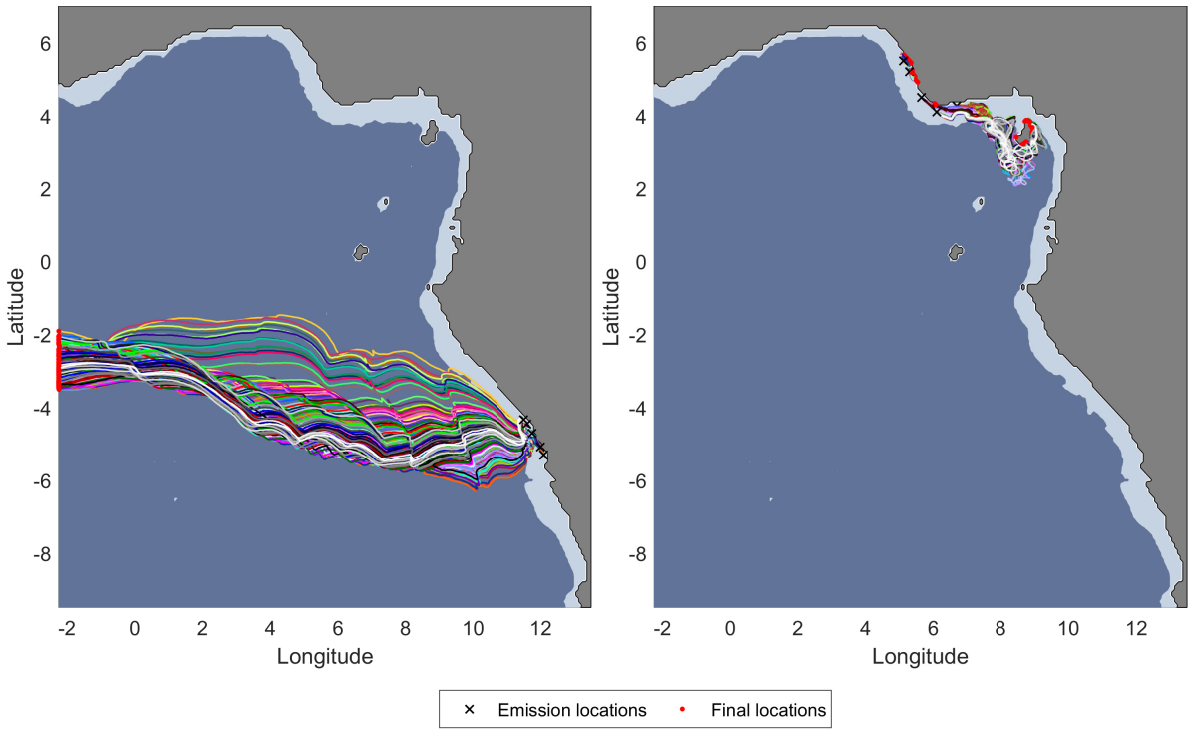

Figure 8.6 Trajectories of 1000 μm EPS fibrous particles emitted in Congo (left) and Gulf of Guinea (right). Light blue: continental scale, dark blue: global scale

Table 8.2 The surface area $[km^2]$ and volume $[km^3]$ of beach and continental marine scales for each emission region

	Beach surface area $[km^2]$	**Beach volume** $[km^3]$	**Continental surface area** $[km^2]$	**Water surface volume** $[km^3]$	**Water column volume** $[km^3]$
East China Sea	839	3.36	3.05E+06	3.96E+03	1.96E+05
Gulf of Guinea - Congo	363	0.73	1.82E+05	1.09+03	7.55E+03
Mediterranean Sea	123	1.23	2.48E+05	2.64E+03	2.02E+04
Bay of Bengal	664	3.52	3.21E+05	1.14E+03	1.18E+04
Okhotsk Sea	421	1.68	3.54E+05	4.60E+02	3.22E+04
Indus	421	0.97	3.58E+05	1.27E+03	1.87E+04

$PAF.m^3/kg$), this difference is mainly related to the fate transfer rates and the size of compartments. Moving from $PAF.m^3.d/kg$ to $PDF.m^2.yr/kg$ (section 5.1) requires the division of partial CFs with the volume of the global compartment and then the multiplication with its surface area. This is equivalent to dividing by the depth, which is equal to 3.68 km for the global scale. It is two orders of magnitude larger than the depths of the beach and continental scale (table 8.3). This is also equivalent to "diluting" the impacts in the deep global scale. Impacts in the global scale are therefore considered negligible compared to those in the continental scale.

Table 8.3 Size of continental marine sub-compartments for each emission region

	Continental width [km]	Beach depth** [m]	Continental water depth [m]	Water surface depth* [m]	Water column depth [m]	Beach length [km]
EC-Japan	363.1	4	65.8	1.3	64.5	8387.7
Gulf of Guinea - Congo	50.2	2	47.37	6	41.37	3633.9
Mediterranean Sea	20.2	1	92.33	10.65	81.68	12255
Bay of Bengal	48.33	5.3	40.36	3.55	36.81	6641.4
Sea of Okhotsk	84	4	92.33	1.3	91.03	4209.9
Indus	84.88	2.3	55.77	3.55	52.22	4212.3

* Water surface depths from [196], ** Beach depths from [188]

Emissions at the global scale are either removed through degradation or burial in sediments. There is no transfer from the global scale to the continental scale because this transfer is considered negligible compared to the transfer from the continental to the global scale [167]. Hence, impacts of emissions at the global scale represent solely the impacts in the scale itself. However, impacts at the beach, water surface, water column and sediments account for both impacts at the continental scale and global scale - if particles manage to reach it. Transfer to the global scale is expected to increase the impacts compared to particles that stay at the continental scale, because an additional fraction of marine ecosystem is exposed. However, due to the large size of the global scale, impacts of particles that stay in the continental scale are larger than the impacts of the ones that reach the global scale. For example, CF_{global} for 10 μm spherical and fibrous EPS emitted in the global scale of Bay of Bengal are 26.2 and 27.7 $PDF.m^2.yr/kg$, respectively. This similarity is expected since they represent solely impacts in the global scale. However, all 10 μm fibrous EPS, emitted at the continental water surface, settle in the continental scale while some of the spherical ones settle at the continental scale and the others reach the global scale (trajectories plotted in figure 8.7). The reason behind this is that biofouled fibrous particles have a higher settling velocity than biofouled spherical particles of the same size and density. However, CFs for emissions at the water surface are 8.57E+03 and 4.37E+02 $PDF.m^2.yr/kg$ for spherical and fibrous 10 μm EPS particles, respectively. This shows that transfers to the global scale reduce the impacts of MPs, due to its large size. Therefore, CFs for emissions at the global scale are small because they account solely for the impacts in this compartment. However, impacts in the continental scale account for impacts at both scales with a variability linked to the fate of the particles between both scales. More details are presented in section 8.5.1.

8.4.2 The GLAM approach

Similar to the IW+ approach, the influence of regionalization for the GLAM approach (figure 8.8), is as important as the influence of physical properties of MPs. As was seen for IW+, the influence of MP physical properties in Sea of Okhotsk and East China is not pronounced

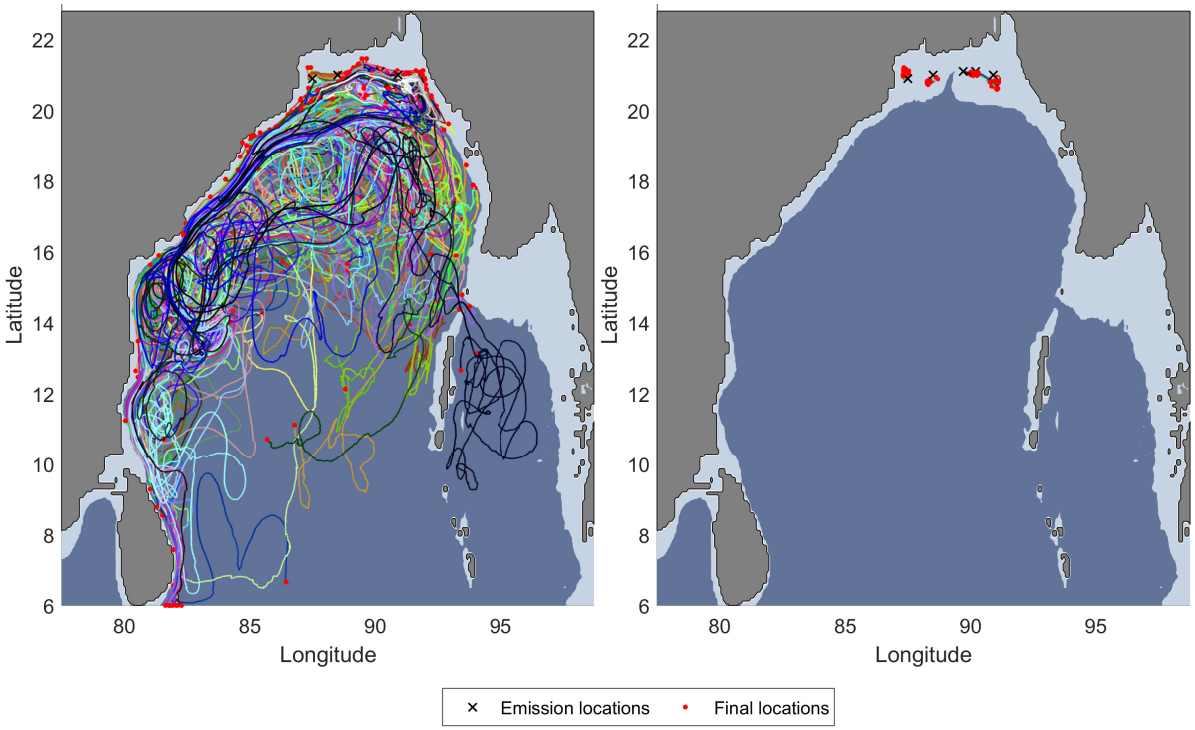

Figure 8.7 Trajectories of EPS 10 μm spherical (left) and fibrous (right) MP in Bay of Bengal. Light blue: continental scale, dark blue: global scale

because all emitted particles mainly end up in continental sediments. Compared to other regions, emitted particles are more dispersed between the global scale, beach and continental sediments (table C.9) depending on the interaction of their physical properties with water currents. Thus, CFs in these regions exhibit greater variability with the physical properties of MPs compared to Okhotsk Sea and East China Sea.

The influence of regionalization is more pronounced in this approach, compared to IW+, because CFs represent the potentially disappeared fraction of species in the entire marine ecosystem over a year [PDF.yr/kg]. As previously presented (section 5.1), the size of different compartments has a high influence on the results. Large volumes tend to "dilute" the impacts of MPs. Thus, the larger the volume, the lower the impacts. This explains the lowest impacts observed for emissions in East China Sea that exhibits the largest marine compartments (table 8.2). Hence, emitted particles in this domain contribute to the least impact on marine ecosystem.

In addition to the influence of the volumes of marine compartments, the GLAM approach gives the same intrinsic values to species living in a low species rich environment as to those living in a rich environment (sections 2.6.2 and 5.1). This means that more impacts are

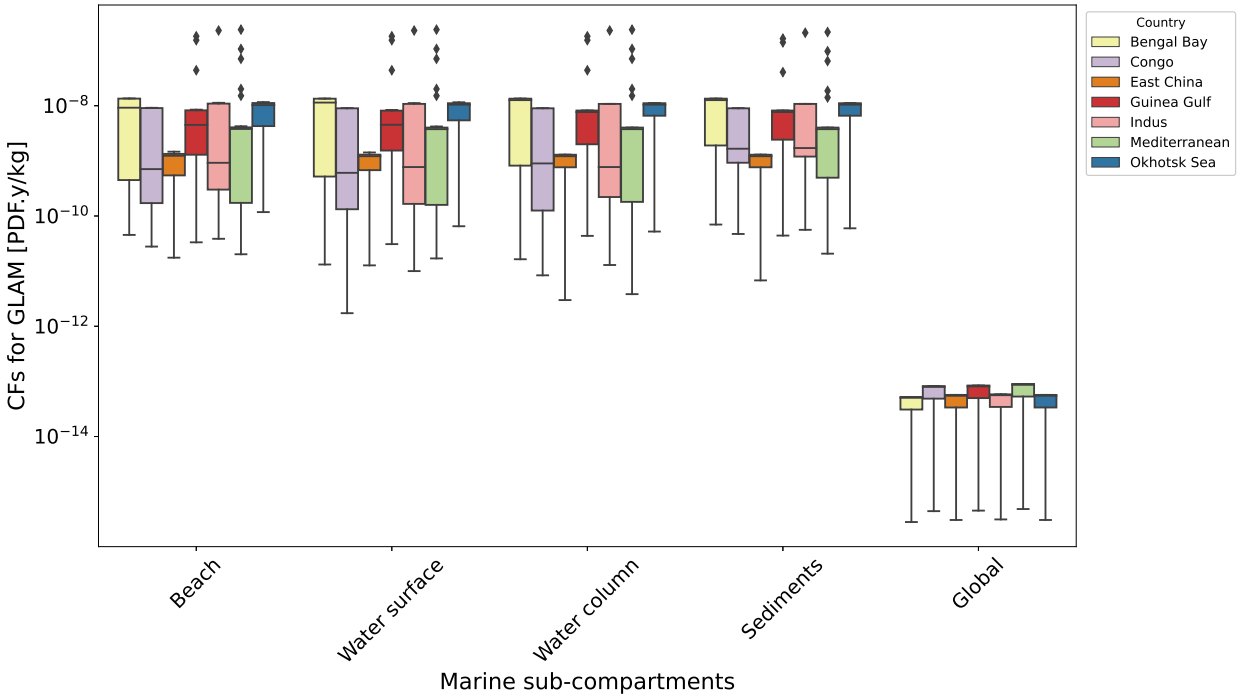

Figure 8.8 The variability of regionalized CFs with the physical properties of MPs, for every emission region, at the endpoint level of GLAM approach

observed in a species rich compartment compared to a species scarce one. Considering the example of 100 μm spherical particles emitted in Congo and Indus. The impacts of these particles are dominated by their impacts in sediments where they reside for 20 years in Congo and 25 years in Indus. The size of marine sub-compartments in Congo is slightly smaller than that of Indus (table 8.2). Following the reasoning presented above on the size of marine compartments, impacts in Congo should be greater than those in the Indus. However, for emissions at the water surface, CF_{Congo} = 5.13E-10 PDF.yr/kg, compared to CF_{Indus} = 1.45E-09 PDF.yr/kg. This is because MPs in the sediments expose 20.65% of marine ecosystems in Indus while they expose only 8.82% in Congo. Therefore, this confirms that both the volume of marine compartments and the species distribution fraction have a significant influence on the CFs of this approach.

8.5 The variability of regionalized CFs for every MP tested

After understanding the influence of interactions between regionalization and physical properties of MPs on the development of CFs, this section presents an in-depth comparison and analysis of regionalized CFs for each MP particle tested. This analysis will help identify for

which types of particle regionalization is important and for which ones it is not pronounced. In addition, it will highlight how each parameter can vary the impacts of MPs.

8.5.1 The IW+ approach

Figure 8.9 allows the comparison between the magnitude of variability of CFs due to the physical properties of MPs and regionalization, for emissions at the beach and the water surface. The variability of CFs for all emission sub-compartments can be found in figure C.3 in section C.2.2. In order to understand the interaction between regionalization and the physical properties of MPs, the spatial variability of CFs will be analyzed for every type (shape, size, density) of MP tested. These analyses are presented in separate subsections. Initially, CFs for large high density spherical and fibrous particles are analyzed in section 8.5.1. Then the analysis of CFs for large low density fibrous particles is presented in section 8.5.1. Later, CFs for small fibrous particles are analyzed in section 8.5.1, with a comparison between small and large low density fibrous particles. Last, the analysis for spherical particles is presented in section 8.5.1 with a focus on large EPS and PP particles.

Large high density fibrous and spherical particles

It can be observed that for both shapes, large fibrous (1000 μm) and spherical (1000 and 5000 μm) high density particles, i.e., PS, PET, PVC and TRWP always have the highest CFs for all emission regions and present no spatial variability for their CFs. The reason behind this is the settling velocity that is directly proportional to the size of the particles. Due to their large size, these particles settle as soon as they reach the marine environment at a fast settling velocity. Therefore, their fate and hence their CFs are the same in every emission region. Fast sedimentation and slow degradation rates result in the accumulation of these particles in sediments, where 55.4% of continental marine species are exposed for a long period of time.

Large low density fibrous particles

Regionalization is mainly significant for low density small (1 and 10 μm) and large (1000 and 5000 μm) particles, for both shapes tested. For large (1000 μm) fibrous low density particles, that is, PP, LDPE, HDPE and EPS, the lowest CFs (3.67E-04 $PDF.m^2.yr/kg$) are for emission in the Congo. The fate of these particles in the Congo is dominated by the transfer rate from the water surface to the global scale, which is at least one order of magnitude higher than other transfer and removal rates (all rate matrices are presented in the

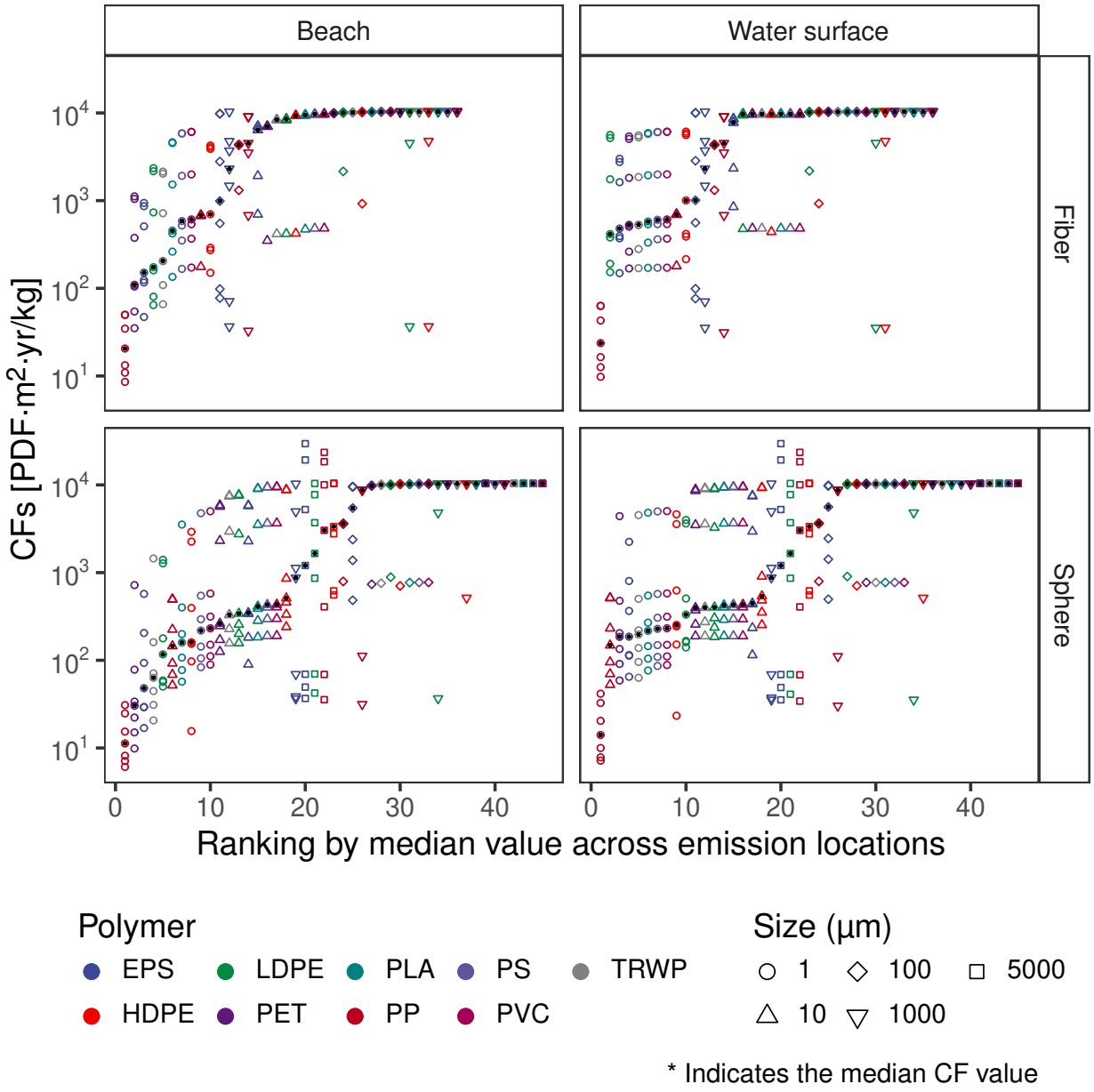

Figure 8.9 The variability of regionalized CFs $[PDF.m^2.yr/kg]$ for all MPs tested, for the IW+ approach. For each type of particle, the spatial variability of CFs is vertically presented. Seven CFs for each emission region for each MP are plotted

Supplementary Information). Consequently, these particles rapidly cross the continental scale of the Congo before any settling can take place. As discussed previously, impacts are "diluted" in the large volume of the global compartment. As a reminder, converting the units from partial $PAF.m^3.d/kg$ to $PDF.m^2.yr/kg$ requires division by the volume and then multiplication by the surface area of the compartment. This is equivalent to dividing by

the compartment depth (1.68 km for the global scale), which is several orders of magnitude deeper than that of continental sub-compartments. Therefore, this explains the low CFs observed in the Congo.

Positively buoyant large fibrous particles (1000 μm), which have medium densities, i.e. HDPE ($\rho = 0.953\ g/cm^3$) and LDPE ($\rho = 0.915\ g/cm^3$), exhibit small variability between their regionalized CFs. As presented above, the lowest values are for emissions in the Congo. The second lowest CFs are for emissions in the Gulf of Guinea because some of these particles manage to reach the global scale, which reduces their impacts. However, the fate of these particles in other regions is similar, which explains their similar CFs.

For low density large fibrous particles (1000 μm), i.e. EPS and PP, the regionalization variability is significant compared to medium density HDPE and LDPE. This is related to the celerity of biofouling and the fate of MPs in each region. Medium-density LDPE and HPDE take 37 and 25 days, respectively, to become negatively buoyant due to biofouling. However, EPS ($\rho = 0.03\ g/cm^3$) and PP ($\rho = 0.88\ g/cm^3$) take 7.5 months and 47.5 days, respectively. Thus, LDPE and HDPE reach the sediments earlier than EPS and PP. Therefore, they are less prone to being carried by water currents. This also justifies the higher CF values observed for LDPE and HDPE compared to EPS and PP. The variability of regionalization for EPS and PP ranges three orders of magnitude. This is because the fate of these particles varies greatly between emission regions. Table 8.4 ranks the emission regions according to the increasing order of their CFs, for 1000 μm fibrous EPS and PP. The table also presents the compartments of ultimate fate of these polymers in each emission region. It can be seen that the fate of EPS and PP differs between the regions. This is also related to the celerity of biofouling, where PP settles faster than EPS. The lowest impacts are always observed in the emission regions where MPs reach the global scale because impacts are reduced. The highest impacts are observed when the particles reach the sediments. This is related to the high residence time in the sediments (figure 8.10) due to slow degradation, resuspension, and burial. When all particles are beached (e.g., in the Mediterranean and Guinea Gulf for EPS), the lower impacts are related to the beaching rate. The faster the beaching (i.e., Mediterranean), the lower the impacts due to fast degradation on the beach, hence a shorter exposure period to marine ecosystems.

Small fibrous particles

The influence of regionalization for small fibrous particles (1 μm) is significant (figure 8.9). Small particles, regardless of their densities, have very slow settling velocities. For this reason, these particles drift for a long period of time in the water before they settle in the sediments.

Table 8.4 Ranking of emission regions by increasing order of their CFs for emissions at the beach and water surface, for 1000 μm fibrous EPS and PP

		Increasing order of regionalized CFs from smallest CFs (left) to highest CFs (right)						
EPS	**Emission regions**	**Congo**	**Okhotsk Sea**	**Mediterranean**	**Bengal Bay**	**East China**	**Guinea Gulf**	**Indus**
	Ultimate fate	Global scale	Global scale Beach	Beach	Global scale Beach Sediments	Global scale Beach Sediments	Beach	Beach Sediments
PP	**Emission regions**	**Congo**	**Bengal Bay**	**Guinea Gulf**	**Okhotsk Sea**	**Mediterranean**	**Indus**	**East China**
	Ultimate fate	Global scale	Global scale Sediments	Global scale Beach Sediments	Global scale Beach Sediments	Beach Sediments	Beach Sediments	Beach Sediments

Therefore, their fate and, thus, their impacts depend greatly on the direction of the water currents in every emission region. If they are carried towards the beach and/or the global scale, their impacts will be smaller than other particles that entirely settle at the continental scale.

In comparison of small and large low density fibrous particles, it can be seen that larger particles always have higher CFs than smaller MPs. For example, CFs of 1 μm in Indus are the smallest. However, larger particles, emitted in Indus, have three orders of magnitude larger CFs than those of smaller ones. The reason behind this is the high settling velocity of large particles compared to smaller ones. Although large particles take a longer duration to become negatively buoyant because of biofouling, they start settling at velocities that are at least four orders of magnitude larger than negatively buoyant small particles. Enhancing the settling of the particles shifts the dominant transfer rate, from the beaching rate ($k_{b,ws}$), observed for 1 μm particles, to the sedimentation rate ($k_{sed,wc}$). Therefore, large particles accumulate fast in sediments where impacts are higher.

For fibrous small (1 μm) MPs, the lowest median CF values are for emissions in Indus, with the lowest value observed for PP. Small particles emitted in Indus accumulate in the sediments. The residence time of PP in sediments is one order of magnitude smaller than that of other particles (figure 8.10). This is because PP degrades the fastest in sediments compared to other polymers, significantly reducing its impacts. This explains the lowest values of CFs for PP in comparison to those of other polymers of the same size and shape.

Spherical particles

CFs for spherical particles follow the same trend as that of fibrous particles. CFs of large (1000 and 5000 μm) high density spherical MPs are always the highest and exhibit no variation with regionalization due to their large settling velocities and fast accumulation in sediments. Small particles (1 μm), and large (1000 and 5000 μm) low density particles present the highest variability with regionalization. These particles linger in the marine environment

longer than large high density particles. Thus, their fate is more influenced by the direction of the water currents in each region. The celerity of biofouling of each particle (defined by its size, density, and shape) versus the direction of the currents, play the key role in defining the fate of the particles and, therefore, their impacts.

Spherical 5000 μm EPS and PP have the highest impacts among all MPs tested. For emissions at the water surface, the highest CF for EPS is in Indus ($CF^{Indus}_{ws,EPS}$ = 2.96E+04 $PDF.m^2.yr/kg$), followed by an emission in the Gulf of Guinea ($CF^{GG}_{ws,EPS}$ = 1.93E+04 $PDF.m^2.yr/kg$). These values are one order of magnitude larger than the particle's CFs for emissions in East China Sea and the Mediterranean, and three orders of magnitude larger than emissions in the other regions. In Gulf of Guinea and Indus, EPS particles are transported toward the beach. However, their fate is mainly dominated by the resurfacing rate ($k_{resurfacing}$ = 4.5E-01 day^{-1}). This results in the accumulation of EPS in the water surface ($FF_{ws,ws}$ = 1.22E+05 days = 335.5 years in Gulf of Guinea, and 1.15E+05 days = 315.6 years in Indus, as presented in figue 8.10). The marine ecosystem at the water surface exhibits the highest sensitivity (EEF_{ws} = 1065.7 $PAF.m^3/kg$) where 29.53% of marine species are exposed to MPs. This significantly increases the CFs of the particles. Similarly, 5000 μm PP have the highest impacts in the Gulf of Guinea ($CF^{GG}_{ws,EPS}$ = 2.35E+04 $PDF.m^2.yr/kg$), followed by the Mediterranean ($CF^{Medit}_{ws,EPS}$ = 1.84E+04 $PDF.m^2.yr/kg$). The fate of these particles is also dominated by their resurfacing rate, which results in their accumulation in the water surface where impacts are high.

8.5.2 The GLAM approach

For the GLAM approach, the influence of regionalization on the CFs (figure 8.8) is more pronounced than in the IW+ approach (figure 8.4). The variability of CFs for all emission compartments is presented in figure C.4. Median CFs for all different polymers across all emission regions range two orders of magnitude with the physical properties of MPs for both shapes. However, the influence of regionalization on CFs ranges up to four and five orders of magnitude for fibrous and spherical particles, respectively. This is mainly related to the species distribution fraction (SDF) and the volume of marine compartments that have a strong influence on the CFs for the GLAM approach. As previously mentioned, this approach gives more intrinsic values for species living in rich sub-compartments. Therefore, the highest impacts are expected to be observed in rich environments. The variability of CFs is first analyzed for large high density particles (section 8.5.3). The variability of CFs for large low density fibrous and spherical particles is then presented in section 8.5.4, with a focus on EPS and HDPE particles. Later, the variability of CFs for small particles is briefly

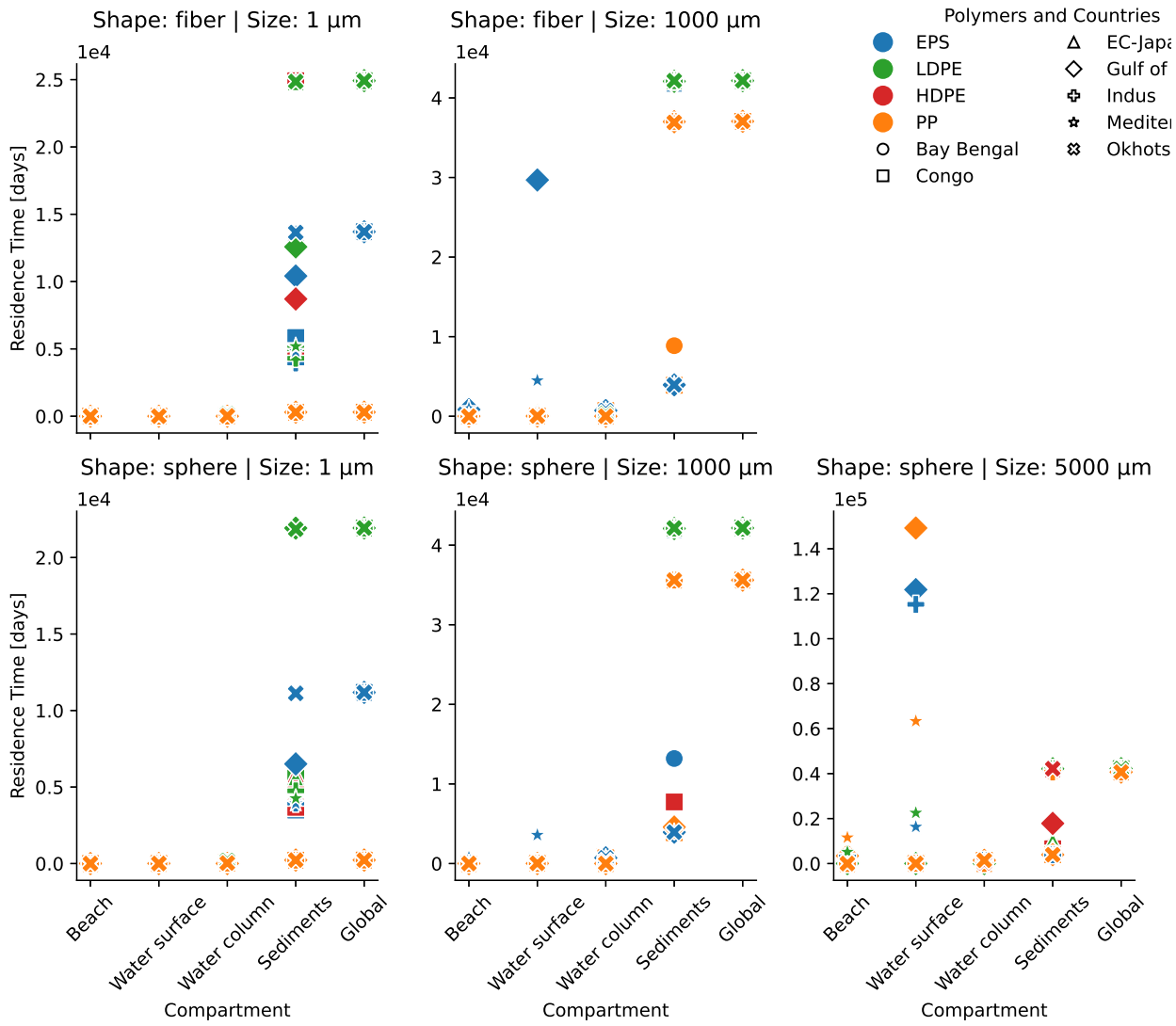

Figure 8.10 Residence times of small (1 μm) and large (1000 and 5000 μm) low density fibrous and spherical MPs in marine sub-compartments

presented in section 8.5.5 to avoid redundant information.

8.5.3 Large high density fibrous and spherical particles

Similar to the IW+ approach, large fibrous (100 and 1000 μm) and spherical (100, 1000 and 5000 μm) high density particles have the highest CFs due to their accumulation in the sediments. While the fate of these particles is the same in all emission regions, CFs vary by up to one order of magnitude, with the lowest for emissions in East China Sea, and the highest in Bay of Bengal. CFs for emissions to the East China Sea are the smallest because

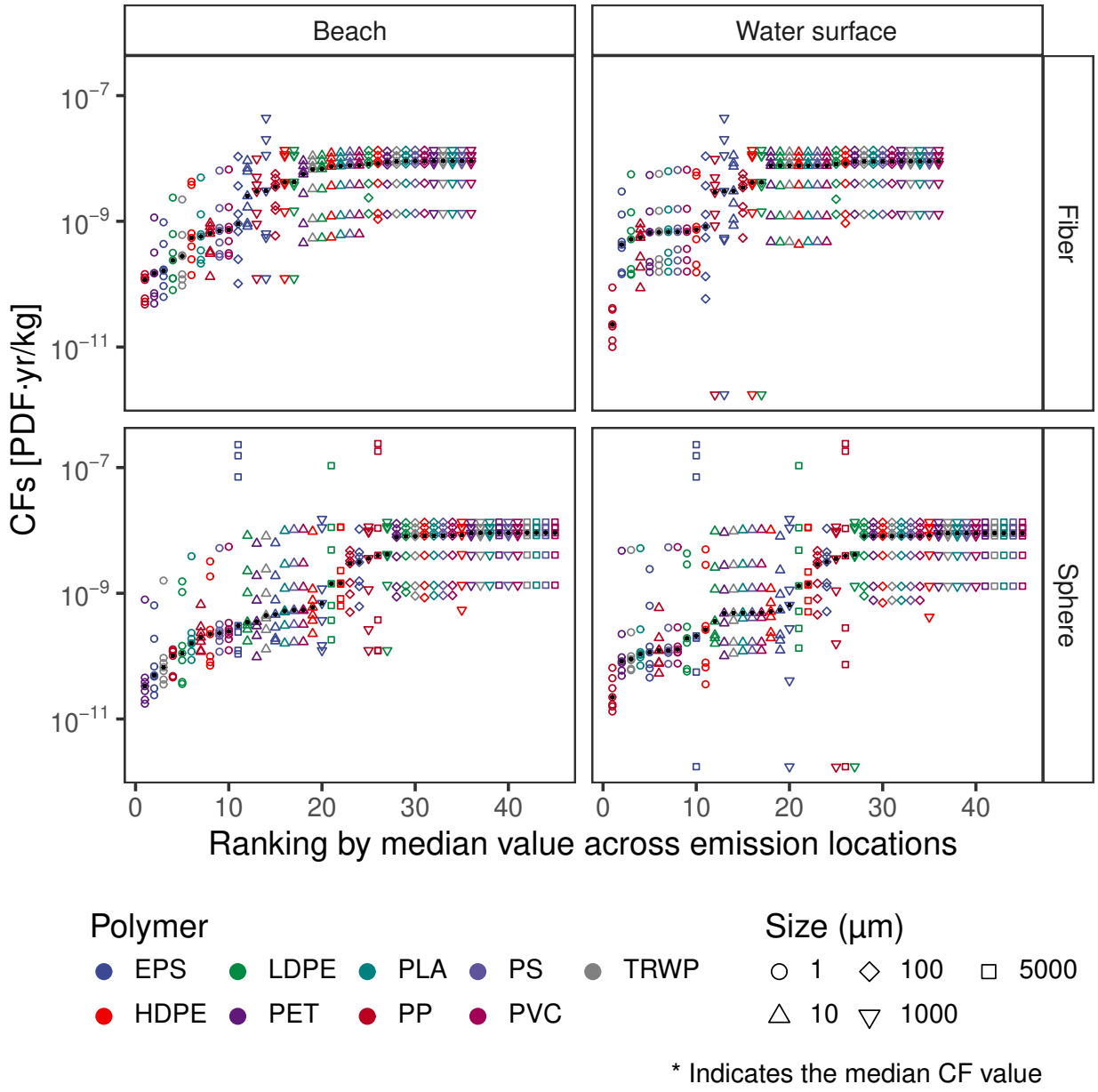

Figure 8.11 The variability of regionalized CFs $[PDF.yr/kg]$ for all MPs tested, for the GLAM approach

this region exhibits the largest volumes of all marine sub-compartments (table 8.2), with up to two orders of magnitude for the volume of the water column. Therefore, impacts in this region are reduced because of the large "diluting" volume of marine compartments. While the size of marine sub-compartments in the Bay of Bengal has similar orders of magnitude as other regions, it presents the highest CFs observed. This is because the Bay of Bengal hosts more marine species at the continental scale than other regions: $SDF_b^{BB} = 6.88\%$, SDF_{ws}^{BB}

= 12.35%, SDF_{wc}^{BB} = 6.31% and SDF_{sed}^{BB} = 23.18%, which are the largest SDFs among all emission regions (SDF matrices can be found in the **Supplementary Information**). Therefore, this explains the high impacts of large high density in the rich sediments of the Bay of Bengal.

8.5.4 Large low density fibrous and spherical particles

As it was observed for the IW+ approach, regionalization is more variable for low density large particles compared to the high density ones, for both spherical and fibrous MPs. The largest variability is observed for EPS 1000 μm fibrous particles and for EPS and HDPE 5000 μm spherical particles. For fibrous 1000 μm EPS, the variability ranges four orders of magnitude, with the lowest value for emissions in Congo, while the highest for Gulf of Guinea. As previously seen, emissions in the Congo have the lowest impacts because low density particles are transported to the global scale. Despite hosting 80.79% of marine species in the global scale for the Congo, impacts are diluted in its large volume (V_{global} = 1.21E+09 m^3), which is at least five orders of magnitude larger than that of the continental scale (table 8.2). Particles emitted in the Gulf of Guinea are transported to the beach. However, their fate is dominated by the resurfacing rate ($k_{resurfacing}$ = 4.5E-01 day^{-1}) which is faster than the beaching rate ($k_{beaching}$ = 1.27E-02 day^{-1}). This increases the residence time of the particles (figure 8.10) in the water surface ($FF_{ws,ws}$ = 2.97E+04 days). Gulf of Guinea has the smallest marine sub-compartments which justifies the high impacts of MPs observed.

The variability of regionalization of 5000 μm EPS and HDPE spherical particles ranges five orders of magnitude. Both particles have the lowest impacts in Congo since all MP particles are transported to the global scale. The lowest CFs for EPS are observed for emissions in Bay of Bengal, East China and Okhotsk Sea. This is also because MPs reach the global scale in these domains, which reduces their impacts. All EPS particles emitted in Gulf of Guinea, Indus and the Mediterranean Sea reach their ultimate fate at the beach. However, the highest CF is observed for emission in Indus. The size of continental marine sub-compartments in these three regions has the same orders of magnitude (table 8.2). However, Indus is the richest among them, hosting 5.56%, 11%, 5.62% and 20.65% at the beach, water surface, water column and sediments, respectively. Therefore, Indus has the highest impacts. Similarly, HDPE particles have low CFs in the Bay of Bengal, Gulf of Guinea and the Mediterranean Sea because particles manage to reach the global scale. In emission regions where HDPE particles show similar fate, i.e., East China Sea, Indus and Okhotsk Sea, lowest impacts are observed for East China Sea due to its large volume. Whereas highest impacts are observed

in Okhotsk Sea that has higher species richness than Indus.

8.5.5 Small particles

As observed for the IW+ approach, small (1 μm) particles have the lowest CFs and present high spatial variability. This is because these particles have a low settling velocity and remain in the marine water. If these particles reach the global scale, their impacts will be reduced. Alternatively, if they reach the beach and/or manage to settle due to water currents, their CFs will increase. Because of their fast degradation rates, the lowest CF values for small MPs are observed for PP.

In-depth analysis of the variability of CFs with regionalization for every MP particle tested, both for the IW + and GLAM approaches, gave a clearer and more concrete explanation of the interaction between the addressed parameters. It is proven once again that regionalization is important for the development of CFs for MPs emitted in the marine environment. The importance of regionalization is more pronounced for small MPs of all densities and shapes, and for low density MPs of all sizes and shapes. However, regionalization is less pronounced for large high density spherical and fibrous particles because the fate of these particles is similar in all emission regions. In addition, the interaction between the direction of water currents and the physical properties of MPs plays a key role in changing the fate and hence the impacts of the particles. Moreover, the characteristics of marine sub-compartments, i.e., their size and species richness can reduce or increase the impacts of emitted MPs, especially for the GLAM approach.

8.6 The influence of seasonality

Figure 8.12 presents the influence of seasonality for both EPS spherical 5000 μm and HDPE fibrous 1000 μm particles, for the IW+ approach.

The variability of CFs with seasonality is less pronounced for HDPE than for EPS particles. CFs in Okhotsk Sea, Mediterranean Sea, Indus, Gulf of Guinea, and East China Sea did not change for HDPE between winter (emissions in January) and summer (emissions in July). However, CFs for emissions in Congo increased by two orders of magnitude in summer compared to winter, whereas CFs for emissions in the Bay of Bengal are reduced by almost two orders of magnitude. The reason behind this, is the difference in the fate between emissions in winter and summer. All HDPE particles emitted in Congo in winter are transported and settle in the global scale where the impact is reduced. However, when particles are emitted in summer, these particles are transported to the beach, where the impacts are much higher

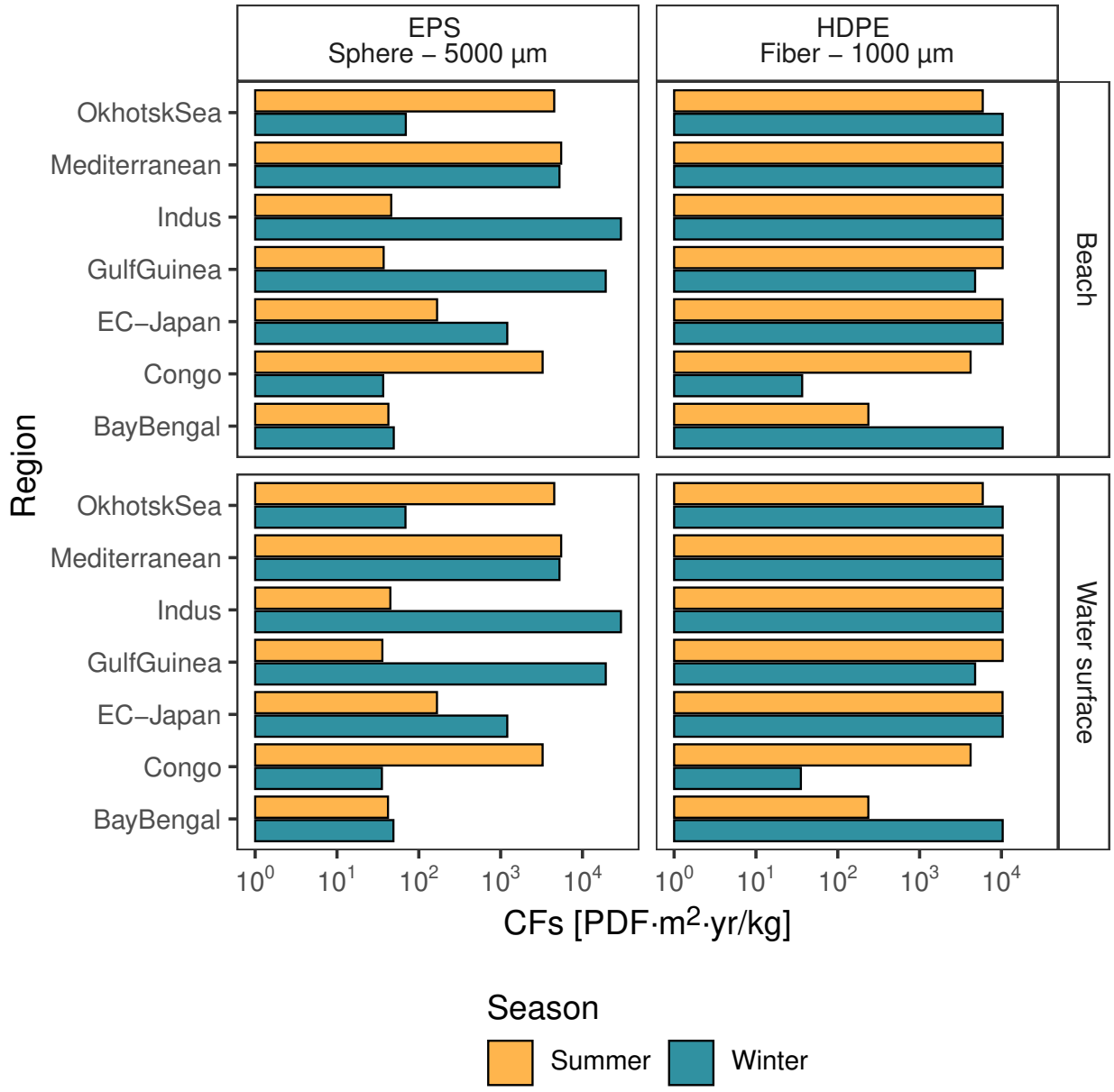

Figure 8.12 The variability of CFs $[PDF.m^2.yr/kg]$ with emissions at the beach and water surface, in January and July, for every emission region, for the IW+ approach

compared to the winter emissions (figure 8.13).

HDPE particles emitted in the Bay of Bengal in winter settle in the continental sediments (figure 8.14). In summer, the majority of particles settle in continental sediments while others reach the global scale. This explains the reduction of impacts between winter and summer.

For EPS particles, the influence of seasonality is pronounced in all emission regions, except

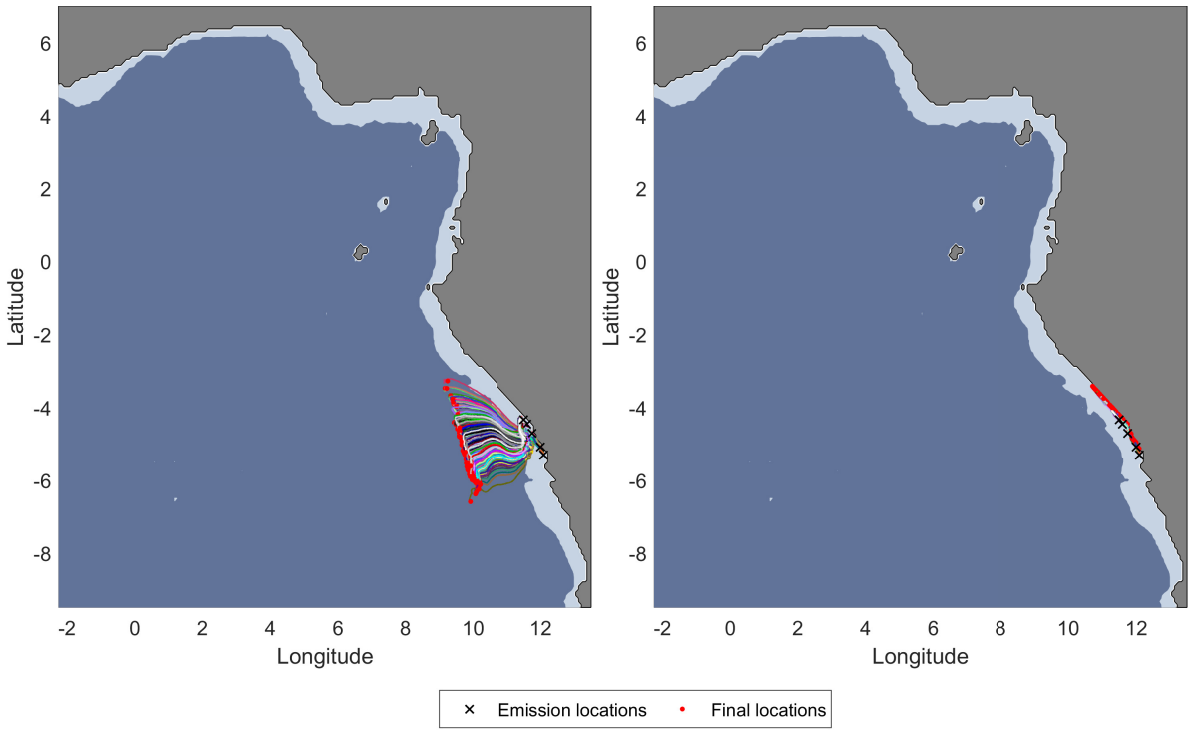

Figure 8.13 Trajectories of 1000 μm HDPE fibrous particles emitted in winter (left) and summer (right), in Congo

for the Mediterranean and Bay of Bengal. Emissions in summer increased the impacts of EPS in the Okhotsk Sea and Congo by about two orders of magnitude and reduced them by about three orders of magnitude for emissions in Indus and Gulf of Guinea. Emissions in summer in East China Sea slightly reduced impacts compared to winter. The reason behind these differences is also related to changes in the direction of the water current due to the monsoon. As a result, the fate of the particles and hence their impacts changed. For instance, emissions of EPS in Indus in winter transported all the particles to the beach, in the east direction. However, emissions in summer drifted the particles more towards the West where part of them beached and the others left towards the global scale (figure 8.15).

In Sea of Okhotsk, some of the EPS particles emitted reach the beach while the others manage to reach the global scale. However, in summer, all particles beach at the entrance to the sea from the river (figure 8.16). This results in an increase in impacts in summer compared to winter.

Although seasonality influences the direction of currents in Bay of Bengal, resulting in a reduction in impacts of HDPE 1000 μm fibrous particles between winter and summer emissions, it does not have an influence on EPS particles. Because EPS is less dense than HDPE,

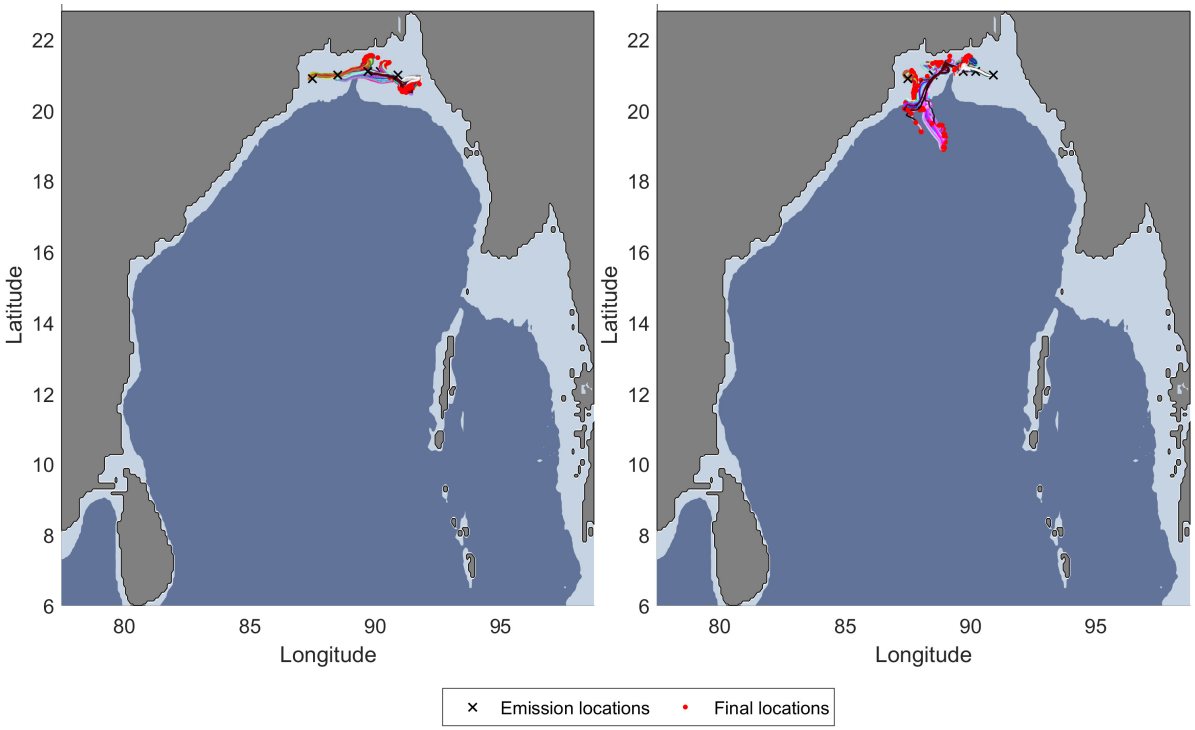

Figure 8.14 Trajectories of 1000 μm HDPE fibrous particles emitted in winter (left) and summer (right), in Bay of Bengal

it disperses longer in marine water before it starts to settle. Thus, its fate in the Bay of Bengal does not change between seasons. Therefore, the influence of seasonality depends not only on the emission region but also on the physical properties of emitted MPs. Nevertheless, seasonality should be treated carefully when addressing the impacts of MPs. Although it is less important than regionalization in some regions, it can reduce or increase the impacts of certain polymers in other regions. Consequently, to better address the influence of seasonality, it should be tested on all MP particles.

Figure 8.17 presents the influence of seasonality for the GLAM approach. As was observed for the IW+ approach, the influence of seasonality is less pronounced for HDPE particles than for EPS particles. CFs for 1000 μm HDPE emitted in Congo also increased by five orders of magnitude, from winter to summer, due to transfer to the beach (figure 8.13). HDPE particles emitted in Bay of Bengal during winter have one to two orders of magnitude reduction in summer due to transfer to the global scale (figure 8.14). Similarly for EPS particles emitted in summer, CFs increase in Sea of Okhotsk and Congo, and decrease in Indus and Gulf of Guinea. Therefore, seasonality influences the impacts of MPs for both approaches, due to changes in the fate of particles in some regions with the direction of water

currents.

8.7 Aggregation of CFs

As described in section 5.8, CFs for every polymer tested in every emission region are aggregated into two continent CFs (Africa and Asia), and then into one global CF, using emissions from rivers (table 5.1). CFs for Asia and Africa are presented in the **Supplementary Information**. Table 8.5 presents the global CFs for every polymer for IW+, for emissions at the beach and the water surface. Table 8.6 presents the same information for the GLAM approach. The complete list for global CFs is presented in **Supplementary Information**. Depending on the availability of LCI flows for MP emissions, LCA practitioners have the flexibility to choose which CF to use. It is important to mention that the uncertainty increases as we move from region-based CFs to continental CFs and then to global CFs.

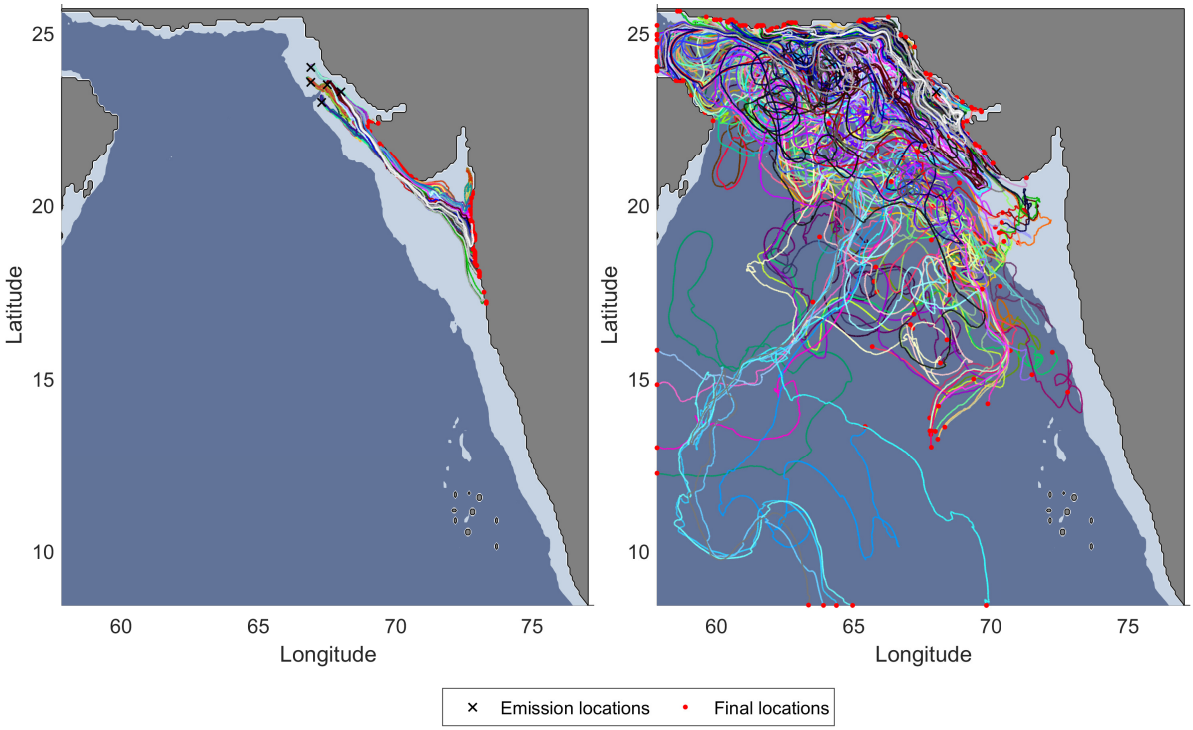

Figure 8.15 Trajectories of 5000 μm EPS spherical particles emitted in winter (left) and summer (right), in Indus

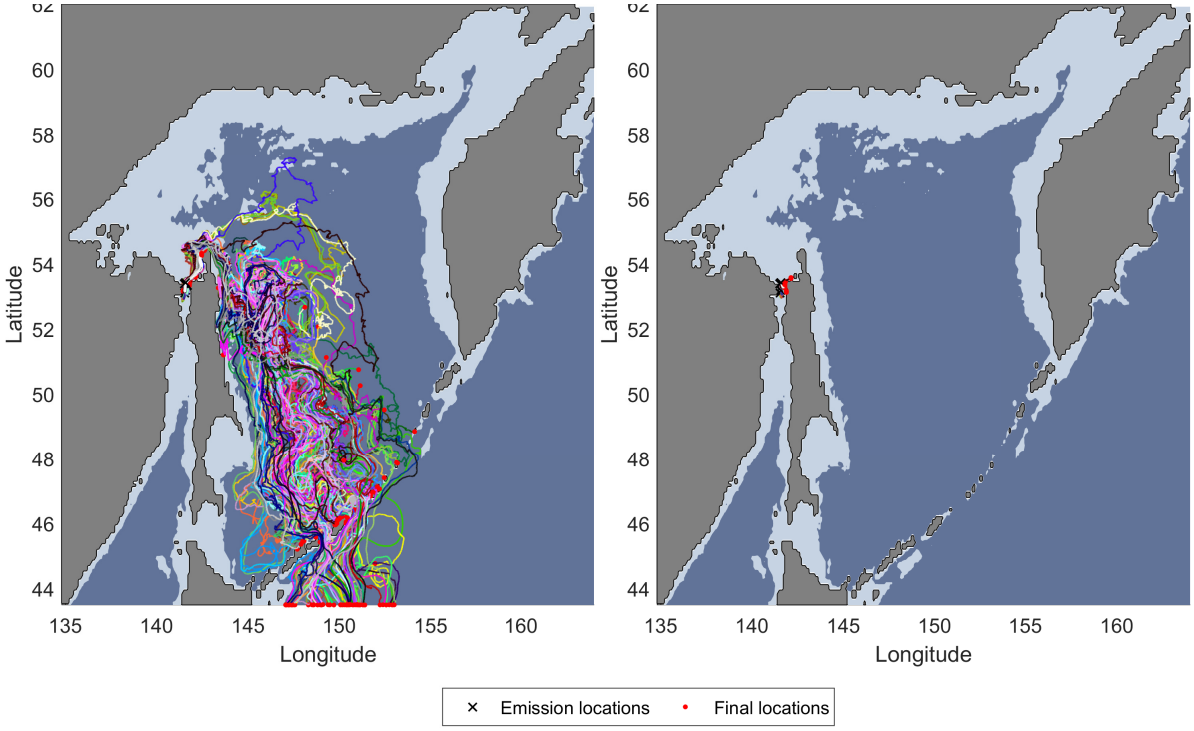

Figure 8.16 Trajectories of 5000 μm EPS spherical particles emitted in winter (left) and summer (right), in Sea of Okhotsk

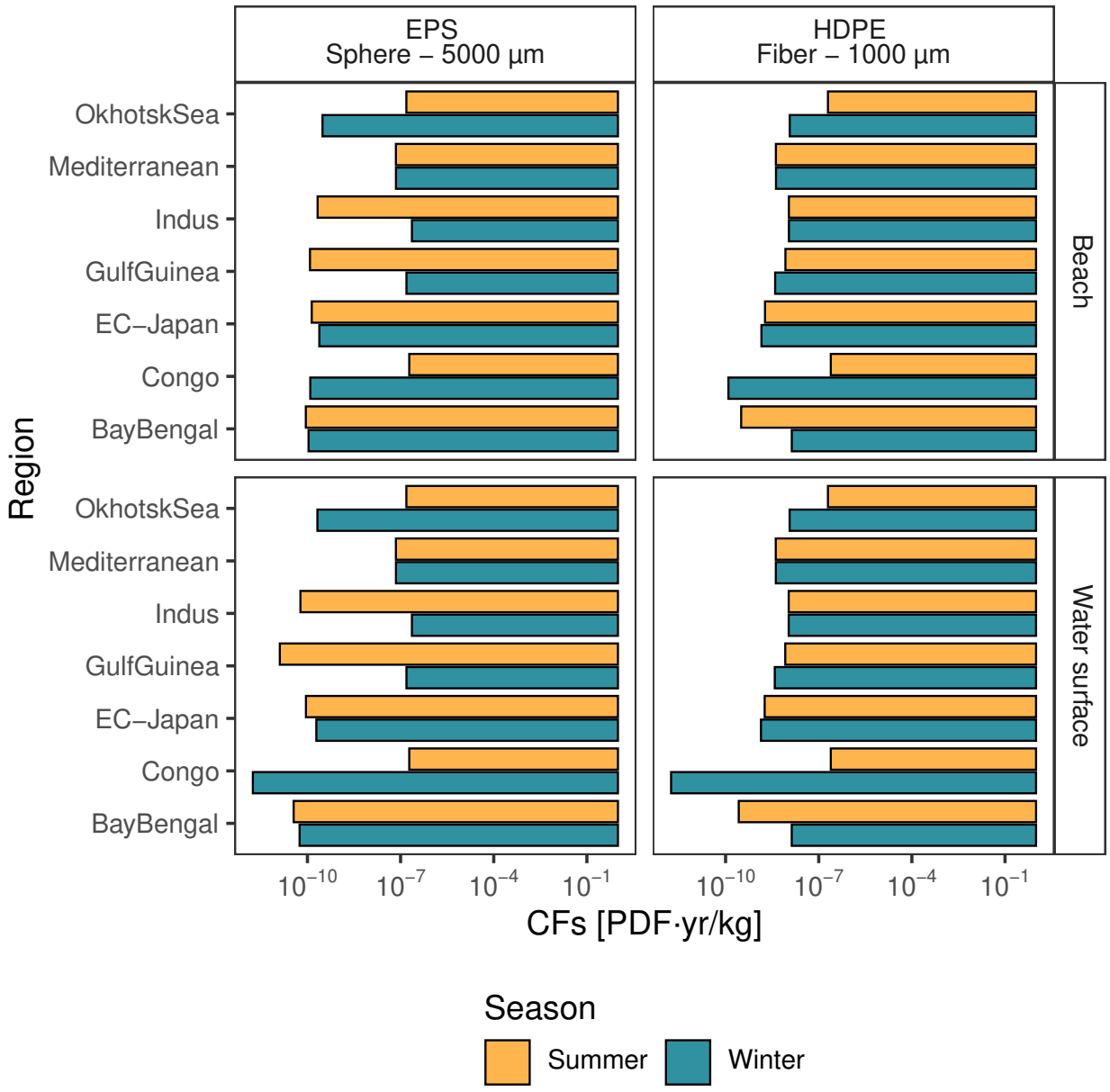

Figure 8.17 The variability of CFs $[PDF.m^2.yr/kg]$ with emissions at the beach and water surface, in January and July, for every emission region, for the GLAM approach. CFs are presented in logarithmic scale. For the values of CF for the GLAM approach, the larger the bars the smaller the CF value

Table 8.5 Global CFs for emissions at the beach and water surface, for IW+ approach, with their spatial variability between minimum and maximum across regions of emissions. b: beach, ws: water surface, glo: global, Min: minimum, Max: maximum

Polymer	**Shape**	**Size**	CF_b^{glo}	**Min** CF_b	**Max** CF_b	CF_{ws}^{glo}	**Min** CF_{ws}	**Max** CF_{ws}
EPS	**fiber**	**1**	7.29E+02	4.71E+01	9.42E+02	2.32E+03	1.49E+02	3.01E+03
		10	5.89E+03	6.97E+02	7.03E+03	7.17E+03	8.48E+02	8.57E+03
		100	7.50E+03	7.74E+01	9.80E+03	7.66E+03	7.65E+01	1.00E+04
		1000	3.65E+03	3.66E+01	1.03E+04	3.66E+03	3.54E+01	1.03E+04
	sphere	**1**	8.87E+01	1.69E+01	5.72E+02	3.47E+02	6.49E+01	2.24E+03
		10	4.47E+03	8.99E+01	5.85E+03	5.77E+03	1.15E+02	7.55E+03
		100	7.79E+03	4.84E+02	9.57E+03	8.01E+03	4.97E+02	9.85E+03
		1000	4.42E+03	3.66E+01	1.03E+04	4.43E+03	3.53E+01	1.03E+04
		5000	3.54E+03	3.67E+01	2.95E+04	3.55E+03	3.54E+01	2.96E+04
HDPE	**fiber**	**1**	3.13E+03	1.50E+02	4.26E+03	4.50E+03	2.15E+02	6.12E+03
		10	7.92E+03	4.23E+02	9.29E+03	8.27E+03	4.40E+02	9.69E+03
		100	8.78E+03	9.23E+02	1.03E+04	8.82E+03	9.26E+02	1.03E+04
		1000	9.32E+03	3.67E+01	1.04E+04	9.32E+03	3.54E+01	1.04E+04
	sphere	**1**	4.12E+02	1.56E+01	2.92E+03	6.51E+02	2.33E+01	4.62E+03
		10	6.64E+03	2.40E+02	8.80E+03	7.02E+03	2.53E+02	9.32E+03
		100	8.73E+03	7.04E+02	1.02E+04	8.78E+03	7.07E+02	1.03E+04
		1000	9.43E+03	5.14E+02	1.04E+04	9.44E+03	5.13E+02	1.04E+04
		5000	8.75E+03	5.56E+02	1.04E+04	8.75E+03	5.54E+02	1.04E+04
LDPE	**fiber**	**1**	1.79E+03	6.45E+01	2.35E+03	4.27E+03	1.53E+02	5.60E+03
		10	7.26E+03	4.20E+02	8.51E+03	8.26E+03	4.77E+02	9.69E+03
		100	8.77E+03	2.15E+03	1.02E+04	8.90E+03	2.18E+03	1.03E+04
		1000	9.29E+03	3.67E+01	1.04E+04	9.30E+03	3.54E+01	1.04E+04

Table 8.5 continued from previous page

Polymer	Shape	Size	CF_b^{glo}	Min CF_b	Max CF_b	CF_{ws}^{glo}	Min CF_{ws}	Max CF_{ws}
LDPE	**sphere**	**1**	1.92E+02	5.01E+01	1.40E+03	5.47E+02	1.40E+02	3.98E+03
		10	5.88E+03	1.57E+02	7.72E+03	6.97E+03	1.85E+02	9.15E+03
		100	8.63E+03	8.87E+02	1.01E+04	8.79E+03	9.02E+02	1.03E+04
		1000	9.31E+03	3.67E+01	1.04E+04	9.32E+03	3.54E+01	1.04E+04
		5000	1.81E+03	4.23E+01	1.04E+04	1.81E+03	4.10E+01	1.04E+04
PET	**fiber**	**1**	8.55E+02	3.51E+01	1.12E+03	4.13E+03	1.68E+02	5.40E+03
		10	5.98E+03	3.50E+02	7.01E+03	8.27E+03	4.83E+02	9.69E+03
		100	9.12E+03	9.92E+03	9.92E+03	9.47E+03	1.03E+04	1.03E+04
		1000	9.50E+03	1.03E+04	1.03E+04	9.53E+03	1.04E+04	1.04E+04
	sphere	**1**	7.53E+01	9.86E+00	7.21E+02	4.60E+02	5.89E+01	4.40E+03
		10	4.48E+03	1.26E+02	5.88E+03	6.76E+03	1.89E+02	8.88E+03
		100	8.36E+03	7.35E+02	9.78E+03	8.79E+03	7.71E+02	1.03E+04
		1000	9.48E+03	1.03E+04	1.03E+04	9.53E+03	1.04E+04	1.04E+04
		5000	9.53E+03	1.04E+04	1.04E+04	9.54E+03	1.04E+04	1.04E+04
PLA	**fiber**	**1**	3.54E+03	1.35E+02	4.63E+03	4.51E+03	1.71E+02	5.90E+03
		10	8.05E+03	4.71E+02	9.44E+03	8.27E+03	4.83E+02	9.70E+03
		100	9.45E+03	1.03E+04	1.03E+04	9.47E+03	1.03E+04	1.03E+04
		1000	9.53E+03	1.04E+04	1.04E+04	9.53E+03	1.04E+04	1.04E+04
	sphere	**1**	3.84E+02	5.70E+01	3.53E+03	5.23E+02	7.65E+01	4.82E+03
		10	6.92E+03	1.83E+02	9.09E+03	7.18E+03	1.89E+02	9.42E+03
		100	8.75E+03	7.70E+02	1.02E+04	8.79E+03	7.72E+02	1.03E+04
		1000	9.53E+03	1.04E+04	1.04E+04	9.53E+03	1.04E+04	1.04E+04
		5000	9.54E+03	1.04E+04	1.04E+04	9.54E+03	1.04E+04	1.04E+04

Table 8.5 continued from previous page

Polymer	Shape	Size	CF_b^{glo}	Min CF_b	Max CF_b	CF_{ws}^{glo}	Min CF_{ws}	Max CF_{ws}
PP	fiber	1	4.01E+01	8.57E+00	5.00E+01	5.05E+01	9.79E+00	6.32E+01
		10	5.87E+02	1.76E+02	6.78E+02	6.03E+02	1.80E+02	6.95E+02
		100	3.77E+03	1.31E+03	4.33E+03	3.78E+03	1.32E+03	4.34E+03
		1000	7.84E+03	3.27E+01	9.12E+03	7.84E+03	3.13E+01	9.12E+03
	sphere	1	1.35E+01	6.08E+00	3.08E+01	1.77E+01	7.17E+00	4.16E+01
		10	3.88E+02	5.19E+01	4.97E+02	4.02E+02	5.26E+01	5.15E+02
		100	3.13E+03	7.93E+02	3.62E+03	3.14E+03	7.95E+02	3.64E+03
		1000	7.80E+03	3.15E+01	8.76E+03	7.80E+03	3.02E+01	8.76E+03
		5000	2.30E+03	3.56E+01	2.35E+04	2.30E+03	3.42E+01	2.35E+04
PS	fiber	1	4.48E+03	1.67E+02	5.85E+03	4.64E+03	1.72E+02	6.07E+03
		10	8.24E+03	4.82E+02	9.66E+03	8.27E+03	4.83E+02	9.70E+03
		100	9.47E+03	1.03E+04	1.03E+04	9.47E+03	1.03E+04	1.03E+04
		1000	9.53E+03	1.04E+04	1.04E+04	9.53E+03	1.04E+04	1.04E+04
	sphere	1	5.23E+02	8.34E+01	4.76E+03	5.47E+02	8.61E+01	4.99E+03
		10	7.19E+03	1.89E+02	9.43E+03	7.22E+03	1.89E+02	9.48E+03
		100	8.78E+03	7.72E+02	1.03E+04	8.79E+03	7.72E+02	1.03E+04
		1000	9.53E+03	1.04E+04	1.04E+04	9.53E+03	1.04E+04	1.04E+04
		5000	9.54E+03	1.04E+04	1.04E+04	9.54E+03	1.04E+04	1.04E+04
PVC	fiber	1	4.65E+03	1.72E+02	6.08E+03	4.67E+03	1.72E+02	6.10E+03
		10	8.27E+03	4.84E+02	9.69E+03	8.27E+03	4.83E+02	9.70E+03
		100	9.47E+03	1.03E+04	1.03E+04	9.47E+03	1.03E+04	1.03E+04
		1000	9.53E+03	1.04E+04	1.04E+04	9.53E+03	1.04E+04	1.04E+04

Table 8.5 continued from previous page

Polymer	Shape	Size	CF_b^{glo}	Min CF_b	Max CF_b	CF_{ws}^{glo}	Min CF_{ws}	Max CF_{ws}
PVC	**sphere**	**1**	5.52E+02	8.92E+01	5.00E+03	5.54E+02	8.83E+01	5.02E+03
		10	7.23E+03	1.90E+02	9.48E+03	7.23E+03	1.89E+02	9.49E+03
		100	8.79E+03	7.73E+02	1.03E+04	8.79E+03	7.72E+02	1.03E+04
		1000	9.53E+03	1.04E+04	1.04E+04	9.53E+03	1.04E+04	1.04E+04
		5000	9.54E+03	1.04E+04	1.04E+04	9.54E+03	1.04E+04	1.04E+04
TRWP	**fiber**	**1**	1.64E+03	6.59E+01	2.14E+03	4.25E+03	1.70E+02	5.55E+03
		10	7.14E+03	4.17E+02	8.36E+03	8.27E+03	4.83E+02	9.69E+03
		100	9.32E+03	1.01E+04	1.01E+04	9.47E+03	1.03E+04	1.03E+04
		1000	9.52E+03	1.03E+04	1.03E+04	9.53E+03	1.04E+04	1.04E+04
	sphere	**1**	1.54E+02	2.06E+01	1.45E+03	4.82E+02	6.31E+01	4.52E+03
		10	5.76E+03	1.57E+02	7.56E+03	6.98E+03	1.89E+02	9.16E+03
		100	8.60E+03	7.57E+02	1.01E+04	8.79E+03	7.72E+02	1.03E+04
		1000	9.51E+03	1.03E+04	1.03E+04	9.53E+03	1.04E+04	1.04E+04
		5000	9.53E+03	1.04E+04	1.04E+04	9.54E+03	1.04E+04	1.04E+04

End of Table

Table 8.6 Global CFs for all polymers, for emissions at the beach and water surface, for the GLAM approach, with their spatial variability between minimum and maximum across regions of emissions. b: beach, ws: water surface, glo: global, Min: minimum, Max: maximum

Polymer	**Shape**	**Size**	CF_b^{glo}	**Min** CF_b	**Max** CF_b	CF_{ws}^{glo}	**Min** CF_{ws}	**Max** CF_{ws}
EPS	**fiber**	**1**	1.41E-10	6.27E-11	9.65E-10	3.96E-10	1.45E-10	2.98E-09
		10	1.34E-09	8.30E-10	9.21E-09	1.58E-09	8.58E-10	1.12E-08
		100	1.35E-09	1.02E-10	1.07E-08	1.32E-09	5.85E-11	1.09E-08
		1000	2.99E-09	1.23E-10	4.40E-08	2.94E-09	1.75E-12	4.40E-08
	sphere	**1**	4.21E-11	2.39E-11	6.43E-10	1.1E-10	4.56E-11	2.42E-09
		10	7.74E-10	1.74E-10	6.30E-09	9.46E-10	1.24E-10	8.05E-09
		100	1.6E-09	6.16E-10	1.05E-08	1.59E-09	5.13E-10	1.07E-08
		1000	1.94E-09	1.23E-10	1.52E-08	1.89E-09	1.74E-12	1.51E-08
		5000	2.23E-08	1.08E-10	2.31E-07	2.23E-08	1.74E-12	2.31E-07
HDPE	**fiber**	**1**	5.69E-10	1.39E-10	4.27E-09	7.63E-10	1.54E-10	6.05E-09
		10	1.87E-09	5.56E-10	1.22E-08	1.89E-09	4.28E-10	1.26E-08
		100	2.09E-09	1.08E-09	1.34E-08	2.05E-09	9.34E-10	1.34E-08
		1000	2.7E-09	1.23E-10	1.36E-08	2.64E-09	1.76E-12	1.35E-08
	sphere	**1**	1.89E-10	7.07E-11	3.21E-09	2.44E-10	3.57E-11	4.99E-09
		10	1.11E-09	2.27E-10	9.61E-09	1.12E-09	1.95E-10	1.01E-08
		100	2.07E-09	8.53E-10	1.34E-08	2.02E-09	7.05E-10	1.34E-08
		1000	2.72E-09	5.41E-10	1.35E-08	2.67E-09	4.20E-10	1.35E-08
		5000	2.17E-09	6.28E-10	1.13E-08	2.11E-09	5.07E-10	1.12E-08
LDPE	**fiber**	**1**	3.1E-10	8.05E-11	2.38E-09	6.87E-10	1.42E-10	5.60E-09
		10	1.71E-09	5.43E-10	1.11E-08	1.89E-09	4.66E-10	1.26E-08
		100	2.16E-09	1.32E-09	1.33E-08	2.13E-09	1.29E-09	1.34E-08
		1000	2.73E-09	1.23E-10	1.35E-08	2.68E-09	1.75E-12	1.35E-08

Table 8.6 continued from previous page

Polymer	Shape	Size	CF_b^{glo}	Min CF_b	Max CF_b	CF_{ws}^{glo}	Min CF_{ws}	Max CF_{ws}
LDPE	**sphere**	**1**	9.34E-11	3.61E-11	1.54E-09	2.12E-10	5.70E-11	4.31E-09
		10	9.93E-10	1.73E-10	8.27E-09	1.12E-09	1.59E-10	9.71E-09
		100	2.05E-09	1.04E-09	1.32E-08	2.04E-09	9.09E-10	1.34E-08
		1000	2.63E-09	1.23E-10	1.35E-08	2.58E-09	1.74E-12	1.35E-08
		5000	5.39E-09	1.82E-10	1.07E-07	5.33E-09	1.34E-10	1.07E-07
PET	**fiber**	**1**	1.51E-10	4.92E-11	1.15E-09	6.74E-10	1.56E-10	5.46E-09
		10	1.41E-09	4.52E-10	9.17E-09	1.9E-09	4.72E-10	1.26E-08
		100	2.68E-09	1.29E-09	1.30E-08	2.73E-09	1.29E-09	1.34E-08
		1000	2.79E-09	1.34E-09	1.35E-08	2.75E-09	1.30E-09	1.35E-08
	sphere	**1**	3.45E-11	1.75E-11	7.93E-10	1.56E-10	4.87E-11	4.75E-09
		10	7.57E-10	9.70E-11	6.19E-09	1.09E-09	1.01E-10	9.25E-09
		100	1.98E-09	8.80E-10	1.28E-08	2.03E-09	7.72E-10	1.34E-08
		1000	2.79E-09	1.34E-09	1.35E-08	2.75E-09	1.30E-09	1.35E-08
		5000	2.8E-09	1.34E-09	1.35E-08	2.75E-09	1.30E-09	1.35E-08
PLA	**fiber**	**1**	6.26E-10	2.13E-10	4.98E-09	7.42E-10	1.58E-10	6.25E-09
		10	1.9E-09	6.09E-10	1.24E-08	1.9E-09	4.72E-10	1.26E-08
		100	2.78E-09	1.33E-09	1.34E-08	2.73E-09	1.29E-09	1.34E-08
		1000	2.8E-09	1.35E-09	1.36E-08	2.75E-09	1.30E-09	1.35E-08
	sphere	**1**	1.71E-10	8.70E-11	3.88E-09	1.79E-10	7.06E-11	5.20E-09
		10	1.17E-09	1.60E-10	9.88E-09	1.16E-09	1.20E-10	1.01E-08
		100	2.07E-09	9.22E-10	1.34E-08	2.03E-09	7.72E-10	1.34E-08
		1000	2.8E-09	1.34E-09	1.35E-08	2.75E-09	1.30E-09	1.35E-08
		5000	2.8E-09	1.35E-09	1.36E-08	2.75E-09	1.30E-09	1.35E-08

Table 8.6 continued from previous page

Polymer	Shape	Size	CF_b^{glo}	Min CF_b	Max CF_b	CF_{ws}^{glo}	Min CF_{ws}	Max CF_{ws}
PP	fiber	1	5.41E-11	4.77E-11	1.44E-10	1.45E-11	1.00E-11	8.85E-11
		10	1.96E-10	1.32E-10	9.33E-10	1.46E-10	8.70E-11	9.06E-10
		100	9.83E-10	5.90E-10	5.69E-09	9.31E-10	5.43E-10	5.66E-09
		1000	2.02E-09	1.23E-10	9.89E-09	1.97E-09	1.74E-12	9.74E-09
	sphere	1	5.19E-11	4.59E-11	1.28E-10	1.65E-11	1.32E-11	6.52E-11
		10	1.34E-10	1.18E-10	6.58E-10	8.47E-11	5.33E-11	5.87E-10
		100	8.09E-10	5.01E-10	4.77E-09	7.57E-10	4.55E-10	4.74E-09
		1000	2.19E-09	1.23E-10	1.15E-08	2.13E-09	1.73E-12	1.14E-08
		5000	1.42E-08	1.22E-10	2.40E-07	1.42E-08	1.74E-12	2.40E-07
PS	fiber	1	7.92E-10	2.74E-10	6.41E-09	7.66E-10	1.59E-10	6.55E-09
		10	1.94E-09	6.23E-10	1.26E-08	1.9E-09	4.72E-10	1.26E-08
		100	2.78E-09	1.34E-09	1.35E-08	2.73E-09	1.29E-09	1.34E-08
		1000	2.8E-09	1.35E-09	1.36E-08	2.75E-09	1.30E-09	1.35E-08
	sphere	1	2.31E-10	1.18E-10	5.23E-09	1.88E-10	7.52E-11	5.39E-09
		10	1.22E-09	1.67E-10	1.03E-08	1.17E-09	1.22E-10	1.02E-08
		100	2.08E-09	9.25E-10	1.34E-08	2.03E-09	7.72E-10	1.34E-08
		1000	2.8E-09	1.35E-09	1.36E-08	2.75E-09	1.30E-09	1.35E-08
		5000	2.8E-09	1.35E-09	1.36E-08	2.75E-09	1.30E-09	1.35E-08
PVC	fiber	1	8.23E-10	2.85E-10	6.67E-09	7.71E-10	1.59E-10	6.60E-09
		10	1.95E-09	6.25E-10	1.27E-08	1.9E-09	4.72E-10	1.26E-08
		100	2.78E-09	1.34E-09	1.35E-08	2.73E-09	1.29E-09	1.34E-08
		1000	2.8E-09	1.35E-09	1.36E-08	2.75E-09	1.30E-09	1.35E-08

Table 8.6 continued from previous page

Polymer	Shape	Size	CF_b^{glo}	Min CF_b	Max CF_b	CF_{ws}^{glo}	Min CF_{ws}	Max CF_{ws}
PVC	sphere	1	2.44E-10	1.24E-10	5.50E-09	1.9E-10	7.64E-11	5.43E-09
		10	1.23E-09	1.69E-10	1.04E-08	1.17E-09	1.23E-10	1.03E-08
		100	2.08E-09	9.25E-10	1.34E-08	2.03E-09	7.72E-10	1.34E-08
		1000	2.8E-09	1.35E-09	1.36E-08	2.75E-09	1.30E-09	1.35E-08
		5000	2.8E-09	1.35E-09	1.36E-08	2.75E-09	1.30E-09	1.35E-08
TRWP	fiber	1	2.89E-10	9.54E-11	2.23E-09	6.94E-10	1.57E-10	5.69E-09
		10	1.68E-09	5.39E-10	1.09E-08	1.9E-09	4.72E-10	1.26E-08
		100	2.74E-09	1.32E-09	1.33E-08	2.73E-09	1.29E-09	1.34E-08
		1000	2.8E-09	1.34E-09	1.35E-08	2.75E-09	1.30E-09	1.35E-08
	sphere	1	6.96E-11	3.55E-11	1.59E-09	1.63E-10	5.96E-11	4.88E-09
		10	9.75E-10	1.29E-10	8.09E-09	1.13E-09	1.11E-10	9.71E-09
		100	2.04E-09	9.06E-10	1.32E-08	2.03E-09	7.72E-10	1.34E-08
		1000	2.79E-09	1.34E-09	1.35E-08	2.75E-09	1.30E-09	1.35E-08
		5000	2.8E-09	1.35E-09	1.36E-08	2.75E-09	1.30E-09	1.35E-08

End of Table

8.8 Discussion of results

This chapter provides regionalized CFs for 9 different polymers, of 5 size classes, 2 shapes, and 9 geographical regions. The aggregation of these factors, using main MP emissions from rivers, generates CFs for two continents (Asia and Africa) and a global CF. Global CFs represent 92% of MP emissions from rivers to oceans and can be used to assess the impacts of MPs emitted to the marine environment, for MarILCA's impact category "Physical effect on biota". These emission points are very relevant for the continental and global scales, since the obtained CFs represent the highest probability of MP emission points at the continent and global scales. Nevertheless, region-based CFs must be addressed and used with caution. The variability of FFs and CFs is high between emission regions, even at a small scale (for instance, Congo and Gulf of Guinea). Thus, it is very delicate to choose a region-based CF to represent the impacts of MPs emitted in another region. Therefore, when CFs for a certain emission region are not available, it is recommended to use continent or global CFs instead.

Using numerical modeling, it was demonstrated that the physical properties of MPs are important for the development of FFs and CFs, as well as regionalization. The same MP particle emitted in a certain region can be transported differently than if it were emitted in another region. Hence, a different impact (CF) is associated to the same particle in different regions. Thus, considering a single fate for MP emissions either underestimate or overestimate their impacts, due to inadequate quantification. The variability of CFs with regionalization is mainly pronounced for small particles and large low density particles because these particles linger in the marine environment before they start settling. Thus, they are more vulnerable to the direction of water currents in determining their fate and hence their impacts.

The largest CFs are observed for larger particles. High density particles settle relatively fast compared to smaller particles, which enhances their accumulation in the sediments, where they expose a large fraction of species hence, increasing their impacts. Low density large particles are the slowest to attain the density of surrounding marine water due to biofouling. However, once they become negatively buoyant, they settle at a high velocity because of their large size. Because these particles float long enough in the marine water prior to their settling, their impacts are highly dependent on their fate. If they settle or beach prior to reaching the global scale, their impacts increase. However, if they drift away from the shore to the global scale, their impacts are reduced. This confirms once again the influence of regionalization on the impacts of these particles.

Characterization factors developed for the IW+ and GLAM approaches should be carefully used since the signification of their impacts is different. As a reminder, $PDF.m^2.yr$ of the

IW+ approach are interpreted as the potentially disappeared fraction of species,over a given surface area over a duration. GLAM units PDF.yr represent the disappeared fraction of species in the whole marine ecosystem as a whole compartment. This justifies the difference in orders of magnitude in CFs developed for the two approaches. The species distribution fraction (SDF) has an influence on the CFs, especially for the GLAM approach. Particles in richer marine sub-compartments have higher impacts than those in less rich environment. In addition, particles that have the same fate in two regions, would have more impact in richer regions (such as Bay of Bengal and Indus) for the GLAM approach. SDF has less influence on the CFs of the IW+ approach, because PDFs are considered equivalent over the surface area of each scale. Thus, SDFs only have an influence in overlapping sub-compartments (for example water surface, water column, sediments) of the same scale (same surface area). These differences highlight the importance to adequately quantify the SDF and understand the interpretation of CF units for each approach when quantifying the impacts of MPs in the marine environment.

Unlike the IW+ approach, the volume of marine compartments greatly influence CFs developed for the GLAM approach. The volume of the global compartment (for GLAM approach) and the depth of the global compartment (for IW+ approach) do have an influence on partial CFs for the global scale (CF of the receiving compartment). This results in a reduction in partial CFs for the global scale when aggregating into CFs for the whole marine ecosystem. The volume of the global scale used here is not regionalized. While the volume of the continental scale is quantified based on the topography of each extracted region, the global volume is not specifically calculated for each extracted domain (figure 5.3). It is rather considered as the global compartment that hosts all oceanic species living outside the world continental shelf. This raised the question to whether the "dilution" of partial impacts in the global scale is done in an arbitrary way by representing the global volume to represent one single box for all global species. Thus, a sensitivity analysis was done in the Mediterranean Sea because the domain is simple and small. In a first scenario, CFs were calculated using the volume of the global scale as the world global volume (V_{global} = 1.21E+09 km^3). In a second scenario, the global volume was calculated based on the domain extracted for the Mediterranean, referred to as "local deep-sea". Since all emitted particles in the Mediterranean Sea stay in the enclosed basin, the size of a global scale (local deep sea) inside the Mediterranean is appropriate for the fate of the particles. The volume of the Mediterranean deep ocean is calculated using the surface area of the Mediterranean deep sea, which is obtained equal to 5.41E+06 km^2 and the deep sea depth 2.23E+03 meters. The resultant volume of the Mediterranean deep sea is then 2.29E+04 km^3. A percentage difference for the CFs, between the two scenarios was calculated, for the two approaches, to compare the influence of the

two values of V_{global} on the CFs. These percentages are presented in the **Supplementary Information**. It was noticed that, for both approaches, the highest influence of V_{global} is for emissions at the global scale only. For the IW+ approach, impacts for emissions at the global scale were reduced by 40%, when the volume of the global scale is increased from the local regionalized Mediterranean deep sea scale to the world global scale. Whereas, for GLAM, CFs for emissions at the global scale were reduced by 99%. Nevertheless, the choice of V_{global} did not present a significant influence on CFs for emissions at the beach, water surface, water column and sediments. However, the majority of MP emissions occur at the beach and the water surface, and MP impacts are reduced in the global scale compared to impacts at the continental scale. Thus, the choice of V_{global} value could be non-regionalized because it has low significance to the compartments of highest impacts. For this reason, the volume that represents all global species around the world was chosen (V_{global} = 1.21E+09 km^3).

The species distribution fraction SDF for the global scale in GLAM includes the world species that live in the global scale, which means the global deep ocean. Therefore, impacts of particles in the global scale are considered on species in the global deep ocean only. However, the fate of some of the particles modeled in this thesis, left the modeling domain. These particles couldn't be tracked further due to limitations linked to data extraction and simulation times. These particles can either settle at a farthest point in the global ocean or can linger in the water until they reach another continental scale/beach. Thus, the fate of these particles require further investigation. These particles represent only 3.6% of total emitted particles. The present model allowed to understand the ultimate fate of 96.4% of emitted particles, of which 92% stayed in the continental zone. The other 8% settled in the "local deep ocean" or "local global", which is the deep ocean defined in section 5.3 as the zone, of the modeling domain, where the depth of the water becomes larger than 200 meters. The remaining 3.6% left the modeling domain from the local global scale or the local deep ocean. In order to better assess their impacts, another global scale can be added, called "global deep ocean". The local deep ocean of the modeling zone can then be connected to the "global deep ocean" that includes the species of the global deep sea (currently taken for the global scale) and species of other continents. This will allow to account for potential impacts of particles that might reach another continental scale. Nevertheless, it is not recommended to add the species of another continent in the current local deep sea, because this will overestimate the impacts of the majority of MPs, that settled in the local deep ocean. However, modeling the ultimate fate of these particles remains the ideal solution to assess their impacts.

Fate factors developed in this chapter are so far the most refined FFs developed for MP emissions in the marine environment. They consider impacts in five marine compartments (beach, water surface, water column, sediments and global scale). The marine environment

was previously considered as a single water compartment [18, 19]. Sediment compartments were later added [21], following the proposition of the fate framework developed in the first article published (chapter 6). The fate at the beach and water surface are integrated for the first time in the development of FFs for MP emissions.

Existing FF models were developed based on estimates of sedimentation and biofouling rates [18, 19]. The present chapter improved the quantification of these mechanisms in several ways. Biofouling is no longer estimated, but rather modeled using various formulations that distinguish differences related to the physical properties of MPs. Sedimentation is also quantified using numerical modeling that incorporates three different formulations of settling velocity, depending on the properties of polymers tested [92, 205, 206]. The formulation used for large particles [92, 204] presents a good fit with the behavior of the particles. It even quantifies the refloating of positively buoyant MPs through their rising velocities. This behavior was never taken into account when modeling the fate of MPs. Thus, these fate mechanisms now represent the fate of the particles more adequately. Moreover, for the first time, numerical modeling is used to quantify both horizontal and vertical transport rates between marine sub-compartments. In this model, three water-current velocity fields, horizontal and vertical dispersion coefficients are used to properly track the transport of the particles. Numerical modeling allows the distinction of dominant transport mechanisms, e.g., beaching versus settling, for each MP particles tested, in each region. Previous simplified models [18, 19] cannot account for these distinctions, because they use a single water flow value to quantify advection.

Using numerical modeling for the quantification of MP transfer rates highlighted the importance of considering water currents and regionalization when quantifying FFs and CFs for various MPs. Based on the results of the present work, it is proven that when it comes to MP emissions, it is crucial not only to know what type of MP is emitted to the marine environment but also to understand where the emission occurs.

The species distribution fraction of species specific for each marine compartment allowed also to allocate the proper weight of MP impacts depending on the species richness of their receiving compartments. This distinction has never been used to aggregate the impacts of MPs between marine sub-compartments.

In order to coherently compare CFs developed in this work with already existing CFs for MP emissions in the marine environment, only endpoint CFs [$PDF.m^2.yr/kg$] for the IW+ approach are used because CFs for the GLAM approach were never developed. In addition, regionalization is not taken into account since it has never been done for MP emissions in the marine environment. In the present thesis, main differences in the FFs are linked

to the size and the density of the particles. However, in the work of Corella-Puertas et al., (2023) [19], the influence of density was mainly related to sedimentation and size to degradation rates. Whereas, in the current work, the interaction between the density and size is taken into consideration when accounting for the sedimentation and other transfer rates. These distinctions lead to different conclusions regarding the impact of MPs. In Corella-Puertas et al., (2023), high density MPs exhibited the lowest impacts, no matter their sizes. This was mainly related to the short residence time of these particles in the water as a result of rapid sedimentation. Having not accounted for an EEF in the sediments, and limiting the impacts solely on the residence time in water, significantly underestimate the impacts of these particles. Taking into account an EEF for benthic species, and aggregating using the proper sediment SDF, our results showed contradicting results, where large high density particles contributed to highest CFs. In addition, because sedimentation was only linked to the density of MPs in the work of Corella-Puertas et al., (2023), all high density particles presented the same fate. However, adequately modeling the sedimentation by considering the interaction between MP physical properties showed significant differences within the fate of high density MPs. Our results showed lower impacts associated to small high density particles, compared to larger ones, because of slow settling velocity. These particles are dispersed in marine water and might be transported to the global scale. Consequently, they present up to three orders of magnitude lower CFs than larger high density particles that accumulate in the sediments. Similarly, in the work of Corella-Puertas et al., (2023), all low density polymers showed similar CFs for same-sized polymers. This was mainly related to slow sedimentation rates. Differences among low density particles were linked to degradation that varies with the size of the particles. In contrast, in our work, the differences between the CFs of low-density particles varied with several orders of magnitude. In addition to the degradation rates and settling velocities that vary with the size of the polymers, differences in the fate were also linked to the celerity of biofouling. Biofouling is the main reason for the settling of these particles. Thus, modeling its variability with the physical properties of MPs presented variation in the FFs of low density polymers. Consequently, based on the receiving sub-compartment, EEF and corresponding SDF, CFs of low density polymers exhibited a larger variability.

It can be concluded that modeling the fate of MPs emitted to the marine environment is very challenging due to the interaction of various environmental parameters with the physical properties of MPs. Adequately addressing these interactions presents significant differences in the FFs. In addition, the variability of FFs, combined with EEFs, and SDFs, results in important differences in the CFs. Because fate plays a key role on the CFs, regionalization is also very important, notably for small particles and low density large polymers.

CHAPTER 9 GENERAL DISCUSSION AND SCIENTIFIC CONTRIBUTIONS

9.1 Objectives achievement

The general objective of this thesis "regionalize fate and characterization factors (CFs) for microplastic emissions in the marine environment, in order to assess the impact of spatial variability on CFs compared to the variability driven by microplastic physical properties" was achieved by answering the following sub-objectives:

9.1.1 Develop a comprehensive, more refined framework for the development of fate and characterization factors for microplastic emissions in the marine environment

The achievement of this sub-objective was presented in chapter 6. The comprehensive literature review conducted to develop the framework proposed for this sub-objective, set the basis to adequately quantify the fate of MPs in the marine environment. Based on this literature, main identified fate mechanisms allowed the division of the marine environment into multiple sub-compartments at two different scales. Each sub-compartment presents a homogeneity in fate mechanisms. The interaction between the physical properties of MP, the environmental parameters and the fate variables highlighted where efforts should be made to develop the fate factors.

The proposed framework was later translated into matrix-based rate matrix **K** where emission compartments are presented on the column and receiving ones on the rows. In this matrix, sub-compartments are connected through identified fate mechanisms. According to this matrix, a mechanistic fate matrix **FF** is then obtained. FFs in this matrix represent the residence time of MPs in each sub-compartment, as well as the mass increase of MPs due to an emission in a certain sub-compartment. Then a mechanistic characterization factor matrix is proposed by multiplying **FF** with an exposure-effect matrix **EEF**. EEFs represent the sensitivity of the marine ecosystem to emitted MPs.

In order to maintain the harmonization between CFs in LCIA, mechanistic fate and characterization matrices proposed followed the structure of emission-based CFs for (eco)toxicity. The proposed framework presented a fundamental structure to rely on for the development of FFs and CFs.

9.1.2 Identify influencing parameters on microplastic transfer rates in the marine environment and the influence of transfer rates on the fate and characterization factors

The achievement of this sub-objective was presented in chapter 7. This sub-objective is an intermediary key step between the mechanistic framework proposed and the operationalization of the framework. Operationalization requires the identification of several key points addressed below:

The literature review developed in the first sub-objective, highlighted the role of various factors in the settling of microplastics (i.e., biofouling, MP size, density, shape, etc.). Thus, the first step was to understand which of these factors is the most influencing on sinking and sedimentation rates. Numerical modeling was used in order to allow the assessment of multiple parameters. This step helped categorize the fate and CF matrices based on the physical properties of MP. It also highlighted the challenges in quantifying fate mechanisms due to the high influence of interacting parameters on sinking and sedimentation rates. In addition, this step showed the importance of spatially variable parameters (such as water currents and turbulence), which indicated the need to assess and consider regionalization in future steps.

In a second step, after identifying the influence on sinking and sedimentation rates using numerical modeling (TrackMPD model [12]), the quantification of remaining fate mechanisms is accomplished based on simplified approaches and data from the literature. This step was important in understanding the influence of fate mechanisms on fate factors. A sensitivity analysis on the mechanisms quantified demonstrated a high influence of multiple rates on FFs, namely the resurfacing rate, the degradation rate on the beach, the sinking and sedimentation rates and the resuspension rates. Among these rates, resurfacing and resuspension rates were quantified assuming the behavior of the MP is similar to that of the sediment particles. Due to lack of data, one value for each rate was used for all MPs. This highlighted the importance of refining these factors, as they have a great influence on FFs. Fast, medium and slow degradation rates, developed as test scenarios in Corella-Puertas et al., (2022, 2023) [18, 19], were used to represent differences in environmental conditions that enhance degradation on the beach (fast) and slow it down in sediments (slow). The influence of degradation rates at the beach equally highlights the need to develop polymer-specific degradation rates that are specific for every marine sub-compartment.

In a third step, a similar sensitivity analysis was performed to assess the influence of quantified mechanisms and EEFs on CFs. Exposure-effect factors, resuspension, and sedimentation rates presented the highest influence on the CFs. Thus, refining these mechanisms is recommended

for future steps to enhance the modeling and quantification of FFs and CFs for MP emissions in the marine environment.

9.1.3 Regionalize the FFs and CFs to assess the importance of spatial variability compared to the variability linked to the physical properties of emitted MPs

The achievement of this sub-objective is presented in chapter 8. The second sub-objective highlighted the need to assess the importance of regionalization, when operationalizing FFs and CFs of the framework proposed in the first sub-objective. Thus, three-dimensional water currents were extracted for seven regions around the main MP emitting rivers: East China, Indus, Bay of Bengal, Gulf of Guinea, Congo, Mediterranean Sea and Sea of Okhotsk. They are used to run the TrackMPD numerical model [12] for nine polymers of five size classes and two shapes. Based on simulation results and data from the literature, transfer rates in the **K** matrix are quantified for each particle tested. Consequently, **FF** and **CF** matrices are constructed for each particle in each region.

In order to aggregate the impacts on each sub-compartment ecosystem, **SDF** matrices were constructed. For the IW+ approach, the SDF values represented the species richness of every scale (beach, continental, global). However, for the GLAM approach, the SDF values represented the species richness of every-compartment relative to the whole marine ecosystem.

Resulting CFs presented high variability linked to both the physical properties of the polymers and regionalization. Large high density particles presented the least variability with regionalization. This is related to their fast sinking because of their large size. Nevertheless, they presented the highest impacts among all particles for both approaches. This was related to their accumulation in the sediments, where removal mechanisms (degradation, resuspension, and burial) are very slow. Alternatively, small particles of all densities and large low density particles presented high variability with regionalization. This is due to their longing in the marine environment. Small particles have slow settling velocities. Thus, they linger in the marine environment and might be transported to the global scale or beaches, depending on water currents. Generally, this also resulted in low impacts compared to larger MPs. Large positively buoyant particles also showed dispersing behavior as small particles, because of slow biofouling. However, once they become negatively buoyant, they settle at velocities larger than those of smaller particles. Hence, they had more chances in accumulating in sediments and thus increase their impacts.

In order to analyze the seasonality, two particles were chosen to be emitted in July (summer season) compared to January (winter season). Resulting CFs, for both approaches, presented

a variability linked to seasonality. This variability was smaller in some regions compared to that of regionalization and MP physical properties. However, it was significant for certain particles in other regions. Nevertheless, it would be more relevant to analyze the influence of seasonality on all MP tested, in order to better capture the variability of CFs.

Based on rivers emissions, region-specific CFs were aggregated into two continent-scale CFs (Asia and Africa) and then into a global CF. CFs provided are coherent with the units of two LCA approaches: IMPACT World+ and GLAM. Nevertheless, the units of the two approaches hold different significance and should be carefully considered when using the CFs provided.

In a nutshell, this thesis provides regionalized and global (default) CFs for nine polymers, two shapes, five size classes, five emission compartments and for two LCIA methods: IMPACT World+ and GLAM. Unlike what is usually done in LCA, the fate model is not simplified but is refined using numerical modeling that tracks MPs more precisely. The beach is modeled and included as a separate sub-compartment in the fate framework, which has not been previously done in LCA. SDFs are used to allocate the proper weight of MP impacts depending on species richness of their receiving compartments.

9.2 Identified limits

As presented throughout this thesis, the main objective and sub-objectives were achieved. Nevertheless, the methodology followed relies on several hypotheses and assumptions. Thus, developed CFs should be used and analyzed while accounting for the identified points addressed in the following sub-sections:

9.2.1 Numerical modeling

As previously presented, numerical modeling is a robust tool to recreate the behavior of MPs emitted in the marine environment. However, with the development and improvement of these tools, many aspects still need to be improved to enhance their performance:

1. The formulation of MP settling velocities for small MPs is still missing. Although improvements have been made for larger particles, more effort should be made in developing formulations that present a good fit for smaller MPs. Currently, these particles are treated similarly to sediment particles. However, this assumption might not be well representative due to differences in densities and sizes between MP and sediment particles.

2. Resuspension and resurfacing rates of MPs are quantified based on a similar assumption where MPs are treated as sediment particles. However, having different sizes, shapes, and densities than sediments, these rates still need to be modeled specifically for MPs. In addition, resuspension is particle-specific. Although some particles might undergo resuspension, others may sediment as soon as they reach the sediments [58]. Thus, resuspension rates should also be particle-specific to better represent this behavior.

3. Biofouling is modeled using an ideal-scenario approach that considers biofilm growth to be uniform on the surface of the polymers. Although the used rate is the most adapted so far, because it is based on numerical values, the ideal approach is still not the most representative. The growth of biofilms is not uniform on the surface of the particles, as has been demonstrated in some experimental studies [58]. Thus, refining the biofouling rate is still missing but highly needed since it is crucial for the fate of low density particles. The approach of Kooi et al. (2017) [66] could be implemented in the future, in TrackMPD. This approach models biofouling due to algae growth. It takes into account the respiration (growth) and mortality (defouling) of algae, which influences the growth of biofilms on the surface of the particles. Adopting this approach based on biological data in the ocean seems to be the most representative way to model biofouling. Therefore, its integration in TrackMPD is highly recommended in future steps.

4. The numerical model TrackMPD used in the present thesis allows for the modeling of MPs in identified geographical zone. The large data needed take time to download and result in long simulation times. This limits the usage of larger domains that allow for the modeling of the fate on the global scale. Therefore, optimizing the TrackMPD to allow for a faster simulation time is important in the future. Also, checking the availability of other fate models that allow large scale simulations is important to improve the modeling of the fate, specifically in the global scale.

9.2.2 Building of FF and CF matrices

As it was discussed in the methodology sections of the present thesis, several assumptions were taken that can be enhanced in future steps:

1. Degradation rates depend on surface degradation rates [19]. Thus, they depend on the physiology of the particles. Although these factors were used from Coarella-Puertas et al. (2022) and (2023) [18, 19] that provide polymer-specific degradation rates, compartment-specific rates are still missing. As it was described in chapter 6,

the degradation of the particles is more enhance at the beach, followed by the surface area, then the water column and the sediments. Thus, using compartment-specific degradation rates that take into account the variations of environmental parameters is important to increase the representativeness of the fate of MPs. This project is an ongoing project within MarILCA's team. Therefore, it would be recommended to implement these factors, when ready, within the rate matrices developed in this thesis.

2. As discussed in section 8.8 and addressed in section 9.2.1, refining the modeling of the global scale is important. The current work considers the global scale as the entire "deep-sea ocean" which reduces the impacts of MPs because of its large volume. In addition, emissions at the global scale are not addressed here because of the variability of the fate between emissions in the deep-sea ocean and the local-ocean. Therefore, it is necessary to enhance the modeling of the global scale to better evaluate and assess the impacts for emissions in the global scale. However, it is important to mention that despite this limitation, the current work adequately models the impact of 92% of MP emissions from rivers into the marine environment.

9.3 Recommendations

The results and conclusions of this thesis raise the need to address regionalization when quantifying CFs for plastic impacts in LCIA. Since developed CFs are based on a refined fate model that quantifies the FFs and CFs based on a robust model, it is recommended to operationalize them in LCIA methods. These CFs are already developed in a coherent way with IMPACT World+ and GLAM which currently represent the most updated LCIA methods. Therefore, they can be easily integrated into these methods. In order to be able to use these CFs, it is also recommended to spatialize the LCI flows in ecoinvent and Plastic Footprint Network (PFN) to cover the influence of regionalization in both phases of the LCA. In addition, it is important to consider the physical properties of MPs, mainly size and shape, in the LCI flows.

As addressed before, it is also recommended to account for a local global scale that is close to continental coasts (as defined in the domains of the present thesis). This coast will allow the assessment of emissions at the global scale that might reach another continental coast nearby. This local-global scale would then connect to a global deep-sea ocean that accounts for the world deep-ocean where the impacts of MPs are diluted because of its large volume.

9.4 Contributions to other scientific articles

Other targeted implications and opportunities led to the publishing of the following articles:

1. Malli, A., Corella-Puertas, E., Hajjar, C., Boulay, A.M. (2022). Transport mechanisms and fate of microplastics in estuarine compartments: A review. *Mar. Pollut. Bull.*, 177(113553). 10.1016/j.marpolbul.2022.113553

2. Corella-Puertas, E., Hajjar, C., Lavoie, J., Boulay, A. (2023). MariLCA characterization factors for microplastic impacts in LCA: physical effects on biota from emissions to aquatic environments. *J. Clean. Prod.*, 418(July). 10.1016/j.jclepro.2023.138197

3. Askham, V.H., Pauna, V., Boulay, A.M., Fantke, P., Jolliet, P., Lavoie, J., Booth, A.M., Coutris, C., Verones, F., Weber, >G., Vijver, M.G., Lusher, A., Hajjar, C. Generating environmental sampling and testing data for micro- and nanoplastics for use in life cycle impact assessment

CHAPTER 10 CONCLUSION

The principal contributions of the present thesis allowed to achieve the main objective: "regionalize the fate and characterization factors (CFs) of microplastic emissions in the marine environment, to assess the impact of spatial variability on CFs compared to the variability driven by the physical properties of microplastics". This was done for two LCIA methods: IMPACT World+ and GLAM. The principle contributions are summarized as follows:

1. A comprehensive framework for the development of FFs and CFs for MP emissions in the marine environment. This framework expanded the marine environment to include more marine sub-compartments: beach, water surface, water column, and sediments at two scales, continental and global scales. It also identified important parameters and fate mechanisms that play a role in the distribution of MPs between marine sub-compartments and need to be quantified. This framework proposed mechanistic fate FFs and characterization factors CFs for microplastic emissions in the marine environment. They are coherent with the structure of emission-based CFs for (eco)toxicity.

2. Identification of influencing parameters on the settling of the particles as well as on the FFs and CFs. Identifying these parameters allowed for a better understanding of the importance of the physical properties of MPs and the need to assess the importance of regionalization for the operationalization of FFs and CFs. This was a key step in determining the parameters that should be focused during the operationalization of CFs.

3. Regionalized FFs and CFs for emissions of nine polymers of two shapes and five size classes, in the marine environment for MarILCA's impact category "physical effects on biota" and the area of protection AoP of two of the most updated LCIA methods: IMPACT World+ and GLAM. These FFs and CFs are the first to include five marine sub-compartments and develop FFs using a numerical model and 3D water velocity fields.

REFERENCES

[1] C. Schmidt, T. Krauth, and S. Wagner, "Export of plastic debris by rivers into the sea," *Environ. Sci. Technol.*, vol. 51, no. 21, pp. 12 246–12 253, 2017. [Online]. Available: https://link.springer.com/10.1007/s10236-007-0123-4

[2] J. T. Quik, J. A. Meesters, and A. A. Koelmans, "A multimedia model to estimate the environmental fate of microplastic particles," *Sci. Total Environ.*, vol. 882, no. December 2022, p. 163437, 2023. [Online]. Available: https://doi.org/10.1016/j.scitotenv.2023.163437

[3] ISO, *Environmental management and life cycle assessment principles and framework*. International Organization for Standardization (ISO) standards 14040, 2006. [Online]. Available: https://www.iso.org/standard/37456.html

[4] J. S. Woods, G. Rødder, and F. Verones, "An effect factor approach for quantifying the entanglement impact on marine species of macroplastic debris within life cycle impact assessment," *Ecol. Indic.*, vol. 99, pp. 61–66, 2019. [Online]. Available: https://linkinghub.elsevier.com/retrieve/pii/S1470160X18309518

[5] A. L. Lusher, "Chapter 10 Microplastics in the marine environment: Distribution, interactions and effects," in *Mar. Anthropog. Litter*. Springer, 2015, pp. 245–307.

[6] C. M. Boerger, G. L. Lattin, S. L. Moore, and C. J. Moore, "Plastic ingestion by planktivorous fishes in the north pacific central gyre," *Mar. Pollut. Bull.*, vol. 60, no. 12, pp. 2275–2278, 2010. [Online]. Available: https://linkinghub.elsevier.com/retrieve/pii/S0025326X10003814

[7] R. Bissen and S. Chawchai, "Microplastics on beaches along the eastern gulf of thailand–a preliminary study," *Marine Pollution Bulletin*, vol. 157, p. 111345, 2020. [Online]. Available: https://doi.org/10.1016/j.marpolbul.2020.111345

[8] M. Tiwari, T. Rathod, P. Ajmal, R. Bhangare, and S. Sahu, "Distribution and characterization of microplastics in beach sand from three different indian coastal environments," *Marine pollution bulletin*, vol. 140, pp. 262–273, 2019. [Online]. Available: https://doi.org/10.1016/j.marpolbul.2019.01.055

[9] T. Maes, M. D. Van der Meulen, L. I. Devriese, H. A. Leslie, A. Huvet, L. Frère, J. Robbens, and A. D. Vethaak, "Microplastics baseline surveys at the water surface

and in sediments of the north-east atlantic," *Frontiers in Marine Science*, vol. 4, p. 135, 2017.

[10] L. Van Cauwenberghe, A. Vanreusel, J. Mees, and C. R. Janssen, "Microplastic pollution in deep-sea sediments," *Environ. Pollut.*, vol. 182, pp. 495–499, 2013. [Online]. Available: http://dx.doi.org/10.1016/j.envpol.2013.08.013

[11] A. L. Lusher, G. Hernandez-Milian, J. O'Brien, S. Berrow, I. O'Connor, and R. Officer, "Microplastic and macroplastic ingestion by a deep diving, oceanic cetacean: The True's beaked whale Mesoplodon mirus," *Environ. Pollut.*, vol. 199, pp. 185–191, 2015.

[12] I. Jalón-rojas, X. Hua, and E. Fredj, "A 3D numerical model to Track Marine Plastic Debris (TrackMPD): Sensitivity of microplastic trajectories and fates to particle dynamical properties and physical processes," *Mar. Pollut. Bull.*, vol. 141, pp. 256–272, 2019.

[13] R. Fischer, D. Lobelle, M. Kooi, A. Koelmans, V. Onink, C. Laufkötter, L. Amaral-Zettler, A. Yool, E. V. Sebille, E. van Sebille, E. V. Sebille, and E. van Sebille, "Modeling submerged biofouled microplastics and their vertical trajectories," *Biogeosciences*, pp. 1–29, 2022.

[14] E. van Sebille, V. Onink, A. L. Shanks, S. Aliani, K. L. Law, N. Maximenko, J. M. Alsina, A. Bagaev, M. Bergmann, B. Chapron, I. Chubarenko, and A. Cózar, "The physical oceanography of the transport of floating marine debris The physical oceanography of the transport of floating marine debris," *Environ. Res. Lett.*, 2020.

[15] C. Bulle, M. Margni, L. Patouillard, A. M. Boulay, G. Bourgault, V. De Bruille, V. Cao, M. Hauschild, A. Henderson, S. Humbert, S. Kashef-Haghighi, A. Kounina, A. Laurent, A. Levasseur, G. Liard, R. K. Rosenbaum, P. O. Roy, S. Shaked, P. Fantke, and O. Jolliet, "IMPACT World+: A globally regionalized life cycle impact assessment method," *Int. J. Life Cycle Assess.*, vol. 24, no. 9, pp. 1653–1674, 2019.

[16] ISO, *Environmental Management and Life Cycle Assessment: Requiremenets and Guidelines*. International Organization for Standardization (ISO) standards 14040, 2006.

[17] A. Boulay, J. S. Woods, I. Vázquez-Rowe, and F. Verones, "MARILCA: A new working group on Marine Impacts in Life Cycle Assessment." SETAC Europe 29th Annual Conference, Helsinki, Finland, 2019.

[18] E. Corella-Puertas, P. Guieu, A. Aufoujal, C. Bulle, A.-M. M. Boulay, P. Guieu, A. Aufoujal, and C. Bulle, "Development of simplified characterization factors for the assessment of expanded polystyrene and tire wear microplastic emissions applied in a food container life cycle assessment," *J. Ind. Ecol.*, pp. 1–13, 2022.

[19] E. Corella-Puertas, C. Hajjar, J. Lavoie, and A. Boulay, "MariLCA characterization factors for microplastic impacts in LCA: physical effects on biota from emissions to aquatic environments," *J. Clean. Prod.*, p. 138197, 2023. [Online]. Available: https://doi.org/10.1016/j.jclepro.2023.138197

[20] J. Lavoie, A. Boulay, and C. Bulle, "Aquatic micro- and nano-plastics in life cycle assessment: Development of an effect factor for the quantification of their physical impact on biota," *J. Ind. Ecol.*, no. 2015, pp. 1–13, 2021.

[21] N. Saadi, J. Lavoie, P. Fantke, P. Redondo-Hasselerharm, and A.-M. Boulay, "Including impacts of microplastics in marine water and sediments in life cycle assessment," *J. Clean. Prod.*, 2024.

[22] C. Morales-Caselles, J. Viejo, E. Martí, D. González-Fernández, H. Pragnell-Raasch, J. I. González-Gordillo, E. Montero, G. M. Arroyo, G. Hanke, V. S. Salvo, O. C. Basurko, N. Mallos, L. Lebreton, F. Echevarría, T. Van Emmerik, C. M. Duarte, J. A. Gálvez, E. Van Sebille, F. Galgani, C. M. García, P. S. Ross, A. Bartual, C. Ioakeimidis, G. Markalain, A. Isobe, and A. Cózar, "An inshore–offshore sorting system revealed from global classification of ocean litter," vol. 4, no. 6, pp. 484–493. [Online]. Available: https://www.nature.com/articles/s41893-021-00720-8

[23] S. B. Borrelle, J. Ringma, K. L. Law, C. C. Monnahan, L. Lebreton, A. McGivern, E. Murphy, J. Jambeck, G. H. Leonard, M. A. Hilleary, M. Eriksen, H. P. Possingham, H. De Frond, L. R. Gerber, B. Polidoro, A. Tahir, M. Bernard, N. Mallos, M. Barnes, and C. M. Rochman, "Predicted growth in plastics waste exceeds efforts to mitigate plastic pollution," *Science*, vol. 369, no. 6510, pp. 1515–1518, 2020. [Online]. Available: http://science.sciencemag.org/content/369/6510/1515

[24] J. S. Woods, F. Verones, I. Vázquez-Rowe, A.-m. Boulay, O. Jolliet, I. Vázquez-Rowe, A.-m. Boulay, O. Jolliet, I. Vázquez-Rowe, A.-m. Boulay, O. Jolliet, I. Vázquez-Rowe, and A.-m. Boulay, "A framework for the assessment of marine litter impacts in life cycle impact assessment," *Ecol. Indic.*, 2021.

[25] A. E. Schwarz, T. N. Ligthart, E. Boukris, and T. Van Harmelen, "Sources, transport, and accumulation of different types of plastic litter in aquatic environments: a

review study," *Mar. Pollut. Bull.*, vol. 143, pp. 92–100, 2019. [Online]. Available: https://linkinghub.elsevier.com/retrieve/pii/S0025326X19302905

[26] GESAMP, *"Sources, fate and effects of microplastics in the marine environment: a global assessment"*. IMO, 2015, vol. 90. [Online]. Available: issn:1020-4873{%}5Cnhttp://ec.europa.eu/environment/marine/good-environmental-status/descriptor-10/pdf/GESAMP{_}microplasticsfullstudy.pdfissn:fullstudy.pdf

[27] M. L. Kaandorp, D. Lobelle, C. Kehl, H. A. Dijkstra, and E. van Sebille, "Global mass of buoyant marine plastics dominated by large long-lived debris," *Nat. Geosci.*, vol. 16, no. 8, pp. 689–694, 2023. [Online]. Available: https://www.nature.com/articles/s41561-023-01216-0

[28] N. Kowalski, A. M. Reichardt, and J. J. Waniek, "Sinking rates of microplastics and potential implications of their alteration by physical, biological, and chemical factors," *Mar. Pollut. Bull.*, vol. 109, no. 1, pp. 310–319, 2016. [Online]. Available: http://dx.doi.org/10.1016/j.marpolbul.2016.05.064

[29] I. Chubarenko, A. Bagaev, M. Zobkov, and E. Esiukova, "On some physical and dynamical properties of microplastic particles in marine environment," *Mar. Pollut. Bull.*, vol. 108, no. 1-2, pp. 105–112, 2016. [Online]. Available: http://dx.doi.org/10.1016/j.marpolbul.2016.04.048

[30] A. Isobe, K. Kubo, Y. Tamura, S. Kako, E. Nakashima, and N. Fujii, "Selective transport of microplastics and mesoplastics by drifting in coastal waters," *Mar. Pollut. Bull.*, vol. 89, no. 1-2, pp. 324–330, 2014.

[31] M. Bergmann, L. Gutow, and M. Klages, *Marine Anthropogenic Litter*. Springer, 2019, vol. 53, no. 9.

[32] S. Qian, X. Qiao, W. Zhang, Z. Yu, S. Dong, and J. Feng, "Machine learning-based prediction for settling velocity of microplastics with various shapes," *Water Research*, vol. 249, p. 121001, 2024. [Online]. Available: https://linkinghub.elsevier.com/retrieve/pii/S0043135423014410

[33] I. Chubarenko, E. Esiukova, A. Bagaev, I. Isachenko, N. Demchenko, M. Zobkov, I. Efimova, M. Bagaeva, and L. Khatmullina, *Behavior of microplastics in coastal zones*. Elsevier Inc., 2018. [Online]. Available: http://dx.doi.org/10.1016/B978-0-12-813747-5.00006-0

[34] E. Zambianchi, I. Iermano, G. Suaria, and S. Aliani, "Marine litter in the Mediterranean Sea: an oceanographic perspective," *Mar. litter Mediterr. Black Sea*, vol. 46, pp. 31–41, 2014.

[35] T. Kukulka and F. Veron, "Lagrangian investigation of wave-driven turbulence in the ocean surface boundary layer," *J. Phys. Oceanogr.*, vol. 49, no. 2, pp. 409–429, 2019.

[36] K. Enders, R. Lenz, C. A. Stedmon, and T. G. Nielsen, "Abundance , size and polymer composition of marine microplastics ≥ 10 μm in the Atlantic Ocean and their modelled vertical distribution," *Mar. Pollut. Bull.*, vol. 100, no. 1, pp. 70–81, 2015. [Online]. Available: http://dx.doi.org/10.1016/j.marpolbul.2015.09.027

[37] T. S. v. d. Bremer and Ø. Breivik, "Stokes drift," *Philos. Trans. A. Math. Phys. Eng. Sci.*, vol. 376, no. 2111, 2017. [Online]. Available: https://doi.org/10.1098/rsta.2017.0104

[38] V. Onink, C. E. Jongedijk, M. J. Hoffman, E. van Sebille, and C. Laufkötter, "Global simulations of marine plastic transport show plastic trapping in coastal zones," *Environ. Res. Lett.*, vol. 16, no. 6, p. 064053, 2021.

[39] K. Brunner, T. Kukulka, G. Proskurowski, and K. L. Law, "Passive buoyant tracers in the ocean surface boundary layer: 2. observations and simulations of microplastic marine debris," *J. Geophys. Res. Ocean.*, pp. 775–791, 2015.

[40] T. Kukulka and K. Brunner, "Passive buoyant tracers in the ocean surface boundary layer: 1. Influence of equilibrium wind-waves on vertical distributions," *J. Geophys. Res. Ocean.*, vol. 120, no. 5, pp. 3837–3858, 2015. [Online]. Available: https://doi.org/10.1002/2014JC010487

[41] T. Kukulka, G. Proskurowski, S. Morét-Ferguson, D. W. Meyer, and K. L. Law, "The effect of wind mixing on the vertical distribution of buoyant plastic debris," *Geophys. Res. Lett.*, vol. 39, no. 7, pp. 1–6, 2012.

[42] M. Kooi, J. Reisser, B. Slat, F. F. Ferrari, M. S. Schmid, S. Cunsolo, R. Brambini, K. Noble, L. A. Sirks, T. E. W. Linders, R. I. Schoeneich-Argent, and A. A. Koelmans, "The effect of particle properties on the depth profile of buoyant plastics in the ocean," *Sci. Rep.*, vol. 6, no. October, pp. 1–10, 2016.

[43] H. Hinata, N. Sagawa, T. Kataoka, and H. Takeoka, "Numerical modeling of the beach process of marine plastics : A probabilistic and diagnostic approach with a

particle tracking method," *Mar. Pollut. Bull.*, vol. 152, no. 110910, 2020. [Online]. Available: https://doi.org/10.1016/j.marpolbul.2020.110910

[44] S. Kim and D.-H. Kim, "Short-term buoyant microplastic transport patterns driven by wave evolution, breaking, and orbital motion in coast," *Mar. Pollut. Bull.*, vol. 201, p. 116248, 2024. [Online]. Available: https://linkinghub.elsevier.com/retrieve/pii/S0025326X2400225X

[45] P. Núñez, A. Romano, J. García-Alba, G. Besio, and R. Medina, "Wave-induced cross-shore distribution of different densities, shapes, and sizes of plastic debris in coastal environments: A laboratory experiment," *Mar. Pollut. Bull.*, vol. 187, p. 114561, 2023. [Online]. Available: https://linkinghub.elsevier.com/retrieve/pii/S0025326X22012437

[46] A. L. Andrady, "Microplastics in the marine environment," *Mar. Pollut. Bull.*, vol. 62, no. 8, pp. 1596–1605, 2011.

[47] M. L. Kaandorp, H. A. Dijkstra, and E. van Sebille, "Modelling size distributions of marine plastics under the influence of continuous cascading fragmentation," *Environ. Res. Lett.*, vol. 16, no. 5, 2021.

[48] N. Maximenko, J. Hafner, and P. Niiler, "Pathways of marine debris derived from trajectories of Lagrangian drifters," *Mar. Pollut. Bull.*, vol. 65, no. 1-3, pp. 51–62, 2012.

[49] E. van Sebille, M. H. England, and G. Froyland, "Origin, dynamics and evolution of ocean garbage patches from observed surface drifters," *Environ. Res. Lett.*, vol. 7, no. 4, 2012.

[50] L. C. Lebreton, S. Greer, and J. Borrero, "Numerical modelling of floating debris in the world's oceans," *Mar. Pollut. Bull.*, vol. 64, no. 3, pp. 653–661, 2012. [Online]. Available: http://dx.doi.org/10.1016/j.marpolbul.2011.10.027

[51] P. Davison and R. G. Asch, "Plastic ingestion by mesopelagic fishes in the North Pacific Subtropical Gyre," *Mar. Ecol. Prog. Ser.*, vol. 432, pp. 173–180, 2011.

[52] E. M. Cunningham, S. M. Ehlers, J. J. T. J. J. T. A. Dick, J. D. Sigwart, K. Linse, J. J. T. J. J. T. A. Dick, and K. Kiriakoulakis, "High Abundances of Microplastic Pollution in Deep-Sea Sediments: Evidence from Antarctica and the Southern Ocean," *Environ. Sci. Technol.*, vol. 54, no. 21, pp. 13 661–13 671, 2020. [Online]. Available: https://pubs.acs.org/doi/10.1021/acs.est.0c03441

[53] D. Kaiser, N. Kowalski, and J. J. Waniek, "Effects of biofouling on the sinking behavior of microplastics," *Environ. Res. Lett.*, vol. 12, no. 12, pp. 20–21, 2017.

[54] C. D. Rummel, A. Jahnke, E. Gorokhova, D. Kühnel, and M. Schmitt-Jansen, "Impacts of biofilm formation on the fate and potential effects of microplastic in the aquatic environment," *Environ. Sci. Technol. Lett.*, vol. 4, no. 7, pp. 258–267, 2017. [Online]. Available: https://pubs.acs.org/doi/10.1021/acs.estlett.7b00164

[55] M. Long, B. Moriceau, M. Gallinari, C. Lambert, A. Huvet, J. Raffray, and P. Soudant, "Interactions between microplastics and phytoplankton aggregates: Impact on their respective fates," *Mar. Chem.*, vol. 175, pp. 39–46, 2015. [Online]. Available: http://dx.doi.org/10.1016/j.marchem.2015.04.003

[56] L. C. Woodall, A. Sanchez-Vidal, M. Canals, G. L. J. Paterson, R. Coppock, V. Sleight, A. Calafat, A. D. Rogers, B. E. Narayanaswamy, and R. C. Thompson, "The deep sea is a major sink for microplastic debris," *R. Soc. Open Sci.*, vol. 1, no. 4, 2014.

[57] D. Lobelle, M. Kooi, A. A. Koelmans, C. Laufkötter, C. E. Jongedijk, C. Kehl, and E. van Sebille, "Global modeled sinking characteristics of biofouled microplastic," *J. Geophys. Res. Ocean.*, vol. 126, 2021.

[58] I. Jalón-Rojas, A. Romero-Ramírez, K. Fauquembergue, L. Rossignol, J. Cachot, D. Sous, and B. Morin, "Effects of Biofilms and Particle Physical Properties on the Rising and Settling Velocities of Microplastic Fibers and Sheets," *Environ. Sci. Technol.*, 2022.

[59] Y. K. Lim, K.-W. Lee, S. H. Hong, J. G. Park, and S. H. Baek, "Differential impact of planktonic and periphytic diatoms on aggregation and sinking of microplastics in a simulated marine environment," *Mar. Pollut. Bull.*, vol. 199, p. 115961, 2024. [Online]. Available: https://linkinghub.elsevier.com/retrieve/pii/S0025326X23013966

[60] J. Hansen, J. Melchiorsen, N. Ciacotich, L. Gram, and C. Sonnenschein, "Effect of polymer type on the colonization of plastic pellets by marine bacteria," *FEMS Microbiol. Lett.*, pp. 1–9, 2021.

[61] A. K. Macleod, M. S. Stanley, J. G. Day, and E. J. Cook, "Biofouling community composition across a range of environmental conditions and geographical locations suitable for floating marine renewable energy generation," *Biofouling*, vol. 32, no. 3, pp. 261–276, 2016.

[62] R. Fischer, D. Lobelle, M. Kooi, A. Koelmans, V. Onink, C. Laufkötter, L. Amaral-Zettler, A. Yool, E. V. Sebille, E. van Sebille, E. V. Sebille, and E. van Sebille, "Modeling submerged biofouled microplastics and their vertical trajectories," *Biogeosciences*, pp. 1–29, 2022.

[63] M. Vladimir, R. Tatiana, S. Evgeniy, S. Veerasingam, and A. Bagaev, "Vertical and seasonal variations in biofilm formation on plastic substrates in coastal waters of the black sea," *Chemosphere*, vol. 317, p. 137843, 2023. [Online]. Available: https://linkinghub.elsevier.com/retrieve/pii/S0045653523001091

[64] T. H. Nguyen, F. H. M. Tang, and F. Maggi, "Sinking of microbial-associated microplastics in natural waters," *PLoS One*, vol. 15, no. 2, pp. 1–20, 2020. [Online]. Available: http://dx.doi.org/10.1371/journal.pone.0228209

[65] L. Miao, Y. Gao, T. M. Adyel, Z. Huo, Z. Liu, J. Wu, and J. Hou, "Effects of biofilm colonization on the sinking of microplastics in three freshwater environments," *J. Hazard. Mater.*, vol. 413, no. 125370, 2021. [Online]. Available: https://doi.org/10.1016/j.jhazmat.2021.125370

[66] M. Kooi, E. H. van Nes, M. Scheffer, and A. A. Koelmans, "Ups and Downs in the Ocean: Effects of Biofouling on Vertical Transport of Microplastics," *Environ. Sci. Technol.*, vol. 51, no. 14, pp. 7963–7971, 2017.

[67] K. Karkanorachaki, E. Syranidou, and N. Kalogerakis, "Sinking characteristics of microplastics in the marine environment," *Sci. Total Environ.*, vol. 793, p. 148526, 2021. [Online]. Available: https://linkinghub.elsevier.com/retrieve/pii/S0048969721035981

[68] A. L. Alldredge and M. W. Silver, "Characteristics, dynamics and significance of marine snow," *Prog. Oceanogr.*, vol. 20, no. 1, pp. 41–82, 1988.

[69] A. L. Alldredge, "House morphology and mechanisms of feeding in the Oikopleuridae (Tunicata, Appendicularia)," *J. Zool.*, vol. 181, no. 2, pp. 175–188, 1977.

[70] C. A. Choy, B. H. Robison, T. O. Gagne, B. Erwin, E. Firl, R. U. Halden, J. A. Hamilton, K. Katija, S. E. Lisin, C. Rolsky, and K. S. Van Houtan, "The vertical distribution and biological transport of marine microplastics across the epipelagic and mesopelagic water column," *Sci. Rep.*, vol. 10, no. 1, pp. 1–9, 2019.

[71] K. Kvale, A. Prowe, C.-T. Chien, A. Landolfi, and A. Oschlies, "The global biological microplastic particle sink," *Sci. Rep.*, vol. 10, no. 1, pp. 1–12, 2020. [Online]. Available: https://doi.org/10.1038/s41598-020-72898-4

[72] K. F. Kvale, A. E. Friederike Prowe, and A. Oschlies, "A Critical Examination of the Role of Marine Snow and Zooplankton Fecal Pellets in Removing Ocean Surface Microplastic," *Front. Mar. Sci.*, vol. 6, no. January, pp. 1–8, 2020.

[73] P. Möhlenkamp, A. Purser, and L. Thomsen, "Plastic microbeads from cosmetic products: An experimental study of their hydrodynamic behaviour, vertical transport and resuspension in phytoplankton and sediment aggregates," *Elementa*, vol. 6, 2018.

[74] A. A. A. Porter, B. P. Lyons, T. S. Galloway, and C. Lewis, "Role of Marine Snows in Microplastic Fate and Bioavailability," *Environ. Sci. Technol.*, vol. 52, no. 12, pp. 7111–7119, 2018.

[75] M. Cole, P. Lindeque, E. Fileman, C. Halsband, R. Goodhead, J. Moger, and T. S. Galloway, "Microplastic ingestion by zooplankton," *Environ. Sci. Technol.*, vol. 47, no. 12, pp. 6646–6655, 2013.

[76] M. Cole, P. K. Lindeque, E. Fileman, J. Clark, C. Lewis, C. Halsband, and T. S. Galloway, "Microplastics Alter the Properties and Sinking Rates of Zooplankton Faecal Pellets," *Environ. Sci. Technol.*, vol. 50, no. 6, pp. 3239–3246, 2016.

[77] A. L. Dawson, S. Kawaguchi, C. K. King, K. A. Townsend, R. King, W. M. Huston, and S. M. Bengtson Nash, "Turning microplastics into nanoplastics through digestive fragmentation by Antarctic krill," *Nat. Commun.*, vol. 9, no. 1, pp. 1–8, 2018. [Online]. Available: http://dx.doi.org/10.1038/s41467-018-03465-9

[78] K. Katija, C. A. Choy, R. E. Sherlock, A. D. Sherman, and B. H. Robison, "From the surface to the seafloor: How giant larvaceans transport microplastics into the deep sea," *Sci. Adv.*, vol. 3, no. 8, pp. 1–6, 2017.

[79] K. W. Lee, W. J. Shim, O. Y. Kwon, and J. H. Kang, "Size-dependent effects of micro polystyrene particles in the marine copepod tigriopus japonicus," *Environ. Sci. Technol.*, vol. 47, no. 19, pp. 11 278–11 283, 2013.

[80] C. A. Choy and J. C. Drazen, "Plastic for dinner? Observations of frequent debris ingestion by pelagic predatory fishes from the central North Pacific," *Mar. Ecol. Prog. Ser.*, vol. 485, pp. 155–163, 2013.

[81] L. Meng, X. Sun, Q. Li, S. Zheng, J. Liang, and C. Zhao, "Quantification of the vertical transport of microplastics by biodeposition of typical mariculture filter-feeding organisms," *Sci. Total Environ.*, vol. 908, p. 168226, 2024. [Online]. Available: https://doi.org/10.1016/j.scitotenv.2023.168226

[82] H. Qu, R. Ma, H. Barrett, B. Wang, J. Han, F. Wang, P. Chen, W. Wang, G. Peng, and G. Yu, "How microplastics affect chiral illicit drug methamphetamine in aquatic food chain? From green alga (Chlorella pyrenoidosa) to freshwater snail (Cipangopaludian cathayensis)," *Environ. Int.*, vol. 136, no. December 2019, p. 105480, 2020. [Online]. Available: https://doi.org/10.1016/j.envint.2020.105480

[83] N. X. Geilfus, K. M. Munson, J. Sousa, Y. Germanov, S. Bhugaloo, D. Babb, and F. Wang, "Distribution and impacts of microplastic incorporation within sea ice," *Mar. Pollut. Bull.*, vol. 145, no. April, pp. 463–473, 2019. [Online]. Available: https://doi.org/10.1016/j.marpolbul.2019.06.029

[84] A. Kelly, D. Lannuzel, T. Rodemann, K. M. Meiners, and H. J. Auman, "Microplastic contamination in east Antarctic sea ice," *Mar. Pollut. Bull.*, vol. 154, no. April, p. 111130, 2020. [Online]. Available: https://doi.org/10.1016/j.marpolbul.2020.111130

[85] I. Peeken, S. Primpke, B. Beyer, J. Gütermann, C. Katlein, T. Krumpen, M. Bergmann, L. Hehemann, and G. Gerdts, "Arctic sea ice is an important temporal sink and means of transport for microplastic," *Nat. Commun.*, vol. 9, no. 1, 2018. [Online]. Available: http://dx.doi.org/10.1038/s41467-018-03825-5

[86] M. Bergmann, I. Peeken, B. Beyer, T. Krumpen, S. Primpke, M. B. Tekman, and G. Gerdts, *Vast Quantities of Microplastics in Arctic Sea Ice—A Prime Temporary Sink for Plastic Litter and a Medium of Transport*. Elsevier Inc., 2017. [Online]. Available: http://dx.doi.org/10.1016/B978-0-12-812271-6.00073-9

[87] Z. Chen, M. Elektorowicz, C. An, X. Tian, Z. Wang, X. Yang, and L. Lyu, "Revealing the freezing-induced alteration in microplastic behavior and its implication for the microplastics released from seasonal ice," *Environ. Sci. Technol.*, vol. 58, no. 30, pp. 13 529–13 539, 2024. [Online]. Available: https://doi.org/10.1021/acs.est.4c05322

[88] Z. Chen, M. Elektorowicz, C. An, and X. Tian, "Seasonal ice encapsulation: the pivotal influence on microplastic transport and fate in cold regions," *Environ. Sci.: Water Res. Technol.*, 2024. [Online]. Available: http://dx.doi.org/10.1039/D4EW00339J

[89] J. H. Trowbridge and S. J. Lentz, "The bottom boundary layer," *Ann. Rev. Mar. Sci.*, vol. 10, pp. 397–420, 2018.

[90] A. Ballent, A. Purser, P. de Jesus Mendes, S. Pando, and L. Thomsen, "Physical transport properties of marine microplastic pollution," *Biogeosciences Discuss.*, vol. 9, no. 12, pp. 18 755–18 798, 2012.

[91] C. Ancey, "Bedload transport: a walk between randomness and determinism. part 1. the state of the art," *J. Hydraul. Res.*, vol. 58, no. 1, pp. 1–17, 2020. [Online]. Available: https://www.tandfonline.com/doi/full/10.1080/00221686.2019.1702594

[92] K. Waldschläger and H. Schüttrumpf, "Effects of particle properties on the settling and rise velocities of microplastics in freshwater under laboratory conditions," *Environ. Sci. Technol.*, vol. 53, no. 4, pp. 1958–1966, 2019. [Online]. Available: https://doi.org/10.1021/acs.est.8b06794

[93] W. Cowger, A. B. Gray, J. J. Guilinger, B. Fong, and K. Waldschläger, "Concentration depth profiles of microplastic particles in river flow and implications for surface sampling," *Environ. Sci. Technol.*, vol. 55, no. 9, pp. 6032–6041, 2021. [Online]. Available: https://pubs.acs.org/doi/10.1021/acs.est.1c01768

[94] M. P. Born, C. Brüll, D. Schaefer, G. Hillebrand, and H. Schuüttrumpf, "Determination of microplastics' vertical concentration transport (rouse) profiles in flumes," *Environ. Sci. Technol.*, vol. 57, no. 14, pp. 5569–5579, 2023. [Online]. Available: https://pubs.acs.org/doi/10.1021/acs.est.2c06885

[95] J. Lofty, D. Valero, C. A. Wilson, M. J. Franca, and P. Ouro, "Microplastic and natural sediment in bed load saltation: Material does not dictate the fate," *Water Res.*, vol. 243, p. 120329, 2023. [Online]. Available: https://linkinghub.elsevier.com/retrieve/pii/S0043135423007650

[96] H. Laermanns, M. Lehmann, M. Klee, M. G. J. Löder, S. Gekle, and C. Bogner, "Tracing the horizontal transport of microplastics on rough surfaces," *Microplast. Nanoplast.*, vol. 1, pp. 1–12, 2021. [Online]. Available: https://microplastics.springeropen.com/articles/10.1186/s43591-021-00010-2

[97] K. Waldschläger, M. Z. Brückner, B. C. Almroth, C. R. Hackney, T. M. Adyel, O. S. Alimi, S. L. Belontz, W. Cowger, D. Doyle, A. Gray *et al.*, "Learning from natural sediments to tackle microplastics challenges: A multidisciplinary perspective," *Earth Sci. Rev.*, vol. 228, p. 104021, 2022. [Online]. Available: https://linkinghub.elsevier.com/retrieve/pii/S0012825222001052

[98] F. Pohl, J. T. Eggenhuisen, I. A. Kane, and M. A. Clare, "Transport and Burial of Microplastics in Deep-Marine Sediments by Turbidity Currents," *Environ. Sci. Technol.*, vol. 54, no. 7, pp. 4180–4189, 2020.

[99] F. Montserrat, C. Van Colen, P. Provoost, M. Milla, M. Ponti, K. Van den Meersche, T. Ysebaert, and P. M. J. Herman, "Sediment segregation by biodiffusing bivalves," *Estuar. Coast. Shelf Sci.*, vol. 83, no. 4, pp. 379–391, 2009. [Online]. Available: http://dx.doi.org/10.1016/j.ecss.2009.04.010

[100] C. Gebhardt and S. Forster, "Size-selective feeding of Arenicola marina promotes long-term burial of microplastic particles in marine sediments," *Environ. Pollut.*, vol. 242, pp. 1777–1786, 2018. [Online]. Available: https://doi.org/10.1016/j.envpol.2018.07.090

[101] C. Van Colen, L. Moereels, B. Vanhove, H. Vrielinck, and T. Moens, "The biological plastic pump: Evidence from a local case study using blue mussel and infaunal benthic communities," *Environ. Pollut.*, vol. 274, no. 115825, 2021. [Online]. Available: https://doi.org/10.1016/j.envpol.2020.115825

[102] P. Näkki, O. Setälä, and M. Lehtiniemi, "Bioturbation transports secondary microplastics to deeper layers in soft marine sediments of the northern Baltic Sea," *Mar. Pollut. Bull.*, vol. 119, no. 1, pp. 255–261, 2017. [Online]. Available: http://dx.doi.org/10.1016/j.marpolbul.2017.03.065

[103] ——, "Seafloor sediments as microplastic sinks in the northern Baltic Sea – Negligible upward transport of buried microplastics by bioturbation," *Environ. Pollut.*, vol. 249, pp. 74–81, 2019.

[104] S. Oberbeckmann and M. Labrenz, "Marine Microbial Assemblages on Microplastics: Diversity, Adaptation, and Role in Degradation," *Ann. Rev. Mar. Sci.*, vol. 12, pp. 209–232, 2020.

[105] P. L. Corcoran, M. C. Biesinger, and M. Grifi, "Plastics and beaches: A degrading relationship," *Mar. Pollut. Bull.*, vol. 58, no. 1, pp. 80–84, 2009.

[106] T. S. Hebner and M. A. Maurer-Jones, "Characterizing microplastic size and morphology of photodegraded polymers placed in simulated moving water conditions," *Environ. Sci. Process. Impacts*, vol. 22, no. 2, pp. 398–407, 2020.

[107] F. Julienne, N. Delorme, and F. Lagarde, "From macroplastics to microplastics: Role of water in the fragmentation of polyethylene," *Chemosphere*, vol. 236, p. 124409, 2019. [Online]. Available: https://doi.org/10.1016/j.chemosphere.2019.124409

[108] B. Gewert, M. M. Plassmann, and M. Macleod, "Pathways for degradation of plastic polymers floating in the marine environment," *Environ. Sci. Process.*

Impacts, vol. 17, no. 9, pp. 1513–1521, 2015. [Online]. Available: http://dx.doi.org/10.1039/C5EM00207A

[109] Plastics Europe, "Plastics - the Facts 2019 An analysis of European plastics production, demand and waste data," pp. 14,35, 2019. [Online]. Available: https://www.plasticseurope.org/en/resources/market-data

[110] J. Wang, Z. Tan, J. Peng, Q. Qiu, and M. Li, "The behaviors of microplastics in the marine environment," *Mar. Environ. Res.*, vol. 113, pp. 7–17, 2016. [Online]. Available: http://dx.doi.org/10.1016/j.marenvres.2015.10.014

[111] Y. K. Song, S. H. Hong, M. Jang, G. M. Han, S. W. Jung, and W. J. Shim, "Combined Effects of UV Exposure Duration and Mechanical Abrasion on Microplastic Fragmentation by Polymer Type," *Environ. Sci. Technol.*, vol. 51, no. 8, pp. 4368–4376, 2017.

[112] D. Feldman, "Polymer weathering: Photo-oxidation," *J. Polym. Environ.*, vol. 10, no. 4, pp. 163–173, 2002.

[113] A. L. Andrady, "Persistence of Plastic Litter in the Oceans," *Mar. Anthropog. Litter*, no. March, pp. 1–447, 2015.

[114] A. L. Andrady, K. Lavender Law, J. Donohue, and B. Koongolla, "Accelerated degradation of low-density polyethylene in air and in sea water," *Sci. Total Environ.*, no. xxxx, p. 151368, 2021. [Online]. Available: https://doi.org/10.1016/j.scitotenv.2021.151368

[115] A. J. Watts, M. A. Urbina, S. Corr, C. Lewis, and T. S. Galloway, "Ingestion of Plastic Microfibers by the Crab Carcinus maenas and Its Effect on Food Consumption and Energy Balance," *Environ. Sci. Technol.*, vol. 49, no. 24, pp. 14 597–14 604, 2015.

[116] G. Kumar Anjana, K. Anjana, . Hinduja, K. Sujitha, and G. Dharani, "Review on plastic wastes in marine environment – Biodegradation and biotechnological solutions," *Mar. Pollut. Bull.*, vol. 150, no. May 2019, p. 110733, 2020. [Online]. Available: https://doi.org/10.1016/j.marpolbul.2019.110733

[117] A. Khoironi, H. Hadiyanto, S. Anggoro, and S. Sudarno, "Evaluation of polypropylene plastic degradation and microplastic identification in sediments at Tambak Lorok coastal area, Semarang, Indonesia," *Mar. Pollut. Bull.*, vol. 151, no. December 2019, p. 110868, 2020. [Online]. Available: https://doi.org/10.1016/j.marpolbul.2019.110868

[118] A. M. Booth, S. Kubowicz, C. J. Beegle-Krause, J. Skancke, T. Nordam, E. Landsem, M. Throne-Holst, and S. Jahren, "Microplastic in global and Norwegian marine environments: Distributions, degradation mechanisms and transport," *Sintef*, vol. M-918, no. 302003604, pp. 1–147, 2018.

[119] L. Cai, J. Wang, J. Peng, Z. Wu, and X. Tan, "Observation of the degradation of three types of plastic pellets exposed to UV irradiation in three different environments," *Sci. Total Environ.*, vol. 628-629, pp. 740–747, 2018. [Online]. Available: https://doi.org/10.1016/j.scitotenv.2018.02.079

[120] A. A. Horton and S. J. Dixon, "Microplastics: An introduction to environmental transport processes," *WIREs Water*, vol. 5, no. 2, pp. 1–10, 2018.

[121] M. R. Gregory and A. L. Andrady, "Plastics in the Marine Environment," *Ann. Rev. Mar. Sci.*, vol. 9, no. 1, pp. 205–229, 2003.

[122] Y. K. Song, S. H. Hong, S. Eo, G. M. Han, and W. J. Shim, "Rapid Production of Micro- and Nanoplastics by Fragmentation of Expanded Polystyrene Exposed to Sunlight," *Environ. Sci. Technol.*, 2020.

[123] W. Courtene-Jones, B. Quinn, C. Ewins, S. F. Gary, and B. E. Narayanaswamy, "Microplastic accumulation in deep-sea sediments from the rockall trough," *Marine Pollution Bulletin*, vol. 154, p. 111092, 2020. [Online]. Available: https://linkinghub.elsevier.com/retrieve/pii/S0025326X20302101

[124] H. Michallet and M. Mory, "Modelling of sediment suspensions in oscillating grid turbulence," *Fluid Dyn. Res.*, vol. 35, no. 2, pp. 87–106, 2004. [Online]. Available: https://iopscience.iop.org/article/10.1016/j.fluiddyn.2004.04.004

[125] J. Chauchat, "A comprehensive two-phase flow model for unidirectional sheet-flows," *J. Hydraul. Res.*, vol. 56, no. 1, pp. 15–28, 2018. [Online]. Available: https://www.tandfonline.com/doi/full/10.1080/00221686.2017.1289260

[126] M. Poulain, M. J. Mercier, L. Brach, M. Martignac, C. Routaboul, E. Perez, M. C. Desjean, and A. Ter Halle, "Small Microplastics As a Main Contributor to Plastic Mass Balance in the North Atlantic Subtropical Gyre," *Environ. Sci. Technol.*, vol. 53, no. 3, pp. 1157–1164, 2019.

[127] M. C. Denes and E. van Sebille, "plasticparcels: A python package for marine plastic dispersal simulations and parameterisation development using parcels," *Journal*

of Open Source Software, vol. 9, no. 102, p. 7094, 2024. [Online]. Available: https://doi.org/10.21105/joss.07094

[128] M. Lange and E. van Sebille, "Parcels v0.9: prototyping a lagrangian ocean analysis framework for the petascale age," *Geosci. Model Dev.*, vol. 10, no. 11, pp. 4175–4186, 2017. [Online]. Available: https://gmd.copernicus.org/articles/10/4175/2017/

[129] P. Delandmeter and E. van Sebille, "The parcels v2.0 lagrangian framework: new field interpolation schemes," *Geosci. Model Dev.*, vol. 12, no. 8, pp. 3571–3584, 2019. [Online]. Available: https://gmd.copernicus.org/articles/12/3571/2019/

[130] K.-F. Dagestad, J. Röhrs, Ø. Breivik, and B. Ådlandsvik, "Opendrift v1.0: a generic framework for trajectory modelling," *Geosci. Model Dev.*, vol. 11, no. 4, pp. 1405–1420, 2018. [Online]. Available: https://gmd.copernicus.org/articles/11/1405/2018/

[131] K. P. Black and S. L. Gay, "A numerical scheme for determining trajectories in particle models," in *Acanthaster and the Coral Reef: A Theoretical Perspective: Proceedings of a Workshop held at the Australian Institute of Marine Science, Townsville, Aug. 6–7, 1988*. Springer, 1990, pp. 151–156.

[132] P. Annika, T. George, P. George, N. Konstantinos, D. Costas, and C. Koutitas, "The poseidon operational tool for the prediction of floating pollutant transport," *Mar. Pollut. Bull.*, vol. 43, no. 7, pp. 270–278, 2001, marine Environmental Modelling. [Online]. Available: https://www.sciencedirect.com/science/article/pii/S0025326X01000807

[133] D. Deltares, "Delft3d-flow user manual," *Deltares Delft, The Netherlands*, vol. 330, 2013.

[134] C. Lett, P. Verley, C. Mullon, C. Parada, T. Brochier, P. Penven, and B. Blanke, "A lagrangian tool for modelling ichthyoplankton dynamics," *Environ. Model. Softw.*, vol. 23, no. 9, pp. 1210–1214, 2008. [Online]. Available: https://linkinghub.elsevier.com/retrieve/pii/S136481520800025X

[135] J. Soto-Navarro, G. Jordá, S. Deudero, C. Alomar, Ángel Amores, and M. Compa, "3d hotspots of marine litter in the mediterranean: A modeling study," *Mar. Pollut. Bull.*, vol. 155, p. 111159, 2020. [Online]. Available: https://www.sciencedirect.com/science/article/pii/S0025326X20302770

[136] K. Tsiaras, E. Costa, S. Morgana, C. Gambardella, V. Piazza, M. Faimali, R. Minetti, C. Zeri, M. Thyssen, S. Ben Ismail *et al.*, "Microplastics in the mediterranean:

variability from observations and model analysis," *Front. Mar. Sci.*, vol. 9, p. 784937, 2022. [Online]. Available: https://www.frontiersin.org/articles/10.3389/fmars.2022.784937/full

[137] M. C. Sousa, M. DeCastro, J. Gago, A. S. Ribeiro, M. Des, J. L. Gómez-Gesteira, J. M. Dias, and M. Gomez-Gesteira, "Modelling the distribution of microplastics released by wastewater treatment plants in ria de vigo (nw iberian peninsula)," *Mar. Pollut. Bull.*, vol. 166, p. 112227, 2021. [Online]. Available: https://linkinghub.elsevier.com/retrieve/pii/S0025326X21002617

[138] J. Röhrs, K.-F. Dagestad, H. Asbjørnsen, T. Nordam, J. Skancke, C. E. Jones, and C. Brekke, "The effect of vertical mixing on the horizontal drift of oil spills," *Ocean. Sci.*, vol. 14, no. 6, pp. 1581–1601, 2018. [Online]. Available: https://doi.org/10.5194/os-14-1581-2018

[139] D. M. Nguyen, L. R. Hole, Ø. Breivik, T. B. Nguyen, and N. K. Pham, "Marine plastic drift from the mekong river to southeast asia," *J. Mar. Sci. Eng.*, vol. 11, no. 5, p. 925, 2023. [Online]. Available: https://www.mdpi.com/2077-1312/11/5/925

[140] V. Onink, M. L. Kaandorp, E. van Sebille, and C. Laufkötter, "Influence of particle size and fragmentation on large-scale microplastic transport in the mediterranean sea," *Environ. Sci. Technol.*, vol. 56, no. 22, pp. 15 528–15 540, 2022. [Online]. Available: https://pubs.acs.org/doi/10.1021/acs.est.2c03363

[141] L. Van Cauwenberghe, M. Claessens, M. B. Vandegehuchte, and C. R. Janssen, "Microplastics are taken up by mussels (mytilus edulis) and lugworms (arenicola marina) living in natural habitats," *Environ. Pollut.*, vol. 199, pp. 10–17, 2015. [Online]. Available: https://linkinghub.elsevier.com/retrieve/pii/S026974911500010X

[142] A. J. Jamieson, L. Brooks, W. D. Reid, S. Piertney, B. E. Narayanaswamy, and T. Linley, "Microplastics and synthetic particles ingested by deep-sea amphipods in six of the deepest marine ecosystems on earth," *R. Soc. Open Sci.*, vol. 6, no. 2, p. 180667, 2019. [Online]. Available: https://royalsocietypublishing.org/doi/10.1098/rsos.180667

[143] X.-Y. Xu, C. Wong, N. Tam, H. Liu, and S. Cheung, "Barnacles as potential bioindicator of microplastic pollution in hong kong," *Mar. Pollut. Bull.*, vol. 154, p. 111081, 2020. [Online]. Available: https://linkinghub.elsevier.com/retrieve/pii/S0025326X20301995

[144] M. Cole, R. Coppock, P. K. Lindeque, D. Altin, S. Reed, D. W. Pond, L. Sørensen, T. S. Galloway, and A. M. Booth, "Effects of nylon microplastic on feeding, lipid accumulation, and moulting in a coldwater copepod," *Environ. Sci. Technol.*, vol. 53, no. 12, pp. 7075–7082, 2019. [Online]. Available: https://pubs.acs.org/doi/10.1021/acs.est.9b01853

[145] C. G. Avio, S. Gorbi, M. Milan, M. Benedetti, D. Fattorini, G. d'Errico, M. Pauletto, L. Bargelloni, and F. Regoli, "Pollutants bioavailability and toxicological risk from microplastics to marine mussels," *Environ. Pollut.*, vol. 198, pp. 211–222, 2015. [Online]. Available: https://linkinghub.elsevier.com/retrieve/pii/S0269749114005211

[146] M. Mohsen, Q. Wang, L. Zhang, L. Sun, C. Lin, and H. Yang, "Microplastic ingestion by the farmed sea cucumber apostichopus japonicus in china," *Environ. Pollut.*, vol. 245, pp. 1071–1078, 2019. [Online]. Available: https://linkinghub.elsevier.com/retrieve/pii/S0269749118339757

[147] C. Fang, R. Zheng, F. Hong, Y. Jiang, J. Chen, H. Lin, L. Lin, R. Lei, C. Bailey, and J. Bo, "Microplastics in three typical benthic species from the arctic: Occurrence, characteristics, sources, and environmental implications," *Environ. Res.*, vol. 192, p. 110326, 2021. [Online]. Available: https://linkinghub.elsevier.com/retrieve/pii/S0013935120312238

[148] M. Long, I. Paul-Pont, H. Hegaret, B. Moriceau, C. Lambert, A. Huvet, and P. Soudant, "Interactions between polystyrene microplastics and marine phytoplankton lead to species-specific hetero-aggregation," *Environ. Pollut.*, vol. 228, pp. 454–463, 2017. [Online]. Available: https://linkinghub.elsevier.com/retrieve/pii/S0269749117303329

[149] L. I. Devriese, M. D. Van der Meulen, T. Maes, K. Bekaert, I. Paul-Pont, L. Frère, J. Robbens, and A. D. Vethaak, "Microplastic contamination in brown shrimp (crangon crangon, linnaeus 1758) from coastal waters of the southern north sea and channel area," *Mar. Pollut. Bull.*, vol. 98, no. 1-2, pp. 179–187, 2015. [Online]. Available: https://linkinghub.elsevier.com/retrieve/pii/S0025326X1500418X

[150] J. Hara, J. Frias, and R. Nash, "Quantification of microplastic ingestion by the decapod crustacean nephrops norvegicus from irish waters," *Mar. Pollut. Bull.*, vol. 152, p. 110905, 2020. [Online]. Available: https://linkinghub.elsevier.com/retrieve/pii/S0025326X20300230

[151] E. Besseling, E. Foekema, J. Van Franeker, M. Leopold, S. Kühn, E. B. Rebolledo, E. Heße, L. Mielke, J. IJzer, P. Kamminga *et al.*, "Microplastic

in a macro filter feeder: humpback whale megaptera novaeangliae," *Mar. Pollut. Bull.*, vol. 95, no. 1, pp. 248–252, 2015. [Online]. Available: https://linkinghub.elsevier.com/retrieve/pii/S0025326X15001952

[152] M. C. Fossi, L. Marsili, M. Baini, M. Giannetti, D. Coppola, C. Guerranti, I. Caliani, R. Minutoli, G. Lauriano, M. G. Finoia *et al.*, "Fin whales and microplastics: The mediterranean sea and the sea of cortez scenarios," *Environ. Pollut.*, vol. 209, pp. 68–78, 2016. [Online]. Available: https://linkinghub.elsevier.com/retrieve/pii/S0269749115301822

[153] E. M. Duncan, A. C. Broderick, W. J. Fuller, T. S. Galloway, M. H. Godfrey, M. Hamann, C. J. Limpus, P. K. Lindeque, A. G. Mayes, L. C. Omeyer, D. Santillo, R. T. Snape, and B. J. Godley, "Microplastic ingestion ubiquitous in marine turtles," *Glob. Chang. Biol.*, vol. 25, no. 2, pp. 744–752, 2019.

[154] Q. A. Schuyler, C. Wilcox, K. Townsend, B. D. Hardesty, and N. J. Marshall, "Mistaken identity? visual similarities of marine debris to natural prey items of sea turtles," *Bmc. Ecol.*, vol. 14, no. 1, pp. 1–7, 2014. [Online]. Available: http://bmcecol.biomedcentral.com/articles/10.1186/1472-6785-14-14

[155] F. Murray and P. R. Cowie, "Plastic contamination in the decapod crustacean nephrops norvegicus (linnaeus, 1758)," *Mar. Pollut. Bull.*, vol. 62, no. 6, pp. 1207–1217, 2011. [Online]. Available: https://linkinghub.elsevier.com/retrieve/pii/S0025326X11001755

[156] P. G. Ryan, G. Cole, K. Spiby, R. Nel, A. Osborne, and V. Perold, "Impacts of plastic ingestion on post-hatchling loggerhead turtles off south africa," *Mar. Pollut. Bull.*, vol. 107, no. 1, pp. 155–160, 2016. [Online]. Available: https://linkinghub.elsevier.com/retrieve/pii/S0025326X16302041

[157] Z. Diana, N. Sawickij, N. A. Rivera Jr, H. Hsu-Kim, and D. Rittschof, "Plastic pellets trigger feeding responses in sea anemones," *Aquat. Toxicol.*, vol. 222, p. 105447, 2020. [Online]. Available: https://linkinghub.elsevier.com/retrieve/pii/S0166445X19308136

[158] G. D'Avignon, S. S. Hsu, I. Gregory-Eaves, and A. Ricciardi, "Feeding behavior and species interactions increase the bioavailability of microplastics to benthic food webs," *Science of The Total Environment*, vol. 896, p. 165261, 2023. [Online]. Available: https://linkinghub.elsevier.com/retrieve/pii/S0048969723038846

[159] M. Ogonowski, C. Schür, Å. Jarsén, and E. Gorokhova, "The effects of natural and anthropogenic microparticles on individual fitness in daphnia magna,"

PloS one, vol. 11, no. 5, p. e0155063, 2016. [Online]. Available: https://dx.plos.org/10.1371/journal.pone.0155063

[160] R. Sussarellu, M. Suquet, Y. Thomas, C. Lambert, C. Fabioux, M. E. J. Pernet, N. Le Goïc, V. Quillien, C. Mingant, Y. Epelboin *et al.*, "Oyster reproduction is affected by exposure to polystyrene microplastics," *Proc. Natl. Acad. Sci.*, vol. 113, no. 9, pp. 2430–2435, 2016. [Online]. Available: https://pnas.org/doi/full/10.1073/pnas.1519019113

[161] F. M. Heindler, F. Alajmi, R. Huerlimann, C. Zeng, S. J. Newman, G. Vamvounis, and L. van Herwerden, "Toxic effects of polyethylene terephthalate microparticles and di (2-ethylhexyl) phthalate on the calanoid copepod, parvocalanus crassirostris," *Ecotoxicol. Environ. Saf.*, vol. 141, pp. 298–305, 2017. [Online]. Available: https://linkinghub.elsevier.com/retrieve/pii/S0147651317301719

[162] D. Brennecke, B. Duarte, F. Paiva, I. Caçador, and J. Canning-Clode, "Microplastics as vector for heavy metal contamination from the marine environment," *Estuar. Coast. Shelf Sci.*, vol. 178, pp. 189–195, 2016.

[163] R. Beiras, E. Verdejo, P. Campoy-López, and L. Vidal-Liñán, "Aquatic toxicity of chemically defined microplastics can be explained by functional additives," *J. Hazard. Mater.*, vol. 406, no. 124338, 2021.

[164] N. Casagrande, C. O. Silva, F. Verones, P. Sobral, and G. Martinho, "Ecotoxicity effect factors for plastic additives on the aquatic environment: a new approach for life cycle impact assessment," *Environ. Pollut.*, vol. 341, p. 122935, 2024. [Online]. Available: https://linkinghub.elsevier.com/retrieve/pii/S0269749123019371

[165] M. Z. Hauschild and M. A. Huijbregts, *Introducing life cycle impact assessment.* Springer, 2015. [Online]. Available: https://link.springer.com/10.1007/978-94-017-9744-3_1

[166] R. K. Rosenbaum, M. Z. Hauschild, A.-M. Boulay, P. Fantke, A. Laurent, M. Núñez, and M. Vieira, "Life cycle impact assessment," in *Life cycle assessment: Theory and practice.* Springer, 2018, ch. 10, pp. 167–270.

[167] P. Fantke, M. Bijster, C. Guignard, M. Hauschild, M. Huijbregts, O. Jolliet, A. Kounina, V. Magaud, M. Margni, T. McKone, L. Posthuma, R. K. Rosenbaum, D. van de Meent, and R. can Zelm, *USEtox 2.0: Documentation (Version 1)*, 2017, no. 2. [Online]. Available: http://dx.doi.org/10.11581/DTU:00000011

[168] U. de Haes, G. Finnveden, M. Goedkoop, M. Hauschild, E. Hertwich, P. Hofstetter, O. Jolliet, W. Klöpffer, W. Krewitt, E. Lindeijer *et al.*, *Life cycle impact assessment: striving towards best practice.* SETAC press, 2002.

[169] A. D. Henderson, M. Z. Hauschild, D. Van De Meent, M. A. J. Huijbregts, H. F. Larsen, M. Margni, T. E. McKone, J. Payet, R. K. Rosenbaum, and O. Jolliet, "USEtox fate and ecotoxicity factors for comparative assessment of toxic emissions in life cycle analysis: Sensitivity to key chemical properties," *Int. J. Life Cycle Assess.*, vol. 16, no. 8, pp. 701–709, 2011. [Online]. Available: https://doi.org/10.1007/s11367-011-0294-6

[170] O. Jolliet, M. Margni, R. Charles, S. Humbert, J. Payet, G. Rebitzer, and R. K. Rosenbaum, "IMPACT 2002+: A New Life Cycle Impact Assessment Methodology," *Int. J. Life Cycle Assess.*, vol. 32, no. 1531, pp. 411–424, 2003.

[171] O. Jolliet, R. Rosenbaum, P. M. Chapman, T. McKone, M. Margni, M. Scheringer, N. Van Straalen, and F. Wania, "Establishing a framework for life cycle toxicity assessment: Findings of the Lausanne review workshop," *Int. J. Life Cycle Assess.*, vol. 11, no. 3, pp. 209–212, 2006.

[172] F. B. Verones, A.-M. Boulay, Corella-Puertas, E. Dorber, M. Douziech, and M. Golstein, "A global consensus life cycle impact assessment method-glam: Impacts on biodiversity."

[173] D. U. Hooper, F. S. Chapin III, J. J. Ewel, A. Hector, P. Inchausti, S. Lavorel, J. H. Lawton, D. M. Lodge, M. Loreau, S. Naeem *et al.*, "Effects of biodiversity on ecosystem functioning: a consensus of current knowledge," *Ecol. Monogr.*, vol. 75, no. 1, pp. 3–35, 2005. [Online]. Available: https://doi.org/10.1890/04-0922

[174] D. Tilman, P. B. Reich, and F. Isbell, "Biodiversity impacts ecosystem productivity as much as resources, disturbance, or herbivory," *Proc. Natl. Acad. Sci.*, vol. 109, no. 26, pp. 10 394–10 397, 2012. [Online]. Available: http://www.pnas.org/cgi/doi/10.1073/pnas.1208240109

[175] L. Peano, A. Kounina, V. Magaud, S. Chalumeau, M. Zgola, J. Boucher, and Quantis EA, "Plastic Leak Project Methodological Guidelines," *Quantis+ea*, vol. v1.3, no. May, 2020.

[176] P. F. N. PFN, "Technical modules," Plasticfootprint.earth, Tech. Rep., 2023. [Online]. Available: https://www.plasticfootprint.earth/

[177] P. Saling, L. Gyuzeleva, K. Wittstock, V. Wessolowski, and R. Griesshammer, "Life cycle impact assessment of microplastics as one component of marine plastic debris," *Int. J. Life Cycle Assess.*, vol. 25, no. 10, pp. 2008–2026, 2020.

[178] D. Maga, C. Galafton, J. Blömer, N. Thonemann, A. Özdamar, and J. Bertling, "Methodology to address potential impacts of plastic emissions in life cycle assessment," *Int. J. Life Cycle Assess.*, vol. 27, no. 3, pp. 469–491, 2022.

[179] M. A. Høiberg, J. S. Woods, and F. Verones, "Global distribution of potential impact hotspots for marine plastic debris entanglement," *Ecol. Indic.*, vol. 135, p. 108509, 2022. [Online]. Available: https://linkinghub.elsevier.com/retrieve/pii/S1470160X21011742

[180] M. A. Høiberg, K. Stadler, and F. Verones, "Disentangling marine plastic impacts in life cycle assessment: Spatially explicit characterization factors for ecosystem quality," *Sci. Total Environ.*, vol. 949, p. 175019, 2024. [Online]. Available: https://linkinghub.elsevier.com/retrieve/pii/S0048969724051696

[181] Y. Tang, R. N. Mankaa, and M. Traverso, "An effect factor approach for quantifying the impact of plastic additives on aquatic biota in life cycle assessment," *Int. J. Life Cycle Assess.*, vol. 27, no. 4, pp. 564–572, 2022. [Online]. Available: https://link.springer.com/10.1007/s11367-022-02046-9

[182] I. A. Kane and M. A. Clare, "Dispersion, accumulation, and the ultimate fate of microplastics in deep-marine environments: a review and future directions," *Front. Earth Sci.*, vol. 7, p. 80, 2019. [Online]. Available: https://doi.org/10.3389/feart.2019.00080

[183] L. C. Lebreton and A. Andrady, "Future scenarios of global plastic waste generation and disposal," *Palgrave Commun.*, vol. 5, no. 1, pp. 1–11, 2019. [Online]. Available: http://dx.doi.org/10.1057/s41599-018-0212-7

[184] P. Schober, C. Boer, and L. A. Schwarte, "Correlation coefficients: appropriate use and interpretation," *Anesth Analg.*, vol. 126, no. 5, pp. 1763–1768, 2018. [Online]. Available: https://journals.lww.com/00000539-201805000-00050

[185] R. K. Rosenbaum, M. Margni, and O. Jolliet, "A flexible matrix algebra framework for the multimedia multipathway modeling of emission to impacts," *Environ. Int.*, vol. 33, no. 5, pp. 624–634, 2007.

[186] S. A. Oginah, L. Posthuma, M. Hauschild, J. Slootweg, M. Kosnik, and P. Fantke, "To split or not to split: Characterizing chemical pollution impacts in aquatic

ecosystems with species sensitivity distributions for specific taxonomic groups," *Environ. Sci. Technol.*, vol. 57, no. 39, pp. 14 526–14 538, 2023. [Online]. Available: https://pubs.acs.org/doi/10.1021/acs.est.3c04968

[187] C. Hajjar, C. Bulle, and A.-M. Boulay, "Life cycle impact assessment framework fro assessing physical effects on biota of marine microplastics emissions," *Int. J. Life Cycle Assess.*, 2023. [Online]. Available: https://doi.org/10.1007/s11367-023-02212-7

[188] E. Bird, "Chapter 2 coastal processes," in *Coastal Geomorphology: An Introduction, Second Edition.* John Wiley & Sons, Ltd, 2008.

[189] R. A. Davis, "Chapter 5 Beach and Nearshore Zone," in *Coast. Sediment. Environ.* Springer New York, NY, 1978, no. 1, ch. 5, pp. 237–280. [Online]. Available: https://doi.org/10.1007/978-1-4684-0056-4

[190] M. J. Costello and C. Chaudhary, "Marine biodiversity, biogeography, deep-sea gradients, and conservation," *Curr. Biol.*, vol. 27, no. 11, pp. R511–R527, 2017. [Online]. Available: https://linkinghub.elsevier.com/retrieve/pii/S0960982217305055

[191] D. P. Tittensor, C. Mora, W. Jetz, H. K. Lotze, D. Ricard, E. V. Berghe, and B. Worm, "Global patterns and predictors of marine biodiversity across taxa," *Nature*, vol. 466, no. 7310, pp. 1098–1101, 2010. [Online]. Available: https://www.nature.com/articles/nature09329

[192] T. O. Gagné, G. Reygondeau, C. N. Jenkins, J. O. Sexton, S. J. Bograd, E. L. Hazen, and K. S. Van Houtan, "Towards a global understanding of the drivers of marine and terrestrial biodiversity," *PLoS One*, vol. 15, no. 2, p. e0228065, 2020. [Online]. Available: https://dx.plos.org/10.1371/journal.pone.0228065

[193] Z. J. Kitchel, H. M. Conrad, R. L. Selden, and M. L. Pinsky, "The role of continental shelf bathymetry in shaping marine range shifts in the face of climate change," *Glob. Change Biol.*, vol. 28, no. 17, pp. 5185–5199, 2022. [Online]. Available: https://onlinelibrary.wiley.com/doi/10.1111/gcb.16276

[194] T. J. Webb, E. Vanden Berghe, and R. O'Dor, "Biodiversity's big wet secret: the global distribution of marine biological records reveals chronic under-exploration of the deep pelagic ocean," *PloS one*, vol. 5, no. 8, p. e10223, 2010. [Online]. Available: https://dx.plos.org/10.1371/journal.pone.0010223

[195] T. Vincenty, "Direct and inverse solutions of geodesics on the ellipsoid with application of nested equations," *Surv. Rev.*, vol. 23, no. 176, pp. 88–93, 1975. [Online]. Available: https://doi.org/10.1179/sre.1975.23.176.88

[196] M. Tedetti and R. Sempéré, "Penetration of Ultraviolet Radiation in the Marine Environment. A Review," *Photochem. Photobiol.*, vol. 82, no. 2, p. 389, 2006.

[197] M. A. Charette and W. H. Smith, "The volume of earth's ocean," *Oceanography*, vol. 23, no. 2, pp. 112–114, 2010. [Online]. Available: https://tos.org/oceanography/article/the-volume-of-earths-ocean

[198] I. Jalón-Rojas, D. Sous, and V. Marieu, "A wave-resolving 2dv lagrangian approach to model microplastic transport in the nearshore," *Geoscientific Model Development Discussions*, vol. 2024, pp. 1–26, 2024. [Online]. Available: https://gmd.copernicus.org/preprints/gmd-2024-100/

[199] GLORYS12V1, "Global ocean physics reanalysis," 2023. [Online]. Available: https://doi.org/10.48670/moi-00021

[200] I. Jalón-Rojas, X.-H. Wang, and E. Fredj, "On the importance of a three-dimensional approach for modelling the transport of neustic microplastics," *Ocean Sci.*, vol. 15, no. 3, pp. 717–724, 2019b. [Online]. Available: https://os.copernicus.org/articles/15/717/2019/

[201] D. Neumann, U. Callies, and M. Matthies, "Marine litter ensemble transport simulations in the southern north sea," *Mar. Pollut. Bull.*, vol. 86, no. 1-2, pp. 219–228, 2014. [Online]. Available: https://linkinghub.elsevier.com/retrieve/pii/S0025326X14004524

[202] M. L. Kaandorp, H. A. Dijkstra, and E. Van Sebille, "Closing the Mediterranean Marine Floating Plastic Mass Budget: Inverse Modeling of Sources and Sinks," *Environ. Sci. Technol.*, vol. 54, no. 19, pp. 11 980–11 989, 2020.

[203] L. D. Talley, G. L. Pickard, W. J. Emery, and J. H. Swift, "Dynamical Processes for Descriptive Ocean Circulation," *Descr. Phys. Oceanogr.*, pp. 1–72, 2011.

[204] K. Waldschläger, M. Born, W. Cowger, A. Gray, and H. Schüttrumpf, "Settling and rising velocities of environmentally weathered micro-and macroplastic particles," *Environ. Res.*, vol. 191, p. 110192, 2020. [Online]. Available: https://linkinghub.elsevier.com/retrieve/pii/S0013935120310896

[205] S. Zhiyao, W. Tingting, X. Fumin, and L. Ruijie, "A simple formula for predicting settling velocity of sediment particles," *Water Sci. Eng.*, vol. 1, no. 1, pp. 37–43, 2008. [Online]. Available: https://doi.org/10.1016/S1674-2370(15)30017-X

[206] L. Khatmullina and I. Isachenko, "Settling velocity of microplastic particles of regular shapes," *Mar. Pollut. Bull.*, vol. 114, no. 2, pp. 871–880, 2017. [Online]. Available: http://dx.doi.org/10.1016/j.marpolbul.2016.11.024

[207] I. Jalón-Rojas, S. Defontaine, M. Bermúdez, and M. Díez-Minguito, "Transport of microplastic debris in estuaries," *Ref. Mod. Earth Syst. Environ. Sci.: Treatise Estuar. Coast. Sci.*, vol. 2, 2024. [Online]. Available: https://linkinghub.elsevier.com/retrieve/pii/B9780323907989000226

[208] J. W. Kamphuis, "Alongshore sediment transport rate," *J. Waterw.*, vol. 117, no. 6, pp. 624–640, 1991.

[209] M. Owsianiak, M. Z. Hauschild, L. Posthuma, E. Saouter, M. G. Vijver, T. Backhaus, M. Douziech, T. Schlekat, and P. Fantke, "Ecotoxicity characterization of chemicals: Global recommendations and implementation in USEtox," *Chemosphere*, vol. 310, no. June 2022, 2023.

[210] IUCN, https://www.iucnredlist.org, 2024, accessed: 2024-10-18.

[211] M. Tunali and B. Nowack, "Towards including soil ecotoxicity of microplastics and tire wear particles into life cycle assessment," 2025.

[212] WoRMS, "Worms editorial board. world register of marine species," 2024. [Online]. Available: https://www.marinespecies.org

[213] D. K. A. Barnes, F. Galgani, R. C. Thompson, M. Barlaz, D. K. A. Barnes, F. Galgani, R. C. Thompson, and M. Barlaz, "Accumulation and fragmentation of plastic debris in global environments," *Philos. Trans. R. Soc. B Biol. Sci.*, vol. 364, no. 1526, pp. 1985–1998, 2009. [Online]. Available: https://doi.org/10.1098/rstb.2008.0205

[214] N. B. Hartmann, S. Rist, J. Bodin, L. H. S. Jensen, S. N. Schmidt, P. Mayer, A. Meibom, and A. Baun, "Microplastics as vectors for environmental contaminants: Exploring sorption, desorption, and transfer to biota," *Integr. Environ. Assess. Manag.*, vol. 13, no. 3, pp. 488–493, 2017.

[215] W. Zhang, X. Ma, Z. Zhang, Y. Wang, J. J. J. Wang, J. J. J. Wang, and D. Ma, "Persistent organic pollutants carried on plastic resin pellets from two beaches in

China," *Mar. Pollut. Bull.*, vol. 99, no. 1-2, pp. 28–34, 2015. [Online]. Available: http://dx.doi.org/10.1016/j.marpolbul.2015.08.002

[216] M. R. Gregory, "Environmental implications of plastic debris in marine settings- entanglement, ingestion, smothering, hangers-on, hitch-hiking and alien invasions," *Philos. Trans. R. Soc. B Biol. Sci.*, vol. 364, no. 1526, pp. 2013–2025, 2009.

[217] S. Humbert, V. Rossi, M. Margni, O. Jolliet, and Y. Loerincik, "Life cycle assessment of two baby food packaging alternatives : glass jars vs . plastic pots," *Int. J. Life Cycle Assess.*, pp. 95–106, 2009.

[218] A. Ahamed, P. Vallam, N. Shiva, A. Veksha, J. Bobacka, and G. Lisak, "Life cycle assessment of plastic grocery bags and their alternatives in cities with con fi ned waste management structure : A Singapore case study," *J. Clean. Prod.*, vol. 278, p. 123956, 2021. [Online]. Available: https://doi.org/10.1016/j.jclepro.2020.123956

[219] L. Peano, A. Kounina, V. Magaud, S. Chalumeau, M. Zgola, and J. Boucher, "Plastic Leak Project Methodological Guidelines," *Quantis+ea*, vol. v1.3, no. May, 2020.

[220] A. Chamas, H. Moon, J. Zheng, Y. Qiu, T. Tabassum, J. H. Jang, M. Abu-omar, S. L. Scott, and S. Suh, "Degradation Rates of Plastics in the Environment," *ACS Sustain. Chem. Eng.*, 2020.

[221] M. A. Browne, P. Crump, S. J. Niven, E. Teuten, A. Tonkin, T. Galloway, and R. Thompson, "Accumulation of microplastic on shorelines woldwide: Sources and sinks," *Environ. Sci. Technol.*, vol. 45, no. 21, pp. 9175–9179, 2011.

[222] P. T. Harris, "The fate of microplastic in marine sedimentary environments: A review and synthesis," *Mar. Pollut. Bull.*, vol. 158, no. 111398, 2020. [Online]. Available: https://doi.org/10.1016/j.marpolbul.2020.111398

[223] S. J. Lentz and M. R. Fewings, "The wind- and wave-driven inner-shelf circulation," *Ann. Rev. Mar. Sci.*, vol. 4, pp. 317–343, 2012.

[224] A. A. Koelmans, M. Kooi, K. L. Law, and E. Van Sebille, "All is not lost: Deriving a top-down mass budget of plastic at sea," *Environ. Res. Lett.*, vol. 12, no. 11, 2017.

[225] A. B. Kara, P. A. Rochford, and H. E. Hurlburt, "An optimal definition for ocean mixed layer depth," *J. Geophys. Res. Ocean.*, vol. 105, no. C7, pp. 16 803–16 821, 2000.

[226] I. Langmuir, "Surface motion of water induced wind," *Science*, vol. 87, pp. 119–123, 1938.

[227] F. J. Tapia, J. Pineda, F. J. Ocampo-Torres, H. L. Fuchs, P. E. Parnell, P. Montero, and S. Ramos, "High-frequency observations of wind-forced onshore transport at a coastal site in Baja California," *Cont. Shelf Res.*, vol. 24, no. 13-14, pp. 1573–1585, 2004.

[228] A. Ter Halle, L. Ladirat, X. Gendre, D. Goudouneche, C. Pusineri, C. Routaboul, C. Tenailleau, B. Duployer, and E. Perez, "Understanding the Fragmentation Pattern of Marine Plastic Debris," *Environ. Sci. Technol.*, vol. 50, no. 11, pp. 5668–5675, 2016.

[229] J. H. Yoon, S. Kawano, and S. Igawa, "Modeling of marine litter drift and beaching in the Japan Sea," *Mar. Pollut. Bull.*, vol. 60, no. 3, pp. 448–463, 2010. [Online]. Available: http://dx.doi.org/10.1016/j.marpolbul.2009.09.033

[230] P. G. Ryan, "Does size and buoyancy affect the long-distance transport of floating debris ?" *Environ. Res. Lett.*, vol. 10, no. 8, 2015. [Online]. Available: https://doi.org/10.1088/1748-9326/10/8/084019

[231] A. Cózar, E. Martí, C. M. Duarte, J. García-de Lomas, E. Van Sebille, T. J. Ballatore, V. M. Eguíluz, J. Ignacio González-Gordillo, M. L. Pedrotti, F. Echevarría, R. Troublè, and X. Irigoien, "The Arctic Ocean as a dead end for floating plastics in the North Atlantic branch of the Thermohaline Circulation," *Sci. Adv.*, vol. 3, no. 4, pp. 1–8, 2017.

[232] X. Chen, G. Huang, and D. D. Dionysiou, "Editorial Overview: Emissions of Microplastics and Their Control in the Environment," *J. Environ. Eng.*, vol. 147, no. 9, p. 01821002, 2021.

[233] R. W. Obbard, "Microplastics in Polar Regions : The role of long range transport," *Curr. Opin. Environ. Sci. Heal.*, vol. 1, pp. 24–29, 2017. [Online]. Available: https://doi.org/10.1016/j.coesh.2017.10.004

[234] X. Wang, C. Li, K. Liu, L. Zhu, Z. Song, and D. Li, "Atmospheric microplastic over the South China Sea and East Indian Ocean: abundance, distribution and source," *J. Hazard. Mater.*, vol. 389, no. 121846, 2019. [Online]. Available: https://doi.org/10.1016/j.jhazmat.2019.121846

[235] K. Liu, T. Wu, X. Wang, Z. Song, C. Zong, N. Wei, and D. Li, "Consistent Transport of Terrestrial Microplastics to the Ocean through Atmosphere," *Environ. Sci. Technol.*, vol. 53, no. 18, pp. 10 612–10 619, 2019.

[236] S. Allen, D. Allen, K. Moss, G. Le Roux, V. R. Phoenix, and J. E. Sonke, "Examination of the ocean as a source for atmospheric microplastics," *PLoS One*, vol. 15, no. 5, pp. 1–14, 2020.

[237] Y. K. Song, S. H. Hong, S. Eo, M. Jang, G. M. Han, A. Isobe, and W. J. Shim, "Horizontal and Vertical Distribution of Microplastics in Korean Coastal Waters," *Environ. Sci. Technol.*, vol. 52, no. 21, pp. 12 188–12 197, 2018.

[238] E. van Sebille, "The oceans' accumulating plastic garbage," *Phys. Today*, vol. 68, no. 2, pp. 60–61, 2015.

[239] J. A. Austin and S. J. Lentz, "The inner shelf response to wind-driven upwelling and downwelling," *J. Phys. Oceanogr.*, vol. 32, no. 7, pp. 2171–2193, 2002.

[240] F. Zhang, C. Yao, J. Xu, L. Zhu, G. Peng, and D. Li, "Composition, spatial distribution and sources of plastic litter on the East China Sea floor," *Sci. Total Environ.*, vol. 742, no. 140525, 2020. [Online]. Available: https://doi.org/10.1016/j.scitotenv.2020.140525

[241] H. C. Flemming, J. Wingender, U. Szewzyk, P. Steinberg, S. A. Rice, and S. Kjelleberg, "Biofilms: An emergent form of bacterial life," *Nat. Rev. Microbiol.*, vol. 14, no. 9, pp. 563–575, 2016. [Online]. Available: http://dx.doi.org/10.1038/nrmicro.2016.94

[242] S. Ye and A. L. Andrady, "Fouling of floating plastic debris under Biscayne Bay exposure conditions," *Mar. Pollut. Bull.*, vol. 22, no. 12, pp. 608–613, 1991.

[243] A. Cózar, F. Echevarría, J. I. González-gordillo, X. Irigoien, and B. Úbeda, "Plastic debris in the open ocean," *Proc. Natl. Acad. Sci.*, vol. 111, no. October, 2014.

[244] M. Egger, R. Nijhof, L. Quiros, G. Leone, S. J. Royer, A. C. McWhirter, G. A. Kantakov, V. I. Radchenko, E. A. Pakhomov, B. P. V. Hunt, and L. Lebreton, "A spatially variable scarcity of floating microplastics in the eastern North Pacific Ocean," *Environ. Res. Lett.*, vol. 15, no. 11, 2020.

[245] J. E. Burris, "Effects of oxygen and inorganic carbon concentrations on the photosynthetic quotients of marine algae," *Mar. Biol.*, vol. 65, no. 3, pp. 215–219, 1981.

[246] K. Unice, M. Weeber, M. Abramson, R. Reid, J. van Gils, A. Markus, A. Vethaak, and J. Panko, "Characterizing export of land-based microplastics to the estuary - Part I: Application of integrated geospatial microplastic transport models to assess tire and road wear particles in the Seine watershed," *Sci. Total Environ.*, vol. 646, pp. 1639–1649, 2019. [Online]. Available: https://doi.org/10.1016/j.scitotenv.2018.07.368

[247] X. Peng, M. Chen, S. Chen, S. Dasgupta, H. Xu, K. Ta, M. Du, J. Li, Z. Guo, and S. Bai, "Microplastics contaminate the deepest part of the world's ocean," *Geochemical Perspect. Lett.*, vol. 9, pp. 1–5, 2018.

[248] E. D. Ingall and P. V. Cappellen, "Relation between sedimentation rate and burial of organic phosphorus and organic carbon in marine sediments," *Geochim. Cosmochim. Acta*, vol. 54, no. 2, pp. 373–386, 1990.

[249] T. S. Galloway, M. Cole, and C. Lewis, "Interactions of microplastic debris throughout the marine ecosystem," *Nat. Ecol. Evol.*, vol. 1, no. 5, pp. 1–8, 2017. [Online]. Available: http://dx.doi.org/10.1038/s41559-017-0116

[250] B. P. Boudreau, "Mean mixed depth of sediments: The wherefore and the why," *Limnol. Oceanogr.*, vol. 43, no. 3, pp. 524–526, 1998.

[251] M. Solan, E. R. Ward, E. L. White, E. E. Hibberd, C. Cassidy, J. M. Schuster, R. Hale, and J. A. Godbold, "Worldwide measurements of bioturbation intensity, ventilation rate, and the mixing depth of marine sediments," *Sci. Data*, vol. 6, no. 1, pp. 1–6, 2019. [Online]. Available: http://dx.doi.org/10.1038/s41597-019-0069-7

[252] E. Yousif and R. Haddad, "Photodegradation and photostabilization of polymers, especially polystyrene: Review," *Springerplus*, vol. 2, no. 1, pp. 1–32, 2013.

[253] A. Mateos-Cárdenas, J. O'Halloran, F. N. A. M. van Pelt, M. A. K. Jansen, J. O'Halloran, F. N. A. M. van Pelt, and M. A. K. Jansen, "Rapid fragmentation of microplastics by the freshwater amphipod Gammarus duebeni (Lillj.)," *Sci. Rep.*, vol. 10, no. 1, pp. 1–12, 2020. [Online]. Available: https://doi.org/10.1038/s41598-020-69635-2

[254] J. E. Pegram and A. L. Andrady, "Outdoor weathering of selected polymeric materials under marine exposure conditions," *Polym. Degrad. Stab.*, vol. 26, no. 4, pp. 333–345, 1989.

[255] C. P. Ward, C. J. Armstrong, A. N. Walsh, J. H. Jackson, and C. M. Reddy, "Sunlight Converts Polystyrene to Carbon Dioxide and Dissolved Organic Carbon," *Environ. Sci. Technol. Lett.*, vol. 6, no. 11, pp. 669–674, 2019.

[256] L. Sørensen, A. S. Groven, I. A. Hovsbakken, O. Del Puerto, D. F. Krause, A. Sarno, and A. M. Booth, "UV degradation of natural and synthetic microfibers causes fragmentation and release of polymer degradation products and chemical

additives," *Sci. Total Environ.*, vol. 755, no. 143170, 2021. [Online]. Available: https://doi.org/10.1016/j.scitotenv.2020.143170

[257] F. Verones, S. Hellweg, A. Antón, L. B. Azevedo, A. Chaudhary, N. Cosme, S. Cucurachi, L. de Baan, Y. Dong, P. Fantke, L. Golsteijn, M. Hauschild, R. Heijungs, O. Jolliet, R. Juraske, H. Larsen, A. Laurent, C. L. Mutel, M. Margni, M. Núñez, M. Owsianiak, S. Pfister, T. Ponsioen, P. Preiss, R. K. Rosenbaum, P. O. Roy, S. Sala, Z. Steinmann, R. van Zelm, R. Van Dingenen, M. Vieira, and M. A. Huijbregts, "LC-IMPACT: A regionalized life cycle damage assessment method," *J. Ind. Ecol.*, vol. 24, no. 6, pp. 1201–1219, 2020.

[258] K. Chomkhamsri, M.-A. Wolf, and R. Pant, "International Reference Life Cycle Data System (ILCD) Handbook: Review Schemes for Life Cycle Assessment," in *Towar. Life Cycle Sustain. Manag.*, 2011, pp. 107–117.

[259] P. Fantke, N. Aurisano, J. Bare, T. Backhaus, C. Bulle, P. M. Chapman, D. De Zwart, R. Dwyer, A. Ernstoff, L. Golsteijn, H. Holmquist, O. Jolliet, T. E. McKone, M. Owsianiak, W. Peijnenburg, L. Posthuma, S. Roos, E. Saouter, D. Schowanek, N. M. van Straalen, M. G. Vijver, and M. Hauschild, "Toward harmonizing ecotoxicity characterization in life cycle impact assessment," *Environ. Toxicol. Chem.*, vol. 37, no. 12, pp. 2955–2971, 2018.

[260] D. Mackay and M. MacLeod, "Multimedia environmental models," *Pract. Period. Hazardous, Toxic, Radioact. Waste Manag.*, vol. 6, no. 2, pp. 63–69, 2002.

[261] M. Margni, D. W. Pennington, D. H. Bennett, and O. Jolliet, "Cyclic exchanges and level of coupling between environmental media: Intermedia feedback in multimedia fate models," *Environ. Sci. Technol.*, vol. 38, no. 20, pp. 5450–5457, 2004.

[262] D. W. Pennington, M. Margni, C. Ammann, and O. Jolliet, "Multimedia fate and human intake modeling: Spatial versus nonspatial insights for chemical emissions in Western Europe," *Environ. Sci. Technol.*, vol. 39, no. 4, pp. 1119–1128, 2005.

[263] R. Heijungs, "Harmonization of methods for impact assessment," *Environ. Sci. Pollut. Res.*, vol. 2, no. 4, pp. 217–224, 1995.

[264] S. Shaked, "Multi-Continental Multimedia Model of Pollutant Intake and Application to Impacts of Global Emissions and Globally Traded Goods," Ph.D. dissertation, University of Michigan, 2011.

[265] P. Webb, "Introduction to Oceanography: Estuaries," *Creat. Commons Attrib. 4.0 Int. Licens.*, pp. 2001–2006, 2017. [Online]. Available: https://rwu.pressbooks.pub/webboceanography/chapter/13-6-estuaries/

[266] R. Park and J. Clough, "Aquatox (Release 3.1 plus) Technical Documentation," vol. 2, no. 344, 2014. [Online]. Available: http://www2.epa.gov/exposure-assessment-models/aquatox

[267] J. A. Arnot and F. A. Gobas, "A food web bioaccumulation model for organic chemicals in aquatic ecosystems," *Environ. Toxicol. Chem.*, vol. 23, no. 10, pp. 2343–2355, 2004.

[268] S. Lambert and M. Wagner, "Characterisation of nanoplastics during the degradation of polystyrene," *Chemosphere*, vol. 145, pp. 265–268, 2016. [Online]. Available: http://dx.doi.org/10.1016/j.chemosphere.2015.11.078

[269] E. van Sebille, P. Delandmeter, M. Lange, C. Kehl, R. Brouwer, D. Reijnders, Reint, W. Rath, Pdnooteboom, J. Scutt Phillips, Simnator101, A. Gibson, J. Kronborg, P. Petersik, Thomas-95, D. Wichmann, Pierrick-giffard, J. Busecke, M. Sterl, and G. Vettoretti, "OceanParcels/parcels: Parcels v2.2.2: a Lagrangian Ocean Analysis tool for the petascale age (v2.2.2)," 2021.

[270] A. Praetorius, M. Scheringer, and K. Hungerbühler, "Development of environmental fate models for engineered nanoparticles - A case study of TiO 2 nanoparticles in the rhine river," *Environ. Sci. Technol.*, vol. 46, no. 12, pp. 6705–6713, 2012.

[271] M. W. Ryberg, A. Laurent, and M. Hauschild, "Mapping of global plastics value chain and plastics losses to the environment (with a particular focus on marine environment)," *United Nations Environ. Program.*, pp. 1–99, 2018. [Online]. Available: https://gefmarineplastics.org/files/2018Mappingofglobalplasticsvaluechainandhotspots-finalversionr181023.pdf

[272] J. van Wijnen, A. M. J. Ragas, and C. Kroeze, "Modelling global river export of microplastics to the marine environment: Sources and future trends," *Sci. Total Environ.*, vol. 673, pp. 392–401, 2019. [Online]. Available: https://doi.org/10.1016/j.scitotenv.2019.04.078

[273] L. C. Lebreton, J. van der Zwet, J.-w. Damsteeg, B. Slat, A. Andrady, and J. Reisser, "River plastic emissions to the world's oceans," *Nat. Commun.*, vol. 8, pp. 1–10, 2017. [Online]. Available: http://dx.doi.org/10.1038/ncomms15611

[274] A. Malli, E. Corella-Puertas, C. Hajjar, and A.-M. M. Boulay, "Transport mechanisms and fate of microplastics in estuarine compartments: A review," *Mar. Pollut. Bull.*, vol. 177, no. 113553, 2022. [Online]. Available: https://doi.org/10.1016/j.marpolbul.2022.113553

[275] E. C. Atwood, F. M. Falcieri, S. Piehl, M. Bochow, M. Matthies, J. Franke, S. Carniel, M. Sclavo, C. Laforsch, and F. Siegert, "Coastal accumulation of microplastic particles emitted from the Po River, Northern Italy: Comparing remote sensing and hydrodynamic modelling with in situ sample collections," *Mar. Pollut. Bull.*, vol. 138, pp. 561–574, 2019. [Online]. Available: https://doi.org/10.1016/j.marpolbul.2018.11.045

[276] S. Kühn, E. L. B. Rebolledo, and J. A. van Franeker, "Deleterious effects of litter on marine life," in *Mar. Anthropog. Litter*. Springer International Publishing, 2015, ch. 4, pp. 75–116. [Online]. Available: https://doi.org/10.1007/978-3-319-16510-3

[277] S. Kühn and J. A. van Franeker, "Quantitative overview of marine debris ingested by marine megafauna," *Mar. Pollut. Bull.*, vol. 151, no. December 2019, p. 110858, 2020. [Online]. Available: https://doi.org/10.1016/j.marpolbul.2019.110858

[278] F. Amélineau, D. Bonnet, O. Heitz, V. Mortreux, A. M. Harding, N. Karnovsky, W. Walkusz, J. Fort, and D. Grémillet, "Microplastic pollution in the Greenland Sea: Background levels and selective contamination of planktivorous diving seabirds," *Environ. Pollut.*, vol. 219, pp. 1131–1139, 2016.

[279] UNEP, *Drowning in plastics - Marine litter and plastic waste vital graphics*, 2021.

[280] P. Villarrubia-Gómez, S. E. Cornell, and J. Fabres, "Marine plastic pollution as a planetary boundary threat – The drifting piece in the sustainability puzzle," *Mar. Policy*, vol. 96, no. November 2017, pp. 213–220, 2018. [Online]. Available: https://doi.org/10.1016/j.marpol.2017.11.035

[281] N. Prinz and Š. Korez, "Understanding how microplastics affect marine biota on the cellular level is important for assessing ecosystem function: a review," in *YOUMARES 9-The Oceans: Our Research, Our Future: Proceedings of the 2018 conference for YOUng MArine RESearcher in Oldenburg, Germany.* Springer International Publishing, 2020, pp. 101–120. [Online]. Available: https://doi.org/10.1007/978-3-030-20389-4_6

[282] B. D. Hardesty, J. Harari, A. Isobe, L. Lebreton, N. Maximenko, J. Potemra, E. V. Sebille, A. D. Vethaak, and C. Wilcox, "Using Numerical Model Simulations to Improve the Understanding of Micro-plastic Distribution and Pathways in the Marine Environment," *Front. Mar. Sci.*, vol. 4, no. March, pp. 1–9, 2017.

[283] E. van Sebille, S. M. Griffies, R. Abernathey, T. P. Adams, P. Berloff, A. Biastoch, B. Blanke, E. P. Chassignet, Y. Cheng, C. J. Cotter, E. Deleersnijder, K. Döös, H. F. Drake, S. Drijfhout, S. F. Gary, A. W. Heemink, J. Kjellsson, M. I. Koszalla, M. Lange, C. Lique, G. A. Macgilchrist, R. Marsh, C. G. Mayorga Adame, R. Mcadam, F. Nencioli, C. B. Paris, M. D. Piggott, J. A. Polton, S. Rühs, S. H. A. M. Shah, M. D. Thomas, J. Wang, P. J. Wolfram, L. Zanna, and J. D. Zika, "Lagrangian ocean analysis : Fundamentals and practices," *Ocean Model.*, vol. 121, no. July 2016, pp. 49–75, 2018.

[284] L. C. M. Lebreton, S. D. Greer, and J. C. Borrero, "Numerical modelling of floating debris in the world's oceans," *Mar. Pollut. Bull.*, vol. 64, no. 3, pp. 653–661, 2012. [Online]. Available: http://dx.doi.org/10.1016/j.marpolbul.2011.10.027

[285] S. K. Kim, H. J. Lee, J. S. Kim, S. H. Kang, E. J. Yang, K. H. Cho, Z. Tian, and A. Andrady, "Importance of seasonal sea ice in the western Arctic ocean to the Arctic and global microplastic budgets," *J. Hazard. Mater.*, vol. 418, no. February, p. 125971, 2021. [Online]. Available: https://doi.org/10.1016/j.jhazmat.2021.125971

[286] C. Gualtieri, "Sediments burial velocity estimation in Venice Lagoon," *XXVIII IAHR Congr.*, no. August 1999, pp. 22–27, 1999.

[287] M. MacLeod, A. J. Fraser, and D. Mackay, "Evaluating and expressing the propagation of uncertainty in chemical fate and bioaccumulation models," *Environ. Toxicol. Chem.*, vol. 21, no. 4, pp. 700–709, 2002.

[288] S. Chapra, *Surface Water-Quality Modeling*, 1997.

[289] G. Voulgaris and M. B. Collins, "Sediment resuspension on beaches: Response to breaking waves," *Mar. Geol.*, vol. 167, no. 1-2, pp. 167–187, 2000.

[290] P. Pfohl, M. Wagner, L. Meyer, P. Domercq, A. Praetorius, T. Hüffer, T. Hofmann, and W. Wohlleben, "Environmental degradation of microplastics: how to measure fragmentation rates to secondary micro-and nanoplastic fragments and dissociation into dissolved organics," *Environ. Sci. Technol.*, vol. 56, no. 16, pp. 11 323–11 334, 2022. [Online]. Available: https://pubs.acs.org/doi/10.1021/acs.est.2c01228

[291] K. Critchell and J. Lambrechts, "Modelling accumulation of marine plastics in the coastal zone; what are the dominant physical processes?" *Estuar. Coast. Shelf Sci*, vol. 171, pp. 111–122, 2016. [Online]. Available: https://linkinghub.elsevier.com/retrieve/pii/S0272771416300361

[292] K. Dunn, "DESIGN AND ANALYSIS OF EXPERIMENTS," in *Process Improv. using Data*, 2022, pp. 231–291.

[293] J. M. Hrycik, J. Chassé, B. R. Ruddick, and C. T. Taggart, "Dispersal kernel estimation : A comparison of empirical and modelled particle dispersion in a coastal marine system," *Estuar. Coast. Shelf Sci.*, vol. 133, pp. 11–22, 2013. [Online]. Available: http://dx.doi.org/10.1016/j.ecss.2013.06.023

[294] I. Jalón-rojas and V. Marieu, "Tutorial. TrackMPD v2.3 A 3D numerical model to Track Maarine Plastic Debris," 2023.

[295] V. Hidalgo-Ruz, L. Gutow, R. C. Thompson, and M. Thiel, "Microplastics in the marine environment: a review of the methods used for identification and quantification," *Environ. Sci. Technol.*, vol. 46, no. 6, pp. 3060–3075, 2012. [Online]. Available: https://doi.org/10.1021/es2031505

[296] R. Soulsby, "Dynamics of marine sands," 1997.

[297] J. Rivers-Auty, A. L. Bond, M. L. Grant, and J. L. Lavers, "The one-two punch of plastic exposure: macro-and micro-plastics induce multi-organ damage in seabirds," *J. Hazard. Mater.*, vol. 442, p. 130117, 2023. [Online]. Available: https://doi.org/10.1016/j.jhazmat.2022.130117

[298] H. Saygin, B. Tilkili, S. Karniyarik, and A. Baysal, "Culture dependent analysis of bacterial activity, biofilm-formation and oxidative stress of seawater with the contamination of microplastics under climate change consideration," *Sci. Total Environ.*, vol. 922, p. 171103, 2024. [Online]. Available: https://linkinghub.elsevier.com/retrieve/pii/S0048969724012427

[299] G. Johnson and S. Wijfells, "Ocean density change contributions to sea level rise," *Oceanogr.*, vol. 4, pp. 112–121, 2011.

[300] J. Hansen, M. Sato, P. Hearty, R. Ruedy, M. Kelley, V. Masson-Delmotte, G. Russell, G. Tselioudis, J. Cao, E. Rignot *et al.*, "Ice melt, sea level rise and superstorms: evidence from paleoclimate data, climate modeling, and modern observations that 2 c

global warming could be dangerous," *Atmos. Chem. Phys.*, vol. 16, no. 6, pp. 3761–3812, 2016. [Online]. Available: https://acp.copernicus.org/articles/16/3761/2016/

[301] M. T. Vu, Y. Lacroix, and V. T. Nguyen, "Modeling investigation of potential sea level rise effect on hydrodynamics and sediment transport in hyères bay, france," *J. ETA Mar. Sci.*, vol. 12, no. 3, pp. 0–0, 2024.

[302] L. Jiang, T. Gerkema, D. Idier, A. Slangen, and K. Soetaert, "Effects of sea-level rise on tides and sediment dynamics in a dutch tidal bay," *Ocean Sci.*, vol. 16, no. 2, pp. 307–321, 2020. [Online]. Available: https://os.copernicus.org/articles/16/307/2020/

[303] C. Heuzé, K. J. Heywood, D. P. Stevens, and J. K. Ridley, "Changes in global ocean bottom properties and volume transports in cmip5 models under climate change scenarios," *J. Clim.*, vol. 28, no. 8, pp. 2917–2944, 2015. [Online]. Available: https://journals.ametsoc.org/view/journals/clim/28/8/jcli-d-14-00381.1.xml

[304] L. A. Amaral-Zettler, E. R. Zettler, T. J. Mincer, M. A. Klaassen, and S. M. Gallager, "Biofouling impacts on polyethylene density and sinking in coastal waters: a macro/micro tipping point?" *Water research*, vol. 201, p. 117289, 2021. [Online]. Available: https://linkinghub.elsevier.com/retrieve/pii/S0043135421004875

[305] E. Van Ierland and L. Peperzak, "Separation of marine seston and density determination of marine diatoms by density gradient centrifugation," *Journal of plankton research*, vol. 6, no. 1, pp. 29–44, 1984. [Online]. Available: https://doi.org/10.1093/plankt/6.1.29

APPENDIX A SI OF ARTICLE 1: LIFE CYCLE IMPACT ASSESSMENT FRAMEWORK FOR ASSESSING PHYSICAL EFFECTS ON BIOTA OF MARINE MICROPLASTICS EMISSIONS

Appendix A includes the supplementary information of Article 1: "Life cycle impact assessment framework for assessing physical effects on biota of marine microplastics emissions". This answers the first objective of this thesis. It can equally be found on the following link: https://link.springer.com/10.1007/s11367-023-02212-7

Supplementary Information: Life cycle impact assessment framework for assessing physical effects on biota of marine microplastics emissions

Carla Hajjar[1*], Cécile Bulle[2] and Anne-Marie Boulay[1]

[1*]Department of Chemical Engineering, CIRAIG, Polytechnique of Montreal, Montreal (QC), Canada.
[2]Department of Strategy and Corporate Social Responsibility, Organization, Montreal (QC), Canada.

*Corresponding author(s). E-mail(s): carla.alchahir-alhajjar@polymtl.ca;
Contributing authors: bulle.cecile@uqam.ca; anne-marie.boulay@polymtl.ca;

S1 Review on fate mechanisms

S1.1 Aggregation

Marine snows are aggregates of particulate organic matter (POM such as detritus, plankton), microorganisms, and clay minerals that are either produced by living marine plants and animals, or by biological aggregation of microaggregates, phytoplankton, organic debris, clay minerals, and fecal pellets egested from plankton, fishes copepods, and mammals (Alldredge & Silver, 1988). Larvaceans build their 'houses', in which they live and through which they move and feed, from complex mucus filters (Alldredge, 1977). Larvaceans houses and marine snows facilitate the phenomenon known as biological pump (Katija et al., 2017) which is the vertical flux of carbon, POM, and nutrients from the surface of the water to deep oceans where benthic ecosystem feeds and the atmospherically derived carbon is stored (Giering et al., 2014; Turner, 2015). Recently, biological transport – which can be due to aggregation - has been

proven to potentially represent an ecological pathway in the redistribution of MPs from the surface to deep sediments and major ocean basins (Choy et al., 2019; K. Kvale et al., 2020). The aggregation of MPs to marine snows can vertically transport these microscopic particles of different densities, shapes, and sizes, from the water surface to the seafloor (K.F. Kvale et al., 2020; Möhlenkamp et al., 2018; Porter et al., 2018) enhancing their bioavailability to benthic organisms. This aggregation is the dominant biological pathway for their vertical transport (K. Kvale et al., 2020). It enhances the sinking rates of dense particles and reduces the buoyancy of floating MPs (Cole et al., 2013, 2016; Dawson et al., 2018; Katija et al., 2017; Lee et al., 2013; Porter et al., 2018). Microplastics aggregated into dense fecal pellets significantly alter their density, physical integrity, structure, and size (Cole et al., 2015; Wieczorek et al., 2019) which might potentially increase (Porter et al., 2018), or reduce their settling velocity (Cole et al., 2016; Wieczorek et al., 2019). Fecal pellets with reduced settling rates are prone to microbial degradation in the water column resulting in their mineralization and the release of POM, carbon, and nutrients prior to their arrival to the sediments hence reducing the vertical carbon flux in deeper oceans (Cole et al., 2016).

S1.2 Transport by biota

A wide variety of marine animals, including fish, turtles, mammals, and invertebrates, are exposed to MPs either by mistaking them for being prey or through trophic transfer (Kühn & van Franeker, 2020; Lusher, 2015). While ingestion is the main pathway (Lusher, 2015), marine organisms can be exposed to MPs through different routes and pathways depending on the species. Benthic invertebrates, i.e., lugworms, amphipods, and blue mussels directly feed on MPs (Thompson et al., 2004). Some species can even selectively ingest microplastic particles (Graham & Thompson, 2009). Planktonic invertebrates are contaminated via absorption (Bhattacharya et al., 2010). Marine turtles ingest MPs through tropic transfer, contaminated seaweeds, or while feeding close to benthic sediments (Duncan et al., 2019; Pham et al., 2017). Shore crabs either ingest contaminated food or inspire them through ventilation across the gills with a higher uptake through the posterior gill (Watts et al., 2014). Large mesopelagic fish, i.e., cetaceans such as True's beaked whales, can inhale MPs at the air-water interface or ingest them while feeding (Lusher et al., 2015). However, trophic transfer is found to be the most dominant pathway (Romeo et al., 2015) with ingestion rates varying with different species and feeding depths (Justino et al., 2022). The bioavailability of microplastics to marine organisms is dependent on particle's abundance, size, density, shape, biofouling, selectivity of species, and prey-resembling colors (Ory et al., 2018).

Once in the body of marine organisms, MPs can either be retained, egested with fecal pellets, or removed through stomach evacuation, which might redistribute MPs within marine sub-compartments. MPs aggregated to egested fecal pellets (section S1.1) have increased density and settling velocity which enhances their vertical movement (K. Kvale et al., 2020). Pelagic species

feeding on fecal pellets result in the suspension of released MPs. Suspended particles will then be repackaged multiple times before they reach the seafloor (Lusher, 2015). Zooplankton (Wright et al., 2013) and mesopelagic fishes such as lantern fishes, myctophids, and other speed up the downward flux of buoyant MPs to deeper depth, a process referred to as "plastic pump" (Wieczorek et al., 2018). These fishes, feeding at the shallow layers during the night (Choy & Drazen, 2013), ingest microplastics particles then undergo diurnal migrations, quickly traveling long distances to the deep ocean where they egest microplastic-laden faeces (Lusher et al., 2016; Wieczorek et al., 2018). The biological interaction of microplastics is not only limited to the retention within feeding organisms, but also to ingestion and egestion (Lusher et al., 2016). While ingestion rates vary with species and feeding depths (Justino et al., 2022), the retention of MPs within marine biota is still unknown as ingestion-excretion rates are poorly understood (Qu et al., 2020). The retention time is influenced by the dispersion of MPs within the whole body of marine organisms through translocation between different organs or adherence into the skin and tissues (Abbasi et al., 2018). In addition, it depends on the species and the route of exposure. For instance, MPs might be retained in crabs for up to 14 days after ingestion and up to 21 days after inspiration through gills (Watts et al., 2014), while some fishes might retain them for an average of 7 days and up to 49 days (Ory et al., 2018). Thus, in order to quantify MPs biological transfer rates, it is important to investigate into their complex behaviour within different marine biota (Sun et al., 2018).

Upon mortality, marine fishes are either consumed by other organisms, i.e., sea turtles or decompose in the marine environment (Muhametsafina et al., 2014). Based on their buoyancy and location at death, they will either float where they drift, or sink to the bottom of the ocean (Moore et al., 2020). The rate of decomposition depends on the temperature and depth of seawater (Chidami & Amyot, 2008). In shallow water, dead fish might refloat after decomposition due to gas release while in deep waters, the decomposition will occur at the bottom (Moore et al., 2020). This indicates that MPs might either be transferred to other marine organisms through ingestion or be released at the sea surface or the bottom sediments. This behaviour might also influence the fate of MPs in the marine environment and needs further investigation.

S1.3 Sea ice transfer

Recent studies have detected MPs in sea ice at concentrations close to those found in accumulation zones, also known as "garbage patches" (Obbard et al., 2014; Peeken et al., 2018). Sea ice in both Arctic and Antarctic represents a major seasonal sink for microplastic particles (Kanhai et al., 2020; Kim, 2021; Obbard et al., 2014; Peeken et al., 2018) while sea ice in Southern ocean presents less plastic concentrations (Mountford & Morales Maqueda, 2021). During ice formation, MPs are entrapped in the uppermost layer of sea ice (Geilfus et al., 2019) formed during the early phases of sea-ice growth (Geilfus et al., 2019; Kelly et al., 2020). However, there is no consistent pattern in the

vertical distribution of MPs in ice cores (Kanhai et al., 2020; Peeken et al., 2018). Upon melting, entrapped particles are released and are redistributed in the water where resulting brine circulation might transport them below the euphotic zone (Peeken et al., 2018). Plastics present in sediments at shallow water levels are resuspended by turbidity currents during storms in autumn/winter seasons and are hypothesized to attach to the bottom of growing ice where they become entrapped (Kelly et al., 2020). Sea ice movement can redistribute MPs both horizontally and vertically in the ocean (Bergmann et al., 2017). Sea ice formation and melting seasonal cycles are responsible for exposing marine organisms to MPs for longer periods of times by increasing their bioavailability at the surface (when ice melts) rather than in the sediments (where they would have reached faster without the ice entrapment) (Kelly et al., 2020). It is important to mention that MPs detection is not uniform in both Arctic and Antarctic waters as their density plays a role in their distribution. Positively buoyant MPs are transported by the circulation of Arctic Sea where they accumulate in the sea ice while neutrally buoyant MPs do not accumulate in well-defined areas but are rather widely transported through the water column (Mountford & Morales Maqueda, 2021). Sea-ice transport was initially studied by Pfirman et al. (1995) while modeling backward trajectories of heavy metals and organochlorines incorporated in sea ice. This model is nowadays used to identify the origins of sea-ice MPs detected in the Arctic sea (Obbard, 2017). Further investigations are still needed to understand the removal and transport of MPs by sea ice. These recent studies reflect on the importance of linking the fate of the particles to both their physical properties and associated physical and ocean dynamics that vary within the ocean.

S2 Results

S2.1 Multimedia fate framework

The interactions between microplastics and marine biota are summarized in figure S1 below.

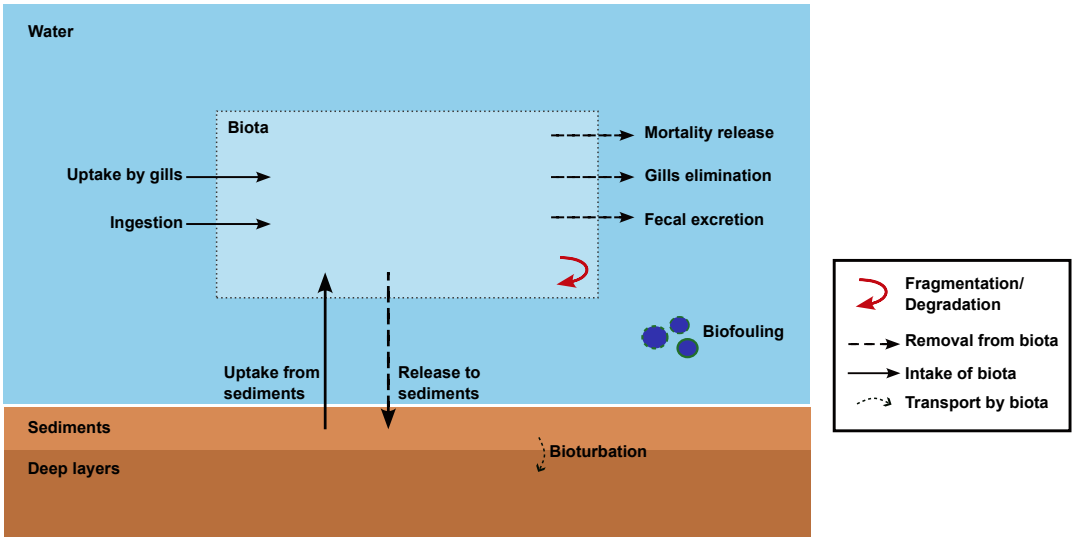

Fig. S1 Interactions between marine biota and microplastics

S2.2 Mass balance equations and rate matrices

Similar to intermedia transfer rates developed for the continental scale, transfer rates between global sub-compartments are developed for the global scale as follows:

$$\begin{aligned} k_{wc.G,ws.G} &= k_{sinking} = k_{aggregation} + k_{biofouling} + k_{biotatransfer} \\ &\quad + k_{advection} \\ k_{sed.G,wc.G} &= k_{sedimentation} = k_{aggregation} + k_{biofouling} + k_{biotatransfer} \\ &\quad + k_{advection} \\ k_{sed.G,wc.G} &= k_{resuspension} \end{aligned} \tag{S1}$$

Table S1 summarizes all mechanisms that play a role in the transport of microplastics in the marine environment at the continental and the global scale.

Table A.1 Summarizing rate matrix for the fate mechanisms of microplastics in the marine environment

	b.C	**ws.C**	**wc.C**	**sed.C**	**ws.G**	**wc.G**	**sed.G**
b.C	Degradation, fragmentation, advection*,burial	advection*	0	0	0	0	0
ws.C	advection*	Degradation, fragmentation, advection*, sinking**	0	0	Advection*, windage	0	0
wc.C	0	Sinking**	Degradation, sedimentation**	Resuspension	0	Advection	0
sed.C	0	0	Sedimentation**	Degradation, resuspension, burial***	0	0	Sediment transport, advection
ws.G	0	Advection*, windage	0	0	Degradation, fragmentation, advection*, sinking**	0	0
wc.G	0	0	Advection	0	0	Degradation, sedimentation*	Resuspension
sed.G	0	0	0	Sediment transport, advection	0	Sinking**	Degradation, resuspension, burial***

* Influenced by Stokes drift, winds, Langmuir circulation, Ekman transport
** Influenced by biofouling, aggregation, biota transfer
*** Influenced by bioturbation and sedimentation

Total removal rates for global scale are:

$$\begin{aligned} k_{ws.G,tot} &= k_{ws.G,deg} + k_{ws.G,frag} + k_{ws.C,ws.G} + k_{wc.G,ws.G} \\ k_{wc.G,tot} &= k_{wc.G,deg} + k_{sed.G,wc.G} + k_{wc.C,wc.G} \\ k_{sed.G,tot} &= k_{sed.G,deg} + k_{sed.C,sed.G} + k_{wc.G,sed.G} \end{aligned} \tag{S2}$$

References

Abbasi, S., Soltani, N., Keshavarzi, B., Moore, F., Turner, A., Hassanaghaei, M. (2018). Microplastics in different tissues of fish and prawn from the Musa Estuary, Persian Gulf. *Chemosphere*, *205*, 80–87. Retrieved from https://doi.org/10.1016/j.chemosphere.2018.04.076

10.1016/j.chemosphere.2018.04.076

Alldredge, A.L. (1977). House morphology and mechanisms of feeding in the Oikopleuridae (Tunicata, Appendicularia). *J. Zool.*, *181*(2), 175–188.

10.1111/j.1469-7998.1977.tb03236.x

Alldredge, A.L., & Silver, M.W. (1988). Characteristics, dynamics and significance of marine snow. *Prog. Oceanogr.*, *20*(1), 41–82.

10.1016/0079-6611(88)90053-5

Bergmann, M., Peeken, I., Beyer, B., Krumpen, T., Primpke, S., Tekman, M.B., Gerdts, G. (2017). *Vast Quantities of Microplastics in Arctic Sea Ice—A Prime Temporary Sink for Plastic Litter and a Medium of Transport*. Elsevier Inc. Retrieved from http://dx.doi.org/10.1016/B978-0-12-812271-6.00073-9 10.1016/b978-0-12-812271-6.00073-9

Bhattacharya, P., Lin, S., Turner, J.P., Ke, P.C. (2010). Physical adsorption of charged plastic nanoparticles affects algal photosynthesis. *J. Phys. Chem. C*, *114*(39), 16556–16561.

10.1021/jp1054759

Chidami, S., & Amyot, M. (2008). Fish decomposition in boreal lakes and biogeochemical implications. *Am. Soc. Limnol. Oceanogr.*, *53*(5), 1988–1996.

Choy, C.A., & Drazen, J.C. (2013). Plastic for dinner? Observations of frequent debris ingestion by pelagic predatory fishes from the central North Pacific. *Mar. Ecol. Prog. Ser.*, *485*, 155–163.

10.3354/meps10342

Choy, C.A., Robison, B.H., Gagne, T.O., Erwin, B., Firl, E., Halden, R.U., ... Van Houtan, K.S. (2019). The vertical distribution and biological transport of marine microplastics across the epipelagic and mesopelagic water column. *Sci. Rep.*, *10*(1), 1–9.

10.1038/s41598-020-57573-y

Cole, M., Lindeque, P., Fileman, E., Halsband, C., Galloway, T.S. (2015). The impact of polystyrene microplastics on feeding, function and fecundity in the marine copepod Calanus helgolandicus. *Environ. Sci. Technol.*, *49*(2), 1130–1137.

10.1021/es504525u

Cole, M., Lindeque, P., Fileman, E., Halsband, C., Goodhead, R., Moger, J., Galloway, T.S. (2013). Microplastic ingestion by zooplankton. *Environ. Sci. Technol.*, *47*(12), 6646–6655.

10.1021/es400663f

Cole, M., Lindeque, P.K., Fileman, E., Clark, J., Lewis, C., Halsband, C., Galloway, T.S. (2016). Microplastics Alter the Properties and Sinking Rates of Zooplankton Faecal Pellets. *Environ. Sci. Technol.*, *50*(6), 3239–3246.

10.1021/acs.est.5b05905

Dawson, A.L., Kawaguchi, S., King, C.K., Townsend, K.A., King, R., Huston, W.M., Bengtson Nash, S.M. (2018). Turning microplastics into nanoplastics through digestive fragmentation by Antarctic krill. *Nat. Commun.*, *9*(1), 1–8. Retrieved from http://dx.doi.org/10.1038/s41467-018-03465-9

10.1038/s41467-018-03465-9

Duncan, E.M., Broderick, A.C., Fuller, W.J., Galloway, T.S., Godfrey, M.H., Hamann, M., ... Godley, B.J. (2019). Microplastic ingestion ubiquitous in marine turtles. *Glob. Chang. Biol.*, *25*(2), 744–752.

10.1111/gcb.14519

Geilfus, N.X., Munson, K.M., Sousa, J., Germanov, Y., Bhugaloo, S., Babb, D., Wang, F. (2019). Distribution and impacts of microplastic incorporation within sea ice. *Mar. Pollut. Bull.*, *145*(April), 463–473. Retrieved from https://doi.org/10.1016/j.marpolbul.2019.06.029

10.1016/j.marpolbul.2019.06.029

Giering, S.L.C., Sanders, R., Lampitt, R.S., Anderson, T.R., Tamburini, C., Boutrif, M., ... Mayor, D.J. (2014). Reconciliation of the carbon budget in the ocean's twilight zone. *Nature*, *507*(7493), 480–483.

10.1038/nature13123

Graham, E.R., & Thompson, J.T. (2009). Deposit- and suspension-feeding sea cucumbers (Echinodermata) ingest plastic fragments. *J. Exp. Mar. Bio. Ecol.*, *368*(1), 22–29. Retrieved from http://dx.doi.org/10.1016/j.jembe.2008.09.007

10.1016/j.jembe.2008.09.007

Justino, A.K.S., Ferreira, G.V.B., Schmidt, N., Eduardo, L.N., Fauvelle, V., Lenoble, V., ... Lucena-Frédou, F. (2022). The role of mesopelagic fishes as microplastics vectors across the deep-sea layers from the Southwestern Tropical Atlantic. *Environ. Pollut.*, *300*(November 2021).

10.1016/j.envpol.2022.118988

Kanhai, L.D.K., Gardfeldt, K., Krumpen, T., Thompson, R.C., O'Connor, I., O'Connor, I. (2020). Microplastics in sea ice and seawater beneath ice floes from the Arctic Ocean. *Sci. Rep.*, *10*(1), 1–11.

10.1038/s41598-020-61948-6

Katija, K., Choy, C.A., Sherlock, R.E., Sherman, A.D., Robison, B.H. (2017). From the surface to the seafloor: How giant larvaceans transport microplastics into the deep sea. *Sci. Adv.*, *3*(8), 1–6.

10.1126/sciadv.1700715

Kelly, A., Lannuzel, D., Rodemann, T., Meiners, K.M., Auman, H.J. (2020). Microplastic contamination in east Antarctic sea ice. *Mar. Pollut. Bull.*, *154*(April), 111130. Retrieved from https://doi.org/10.1016/j.marpolbul.2020.111130

10.1016/j.marpolbul.2020.111130

Kim, M.S. (2021). Modeling study on fate of micro/nano-plastics in micro/nano-hydrodynamic flow of freshwater. *J. Hazard. Mater.*, *419*(February 2020).

10.1016/j.jhazmat.2021.126397

Kühn, S., & van Franeker, J.A. (2020). Quantitative overview of marine debris ingested by marine megafauna. *Mar. Pollut. Bull.*, *151*(December 2019), 110858. Retrieved from https://doi.org/10.1016/j.marpolbul.2019.110858

10.1016/j.marpolbul.2019.110858

Kvale, K., Prowe, A., Chien, C.-T., Landolfi, A., Oschlies, A. (2020). The global biological microplastic particle sink. *Sci. Rep.*, *10*(1), 1–12. Retrieved from https://doi.org/10.1038/s41598-020-72898-4

10.1038/s41598-020-72898-4

Kvale, K.F., Friederike Prowe, A.E., Oschlies, A. (2020). A Critical Examination of the Role of Marine Snow and Zooplankton Fecal Pellets in Removing Ocean Surface Microplastic. *Front. Mar. Sci.*, *6*(January), 1–8.

10.3389/fmars.2019.00808

Lee, K.W., Shim, W.J., Kwon, O.Y., Kang, J.H. (2013). Size-dependent effects of micro polystyrene particles in the marine copepod tigriopus japonicus. *Environ. Sci. Technol.*, *47*(19), 11278–11283.

10.1021/es401932b

Lusher, A.L. (2015). Chapter 10 Microplastics in the marine environment: Distribution, interactions and effects. *Mar. anthropog. litter* (pp. 245–307). 10.1007/978-3-319-16510-3

Lusher, A.L., Hernandez-Milian, G., O'Brien, J., Berrow, S., O'Connor, I., Officer, R. (2015). Microplastic and macroplastic ingestion by a deep diving, oceanic cetacean: The True's beaked whale Mesoplodon mirus. *Environ. Pollut.*, *199*, 185–191.

10.1016/j.envpol.2015.01.023

Lusher, A.L., O'Donnell, C., Officer, R., O'Connor, I. (2016). Microplastic interactions with North Atlantic mesopelagic fish. *ICES J. Mar. Sci.*, *73*, 1214–1225.

10.4135/9781412953924.n678

Möhlenkamp, P., Purser, A., Thomsen, L. (2018). Plastic microbeads from cosmetic products: An experimental study of their hydrodynamic behaviour, vertical transport and resuspension in phytoplankton and sediment aggregates. *Elementa*, *6*.

10.1525/elementa.317

Moore, M.J., Mitchell, G.H., Rowles, T.K., Early, G., Moore, M.J. (2020). Dead Cetacean ? Beach, Bloat, Float, Sink. *Front. Mar. Sci.*, *7*(May), 1–6.

10.3389/fmars.2020.00333

Mountford, A.S., & Morales Maqueda, M.A. (2021). Modeling the accumulation and transport of microplastics by sea ice. *J. Geophys. Res. Ocean.*, *126*(2), 1–19.

10.1029/2020JC016826

Muhametsafina, A., Midwood, J.D., Bliss, S.M., Stamplecoskie, K.M., Cooke, S.J. (2014). The fate of dead fish tagged with biotelemetry transmitters in an urban stream. *Aquat Ecol*, 23–33.

10.1007/s10452-013-9463-y

Obbard, R.W. (2017). Microplastics in Polar Regions : The role of long range transport. *Curr. Opin. Environ. Sci. Heal.*, *1*, 24–29. Retrieved from https://doi.org/10.1016/j.coesh.2017.10.004

10.1016/j.coesh.2017.10.004

Obbard, R.W., Sadri, S., Wong, Y.Q., Khitun, A.A., Baker, I., Thompson, R.C. (2014). Global warming releases microplastics legacy frozen in arctic. *Earth's Futur.*, *2*, 315–320.

10.1002/2014EF000240.Abstract

Ory, N.C., Gallardo, C., Lenz, M., Thiel, M. (2018). Capture, swallowing, and egestion of microplastics by a planktivorous juvenile fish. *Environ. Pollut.*, *240*, 566–573. Retrieved from https://doi.org/10.1016/j.envpol.2018.04.093

10.1016/j.envpol.2018.04.093

Peeken, I., Primpke, S., Beyer, B., Gütermann, J., Katlein, C., Krumpen, T., ... Gerdts, G. (2018). Arctic sea ice is an important temporal sink and means of transport for microplastic. *Nat. Commun.*, *9*(1). Retrieved from http://dx.doi.org/10.1038/s41467-018-03825-5

10.1038/s41467-018-03825-5

Pfirman, S.L., Eickenb, H., Bauchc, D., Weeksd, W.F. (1995). The potential transport of pollutants by Arctic sea ice. , *159*, 129–146.

Pham, C.K., Rodríguez, Y., Dauphin, A., Carriço, R., Frias, J.P.G.L., Vandeperre, F., ... Bjorndal, K.A. (2017). Plastic ingestion in oceanic-stage loggerhead sea turtles (Caretta caretta) off the North Atlantic subtropical gyre. *Mar. Pollut. Bull.*, *121*(1-2), 222–229. Retrieved from http://dx.doi.org/10.1016/j.marpolbul.2017.06.008

10.1016/j.marpolbul.2017.06.008

Porter, A.A.A., Lyons, B.P., Galloway, T.S., Lewis, C. (2018). Role of Marine Snows in Microplastic Fate and Bioavailability. *Environ. Sci. Technol.*, *52*(12), 7111–7119.

10.1021/acs.est.8b01000

Qu, H., Ma, R., Barrett, H., Wang, B., Han, J., Wang, F., ... Yu, G. (2020). How microplastics affect chiral illicit drug methamphetamine in aquatic food chain? From green alga (Chlorella pyrenoidosa) to freshwater snail (Cipangopaludian cathayensis). *Environ. Int.*, *136*(December 2019), 105480. Retrieved from https://doi.org/10.1016/j.envint.2020.105480

10.1016/j.envint.2020.105480

Romeo, T., Pietro, B., Pedà, C., Consoli, P., Andaloro, F., Fossi, M.C. (2015). First evidence of presence of plastic debris in stomach of large pelagic fish in the Mediterranean Sea. *Mar. Pollut. Bull.*, *95*(1), 358–361. Retrieved from http://dx.doi.org/10.1016/j.marpolbul.2015.04.048

10.1016/j.marpolbul.2015.04.048

Sun, X., Liang, J., Zhu, M., Zhao, Y., Zhang, B. (2018). Microplastics in seawater and zooplankton from the Yellow Sea. *Environ. Pollut.*, *242*, 585–595. Retrieved from https://doi.org/10.1016/j.envpol.2018.07.014

10.1016/j.envpol.2018.07.014

Thompson, R.C., Olson, Y., Mitchell, R.P., Davis, A., Rowland, S.J., John, A.W., ... Russell, A.E. (2004). Lost at Sea: Where Is All the Plastic? *Science (80-.).*, *304*(5672), 838.

10.1126/science.1094559

Turner, J.T. (2015). Zooplankton fecal pellets, marine snow, phytodetritus and the ocean's biological pump. *Prog. Oceanogr.*, *130*, 205–248. Retrieved

from http://dx.doi.org/10.1016/j.pocean.2014.08.005

10.1016/j.pocean.2014.08.005

Watts, A.J., Lewis, C., Goodhead, R.M., Beckett, S.J., Moger, J., Tyler, C.R., Galloway, T.S. (2014). Uptake and retention of microplastics by the shore crab carcinus maenas. *Environ. Sci. Technol.*, *48*(15), 8823–8830.

10.1021/es501090e

Wieczorek, A.M., Croot, P.L., Lombard, F., Sheahan, J.N., Doyle, T.K. (2019). Microplastic Ingestion by Gelatinous Zooplankton May Lower Efficiency of the Biological Pump. *Environ. Sci. Technol.*, *53*(9), 5387–5395.

10.1021/acs.est.8b07174

Wieczorek, A.M., Morrison, L., Croot, P.L., Allcock, A.L., MacLoughlin, E., Savard, O., ... Doyle, T.K. (2018). Frequency of microplastics in mesopelagic fishes from the Northwest Atlantic. *Front. Mar. Sci.*, *5*(FEB), 1–9.

10.3389/fmars.2018.00039

Wright, S.L., Thompson, R.C., Galloway, T.S. (2013). The physical impacts of microplastics on marine organisms: a review. *Environ. Pollut.*, *178*, 483–492. Retrieved from http://dx.doi.org/10.1016/j.envpol.2013.02.031

10.1016/j.envpol.2013.02.031

APPENDIX B SI OF ARTICLE 2: IDENTIFYING INFLUENCING PHYSICAL AND ENVIRONMENTAL PARAMETERS THROUGH THE DEVELOPMENT OF SITE-SPECIFIC FATE AND CHARACTERIZATION FACTORS FOR MICROPLASTIC EMISSIONS IN THE MARINE ENVIRONMENT

Appendix B includes the supplementary information of Article 2: "Identifying influencing physical and environmental parameters for fate and characterization factors for microplastic emissions in the marine environment". This article answers the second objective of this thesis.

202

Supplementary Information: Identifying influencing physical and environmental parameters through the development of site-specific fate and characterization factors for microplastic emissions in the marine environment

Carla Ha jjar[1*], Cécile Bulle[2], Maxime Agez[1], Elena Corella-Puertas[1] and Anne-Marie Boulay[1]

[1*]Department of Chemical Engineering, CIRAIG, Polytechnique of Montreal, Montreal (QC), Canada.

[2]Department of Strategy and Corporate Social Responsibility, Organization, Montreal (QC), Canada.

*Corresponding author(s). E-mail(s):
carla.alchahir-alha jjar@polymtl.ca;
Contributing authors: bulle.cecile@uqam.ca;
maxime.agez@polymtl.ca;
maria-elena.corella-puertas@polymtl.ca;
anne-marie.boulay@polymtl.ca;

Outline.....

S1 Methodology

S1.1 Quantification of intermedia transfer and degradation rates

S1.1.1 Resuspension and burial rates

Resuspension and burial rates are considered as advective processes occurring on the top and the bottom layers of the sediments sub-compartments, as shown in figure S1.

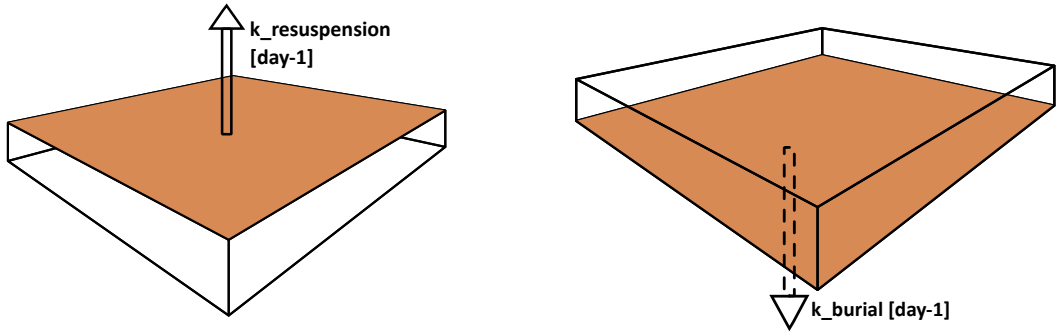

(a) Resuspension (b) Burial

Fig. S1 Resuspension and burial rates of MPs in the sediments sub-compartment

S1.1.2 Resurfacing rate

Based on the virtual wave basin of Kamphuis (1991), a beach box is constructed where the length and width are taken as 10 meters and 3.55 meters, respectively (figure S2). The depth of the box is taken as 50 mm, which is the depth of sands remaining on their sand beach when steady-state is reached. Data of their total sediment load mass [kg] are collected after equilibrium is reached (3 hours after the beginning of the authors' experiments). Consequently, the graph of sediments mass load [kg] versus time [h] is plotted (figure S3). The flux of sediments leaving the beach box (Q_{out} [kg/h]) is then obtained as the slope of the linear regression equation (red equation in figure S3). Accordingly, applying the mass balance to the beach box, $k_{resurfacing}$ $[day^{-1}]$ is obtained as follows:

$$k_{resurfacing} = k_{ws,b} = \frac{Q_{out}.24}{M_{s.s}} = \frac{Q_{out}.24}{\rho_{sediments}.V_{beach}} \quad \text{(S1)}$$

Where $M_{s.s}$ [kg] is the mass in the beach sub-compartment at steady-state. $\rho_{sediments}$ $[kg/m^3]$ and V_{beach} $[m^3]$ are the density and volume of the sand beach, respectively. 24 is the unit conversion from hours to days.

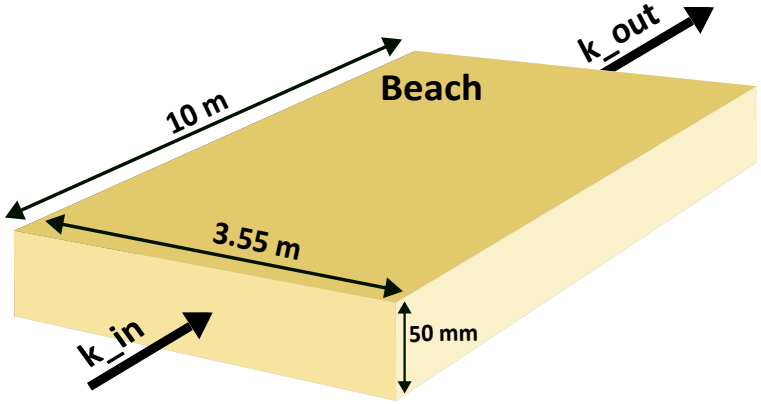

Fig. S2 Beach box recreated from (Kamphuis, 1991) at steady-state

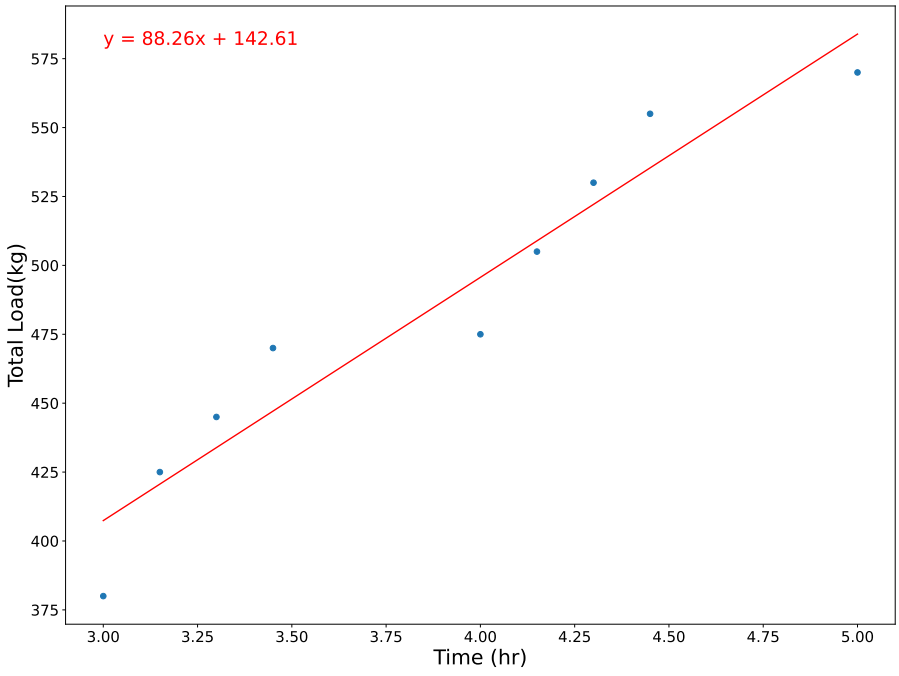

Fig. S3 Total sediment load [kg] collected versus time as taken from (Kamphuis, 1991)

S1.2 Emission Locations

The coordinates of each emission point presented in figure 1 of the manuscript are presented in the table below:

Table S1 Coordinates of emission locations for points A, B and C in figure 1 of the manuscript (Coordinate reference system: EPSG 4326 WGS 84 - World Geodetic System)

Emission locations	Longitude	Latitude	Depth [m]
A	-63.97632	43.98452	-0.5
B	-69.12746	43.56431	-0.5
C	-70.49068	40.93734	-0.5

S1.3 Simulation Plan

The full factorial design for 6 factors at two levels per factor (minimum and maximum) would require a total of 64 runs (2^6) in order to understand the influence of each parameter as well as the interaction between them on the output, which is the settling time of MPs. Due to the high computation time required for each simulation, a simulation plan is developed to run the least number of simulations while getting the most robust results possible. The half-fraction design was adopted in this work where 32 simulations were run. According to the trade-off table presented in Dunn (2022), the set of minimum and maximum values for each parameter per scenario is constructed (as seen in table S2). Negative numbers (-1) represent minimum values while positive ones (+1) represent maximum values (Table 1). The settling time for each particle is then recorded for each simulation. The median value for 150 particles simulated per scenario is then used. According to Dunn (2022), the least square model, a type of linear models, is used to determine the magnitude of effect of each parameter tested. It represents the change in the simulations response (output) due to the change of input parameters. The linear system of the 32 simulations run is then solved in a matrix form in RStudio according to the formula:

$$y = X.b \tag{S2}$$

where y is the output of each scenario, X the parameters tested, and b the magnitude of effect of each parameter. In this simulation plan, the influence of individual parameters can be overlapped with five-parameter interactions. However, it is hypothesized that the interaction between five parameters at the same time is rare to be encountered in real life. For this reason, influences of individual parameters on the settling time can only be linked to their independent behaviour. The Pareto plot is then constructed to compare the significance of each parameter and/or interactions on the settling time of MPs.

Table S2 Simulation Plan: Parameters minimum and maximum values

Scenario number	Density	Shape	BR	kh	kv	Size
1	-1	-1	-1	-1	-1	-1
2	1	-1	-1	-1	-1	1
3	-1	1	-1	-1	-1	1
4	1	1	-1	-1	-1	-1
5	-1	-1	1	-1	-1	1
6	1	-1	1	-1	-1	-1
7	-1	1	1	-1	-1	-1
8	1	1	1	-1	-1	-1
9	-1	-1	-1	1	-1	-1
10	1	-1	-1	1	-1	-1
11	-1	1	-1	1	-1	-1
12	1	1	-1	1	-1	1
13	-1	-1	1	1	-1	-1
14	1	-1	1	1	-1	1
15	-1	1	1	1	-1	1
16	1	1	1	1	-1	-1
17	-1	-1	-1	-1	1	1
18	1	-1	-1	-1	1	-1
19	-1	1	-1	-1	1	-1
20	1	1	-1	-1	1	1
21	-1	-1	1	-1	1	-1
22	1	-1	1	-1	1	1
23	-1	1	1	-1	1	1
24	1	1	1	-1	1	-1
25	-1	-1	-1	1	1	-1
26	1	-1	-1	1	1	1
27	-1	1	-1	1	1	1
28	1	1	-1	1	1	-1
29	-1	-1	1	1	1	-1
30	1	-1	1	1	1	-1
31	-1	1	1	1	1	-1
32	1	1	1	1	1	1

1: Maximum values
-1: Minimum values

S2 Results

S2.1 Rate matrices for microplastic categories

Different rates calculated for different MPs categories are presented in table S3 below.

Table S3 Parameters per microplastics category. All rates are expressed in $[day^{-1}]$.

	Sphere				Cylinder			
	High density		Low density		High density		Low density	
	Big	Small	Big	Small	Big	Small	Big	Small
Simulation numbers	2-14-22-26	6-10-18-30	5-9-17-29	1-13-21-25	8-12-20-32	4-16-24-28	3-15-23-27	7-11-19-31
$k_{resurfacing}$	$4.5E-01$	$4.5E-01$	$4.5E-01$	$4.5E-01$	$4.5E-01$	$4.5E-01$	$4.5E-01$	$4.5E-01$
$k_{wc,ws}$	$2.03E+03$	$5.23E-01$	$6.35E-02$	$5.23E-01$	$9.3E+01$	$4.78E-01$	$3.09E-01$	$5.28E-01$
$k_{sed,wc}$	$1.19E+02$	$2.45E-01$	$6.9E-02$	$2.74E-01$	5.38	$1.72E-01$	$4.46E-01$	$1.7E-01$
$k_{resuspension}$	$2.3E-04$	$2.3E-04$	$2.3E-04$	$2.3E-04$	$2.3E-04$	$2.3E-04$	$2.3E-04$	$2.3E-04$
k_{burial}	$2.4E-05$	$2.4E-05$	$2.4E-05$	$2.4E-05$	$2.4E-05$	$2.4E-05$	$2.4E-05$	$2.4E-05$
k_{deg}(Fast)	$4.6E{-}4$	2.3	$2.63E{-}4$	1.3	$3.45E{-}4$	1.72	$1.97E{-}4$	0.98
k_{deg}(Medium)	$1.42E{-}8$	$7.1E{-}3$	$1.53E{-}6$	$6.92E{-}3$	$1.06E{-}6$	$5.31E{-}3$	$1.04E{-}6$	$5.2E{-}3$
k_{deg}(Slow)	$4.4E{-}9$	$2.2E{-}3$	$1.3E{-}8$	$6.57E{-}5$	$3.3E{-}9$	$1.64E{-}5$	$9.85E{-}9$	$4.92E{-}5$

Different rate matrices obtained for microplastic eight categories are presented in table S4 below.

Table S4 Rate **K** matrices for each microplastic category

		beach	water surface	water column	sediments
Sp-HD-B	**beach**	-4.51E-01	0	0	0
	water surface	4.50E-01	-2.03E+03	0	0
	water column	0	2.03E+03	-1.19E+02	2.26E-04
	sediments	0	0	1.19E+02	-2.5E-04
Sp-HD-S	**beach**	-2.75E+00	0	0	0
	water surface	4.50E-01	-5.30E-01	0	0
	water column	0	5.23E-01	-2.45E-01	2.26E-04
	sediments	0	0	2.45E-01	-2.72E-04
Sp-LD-B	**beach**	-4.51E-01	0	0	0
	water surface	4.50E-01	-6.35E-02	0	0
	water column	0	6.35E-02	-6.90E-02	2.26E-04
	sediments	0	0	6.90E-02	-2.5E-04
Sp-LD-S	**beach**	-1.76E+00	0	0	0
	water surface	4.50E-01	-5.30E-01	0	0
	water column	0	5.23E-01	-2.74E-01	2.26E-04
	sediments	0	0	2.74E-01	-3.16E-04
Cy-HD-B	**beach**	-4.68E-01	0	0	0
	water surface	4.50E-01	-9.30E+01	0	0
	water column	0	9.30E+01	-5.38E+00	2.26E-04
	sediments	0	0	5.38E+00	-2.5E-04
Cy-HD-S	**beach**	-2.18E+00	0	0	0
	water surface	4.50E-01	-4.83E-01	0	0
	water column	0	4.78E-01	-1.72E-01	2.26E-04
	sediments	0	0	1.72E-01	-2.66E-04
Cy-LD-B	**beach**	-4.60E-01	0	0	0
	water surface	4.50E-01	-3.09E-01	0	0
	water column	0	3.09E-01	-4.46E-01	2.26E-04
	sediments	0	0	4.46E-01	-2.5E-04
Cy-LD-S	**beach**	-1.44E+00	0	0	0
	water surface	4.50E-01	-5.33E-01	0	0
	water column	0	5.28E-01	-1.70E-01	2.26E-04
	sediments	0	0	1.70E-01	-2.99E-04

S2.2 Fate matrices for microplastic categories

Fate matrices for microplastic eight categories are presented in the table S5. The percentage of distribution for every emission sub-compartment for each category is also presented in table S6 below.

The results of the simulations in TrackMPD show that the water dynamic in this region transports the particles away from the shore. This is translated by a zero value for the transfer rate from the water surface to the beach for all MPs categories. This is the reason why the percentage of distribution is equal to zero for all MPs categories for emissions into water surface, water column, and sediments (see table S6).

Table S5 FF matrices for each microplastic category

		beach	water surface	water column	sediments
Sp-HD-B	**beach**	2.22E+00	0	0	0
	water surface	4.93E-04	4.94E-04	0	0
	water column	8.71E-02	8.72E-02	38.72E-02	7.88E-02
	sediments	4.16E+04	4.17E+04	14.17E+04	4.17E+04
Sp-HD-S	**beach**	3.64E-01	0	0	0
	water surface	3.09E-01	1.89E+00	0	0
	water column	3.91E+00	2.39E+01	2.18E+04	2.01E+01
	sediments	3.52E+03	2.15E+04	2.18E+04	2.18E+04
Sp-LD-B	**beach**	2.22E+00	0	0	0
	water surface	1.57E+01	1.57E+01	0	0
	water column	1.51E+02	1.51E+02	1.51E+02	1.36E+02
	sediments	4.16E+04	4.16E+04	4.16E+04	4.16E+04
Sp-LD-S	**beach**	5.67E-01	0	0	0
	water surface	4.82E-01	1.89E+00	0	0
	water column	3.24E+00	1.27E+01	1.28E+01	9.19E+00
	sediments	2.81E+03	1.1E+04	1.11E+04	1.11E+04
Cy-HD-B	**beach**	2.14E+00	0	0	0
	water surface	1.04E-02	1.08E-02	0	0
	water column	1.85E+00	1.92E+00	1.92E+00	1.74E+00
	sediments	3.99E+04	4.14E+04	4.14E+04	4.14E+04
Cy-HD-S	**beach**	4.60E-01	0	0	0
	water surface	4.28E-01	2.07E+00	0	0
	water column	7.86E+00	3.79E+01	3.84E+01	3.25E+01
	sediments	5.06E+03	2.44E+04	2.47E+04	2.47E+04
Cy-LD-B	**beach**	2.17E+00	0	0	0
	water surface	3.17E+00	3.23E+00	0	0
	water column	3.24E+01	2.29E+01	2.29E+01	2.07E+01
	sediments	3.99E+04	1.08E+04	4.08E+04	4.08E+04
Cy-LD-S	**beach**	6.96E-01	0	0	0
	water surface	5.88E-01	1.88E+00	0	0
	water column	7.43E+00	2.37E+01	2.39E+01	1.81E+01
	sediments	4.23E+03	1.35E+04	1.36E+04	1.36E+04

S2.3 Characterization factors

Table S7 presents characterization factors ($PAF.m^3.d/kg$) for microplastic emissions into all marine sub-compartments. EFs are only applied to water sub-compartments. Therefore CF_{beach} and $CF_{sediments}$ represent potential impacts of MPs on the overall ecosystem.

Table S7 demonstrates characterization factors for microplastics emitted to the water surface and water column (characterization factors for beach and sediments can be found in table S6). The characterization factor is the highest for an emission in the water surface CF_{ws} for all microplastic categories with the maximum value (6397.1 $PAF.m^3.d/kg$) for spherical low density big particles (Sp-LD-B) that are the slowest to leave the water surface. The lowest impacts (3.37 $PAF.m^3.d/kg$) are for the particles that spend the shortest period of time in the water due to fast settling. Since the same value for the effect factor (28 $PAF.m^3/kg$ (**?**)) is applied in the marine environment, differences in characterization factors are mainly linked to the fate factors. Therefore, difference between the CFs are mainly driven by fate factors influenced by the variability of microplastic physical properties and environmental properties. However, the impacts represented by these CFs account for the impacts in the water

Table S6 Matrix of microplastic percentage of distribution for an emission in every sub-compartment (columns) for the eight categories

		beach	water surface	water column	sediments
Sp-HD-B	**beach**	5.33E-03	0.00E+00	0.00E+00	0.00E+00
	water surface	1.19E-06	1.19E-06	0.00E+00	0.00E+00
	water column	2.09E-04	2.09E-04	2.09E-04	1.89E-04
	sediments	1.00E+02	1.00E+02	1.00E+02	1.00E+02
Sp-HD-S	**beach**	1.03E-02	0.00E+00	0.00E+00	0.00E+00
	water surface	8.77E-03	8.77E-03	0.00E+00	0.00E+00
	water column	1.11E-01	1.11E-01	1.11E-01	9.23E-02
	sediments	9.99E+01	9.99E+01	9.99E+01	9.99E+01
Sp-LD-B	**beach**	5.31E-03	0.00E+00	0.00E+00	0.00E+00
	water surface	3.77E-02	3.77E-02	0.00E+00	0.00E+00
	water column	3.61E-01	3.61E-01	3.61E-01	3.26E-01
	sediments	9.96E+01	9.96E+01	9.96E+01	9.97E+01
Sp-LD-S	**beach**	2.02E-02	0.00E+00	0.00E+00	0.00E+00
	water surface	1.72E-02	1.72E-02	0.00E+00	0.00E+00
	water column	1.15E-01	1.15E-01	1.15E-01	8.25E-02
	sediments	9.98E+01	9.99E+01	9.99E+01	9.99E+01
Cy-HD-B	**beach**	5.37E-03	0.00E+00	0.00E+00	0.00E+00
	water surface	2.60E-05	2.60E-05	0.00E+00	0.00E+00
	water column	4.65E-03	4.65E-03	4.65E-03	4.20E-03
	sediments	1.00E+02	1.00E+02	1.00E+02	1.00E+02
Cy-HD-S	**beach**	9.07E-03	0.00E+00	0.00E+00	0.00E+00
	water surface	8.45E-03	8.45E-03	0.00E+00	0.00E+00
	water column	1.55E-01	1.55E-01	1.55E-01	1.31E-01
	sediments	9.98E+01	9.98E+01	9.98E+01	9.99E+01
Cy-LD-B	**beach**	5.44E-03	0.00E+00	0.00E+00	0.00E+00
	water surface	7.92E-03	7.92E-03	0.00E+00	0.00E+00
	water column	5.61E-02	5.61E-02	5.61E-02	5.07E-02
	sediments	9.99E+01	9.99E+01	9.99E+01	9.99E+01
Cy-LD-S	**beach**	1.64E-02	0.00E+00	0.00E+00	0.00E+00
	water surface	1.39E-02	1.39E-02	0.00E+00	0.00E+00
	water column	1.75E-01	1.75E-01	1.75E-01	1.32E-01
	sediments	9.98E+01	9.98E+01	9.98E+01	9.99E+01

surface and water column as the effect factor is only applied for the water sub-compartments. Since the longest residence time for MPs is the sediments, it is important to develop an effect factor to account for differences linked to different exposure routes of benthic species (i.e., exposure via water, sediments or both). Characterization factors for emissions at the beach (CF_{beach}) (table S6) and the water surface ($CF_{watersurface}$) are currently the most relevant to present here as it is assumed that microplastics flows assessed in LCA can only be emitted to these sub-compartments. Characterization factors for the water column ($CF_{watercolumn}$) and the sediments ($CF_{sediments}$) are still needed to be implemented for microplastics generated via the fragmentation of larger macroplastics, which is an ongoing project within MariLCA.

S2.3.1 Influence of environmental parameters

In order to analyze the influence of environmental parameters tested, which are the horizontal dispersion, vertical dispersion, and biofouling rate, eight categories are defined based on the minimum and maximum values of the parameters tested in the simulation plan (section S1.3) as seen in table S8.

Table S7 Characterization factors ($PAF.m^3.d/kg$) for MPs emitted in the marine environment for the impact category "Physical effects o n biota"

	Beach	**Water surface**	**Water column**	**Sediments**
Sp-HD-B	3.36E+00	3.37Ee+0	3.35E+0	3.03E+00
Sp-HD-S	1.62E+02	9.89E+02	9.29E+02	7.72E+02
Sp-LD-B	6.39E+03	6.4E+03	5.79E+03	5.24E+03
Sp-LD-S	1.43E+02	5.59E+02	4.93E+02	3.53E+02
Cy-HD-B	7.16E+01	7.43E+01	7.39E+01	6.68E+01
Cy-HD-S	3.18E+02	1.54E+03	1.47E+03	1.25E+03
Cy-LD-B	9.83E+02	1.00E+03	8.81E+02	7.95E+02
Cy-LD-S	3.08E+02	9.82E+02	9.19E+02	6.94E+02

Sp: spherical - Cy: cylinder - HD: high density - LD: low density - B: big - S: small

Table S8 Simulations categorized based on environmental properties

	kh_max				kh_min			
	kv_max		kv_min		kv_max		kv_min	
	BR_max	BR_min	BR_max	BR_min	BR_max	BR_min	BR_max	BR_min
Number of simulations	29-30-31-32	25-26-27-28	13-14-15-16	9-10-11-12	21-22-23-24	17-18-19-20	5-6-7-8	1-2-3-4

Degradation rates used as removal mechanisms in the rate matrices, are polymer-based. Thus, various rates are considered within the same environmental category. Within each environmental category, influences can be linked with the physical properties of the particles. In order to avoid this confusion, comparison is made at the level of the characterization factors. Therefore, the 32 rate and fate matrices developed for each simulation are used to develop characterization factor matrices (as explained in section 2.3 of the manuscript). They are then classified based on the categories defined in S8. Minimum and maximum values for each category are then calculated, as presented in log scale in figure S4. Because the same effect factors are used for the development of the CFs, the variability of the CFs can be linked to the fate factors influenced by differences in environmental properties. It can be noticed that the variability of these environmental parameters influences the CFs. However, it cannot be determined which variable is responsible for the changes. For instance, increasing the biofouling rate (BR) from its minimum to its maximum value reduces the characterization factors for every emission compartment. This is obtained when the horizontal or the vertical dispersion are at their maximum or minimum values. However, when kh and kv are either both at their maximum or both at their minimum, biofouling rate increases the characterization factors. The reason behind this is explained in the Pareto plot (figure 2 in the manuscript) where the influence of environmental parameters is mainly pronounced when interacting with other variables including microplastic physical properties. This emphasizes on the challenges when modeling the fate of microplastics and the need for considering all varying parameters as their interactions have bigger influence than individual variables.

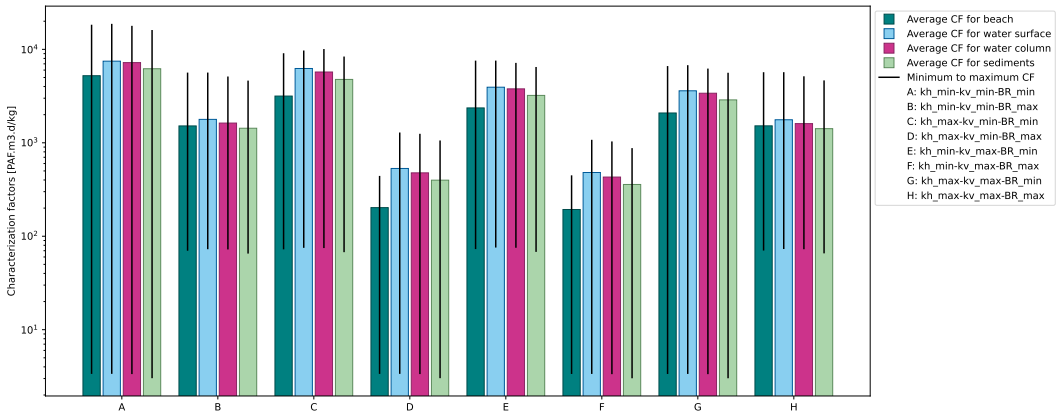

Fig. S4 Average, minimum and maximum characterization factors $[PAF.m^3.d/kg]$, in log scale, classified based on a fixed set of environmental parameters. Vertical lines represent the minimum and maximum CFs for each category and for the water surface and water column sub-compartments. kh: horizontal dispersion, kv: vertical dispersion, BR: biofouling rate

S2.4 Sensitivity Analysis

The results of the sensitivity analysis on the fate factors of each microplastic category is presented in figure S5.

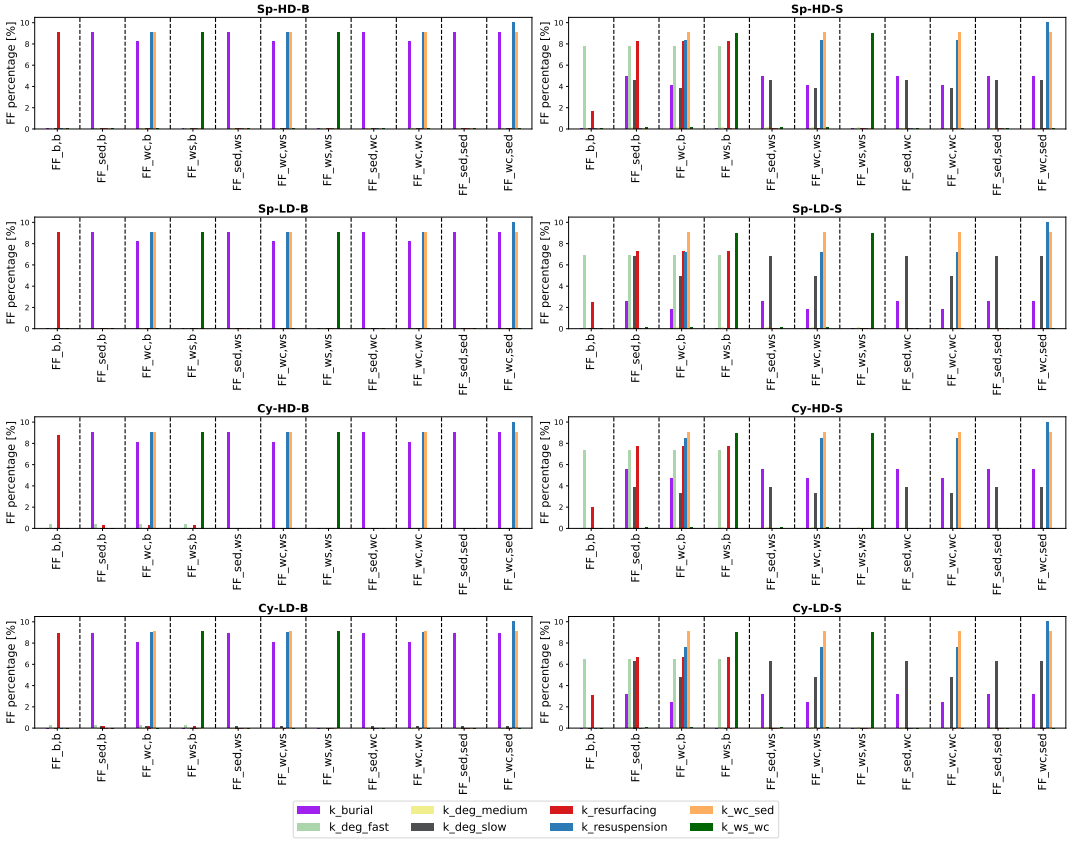

Fig. S5 Sensitivity analysis of different rates on the FF matrix of each microplastic category (k_deg_i: degradation rates for different intensities i, k_ws_wc: transfer rate from the water surface to the water column, k_wc_sed: transfer rate from the water column to the sediments)

The results of the sensitivity analysis on the characterization factors of each microplastic category is presented in figure S6.

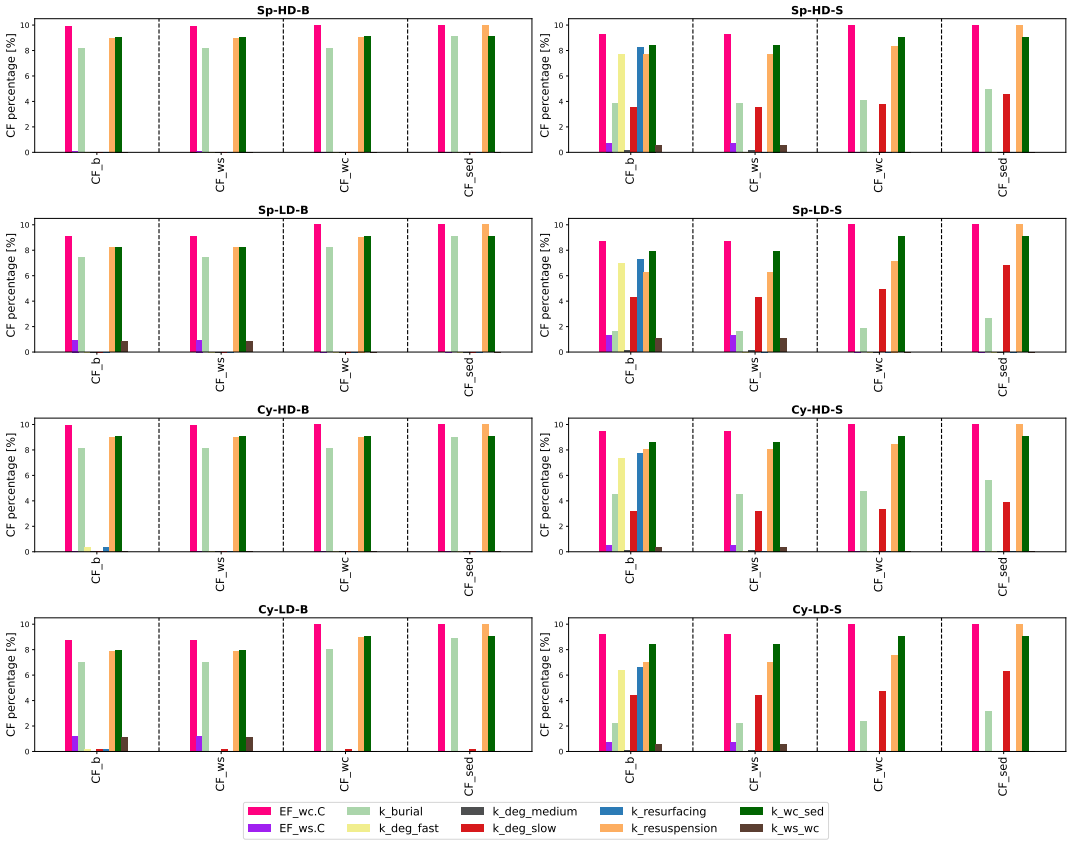

Fig. S6 Sensitivity analysis of different quantified rates on the CF matrix of each microplastic category (k_deg_i: degradation rates for different intensities i, k_ws_wc: transfer rate from the water surface to the water column, k_wc_sed: transfer rate from the water column to the sediments)

S2.5 Rate matrices for each simulation

The rate matrices for the 32 simulations are presented in the tables below.

Table S9: Rate matrices [day^{-1}] for 32 simulations (b: beach, ws: water surface, wc: water column, sed: sediments)

Simulation		b	ws	wc	sed
1	**b**	-1.76E+00	0.00E+00	0.00E+00	0.00E+00
	ws	4.50E-01	-4.29E-02	0.00E+00	0.00E+00
	wc	0.00E+00	3.60E-02	-2.78E-02	2.26E-04
	sed	0.00E+00	0.00E+00	2.77E-02	-3.16E-04
2	**b**	-4.51E-01	0.00E+00	0.00E+00	0.00E+00
	ws	4.50E-01	-2.03E+03	0.00E+00	0.00E+00

Table S9 – continued from previous page

		b	ws	wc	sed
	wc	0.00E+00	2.03E+03	-1.19E+02	2.26E-04
	sed	0.00E+00	0.00E+00	1.19E+02	-2.5E-04
3	**b**	-4.60E-01	0.00E+00	0.00E+00	0.00E+00
	ws	4.50E-01	-4.18E-02	0.00E+00	0.00E+00
	wc	0.00E+00	4.18E-02	-2.20E-02	2.26E-04
	sed	0.00E+00	0.00E+00	2.20E-02	-2.5E-04
4	**b**	-2.18E+00	0.00E+00	0.00E+00	0.00E+00
	ws	4.50E-01	-1.73E-01	0.00E+00	0.00E+00
	wc	0.00E+00	1.67E-01	-4.09E-02	2.26E-04
	sed	0.00E+00	0.00E+00	4.09E-02	-2.7E-04
5	**b**	-4.51E-01	0.00E+00	0.00E+00	0.00E+00
	ws	4.50E-01	-7.36E-02	0.00E+00	0.00E+00
	wc	0.00E+00	7.36E-02	-7.81E-02	2.26E-04
	sed	0.00E+00	0.00E+00	7.81E-02	-2.5E-04
6	**b**	-2.75E+00	0.00E+00	0.00E+00	0.00E+00
	ws	4.50E-01	-6.59E-01	0.00E+00	0.00E+00
	wc	0.00E+00	6.52E-01	-4.20E-01	2.26E-04
	sed	0.00E+00	0.00E+00	4.20E-01	-2.72E-04
7	**b**	-1.44E+00	0.00E+00	0.00E+00	0.00E+00
	ws	4.50E-01	-7.84E-01	0.00E+00	0.00E+00
	wc	0.00E+00	7.79E-01	-2.03E-01	2.26E-04
	sed	0.00E+00	0.00E+00	2.03E-01	-2.99E-04
8	**b**	-4.68E-01	0.00E+00	0.00E+00	0.00E+00
	ws	4.50E-01	-9.24E+01	0.00E+00	0.00E+00
	wc	0.00E+00	9.24E+01	-5.50E+00	2.99E-04
	sed	0.00E+00	0.00E+00	5.50E+00	-2.5E-04
9	**b**	-4.51E-01	0.00E+00	0.00E+00	0.00E+00
	ws	4.50E-01	-1.62E-02	0.00E+00	0.00E+00
	wc	0.00E+00	1.62E-02	-5.95E-02	2.26E-04
	sed	0.00E+00	0.00E+00	5.95E-02	-2.5E-04
10	**b**	-2.75E+00	0.00E+00	0.00E+00	0.00E+00
	ws	4.50E-01	-9.22E-02	0.00E+00	0.00E+00
	wc	0.00E+00	8.51E-02	-2.25E-02	2.26E-04
	sed	0.00E+00	0.00E+00	2.24E-02	-2.72E-04
11	**b**	-1.44E+00	0.00E+00	0.00E+00	0.00E+00
	ws	4.50E-01	-1.43E-01	0.00E+00	0.00E+00
	wc	0.00E+00	1.38E-01	-2.59E-02	2.26E-04
	sed	0.00E+00	0.00E+00	2.58E-02	-2.99E-04
12	**b**	-4.68E-01	0.00E+00	0.00E+00	0.00E+00
	ws	4.50E-01	-9.22E+01	0.00E+00	0.00E+00
	wc	0.00E+00	9.22E+01	-5.32E+00	2.26E-04
	sed	0.00E+00	0.00E+00	5.32E+00	-2.5E-04

Table S9 – continued from previous page

		b	ws	wc	sed
13	**b**	-1.76E+00	0.00E+00	0.00E+00	0.00E+00
	ws	4.50E-01	-6.59E-01	0.00E+00	0.00E+00
	wc	0.00E+00	6.52E-01	-4.14E-01	2.26E-04
	sed	0.00E+00	0.00E+00	4.14E-01	-3.2E-04
14	**b**	-4.51E-01	0.00E+00	0.00E+00	0.00E+00
	ws	4.50E-01	-2.03E+03	0.00E+00	0.00E+00
	wc	0.00E+00	2.03E+03	-1.19E+02	2.26E-04
	sed	0.00E+00	0.00E+00	1.19E+02	-2.5E-04
15	**b**	-4.60E-01	0.00E+00	0.00E+00	0.00E+00
	ws	4.50E-01	-3.14E-01	0.00E+00	0.00E+00
	wc	0.00E+00	3.14E-01	-1.19E+00	2.26E-04
	sed	0.00E+00	0.00E+00	1.19E+00	-2.5E-04
16	**b**	-2.18E+00	0.00E+00	0.00E+00	0.00E+00
	ws	4.50E-01	-7.85E-01	0.00E+00	0.00E+00
	wc	0.00E+00	7.80E-01	-2.03E-01	2.26E-04
	sed	0.00E+00	0.00E+00	2.03E-01	-2.66E-04
17	**b**	-4.51E-01	0.00E+00	0.00E+00	0.00E+00
	ws	4.50E-01	-9.24E-02	0.00E+00	0.00E+00
	wc	0.00E+00	9.24E-02	-5.58E-02	2.26E-04
	sed	0.00E+00	0.00E+00	5.58E-02	-2.5E-04
18	**b**	-2.75E+00	0.00E+00	0.00E+00	0.00E+00
	ws	4.50E-01	-6.79E-02	0.00E+00	0.00E+00
	wc	0.00E+00	6.08E-02	-4.68E-02	2.26E-04
	sed	0.00E+00	0.00E+00	4.68E-02	-2.72E-04
19	**b**	-1.44E+00	0.00E+00	0.00E+00	0.00E+00
	ws	4.50E-01	-1.47E-01	0.00E+00	0.00E+00
	wc	0.00E+00	1.42E-01	-5.16E-02	2.26E-04
	sed	0.00E+00	0.00E+00	5.16E-02	-2.99E-04
20	**b**	-4.68E-01	0.00E+00	0.00E+00	0.00E+00
	ws	4.50E-01	-9.60E+01	0.00E+00	0.00E+00
	wc	0.00E+00	9.60E+01	-5.28E+00	2.26E-04
	sed	0.00E+00	0.00E+00	5.28E+00	-2.5E-04
21	**b**	-1.76E+00	0.00E+00	0.00E+00	0.00E+00
	ws	4.50E-01	-7.58E-01	0.00E+00	0.00E+00
	wc	0.00E+00	7.51E-01	-4.00E-01	2.26E-04
	sed	0.00E+00	0.00E+00	4.00E-01	-3.16E-04
22	**b**	-4.51E-01	0.00E+00	0.00E+00	0.00E+00
	ws	4.50E-01	-2.01E+03	0.00E+00	0.00E+00
	wc	0.00E+00	2.01E+03	-1.20E+02	2.26E-04
	sed	0.00E+00	0.00E+00	1.20E+02	-3.05E-04
23	**b**	-4.60E-01	0.00E+00	0.00E+00	0.00E+00
	ws	4.50E-01	-3.36E-01	0.00E+00	0.00E+00

Table S9 – continued from previous page

		b	ws	wc	sed
	wc	0.00E+00	3.35E-01	-1.14E+00	2.26E-04
	sed	0.00E+00	0.00E+00	1.14E+00	-2.5E-04
24	**b**	-2.18E+00	0.00E+00	0.00E+00	0.00E+00
	ws	4.50E-01	-7.76E-01	0.00E+00	0.00E+00
	wc	0.00E+00	7.71E-01	-2.45E-01	2.26E-04
	sed	0.00E+00	0.00E+00	2.45E-01	-2.66E-04
25	**b**	-1.76E+00	0.00E+00	0.00E+00	0.00E+00
	ws	4.50E-01	-9.97E-02	0.00E+00	0.00E+00
	wc	0.00E+00	9.28E-02	-5.31E-02	2.26E-04
	sed	0.00E+00	0.00E+00	5.31E-02	-3.16E-04
26	**b**	-4.51E-01	0.00E+00	0.00E+00	0.00E+00
	ws	4.50E-01	-2.01E+03	0.00E+00	0.00E+00
	wc	0.00E+00	2.01E+03	-1.20E+02	2.26E-04
	sed	0.00E+00	0.00E+00	1.20E+02	-2.5E-04
27	**b**	-4.60E-01	0.00E+00	0.00E+00	0.00E+00
	ws	4.50E-01	-7.00E-02	0.00E+00	0.00E+00
	wc	0.00E+00	6.99E-02	-6.31E-02	2.26E-04
	sed	0.00E+00	0.00E+00	6.31E-02	-2.5E-04
28	**b**	-2.18E+00	0.00E+00	0.00E+00	0.00E+00
	ws	4.50E-01	-1.56E-01	0.00E+00	0.00E+00
	wc	0.00E+00	1.50E-01	-5.26E-02	2.26E-04
	sed	0.00E+00	0.00E+00	5.26E-02	-2.66E-04
29	**b**	-4.51E-01	0.00E+00	0.00E+00	0.00E+00
	ws	4.50E-01	-6.99E-02	0.00E+00	0.00E+00
	wc	0.00E+00	6.99E-02	-7.76E-02	2.26E-04
	sed	0.00E+00	0.00E+00	7.76E-02	-2.5E-04
30	**b**	-2.75E+00	0.00E+00	0.00E+00	0.00E+00
	ws	4.50E-01	-7.58E-01	0.00E+00	0.00E+00
	wc	0.00E+00	7.51E-01	-3.98E-01	2.26E-04
	sed	0.00E+00	0.00E+00	3.98E-01	-2.72E-04
31	**b**	-1.44E+00	0.00E+00	0.00E+00	0.00E+00
	ws	4.50E-01	-7.71E-01	0.00E+00	0.00E+00
	wc	0.00E+00	7.66E-01	-2.51E-01	2.26E-04
	sed	0.00E+00	0.00E+00	2.51E-01	-2.99E-04
32	**b**	-4.68E-01	0.00E+00	0.00E+00	0.00E+00
	ws	4.50E-01	-9.61E+01	0.00E+00	0.00E+00
	wc	0.00E+00	9.61E+01	-5.48E+00	2.26E-04
	sed	0.00E+00	0.00E+00	5.48E+00	-2.5E-04

S2.6 Fate matrices for each simulation

Fate matrices for each of the 32 simulations are presented in table S10 below.

Table S10: Fate matrices [day] for 32 simulations (b: beach, ws: water surface, wc: water column, sed: sediments)

Simulation		b	ws	wc	sed
1	**b**	5.67E-01	0.00E+00	0.00E+00	0.00E+00
	ws	5.95E+00	2.33E+01	0.00E+00	0.00E+00
	wc	2.69E+01	1.06E+02	1.26E+02	9.01E+01
	sed	2.37E+03	9.27E+03	1.11E+04	1.11E+04
2	**b**	2.22E+00	0.00E+00	0.00E+00	0.00E+00
	ws	4.92E-04	4.93E-04	0.00E+00	0.00E+00
	wc	8.71E-02	8.72E-02	8.72E-02	7.88E-02
	sed	4.16E+04	4.17E+04	4.17E+04	4.17E+04
3	**b**	2.17E+00	0.00E+00	0.00E+00	0.00E+00
	ws	2.34E+01	2.39E+01	0.00E+00	0.00E+00
	wc	4.54E+02	4.64E+02	4.65E+02	4.20E+02
	sed	3.99E+04	4.08E+04	4.08E+04	4.08E+04
4	**b**	4.60E-01	0.00E+00	0.00E+00	0.00E+00
	ws	1.20E+00	5.79E+00	0.00E+00	0.00E+00
	wc	3.22E+01	1.56E+02	1.61E+02	1.36E+02
	sed	4.95E+03	2.39E+04	2.47E+04	2.47E+04
5	**b**	2.22E+00	0.00E+00	0.00E+00	0.00E+00
	ws	1.36E+01	1.36E+01	0.00E+00	0.00E+00
	wc	1.33E+02	1.33E+02	1.33E+02	1.21E+02
	sed	4.16E+04	4.16E+04	4.16E+04	4.16E+04
6	**b**	3.64E-01	0.00E+00	0.00E+00	0.00E+00
	ws	2.48E-01	1.52E+00	0.00E+00	0.00E+00
	wc	2.29E+00	1.40E+01	1.41E+01	1.17E+01
	sed	3.53E+03	2.15E+04	2.18E+04	2.18E+04
7	**b**	6.96E-01	0.00E+00	0.00E+00	0.00E+00
	ws	4.00E-01	1.28E+00	0.00E+00	0.00E+00
	wc	6.25E+00	1.99E+01	2.01E+01	1.51E+01
	sed	4.25E+03	1.35E+04	1.36E+04	1.36E+04
8	**b**	2.14E+00	0.00E+00	0.00E+00	0.00E+00
	ws	1.04E-02	1.08E-02	0.00E+00	0.00E+00
	wc	1.81E+00	1.88E+00	1.88E+00	1.70E+00
	sed	3.99E+04	4.14E+04	4.14E+04	4.14E+04
9	**b**	2.22E+00	0.00E+00	0.00E+00	0.00E+00
	ws	6.18E+01	6.19E+01	0.00E+00	0.00E+00
	wc	1.75E+02	1.75E+02	1.75E+02	1.58E+02
	sed	4.16E+04	4.16E+04	4.16E+04	4.16E+04
10	**b**	3.64E-01	0.00E+00	0.00E+00	0.00E+00
	ws	1.78E+00	1.08E+01	0.00E+00	0.00E+00
	wc	3.97E+01	2.42E+02	2.63E+02	2.18E+02
	sed	3.27E+03	2.00E+04	2.17E+04	2.17E+04
11	**b**	6.96E-01	0.00E+00	0.00E+00	0.00E+00

Table S10 continued from previous page

	ws	2.20E+00	7.00E+00	0.00E+00	0.00E+00
	wc	4.74E+01	1.51E+02	1.57E+02	1.18E+02
	sed	4.09E+03	1.30E+04	1.35E+04	1.36E+04
12	**b**	2.14E+00	0.00E+00	0.00E+00	0.00E+00
	ws	1.04E-02	1.08E-02	0.00E+00	0.00E+00
	wc	1.87E+00	1.95E+00	1.95E+00	1.76E+00
	sed	3.99E+04	4.14E+04	4.14E+04	4.14E+04
13	**b**	5.67E-01	0.00E+00	0.00E+00	0.00E+00
	ws	3.88E-01	1.52E+00	0.00E+00	0.00E+00
	wc	2.15E+00	8.41E+00	8.50E+00	6.08E+00
	sed	2.81E+03	1.10E+04	1.11E+04	1.11E+04
14	**b**	2.22E+00	0.00E+00	0.00E+00	0.00E+00
	ws	4.92E-04	4.93E-04	0.00E+00	0.00E+00
	wc	8.71E-02	8.72E-02	8.72E-02	7.88E-02
	sed	4.16E+04	4.17E+04	4.17E+04	4.17E+04
15	**b**	2.17E+00	0.00E+00	0.00E+00	0.00E+00
	ws	3.12E+00	3.19E+00	0.00E+00	0.00E+00
	wc	8.40E+00	8.59E+00	8.59E+00	7.75E+00
	sed	3.99E+04	4.08E+04	4.08E+04	4.08E+04
16	**b**	4.60E-01	0.00E+00	0.00E+00	0.00E+00
	ws	2.64E-01	1.27E+00	0.00E+00	0.00E+00
	wc	6.68E+00	3.23E+01	3.25E+01	2.76E+01
	sed	5.08E+03	2.46E+04	2.47E+04	2.47E+04
17	**b**	2.22E+00	0.00E+00	0.00E+00	0.00E+00
	ws	1.08E+01	1.08E+01	0.00E+00	0.00E+00
	wc	1.86E+02	1.87E+02	1.87E+02	1.69E+02
	sed	4.16E+04	4.16E+04	4.16E+04	4.16E+04
18	**b**	3.64E-01	0.00E+00	0.00E+00	0.00E+00
	ws	2.41E+00	1.47E+01	0.00E+00	0.00E+00
	wc	1.85E+01	1.13E+02	1.26E+02	1.05E+02
	sed	3.19E+03	1.95E+04	2.17E+04	2.17E+04
19	**b**	6.96E-01	0.00E+00	0.00E+00	0.00E+00
	ws	2.13E+00	6.80E+00	0.00E+00	0.00E+00
	wc	2.39E+01	7.61E+01	7.89E+01	5.96E+01
	sed	4.11E+03	1.31E+04	1.36E+04	1.36E+04
20	**b**	2.14E+00	0.00E+00	0.00E+00	0.00E+00
	ws	1.00E-02	1.04E-02	0.00E+00	0.00E+00
	wc	1.89E+00	1.96E+00	1.96E+00	1.77E+00
	sed	3.99E+04	4.14E+04	4.14E+04	4.14E+04
21	**b**	5.67E-01	0.00E+00	0.00E+00	0.00E+00
	ws	3.37E-01	1.32E+00	0.00E+00	0.00E+00
	wc	2.23E+00	8.72E+00	8.80E+00	6.30E+00
	sed	2.82E+03	1.10E+04	1.11E+04	1.11E+04
22	**b**	2.22E+00	0.00E+00	0.00E+00	0.00E+00

Table S10 continued from previous page

	ws	4.97E-04	4.98E-04	0.00E+00	0.00E+00
	wc	8.69E-02	8.70E-02	8.70E-02	7.87E-02
	sed	4.16E+04	4.17E+04	4.17E+04	4.17E+04
23	**b**	2.17E+00	0.00E+00	0.00E+00	0.00E+00
	ws	2.92E+00	2.98E+00	0.00E+00	0.00E+00
	wc	8.77E+00	8.96E+00	8.96E+00	8.08E+00
	sed	3.99E+04	4.08E+04	4.08E+04	4.08E+04
24	**b**	4.60E-01	0.00E+00	0.00E+00	0.00E+00
	ws	2.67E-01	1.29E+00	0.00E+00	0.00E+00
	wc	5.54E+00	2.68E+01	2.69E+01	2.28E+01
	sed	5.08E+03	2.46E+04	2.47E+04	2.47E+04
25	**b**	5.67E-01	0.00E+00	0.00E+00	0.00E+00
	ws	2.56E+00	1.00E+01	0.00E+00	0.00E+00
	wc	1.57E+01	6.15E+01	6.60E+01	4.73E+01
	sed	2.64E+03	1.03E+04	1.11E+04	1.11E+04
26	**b**	2.22E+00	0.00E+00	0.00E+00	0.00E+00
	ws	4.97E-04	4.98E-04	0.00E+00	0.00E+00
	wc	8.69E-02	8.70E-02	8.70E-02	7.87E-02
	sed	4.16E+04	4.17E+04	4.17E+04	4.17E+04
27	**b**	2.17E+00	0.00E+00	0.00E+00	0.00E+00
	ws	1.40E+01	1.43E+01	0.00E+00	0.00E+00
	wc	1.59E+02	1.62E+02	1.62E+02	1.46E+02
	sed	3.99E+04	4.08E+04	4.08E+04	4.08E+04
28	**b**	4.60E-01	0.00E+00	0.00E+00	0.00E+00
	ws	1.33E+00	6.42E+00	0.00E+00	0.00E+00
	wc	2.50E+01	1.21E+02	1.25E+02	1.06E+02
	sed	4.94E+03	2.38E+04	2.47E+04	2.47E+04
29	**b**	2.22E+00	0.00E+00	0.00E+00	0.00E+00
	ws	1.43E+01	1.43E+01	0.00E+00	0.00E+00
	wc	1.34E+02	1.34E+02	1.34E+02	1.21E+02
	sed	4.16E+04	4.16E+04	4.16E+04	4.16E+04
30	**b**	3.64E-01	0.00E+00	0.00E+00	0.00E+00
	ws	2.16E-01	1.32E+00	0.00E+00	0.00E+00
	wc	2.41E+00	1.47E+01	1.49E+01	1.24E+01
	sed	3.53E+03	2.16E+04	2.18E+04	2.18E+04
31	**b**	6.96E-01	0.00E+00	0.00E+00	0.00E+00
	ws	4.07E-01	1.30E+00	0.00E+00	0.00E+00
	wc	5.07E+00	1.62E+01	1.63E+01	1.23E+01
	sed	4.25E+03	1.35E+04	1.36E+04	1.36E+04
32	**b**	2.14E+00	0.00E+00	0.00E+00	0.00E+00
	ws	1.00E-02	1.04E-02	0.00E+00	0.00E+00
	wc	1.82E+00	1.89E+00	1.89E+00	1.71E+00
	sed	3.99E+04	4.14E+04	4.14E+04	4.14E+04

S2.7 Characterization factor matrices for each simulation

Characterization factors $[PAF.m^3.d/kg]$ for each of the 32 simulations are presented in table S11 below.

Table S11: Characterization factors $[PAF.m^3.d/kg]$ for each simulation

Simulation	beach	water surface	water column	sediments
1	1.26E+03	4.95E+03	4.83E+03	3.46E+03
2	3.36E+00	3.37E+00	3.35E+00	3.03E+00
3	1.83E+04	1.88E+04	1.79E+04	1.61E+04
4	1.28E+03	6.2E+03	6.17E+03	5.23E+03
5	5.64E+03	5.64E+03	5.12E+03	4.63E+03
6	9.73E+01	5.94E+02	5.42E+02	4.5E+02
7	2.55E+02	8.14E+02	7.7E+02	5.82E+02
8	6.99E+01	7.26E+01	7.22E+01	6.52E+01
9	9.09E+03	9.09E+03	6.72E+03	6.07E+03
10	1.59E+03	9.72E+03	1.01E+04	8.38E+03
11	1.9E+03	6.07E+03	6.02E+03	4.55E+03
12	7.24E+01	7.52E+01	7.47E+01	6.75E+01
13	9.73E+01	3.81E+02	3.26E+02	2.34E+02
14	3.36E+00	3.37E+00	3.35E+00	3.03E+00
15	4.42E+02	4.52E+02	3.3E+02	2.97E+02
16	2.67E+02	1.29E+03	1.25E+03	1.06E+03
17	7.58E+03	7.58E+03	7.17E+03	6.48E+03
18	8.03E+02	4.9E+03	4.85E+03	4.03E+03
19	9.98E+02	3.18E+03	3.03E+03	2.29E+03
20	7.29E+01	7.57E+01	7.53E+01	6.8E+01
21	9.84E+01	3.86E+02	3.38E+02	2.42E+02
22	3.36E+00	3.36E+00	3.34E+00	3.02E+00
23	4.49E+02	4.58E+02	3.44E+02	3.10E+02
24	2.23E+02	1.08E+03	1.03E+03	8.77E+02
25	7.01E+02	2.74E+03	2.54E+03	1.82E+03
26	3.36E+00	3.36E+00	3.34E+00	3.02E+00
27	6.63E+03	6.77E+03	6.23E+03	5.62E+03
28	1.01E+03	4.89E+03	4.81E+03	4.08E+03
29	5.69E+03	5.7E+03	5.15E+03	4.65E+03
30	1.01E+02	6.16E+02	5.71E+02	4.74E+02
31	2.10E+02	6.70E+02	6.25E+02	4.72E+02
32	7.03E+01	7.3E+01	7.26E+01	6.56E+01

References

Dunn, K. (2022). DESIGN AND ANALYSIS OF EXPERIMENTS. *Process improv. using data* (pp. 231–291).

Kamphuis, J.W. (1991). Alongshore sediment transport rate. *J. Waterw.*, *117*(6), 624–640.

APPENDIX C SI OF CHAPTER 8: REGIONALIZE FF AND CF TO ASSESS THE IMPORTANCE OF SPATIAL VARIABILITY COMPARED TO THE VARIABILITY LINKED TO THE PHYSICAL PROPERTIES OF EMITTED MP

Appendix C includes the supplementary information of chapter 8 that responds to the third sub-objective: "Regionalize the FFs and CFs to assess the importance of spatial variability compared to the variability linked to the physical properties of emitted MPs".

C.1 Methodology

C.1.1 Characterization factors CFs

The partial characterization factor matrix **CF** that include sub-compartment specific characterization factors, is presented in equation C.1. CFs are expressed in $PAF.m_i^3.d/kg$ where i represents considered sub-compartment. "b" represents beach, "ws" represents water surface, "wc" represents water column, "sed" represents sediments sub-compartments, and "glo" represents the global scale.

$$\mathbf{CF} = \begin{bmatrix} CF_{b,b} & CF_{b,ws} & 0 & 0 & 0 \\ CF_{ws,b} & CF_{ws,ws} & 0 & 0 & 0 \\ CF_{wc,b} & CF_{wc,ws} & CF_{wc,wc} & CF_{wc,sed} & 0 \\ CF_{sed,b} & CF_{sed,ws} & CF_{sed,wc} & CF_{sed,sed} & 0 \\ CF_{glo,b} & CF_{glo,ws} & CF_{glo,wc} & CF_{glo,sed} & CF_{glo,glo} \end{bmatrix} \quad \text{(C.1)}$$

C.1.2 Parametrization of TrackMPD

Table C.1 presents the coordinates that define each extracted domain presented in figure 5.3. Table C.2 provides the coordinates of all emission locations in all domains (figure 5.3). As explained in section 5.4.1, 50 particles are emitted in every emission location to give a total of 250 particles emitted per domain.

Table C.1 Coordinates of the extracted domains present in figure 5.3

Region	Minimum Longitude	Maximum Longitude	Minimum Latitude	Maximum Latitude
Gulf of Guinea - Congo	-2.3	13.5	-9.5	6.5
Mediterranean	12.403	36.104	30.249	39.243
Indus	57.793	77.301	8.346	25.865
Bay of Bengal	77.5	98.825	6	23
EC-Japan	117	136	25.496	43.6
Okhotsk Sea	135	164	43.5	61.96

Table C.2 Coordinates of all emission points in all the domains tested

Emission locations per region		
Region	**Longitude**	**Latitude**
Okhotsk Sea	141.55	53.1
	141.583	53.19
	141.7	53.33
	141.509	53.38
	141.583	53.4167
Bay of Bengal	87.5	20.9
	90.2	21.1
	88.5	21
	89.7	21.1
	90.9	21
EC-Japan	121.7	36.5
	120	35
	122.2	31.1
	121.4	33
	122.3	29
Gulf of Guinea	6.7	4.27
	5.125	5.5
	5.3	5.2
	5.65	4.5
	6.1	4.1
Congo	12.1	-5.3
	12	-5.083
	11.75	-4.7083
	11.6	-4.4583

Table C.3 continued from previous page

Region	Longitude	Latitude
Congo	11.5	-4.33
Mediterranean	31.17	31.83
	31.67	31.613
	30.75	31.7
	30.42	31.67
	32	31.57
Indus	66.9	23.58
	67.3	23
	66.9	24
	67.5	23.5
	68	23.3
End of Table		

Number of particles per region

In order to determine the number of particles released per oceanographic region, a sensitivity analysis is carried out in East China (Asia) and the Gulf of Guinea (Africa). In each domain 250, 500, 1000 and 2000 particles are emitted in different locations. The settling velocity of the particles was set to zero to omit the influence of the physical properties of the particles and account only for the influence of water currents. A time step of 1 hour was chosen and the simulations were run for 30 days. The trajectories of the particles can be seen in figures C.1 and C.2. The percentage of distribution of the final position (water, beach, bottom and outside the domain) was calculated. Results are presented in table C.4.

Table C.4 The percentage of distribution of 250, 500, 1000, 2000 MPs emitted in East China Sea and Gulf of Guinea

Domain	Number of particles	Water	Beached	Bottom	Out of Domain
East China	250	29.4%	1.6%	19%	0%
	500	29.8%	2.1%	18.1%	0%
	1000	30.2%	1.7%	18.2%	0%
	2000	31.5%	2.1%	16.5%	0%
Gulf of Guinea	250	17.6%	2.4%	30%	0%
	500	18.9%	1.6%	29.5%	0%
	1000	18.8%	1.8%	29.4%	0%
	2000	18.45%	2.25%	29.3%	0%

As presented in table C.4 and in figures C.1 and C.2, the number of particles does not change

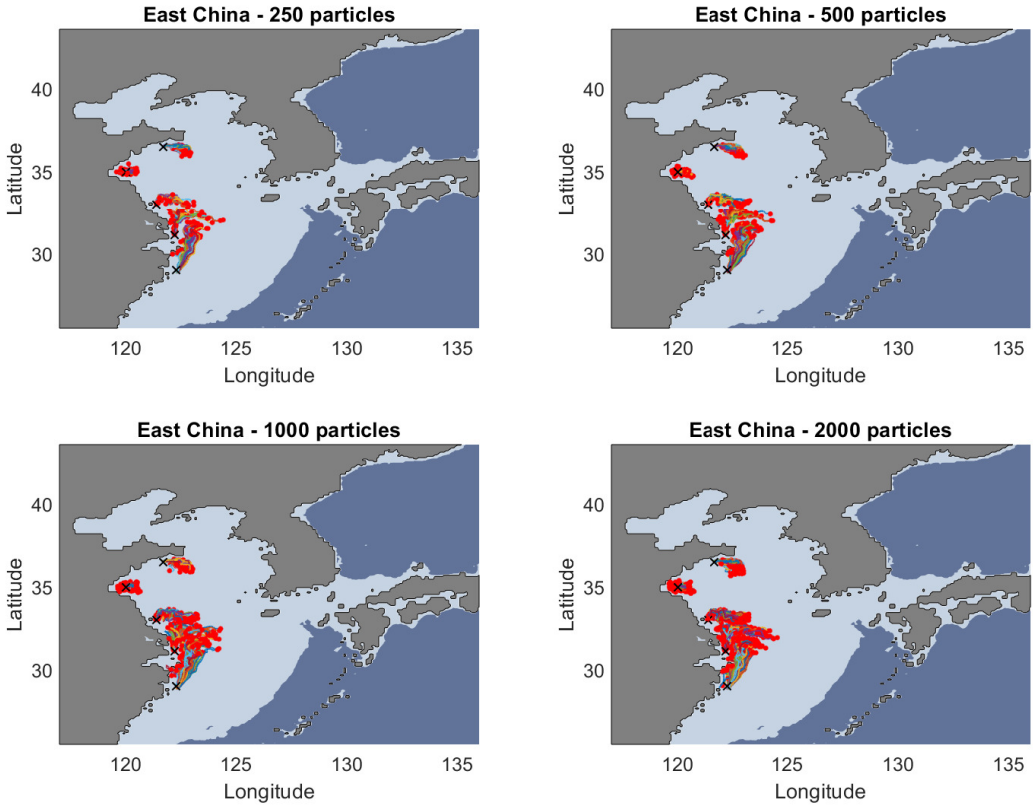

Figure C.1 The trajectory of 250, 500, 1000 and 2000 MP particles emitted around East China Sea

their fate in East China and Gulf of Guinea. Therefore, in order to avoid high computation time, a number of 250 particles is released for every simulation (see methodology section 2.4 in the main manuscript).

Properties of particles tested

The physical properties of microplastics tested are presented in table C.5.

Settling velocities

As described in the main manuscript (section 2.4.2), the settling velocity is calculated according to three formulations depending on the physical properties of microplastics (table C.6). The settling velocity for large spherical and fibrous microplastics (>= 100 µm) is calculated according to the formulation of Waldschlager et al. (2019) and (2020) [92, 204]:

Table C.5 The physical properties of microplastics tested in each simulation scenario

Scenario	**Polymer type**	**Density** $[g/cm^3]$	**Shape**	**Diameter** d_{equi} **[m]**	**Length [m]**	CSF
1	EPS	0.03	Sphere	0.005	-	1
2	EPS	0.03	Sphere	0.001	-	1
3	EPS	0.03	Sphere	10^{-4}	-	1
4	EPS	0.03	Sphere	10^{-5}	-	1
5	EPS	0.03	Sphere	10^{-6}	-	1
6	PP	0.88	Sphere	0.005	-	1
7	PP	0.88	Sphere	0.001	-	1
8	PP	0.88	Sphere	10^{-4}	-	1
9	PP	0.88	Sphere	10^{-5}	-	1
10	PP	0.88	Sphere	10^{-6}	-	1
11	LDPE	0.915	Sphere	0.005	-	1
12	LDPE	0.915	Sphere	0.001	-	1
13	LDPE	0.915	Sphere	10^{-4}	-	1
14	LDPE	0.915	Sphere	10^{-5}	-	1
15	LDPE	0.915	Sphere	10^{-6}	-	1
16	HDPE	0.953	Sphere	0.005	-	1
17	HDPE	0.953	Sphere	0.001	-	1
18	HDPE	0.953	Sphere	10^{-4}	-	1
19	HDPE	0.953	Sphere	10^{-5}	-	1
20	HDPE	0.953	Sphere	10^{-6}	-	1
21	PS	1.06	Sphere	0.005	-	1
22	PS	1.06	Sphere	0.001	-	1
23	PS	1.06	Sphere	10^{-4}	-	1
24	PS	1.06	Sphere	10^{-5}	-	1
25	PS	1.06	Sphere	10^{-6}	-	1
26	EPS	0.03	Fiber	0.001	0.005	0.45
27	EPS	0.03	Fiber	10^{-4}	0.001	0.32
28	EPS	0.03	Fiber	10^{-5}	10^{-4}	0.32
29	EPS	0.03	Fiber	10^{-6}	$5E{-}5$	0.14
30	PP	0.88	Fiber	0.001	0.005	0.45
31	PP	0.88	Fiber	10^{-4}	0.001	0.32
32	PP	0.88	Fiber	10^{-5}	10^{-4}	0.32
33	PP	0.88	Fiber	10^{-6}	$5E{-}5$	0.14
34	LDPE	0.915	Fiber	0.001	0.005	0.45
35	LDPE	0.915	Fiber	10^{-4}	0.001	0.32
36	LDPE	0.915	Fiber	10^{-5}	10^{-4}	0.32
37	LDPE	0.915	Fiber	10^{-6}	$5E{-}5$	0.14
38	HDPE	0.953	Fiber	0.001	0.005	0.45
39	HDPE	0.953	Fiber	10^{-4}	0.001	0.32
40	HDPE	0.953	Fiber	10^{-5}	10^{-4}	0.32
41	HDPE	0.953	Fiber	10^{-6}	$5E{-}5$	0.14
42	PS	1.06	Fiber	0.001	0.005	0.45
43	PS	1.06	Fiber	10^{-4}	0.001	0.32
44	PS	1.06	Fiber	10^{-5}	10^{-4}	0.32
45	PS	1.06	Fiber	10^{-6}	$5E{-}5$	0.14

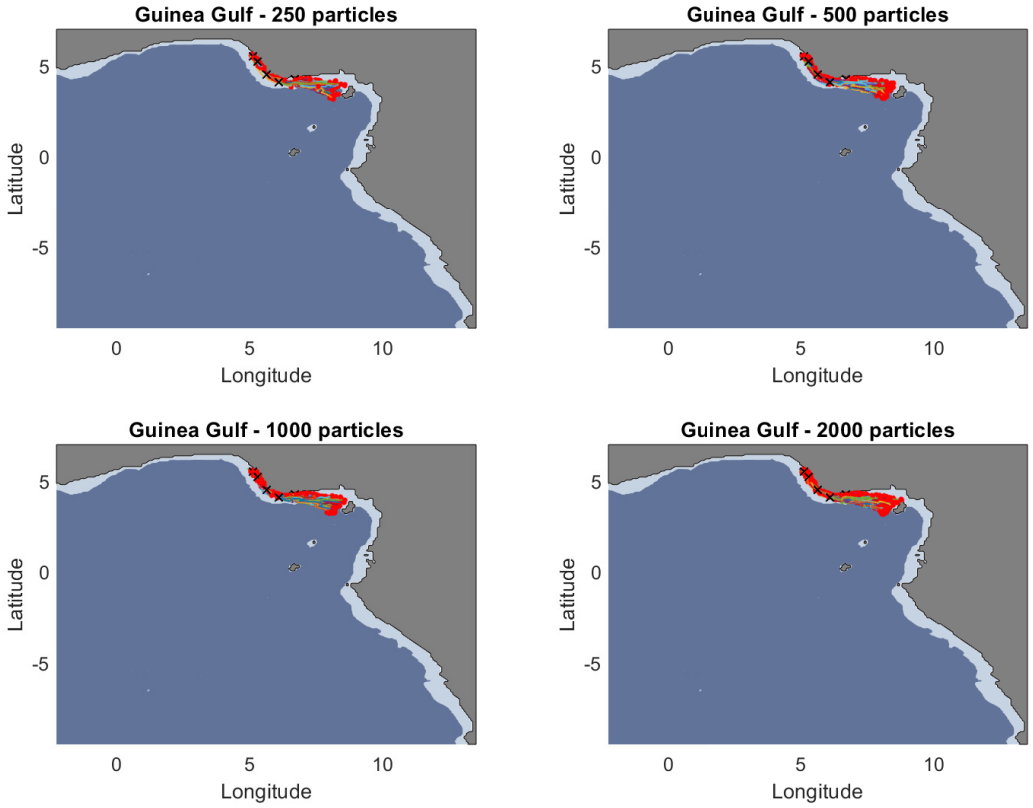

Figure C.2 The trajectory of 250, 500, 1000 and 2000 MP particles emitted around Gulf of Guinea

$$w_s = \sqrt{\frac{4}{3}\frac{d_{equi}}{C_D}\frac{\rho_p - \rho}{\rho}g} \tag{C.2}$$

where w_s is the settling velocity [m/s], d_{equi} is the equivalent diameter [m], ρ is the density of seawater $[g/cm^3]$ and ρ_p is the density of MP particles $[g/cm^3]$, g is the gravity acceleration $[m/s^2]$, and C_D is the drag coefficient [-].

The equivalent diameter d_{equi} [m] is calculated using the shortest c, middle b and longest a sides of spherical (equation C.3) and fibrous (equation C.4) [92]:

$$d_{equi} = \sqrt[3]{abc} \tag{C.3}$$

$$d_{equi} = c \tag{C.4}$$

C_D depends on the physical properties of the particles, i.e., power roundness P and the Corey Shape Factor (CSF). The power roundness P ranges from 0 (very angular particles) to 6 (well-rounded particles). It is taken as 6 for spherical particles, assuming that they are perfect spheres (table C.5). For cylindrical particles, it is taken as 1 [58]. The CSF represents the sphericity of particles. It is calculated as follows [92]:

$$CSF = \frac{c}{\sqrt{ab}} \tag{C.5}$$

Readers can refer to [92, 204] for more details on the calculation of C_D for each type of particles.

For smaller microplastics (< 100 µm), the settling velocity is calculated according to Zhiyao et al. (2008) [205] (equation C.6) for spherical particles and Khatmullina et al., (2017) [206] (equation C.7) for cylindrical particles:

$$w_s = \frac{\nu}{2R} d_*^3 (38.1 + 0.93 d_*^{12/7})^{-7/8} \tag{C.6}$$

where ν is the water kinematic viscosity. It is taken as $1.04E-06 m^2/s$ [58]. R is the radius of MPs [m], and d_* the dimensionless particle diameter. It is calculated using: $d_* = 2R(g\frac{\rho_p - \rho}{\rho\nu^2})^{1/3}$

$$w_s = \frac{\pi}{2}\frac{1}{\nu} g \frac{\rho_p - \rho}{\rho} \frac{2RL}{55.238L + 12.691} \tag{C.7}$$

where L is the length [m] of the cylindrical microplastic particle.

Settling velocities (equation C.2, C.6 and C.7) require the density of seawater. The values of each geographical emission site are taken from (`https://ilp-media.wgbh.org/filer_public/4b/cd/4bcd231d-e60d-4e92-96f4-8047737f2dd6/ssdensemap_17-6-20.png`) and

Table C.6 Summary of the usage of the three settling velocity formulations according to MP physical properties

Shape	**Size**	**Formulation**
Sphere	>= 100 µm	[204]
	< 100 µm	[205]
Cylinders	>= 100 µm	[204]
	< 100 µm	[206]

summarized in table C.7.

Table C.7 Densities of seawater [g/cm^3] for each emission site

Emission site	**Seawater density**
Bay of Bengal	1.02
Congo	1.02
East China	1.021
Indus	1.024
Gulf of Guinea	1.02
Mediterranean	1.027
Okhotsk Sea	1.025

Biofouling

Biofouling densities found in the literature are summarized in table C.8 below:

Karkanorachaki et al. (2021) [67] studied the influence of biofouling on the settling velocities of various PP, LDPE, HDPE, PS and PE films, and PP, LDPE and HDPE fragments. In our study, only spherical and cylindrical shapes are tested. Thus, data on fragments tested in their study are excluded. Only results about LDPE, HDPE, and PP pellets are considered. In their experiments, extreme weather resulted in the detachment of biofilms from the surface of the particles, which affected their densities and settling velocities. Although these findings were excluded from their analysis, it was decided to consider them in this study to represent defouling in the quantification of the biofouling rate, in a simplified way. Having the weight increase (dm/dt) [g/d] and the duration time [d] of their sampling experiment, the biofouling rate (dr/dt) was determined following these iterative steps:

1. For a given initial density, the radius is calculated using the mass increase (Δ m) taken from the empirical data of [67], the initial radius r_0 [m] and density ρ_0 [g/cm^3], and the density ρ at each iteration, according to the following equation:

Table C.8 Biofouling film densities found in literature

Type of biofilm density	**Value** [g/cm^3]	**References**
Algae	1.388	[66]
Microbial mass	1.5	[29]
Diatom species	1.15-1.17-1.18	[304]
Diatom species	1.03	[305]

$$r = \sqrt[3]{\frac{\frac{3\Delta m}{4\pi} + \rho_0 r_0^3}{\rho}} \tag{C.8}$$

2. The biofouling rate (BR = dr/dt [m/d]) is calculated as the difference in radius, at each iteration, with time

3. The biofouling thickness BT [m] by multiplying the biofouling rate with time

4. The density of the particles ρ [g/cm^3] is calculated according to the following equation:

$$\rho.\frac{4}{3}\pi r^3 = \Delta m + \rho_0.\frac{4}{3}\pi r_0^3 \tag{C.9}$$

These steps are iteratively repeated until the density converges, which means that the density calculated in step 4 no longer changes with the change of the other parameters calculated in steps 1 to 3. These steps were followed for the three pellets tested in [67]. The biofouling rate for each pellet is taken when the density converges. An average value (BR = 3.07E-06 m/d) of the three calculated rates (BR_{LDPE} = 3.1E-06 m/d, BR_{HDPE} = 2.5E-06 m/d, and BR_{PP} = 3.6E-06 m/d) was then adopted for the simulations of the particles modeled in this study (table C.5).

C.1.3 Fate matrix

The fate matrix obtained from the inversion of the rate **K** matrix (equation 5.7 in the manuscript) is presented in equation C.10.

$$\mathbf{FF} = \begin{bmatrix} FF_{b,b} & FF_{b,ws} & 0 & 0 & 0 \\ FF_{ws,b} & FF_{ws,ws} & FF_{ws,wc} & 0 & 0 \\ FF_{wc,b} & FF_{wc,ws} & FF_{wc,wc} & FF_{wc,sed} & 0 \\ FF_{sed,b} & FF_{sed,ws} & FF_{sed,wc} & FF_{sed,sed} & 0 \\ FF_{glo,b} & FF_{glo,ws} & FF_{glo,wc} & FF_{glo,sed} & FF_{glo,glo} \end{bmatrix} \tag{C.10}$$

C.1.4 Exposure-effect and species distribution matrices

The exposure-effect matrix **EEF** is presented in equation C.11:

$$\mathbf{EEF} = \begin{bmatrix} EEF_{beach} & 0 & 0 & 0 & 0 \\ 0 & EEF_{ws} & 0 & 0 & 0 \\ 0 & 0 & EEF_{wc} & 0 & 0 \\ 0 & 0 & 0 & EEF_{sed} & 0 \\ 0 & 0 & 0 & 0 & EEF_{glo} \end{bmatrix} \quad \text{(C.11)}$$

C.2 Results

C.2.1 The variability of CFs due to MP physical properties within each region

Table C.9 presents the percentage of particles in the compartments of their final fate within each region.

Table C.9 The percentage of particles in the marine compartment of their ultimate within every emission region

Region	Beached	Sediments	Global
Bay of Bengal	6.66	76.47	16.68
Congo	1.24	63.55	35.04
East China Sea	7.45	90.68	1.79
Gulf of Guinea	19.3	73.73	6.88
Indus	14.13	76.71	9.05
Mediterranean Sea	32.73	62.41	0.853
Okhotsk Sea	16.32	78.06	5.61

C.2.2 The variability of regionalized CFs for every MP tested

The IW+ approach

Figure C.3 presents the variability of CFs due to regionalization for every MP particle tested, for emissions in every marine compartment, for the IW+ approach.

The GLAM approach

Figure C.4 presents the variability of CFs for all MP particles in every emission region and for every emission compartment, for the GLAM approach.

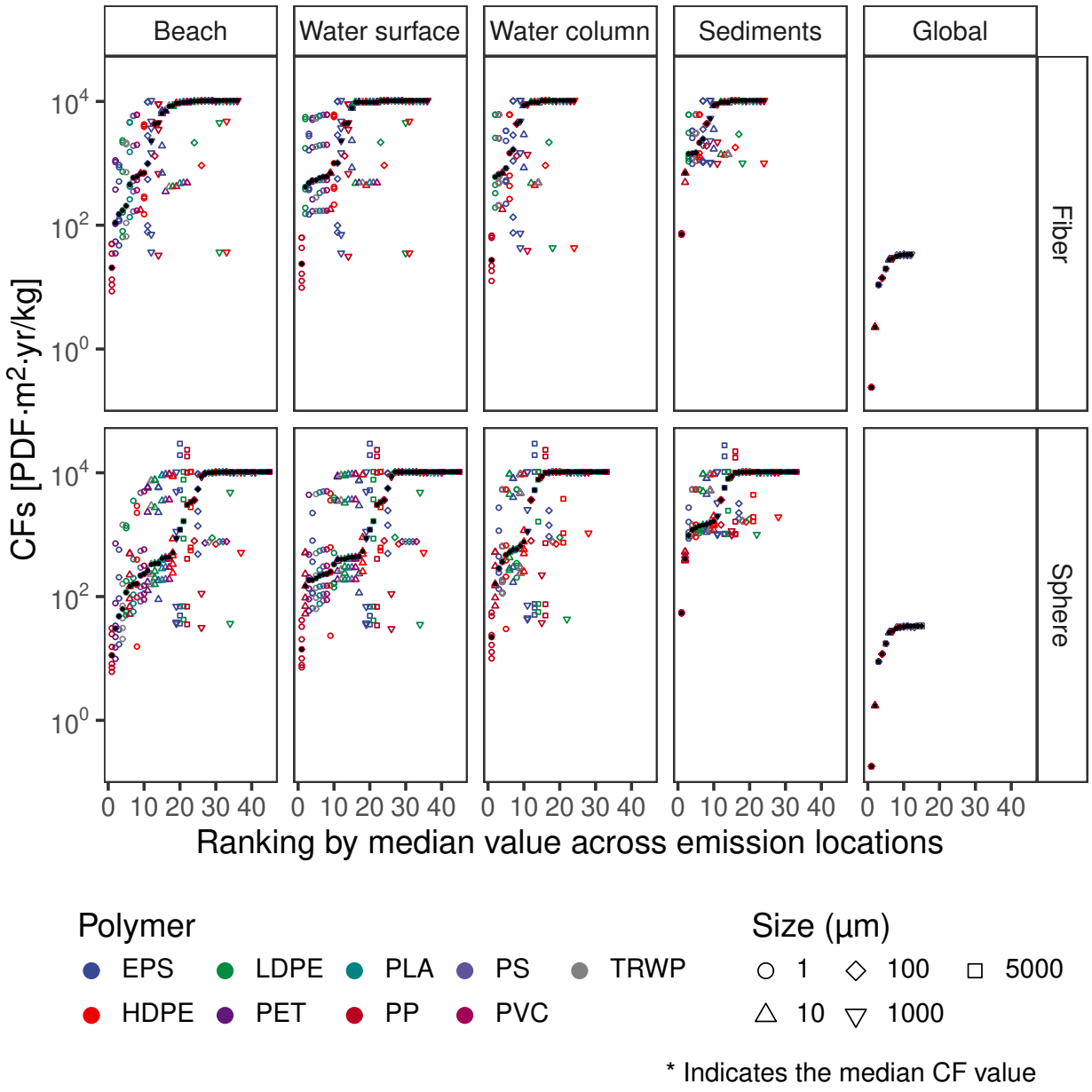

Figure C.3 The variability of regionalized CFs $[PDF.m^2.yr/kg]$ for all MPs emitted in every marine compartment, for the IW+ approach

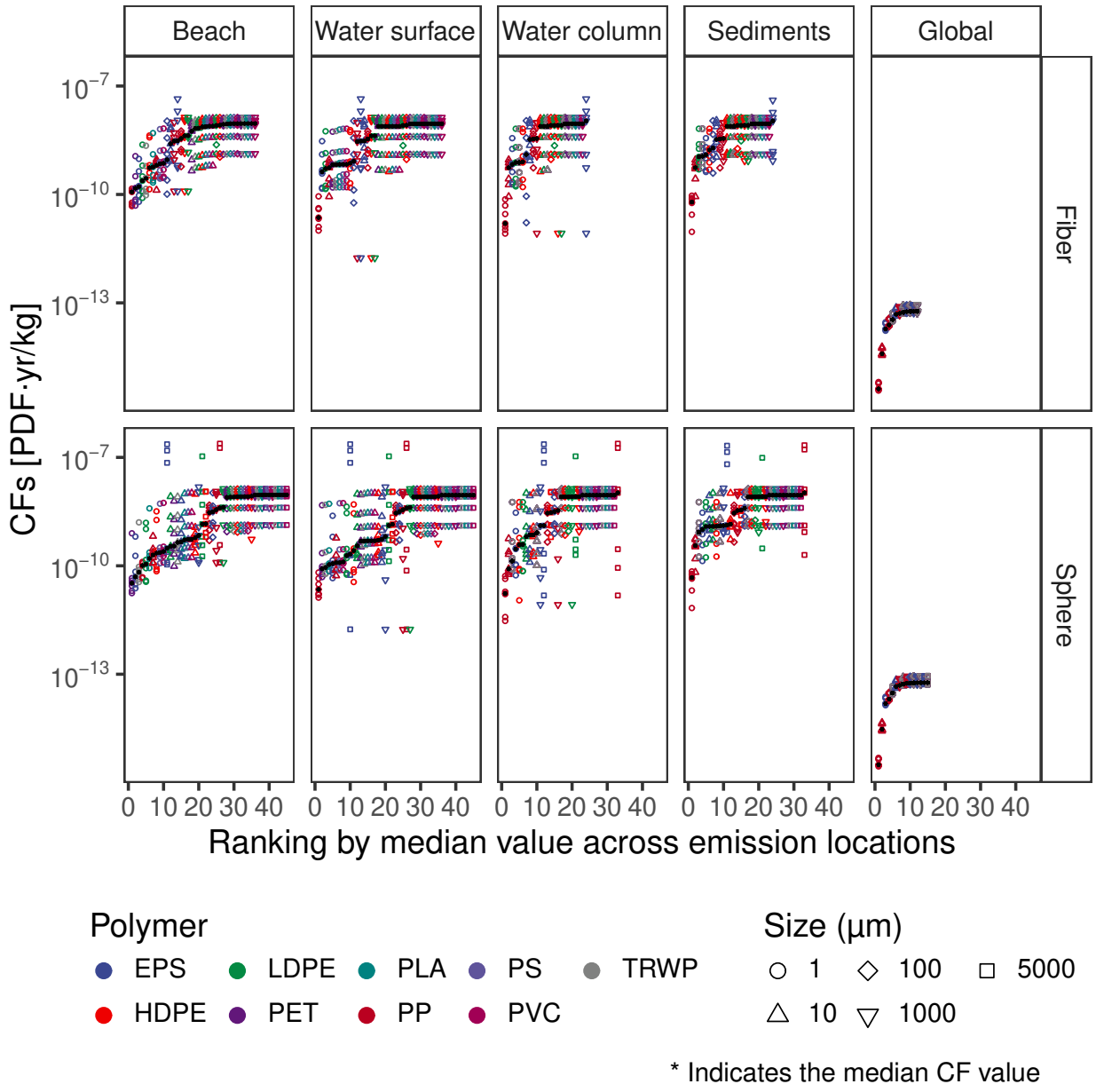

Figure C.4 The variability of regionalized CFs $[PDF.yr/kg]$ for all MPs emitted in every marine compartment, for the GLAM approach